Lawrence Berkeley Laboratory
UNIVERSITY OF CALIFORNIA

CHEMICAL BIODYNAMICS DIVISION

I. CONFORMATIONAL ANALYSIS OF CYCLIC PEPTIDES
II. MULTINUCLEAR NMR SPECTROMETER FOR THE STUDY OF BIOLOGICAL SYSTEMS

Willy Chao-Wei Shih
(Ph.D. thesis)

November 1979

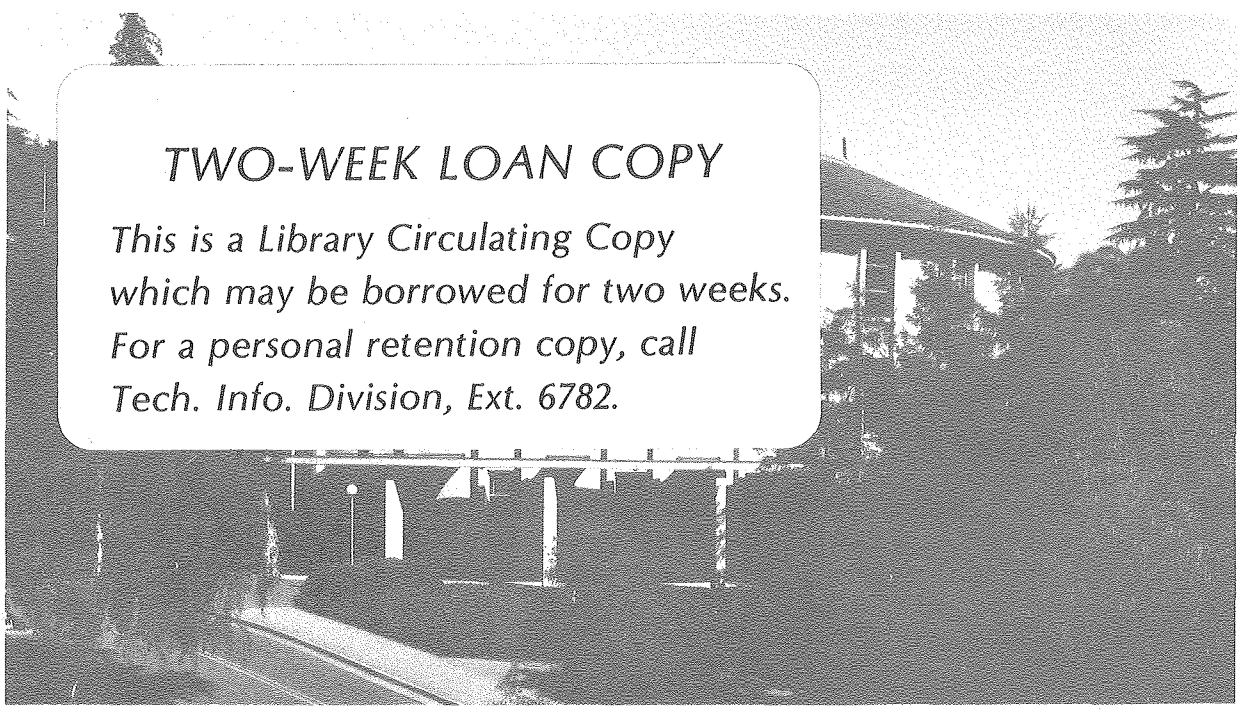

Prepared for the U.S. Department of Energy under Contract W-7405-ENG-48

I. Conformational Analysis of Cyclic Peptides

II. Multinuclear NMR Spectrometer for the Study of Biological Systems

I. Conformational Analysis of Cyclic Peptides

II. Multinuclear NMR Spectrometer for the Study of Biological Systems

Willy Chao-Wei Shih
Lawrence Berkeley Laboratory, University of California
Berkeley, California 94720

ABSTRACT

A systematic approach to the employment of ^{1}H NMR data to the analysis of the solution conformations of small polypeptides is outlined. Two-dimensional homonuclear J-spectra along with the corresponding 45° projections and contour maps simplify the task of homonuclear decoupling experiments, and the assignments of lines is made very straightforward. The vicinal couplings that are likely to vary as the conformation changes are then examined. Spectrum simulations coupled with x-ray data for model systems allow the formulation of Karplus relationships for the vicinal couplings, and solution conformations may then be inferred.

This approach to conformational analysis was applied to an examination of the metal affinities of *cyclo*-[3-(4-β-aminoethyl)-phenyloxypropanoyl-L-prolyl] and *cyclo*-[3-(4-β-N-methylaminoethyl)-

phenyloxypropanoyl-L-prolyl]. The NMR data revealed that the metal affinity of the former is probably a result of the orientation of both carbonyl groups towards the same face of the ring; the sharply lower affinity of the N-methyl cyclopeptide for divalent cations is likely a result of the carbonyl facing opposite sides of the ring.

Part II describes the design approach, major construction details, and the test and characterization procedures associated with the construction of a broadband multinuclear NMR spectrometer system. The design emphasis was on incorporating features that would be useful for biological experiments. Summaries of original designs are included with schematic documentation.

Melvin P. Klein

ACKNOWLEDGMENTS

It is nearly impossible to acknowledge the assistance of all the people who contributed to the completion of this work. I would particularly like to thank Prof. Melvin Calvin for his support, and for providing a unique educational opportunity. I am especially grateful to Dr. Melvin P. Klein for his wisdom, counsel, and guidance. I shall always respect him as a scientist, an educator, and as a friend.

Prof. Henry Rapoport and Dr. J. Clark Lagarias made major contributions to the cyclopeptide work, and Prof. F. Bordner kindly supplied the x-ray data on the N-methyl cyclopeptide. John Griffin, Ferenc Kovac, Dick O'Brien, Cees DeGroot, and Mike Press provided technical assistance; Sheldon Wong and Ken Wiley assisted in the VAX data transmission and contour plotting work.

Special thanks are due Gary Lee, for filling the liquid nitrogen and liquid helium on the magnets countless times, and for helping on innumerable other tasks. Karen Cornwell and Maria Fassett provided expert assistance in the nitrogenase isolation work; Ben Gordon and Wally Erwin assisted with GCs, plumbing, and many other problems. I thank Howard Wood for teaching me how to use machine tools, and for helping me salvage many projects.

Special thanks are due members of the Electronics Research and Development Group at the Lawrence Berkeley Laboratory, headed by Dr. Branko Leskovar. C.C. Lo and Eric Young provided much valuable advice (and the loan of much valuable test equipment), and I deeply appreciate their help. Thanks are also due Dr. J.D. Swalen for discussions on the iterative fit procedures, and for providing program tapes.

I am especially grateful to Dr. David Dalrymple of Nicolet Technology Corp. Even though we had a customer relationship, he displayed extraordinary patience during many hours on the phone.

I thank my friends around LCB -- Beth Klingel and Lois Soule in particular -- for helping me to maintain a sense of humor, and I particularly thank Craig Hodges and Mary McLean for many valuable consultations.

A special thanks is reserved for the people without whom this work would not have been completed. Gary Smith, in addition to being a good friend, taught me an approach to doing design work and troubleshooting. Without his guidance, the spectrometer system would not approach its current performance level.

I thank Janice DelMar for her friendship, understanding, and counsel. Her wisdom and guidance during many difficult times will always be remembered and appreciated. I thank Barbara Plowman for her friendship and understanding, and for her patience during the preparation of this work. Finally I thank my parents, who have stood by me from the start, hoping to see this day.

This work was supported, in part, by the Biomedical and Environmental Research Division of the U.S. Department of Energy under contract W-7405-eng-48.

TABLE OF CONTENTS

FIGURE LIST

LIST OF TABLES

I. Conformational Analysis of Cyclic Peptides

"Nothing will ever be attempted if all possible objections must first be overcome."

- Samuel Johnson

1.1 Introduction

The physical properties and biological activity of proteins is primarily dependent on levels of structure higher than just the primary amino acid sequence. The analysis of peptide backbone conformations therefore is an important route to the understanding of the three-dimensional arrangement of amino acids in proteins. In recent years, a great deal of attention has been focused on conformational studies of small cyclic polypeptides, both natural and synthetic. These substances, in addition to being interesting because of their own biological activity, have been used as models for larger proteins because of the simplified analysis that is possible.

Of the spectroscopic techniques that are applicable to conformational analysis, nuclear magnetic resonance (NMR) has found increasing use.[1-5] In part this is due to the wealth of information that is provided by the NMR spectrum, *i.e.* chemical shifts and spin-spin couplings. Proton NMR has been used for the majority of these studies, primarily because of the ease of acquiring and analyzing data. Proton spectral parameters which can provide the most information with regard to conformation are:

1. Vicinal coupling constants, which can be interpreted in terms of Karplus type relationships:[6,7]

$$^3J\ (\theta) = A \cos^2\theta + B \cos\theta + C \qquad (1)$$

where θ is the dihedral angle between the planes formed by $H\text{-}C_1\text{-}C_2$ and $C_1\text{-}C_2\text{-}H$, and $A = 4.22$, $B = -0.5$, $C = 4.5$.

Strictly speaking, (1) is only valid for saturated tetrahedral carbons. The presence of electronegative substituents alters this relationship; many groups have assumed that the general form of the equation is correct in such instances, and they have empirically added or modified constants. The simple relationship (1) is often restated in the form

$$^{3}J\ (\theta) = K_1 \cos^2\theta - 0.28 \qquad 0° \leq \theta \leq 90° \qquad (2)$$

$$^{3}J\ (\theta) = K_2 \cos^2\theta - 0.28 \qquad 90° \leq \theta \leq 180° \qquad (3)$$

with $K_1 = 8.5$ and $K_2 = 9.5$.

Another variation on (1) has been proposed for the dependence of $^{3}J_{NH\text{-}C^{\alpha}H}$ on dihedral angle:[8,9]

$$^{3}J_{NH\text{-}C^{\alpha}H} = A \cos^2\theta + B \cos\theta + C \sin^2\theta \qquad (4)$$

The values $A = 7.9$, $B = -1.55$, and $C = 1.35$ gave a reasonable fit for cyclic oligopeptides where both NMR and other types of structural data were available.

It is readily apparent that the application of coupling constant data to the analysis of bond angles and solution conformations depends on the use of good model systems for the evaluation of constants.

2. Chemical shift assignments, which are of more limited utility in systems of higher complexity because of the difficulty in making assignments. The advent of high field superconducting magnet spectrometers has helped to spread out

resonances, making this task easier. An important aspect of making assignments is that line positions together with coupling constant estimates make theoretical simulation of spectra possible.

3. Temperature dependence of NH chemical shifts -- in polar protic solvents, amide protons that are intramolecularly hydrogen bonded tend to experience less of an upfield shift than amide protons that are exposed to the solvent.

4. *Cis-trans* peptide bond isomerism -- the planer nature of the peptide bond, owing to resonance stabilization

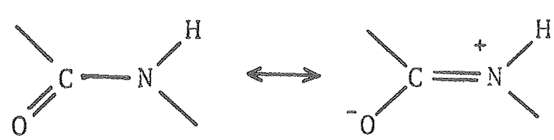

(5)

means that *cis* and *trans* peptide bond configurations are possible. NMR can often reveal the presence of both forms due to the generally high barrier to internal rotation.

Natural abundance ^{13}C NMR has also come into wider use for solution spectra of small polypeptides. The principal advantage is the greater range of chemical shifts (> 200 PPM) due to the increased sensitivity of shifts to the local environment. Most ^{13}C work has employed broadband decoupling of the coupled protons to improve the signal to noise, as a result, ^{13}C-^{1}H J couplings have not been revealed. The low natural abundance (1.1%) of ^{13}C implies that ^{13}C-^{13}C couplings are not generally seen. The primary utility of ^{13}C NMR has been looking at chemical shift variation resulting from conformational effects.

In the text that follows, a different approach to conformational analysis using ^{1}H NMR will be delineated. One of the great difficulties in using ^{1}H NMR for conformational studies has been the extraction of chemical shift and coupling information, because of the multitude of lines and the incidence of non-first-order coupled systems. The approach that has been taken employs the acquisition of two-dimensional NMR J spectra and the generation of suitable projections to extract shifts and couplings, followed by computer simulation of spin subsystems to generate accurate coupling constants for bond angle calculations.

1.2 Two-Dimensional J-Resolved Spectroscopy

In most NMR experiments, the relative intensities of the observed lines are subject to a variety of external influences. Observed intensities may show a time dependence due to relaxation processes, or observed linewidths (and relaxation rates) may show variation with field strength or other parameters. In such instances, the logical extension for the presentation of spectral data has been the utilization of a second dimension to represent this other functional dependence.

The idea of applying a two-dimensional Fourier transform to experiments where the external variable is time was first suggested by Jeener in 1971.[10] Since that time, an increasing volume of work has appeared, along with several reviews.[11-16] The concept is quite simple; normal one-dimensional spectra are acquired as a time domain decay of a transient free precession signal, which may be called $S(t_2)$ where t_2 is the time variable associated with the data acquisition process. Fourier transformation of this signal yields the normal frequency domain spectrum, $S(f_2)$. The appearance of $S(f_2)$, however, depends on the behavior of the nuclear magnetization prior to time $t_2 = 0$. If as a result of some pulse sequence, the nuclear spins execute some motion during this time (called the evolution time t_1), this history will be reflected in the relative phases and amplitudes of the components of $S(t_2)$. The systematic variation of the evolution time t_1 over an appropriate range will then yield a signal matrix $S(t_1,t_2)$ which upon double Fourier transformation yields a two-dimensional spectrum $S(f_1,f_2)$ in two orthogonal frequency dimensions that correlates the behavior of spins during the evolution time t_1 to their behavior during detection

(t_2).

The purpose of acquiring data in two dimensions is to try to spread out complex spectra that are not amenable to analysis in the conventional fashion. The feature of 2-D that makes this possible is that it is often possible to restrict different nuclear parameters to distinct dimensions. This separation is exemplified by the case of echo modulation by scaler coupling that was first described by Hahn and Maxwell in the basic $90°$-τ-$180°$-τ spin-echo experiment (Figure 1.1).[17] For a coupled homonuclear spin system, the 180° pulse produces a refocusing of magnetization components that are dephased by chemical shift and field inhomogeneity effects, but the J splitting is not refocused because the 180° pulse also interchanges the spin state labels of the multiplet components. This is conveniently illustrated by the phase-time diagram for a coupled two-spin system IS of Figure 1.2 (after Freeman).[15] The phase shift of the two vectors representing the I spins in the rotating frame are shown as a function of time during the defocusing and refocusing intervals. If the 180° pulse is applied only to the I spins (top), the signs of the accumulated phase errors are changed, resulting in reconvergence at the end of the refocusing interval with zero phase error. If on the other hand the 180° pulse is simultaneously applied to the S spins (bottom), the two vectors are also interchanged. At the end of the refocusing period, the accumulated phase errors are $\pm 1/2\ J_{IS}t_1$.

The J-resolved two-dimensional experiment may be summarized by Figure 1.3. There is an evolution period of length t_1 followed by a detection period with running time variable t_2. During these two times, different effective Hamiltonians apply. During t_2, the

Figure 1.1 $90°$-τ-$180°$-τ Spin-Echo Experiment

CARR-PURCELL SPIN ECHO SEQUENCE

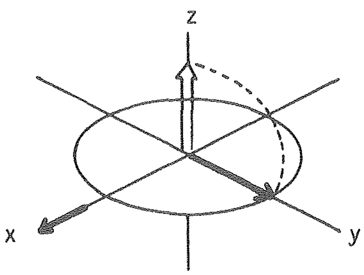

1. 90° PULSE ALONG X AT TIME 0

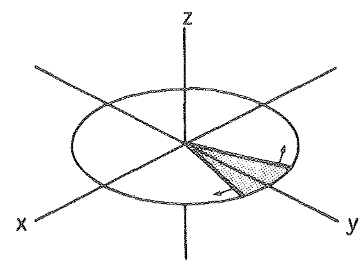

2. MACROSCOPIC MAGNETIZATIONS DEPHASE

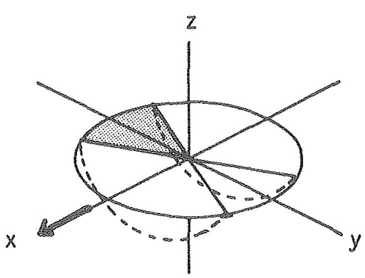

3. 180° PULSE ALONG X AT TIME τ

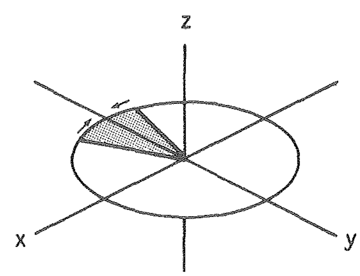

4. REPHASING

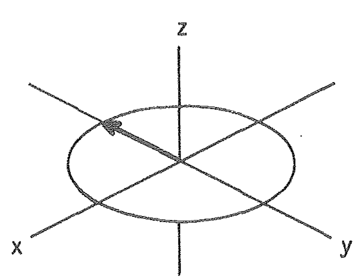

5. ECHO AT TIME 2τ

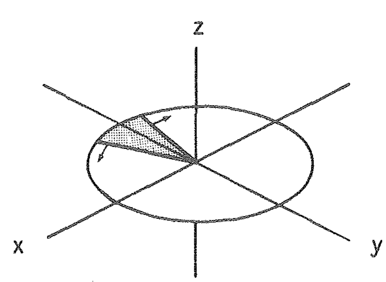

6. DEPHASING

XBL 7910-12482

Hamiltonian is just that for a spin system under high resolution conditions:

$$\mathcal{H}^{(2)} = \sum_i h\gamma_i(1 - \sigma_i)\, H\cdot \mathrm{I}_i + \sum_{i<j}\sum J_{ij}\mathrm{I}_i\cdot \mathrm{I}_j \tag{6}$$

which consists of chemical shielding terms and spin-spin coupling terms. During the evolution period t_1, chemical shift effects are eliminated by the refocusing process, so the effective Hamiltonian is only the spin-spin coupling term:

$$\mathcal{H}^{(1)} = \sum_{i<j}\sum J_{ij}\mathrm{I}_i\cdot \mathrm{I}_j \tag{7}$$

Thus the f_1 dimension of the transformation should reflect only spin coupling effects, while the f_2 dimension should show both spin couplings and chemical shift effects.

Figure 1.2 Phase-Time Diagram for a Coupled Two-spin System, IS

Top: The two components of the I spin multiplet are exactly refocused at the end of the evolution period.

Lower: The 180° pulse applied to the S spins leads to phase modulation at the end of the evolution period.

Figure 1.3 J-Resolved Two-dimensional Experiment

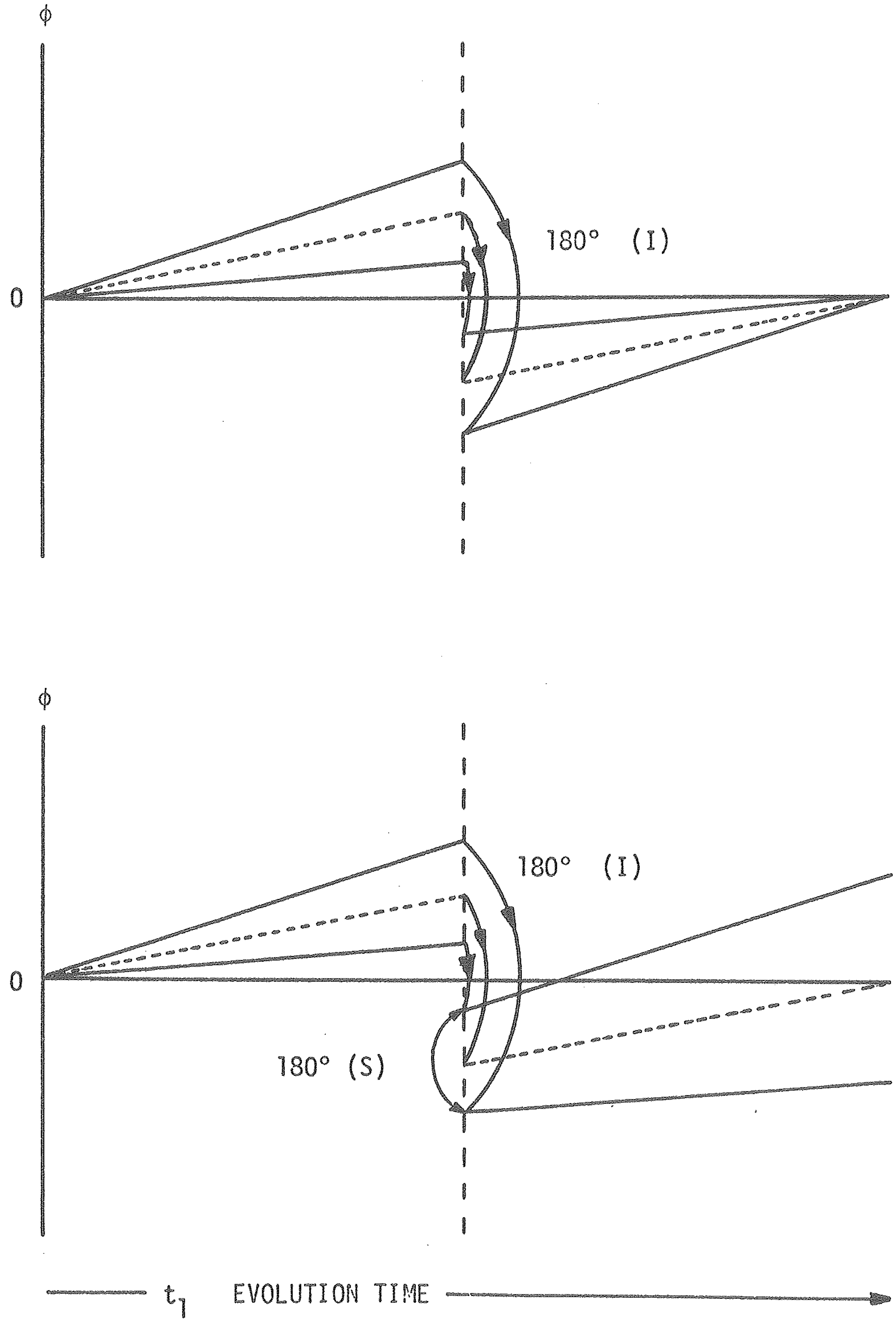
ϕ
0
180° (I)
ϕ
0
180° (I)
180° (S)
t_1 EVOLUTION TIME

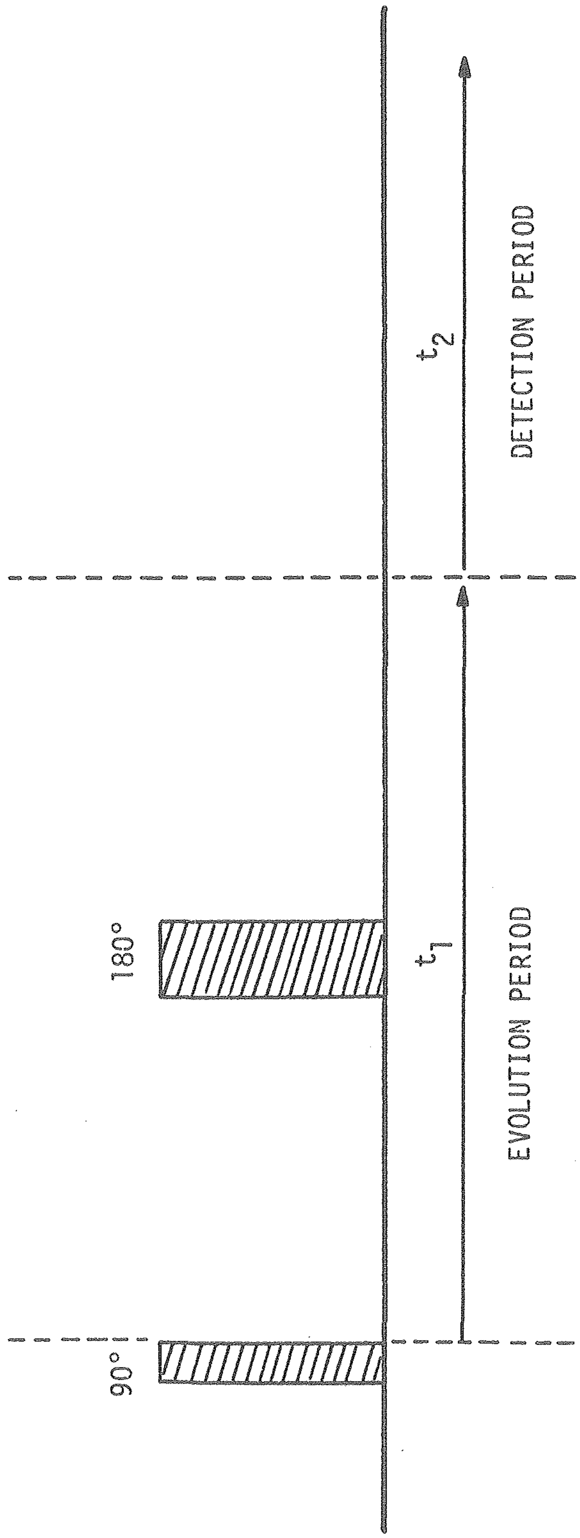

90°
180°
t_1
t_2
EVOLUTION PERIOD
DETECTION PERIOD

1.3 Cyclopeptide Alkaloids

A. Occurrrence, Structure, Model Systems

The term *peptide alkaloids*, first suggested by Goutarel, et al,[18] has been used to describe a large class of polyamide plant bases that are particularly common in plants of the Rhamnaceae family.[19] These compounds often represent *ca.* 0.02 to 0.9% of the dry weight of the plant, and they are usually distributed throughout the plant although often they are more abundant in the root bark and seeds. Isolation procedures produce complex alkaloidal mixtures, the composition of which may depend on the relative maturity and the region of growth of the plant.

Most peptide alkaloids that have been isolated are cyclic, and it has been suggested that the term *cyclopeptide alkaloids* is a more apt description of the class.[20]

The largest group of these compounds are based on 14 membered rings; they are characterized by a β-hydroxyamino acid unit, and an aryl ether linkage to a *p*-hydroxystyrlamine unit. The β-hydroxyamino acid may be β-hydroxyleucine (as in frangulanine, **1**), β-hydroxyphenylalanine (as in integerrine, **2**), *trans*-3-hydroxyproline (amphibine-B type, **3**), β-hydroxyisoleucine (*e.g.* ceanothine-B, **4**), among the more prevalent types. Functionalization of the benzyllic position may also vary (**5**).

NMR has been one of the important techniques used for the structure elucidation work on the cyclopeptides. Its use has been far more limited, though, in the analysis of solution conformations

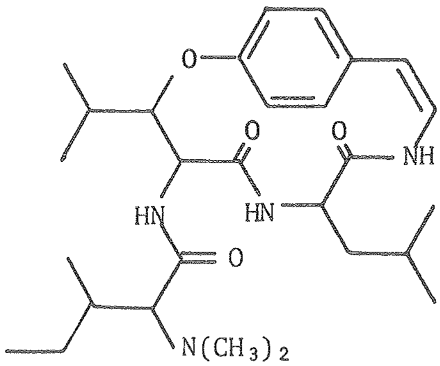

1

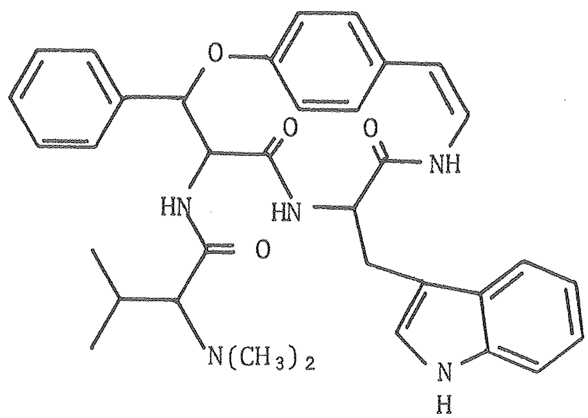

2

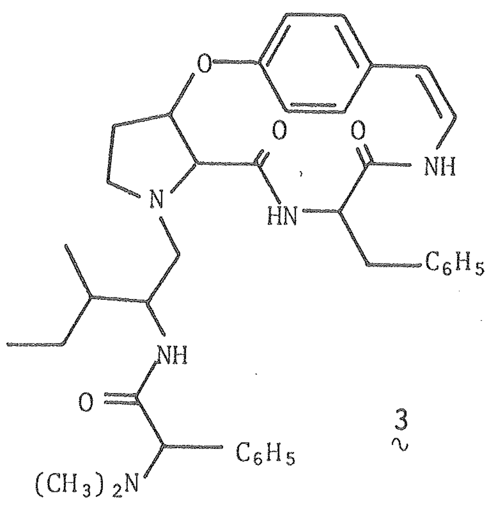

3

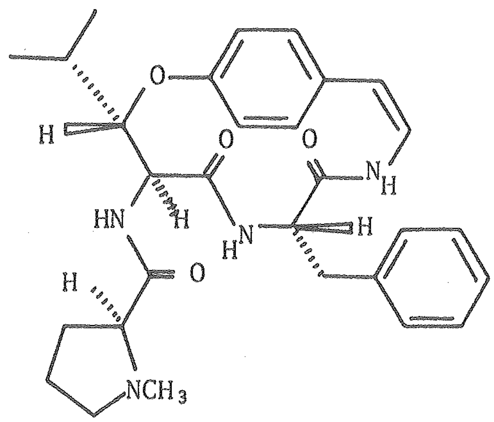

4

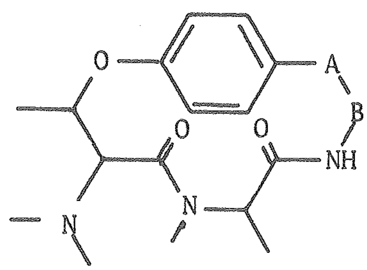

A—B = CH=CH
$CO\text{-}CH_3$
$CH(OH)CH_2$

5

and conformational changes in these compounds. The latter question is of interest because of the suggestion that cyclopeptides may function as ionophores in plants,[22,23] and that they undergo metal induced conformational changes.[24]

The analysis of metal induced conformational changes in cyclopeptide alkaloids has been addressed via the study of models for the natural products: *cyclo*-[3-(4-β-N-methylaminoethyl)phenyloxypropanoyl-L-prolyl], 6a, *cyclo*-[3-(4-β-aminoethyl)phenyloxypropanoyl-L-prolyl], 6b, and *cyclo*-[3-(4-β-aminoethyl)phenyloxy-4-methylpentanoyl-L-prolyl], 6c. These compounds differ from the ring backbone of most of the natural products in the saturated C_1-C_2 linkage (which results in fewer conformational possibilities) and the substitution of an L-proline residue for the β-hydroxy-α-amino acid residue (which eliminates the need to separate diastereomers during synthesis). All three compounds were prepared via high dilution active ester cyclizations from the *p*-nitrophenyl esters of the corresponding *tert*-butoxycarbonyl protected L-prolyl-(4-β-aminoethyl)phenyloxypropanoates.[22] The N-*tert*-butoxycarbonyl group was removed by dissolving in anhydrous trifluoroacetic acid; the resulting amine salt was dissolved in N,N-dimethylacetamide and added slowly to pyridine maintained at 90° C, giving cyclic monomers (*ca.* 25%) contaminated by cyclic dimers and oligomers. Pure cyclopeptide monomers were isolated by chromatography, then sublimed prior to NMR experiments.

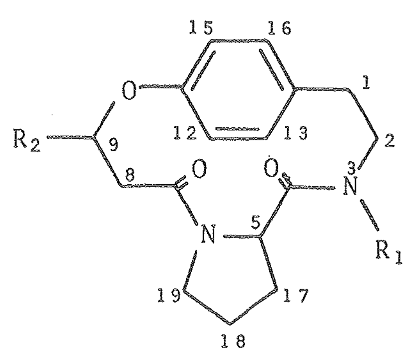

6a: $R_1 = CH_3$, $R_2 = H$
6b: $R_1 = H$, $R_2 = H$
6c: $R_1 = H$, $R_2 = CH(CH_3)_2$

B. Metal Binding Properties

Circular dichroism (CD) studies of metal binding by certain natural and synthetic polypeptides have shown that in aprotic solvents like acetonitrile, large shifts in the dichroic absorption are observable upon the addition of certain metals.[24,25] The natural cyclopeptide alkaloid Ceanothine-B[26] exhibits such behavior; Figure 1.4 shows the change in the near UV region (aromatic) observed upon the addition of Ca^{2+} or Mg^{2+}. No change was observed upon addition of Na^+ however.

The CD spectra of the two principal models, the N-methyl cyclopeptide **6a**, and the N-H cyclopeptide **6b**, are shown in Figures 1.5 and 1.6 (near and far UV regions). The metal binding properties of the N-H case **6b** have been reported;[22] the observed shift in dichroic absorption and metal selectivity mimicked the natural product surprisingly well (Figure 1.7).

The metal binding properties of the N-H cyclopeptide **6b** were consistent with a conformation in which both carbonyl groups were directed towards the same face of the ring. The inability to crystallize the compound, however, made it impossible to obtain an x-ray crystal structure. An x-ray crystal structure was obtained for the N-methyl cyclopeptide **6a**, though, and it showed the carbonyl groups at C_4 and C_7 pointing towards opposite sides of the ring (Figure 1.8).

Infrared absorption spectra of **6a** and **6b** indicated that the two rings might have quite different conformations. The N-methyl case shows a single amide carbonyl stretch at 1630 cm^{-1}, which is consistent with a *trans* configuration of both amide bonds as shown by the x-ray.

The N-H case **6b** on the other hand shows two amide carbonyl absorptions, one at 1675 cm^{-1} and the other at 1615 cm^{-1}. A lower frequency amide absorption is characteristic of a *cis* amide bond, thus the infrared data suggests one *cis* and one *trans* linkage.

Cumulatively, this data suggested that ring conformation might be a key factor in the metal binding properties of the cyclopeptide model systems. If it was necessary for both carbonyls to be on the same side of the ring to participate in metal complexation, the N-methyl cyclopeptide would likely exhibit vastly different or perhaps no metal affinity. Before testing this hypothesis on the small sample of **6a** that had been prepared, a series of NMR experiments was performed to see if detailed solution conformation data could be obtained. If the solution conformations of **6a** and **6b** could be ascertained by NMR, an approach that is very complementary to x-ray crystallography could be demonstrated for small polypeptides.

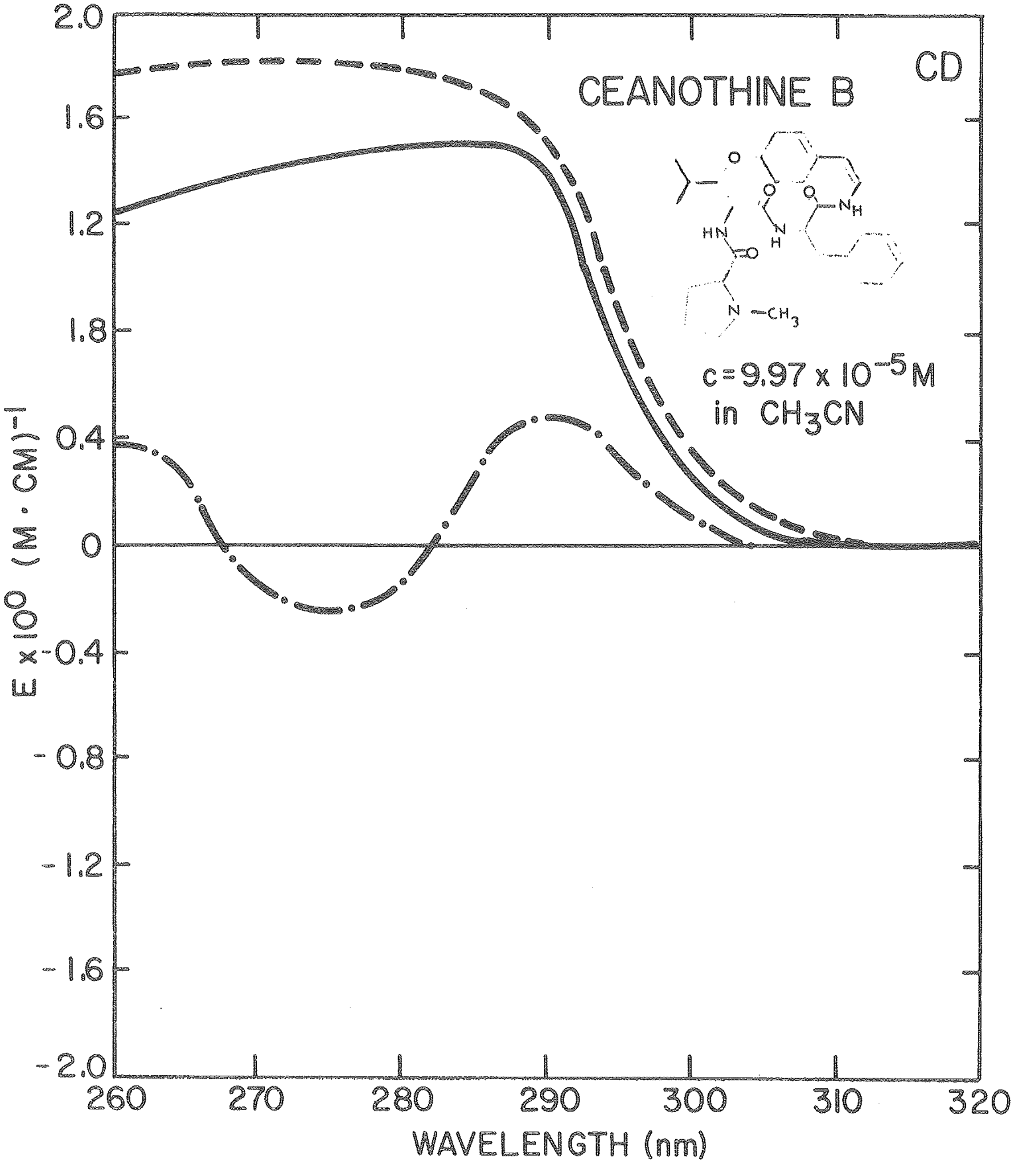

No salt

Sodium perchlorate 1.10 x 10^{-3}M

Magnesium perchlorate 9.21 x 10^{-4}M

Calcium perchlorate 1.45 x 10^{-3}M

XBL 7710-4693

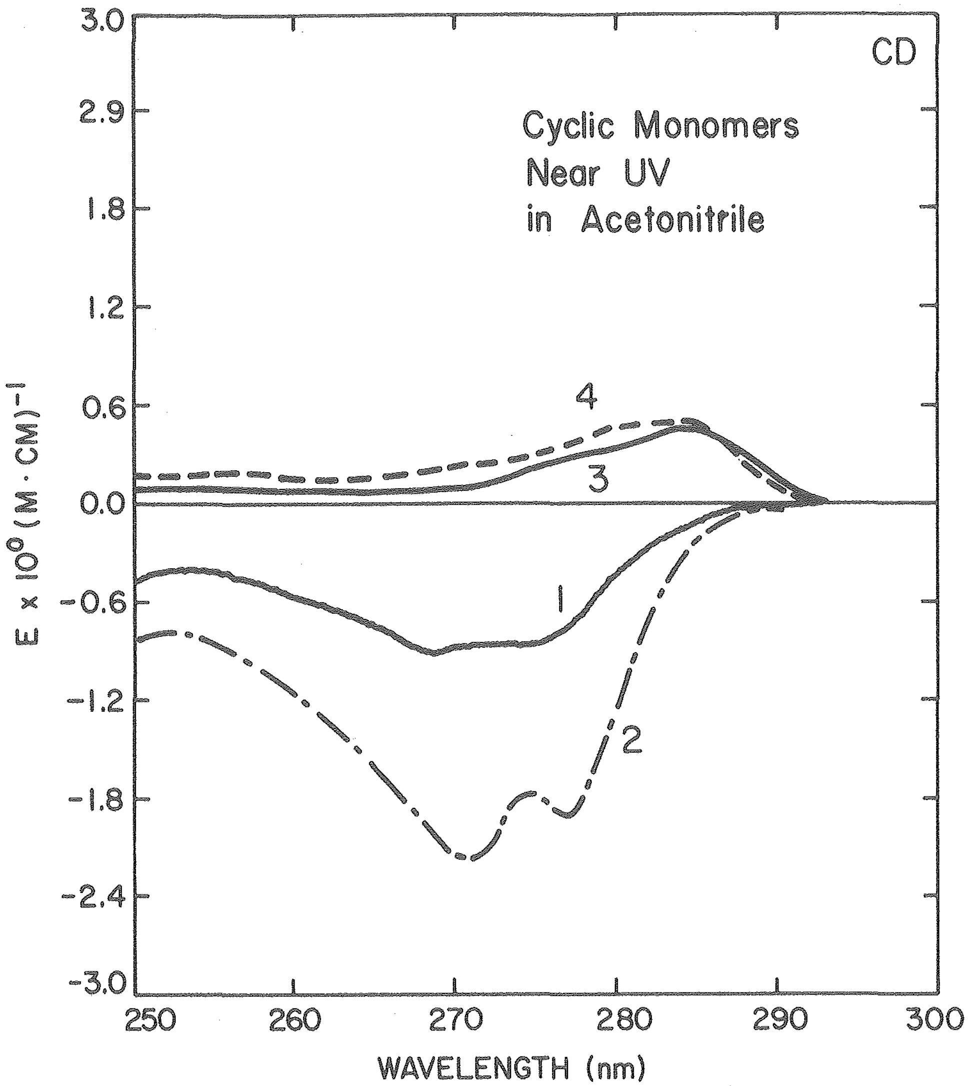

(1) Cyclo[3-(4-β-N-methylaminoethylphenoxy) propanoyl L-prolyl] (c = 1.33×10^{-3}M)

(2) Cyclo[3-(4-β-aminoethylphenoxy) propanoyl L-prolyl] (c = 1.31×10^{-3}M)

(3) Cyclo[3-(4-β-N-methylaminoethylphenoxy) propanoyl L-leucyl] (c = 1.47×10^{-3}M)

(4) Cyclo[3-4-β-aminoethyl phenoxy) propanoyl L-leucyl] (c = 1.09×10^{-3}M)

XBL 7710-4686

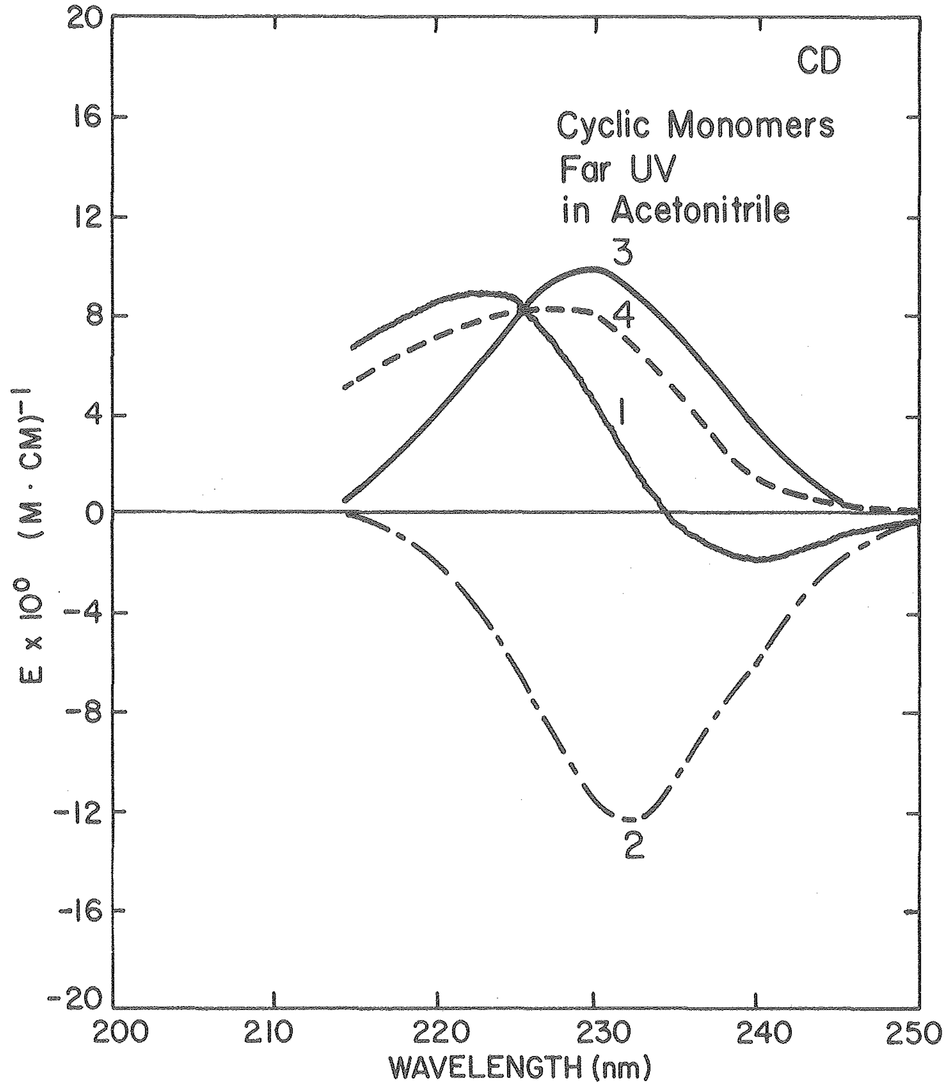

(——1——) Cyclo[3-(4-β-N-methylaminoethylphenoxy) propanoyl L-prolyl] (c = 1.75×10^{-4}M)

(—.2—.—) Cyclo[3-(4-β-aminoethylphenoxy) propanoyl L-prolyl] (c = 1.31×10^{-4}M)

(——3——) Cyclo[3-(4-β-N-methylaminoethylphenoxy) propanoyl L-leucyl] (c = 1.55×10^{-4}M)

(– –4– –) Cyclo[3-4-β-aminoethyl phenoxy) propanoyl L-leucyl] (c = 6.68×10^{-5}M)

XBL 7710-4689

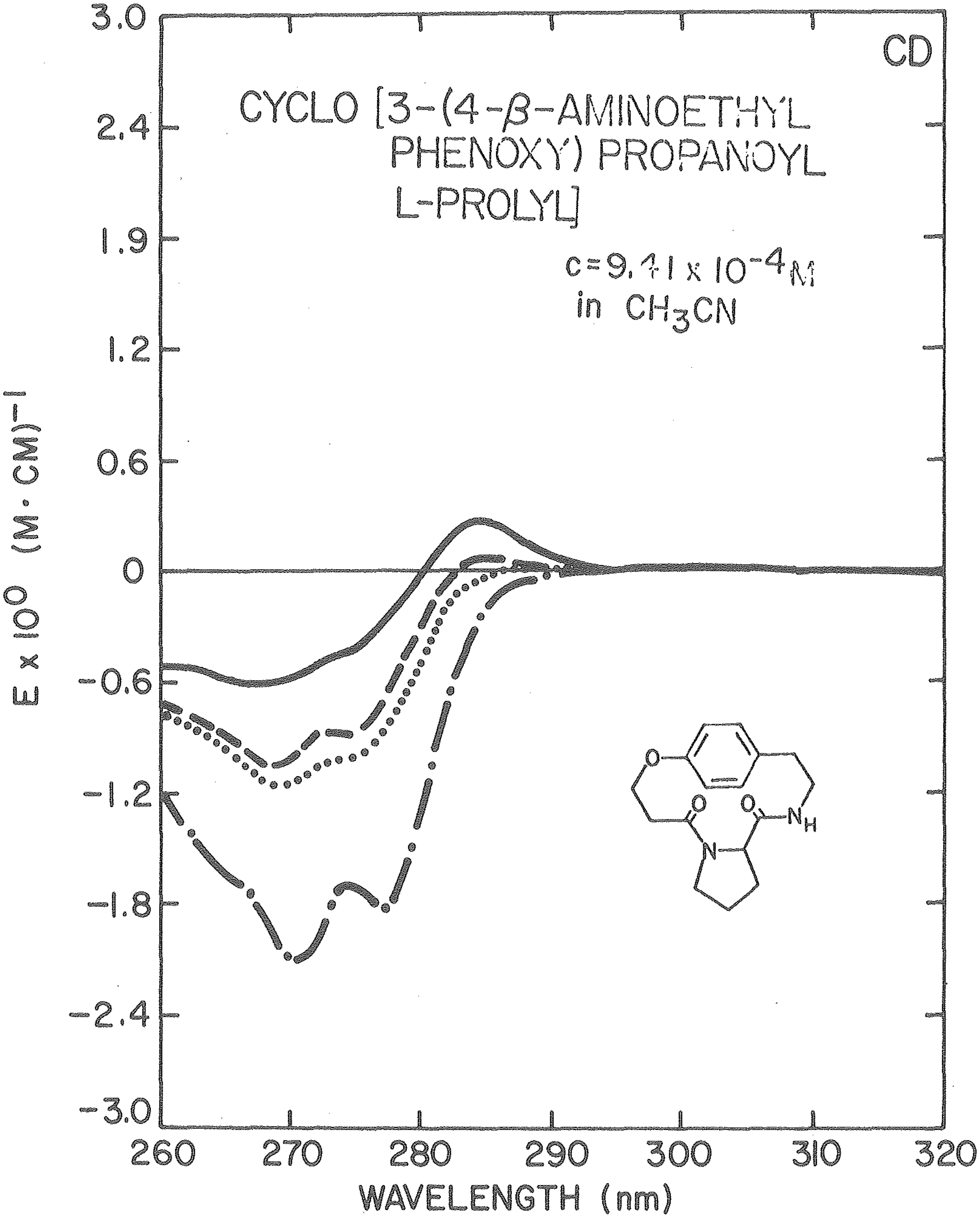

No salt
Sodium perchlorate 9.45 x 10^{-3}M
Potassium hexafluorophosphate 8.61 x 10^{-3}M
Lithium perchlorate 8.33 x 10^{-3}M
Magnesium perchlorate 9.17 x 10^{-4}M
Calcium perchlorate 1.45 x 10^{-3}M

XBL 7710-4692

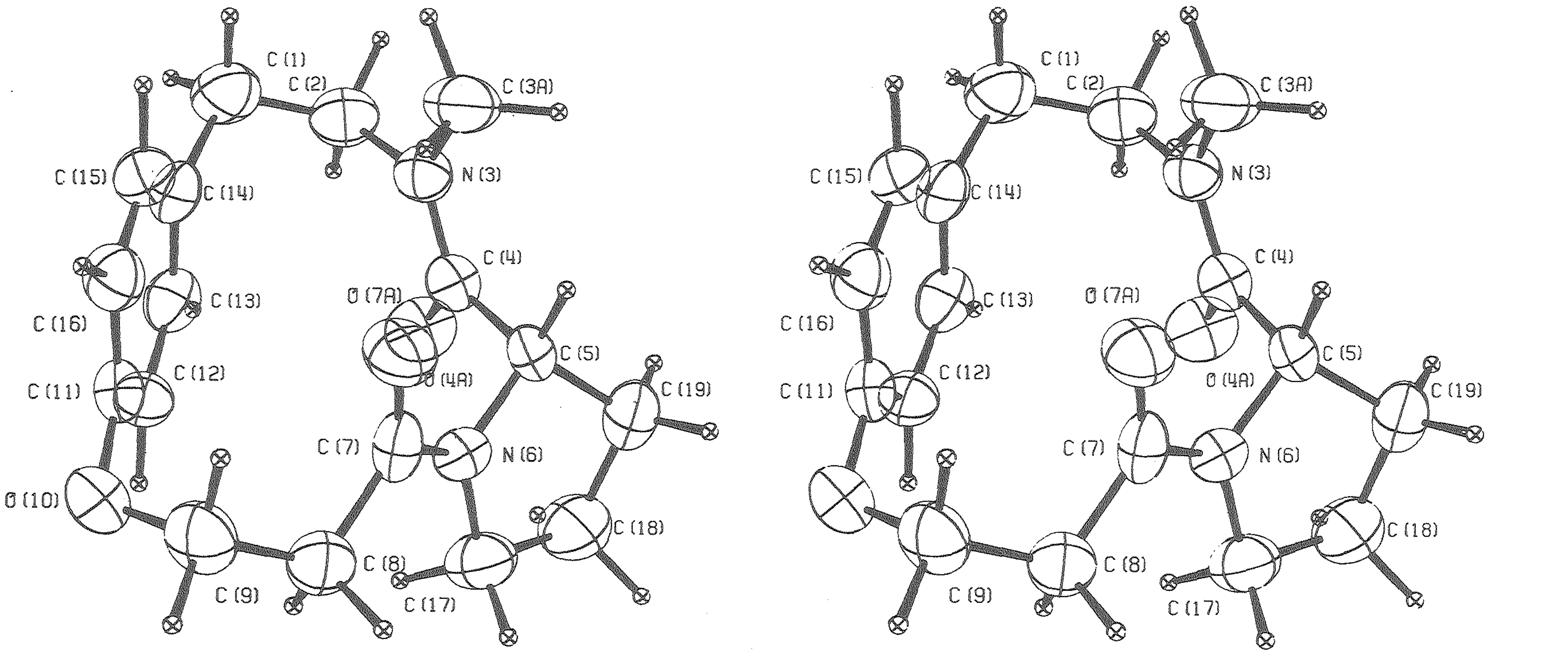

XBL 799-11732

1.4 NMR Spectral Data for Cyclopeptide Alkaloid Model Compounds

A. Assignment of Lines

The 270 MHz ^1H NMR spectra of the cyclopeptides 6a and 6b in $CDCl_3$ (Figures 1.9 and 1.10 respectively) show perhaps not surprising patterns of complex overlapping multiplets. The only lines that were readily assigned were the aromatic C_{12}-C_{13}-C_{15}-C_{16} four spin multiplet in both cases, and the N-methyl group of 6a (2.95 δ, Figure 1.9).

The traditional approach to making assignments involves exhaustive homonuclear decoupling experiments. The time-consuming part of this task is determing the exact H_2 irradiation frequency in complex regions such as 2.7 - 3.1 δ of the N-H case (6b, Figure 1.10) where integration indicates the presence of four lines. When lines are this closely spaced, the careful application of the correct level of decoupler power is also required. Too high a power level would lead to the collapse of multiplets coupled to adjacent lines, making assignments very difficult. Thus both exact frequency information and a proper decoupling power level are important.

The two-dimensional J-spectra technique described in Section 1.2 was used to make the assignment procedure very simple. Two-dimensional homonuclear J-spectra were acquired with f_1 (J) frequency ranges of ± 25 Hz and f_2 frequency ranges spanning the normal spectral region. The 2-D spectrum of the N-methyl case 6a is shown along with the normal spectrum in Figure 1.11, and the N-H case 6b is similarly shown in Figure 1.12. It may be seen that the complex multiplets of the normal one-dimensional spectra (lower) are effectively rotated by 45° into the

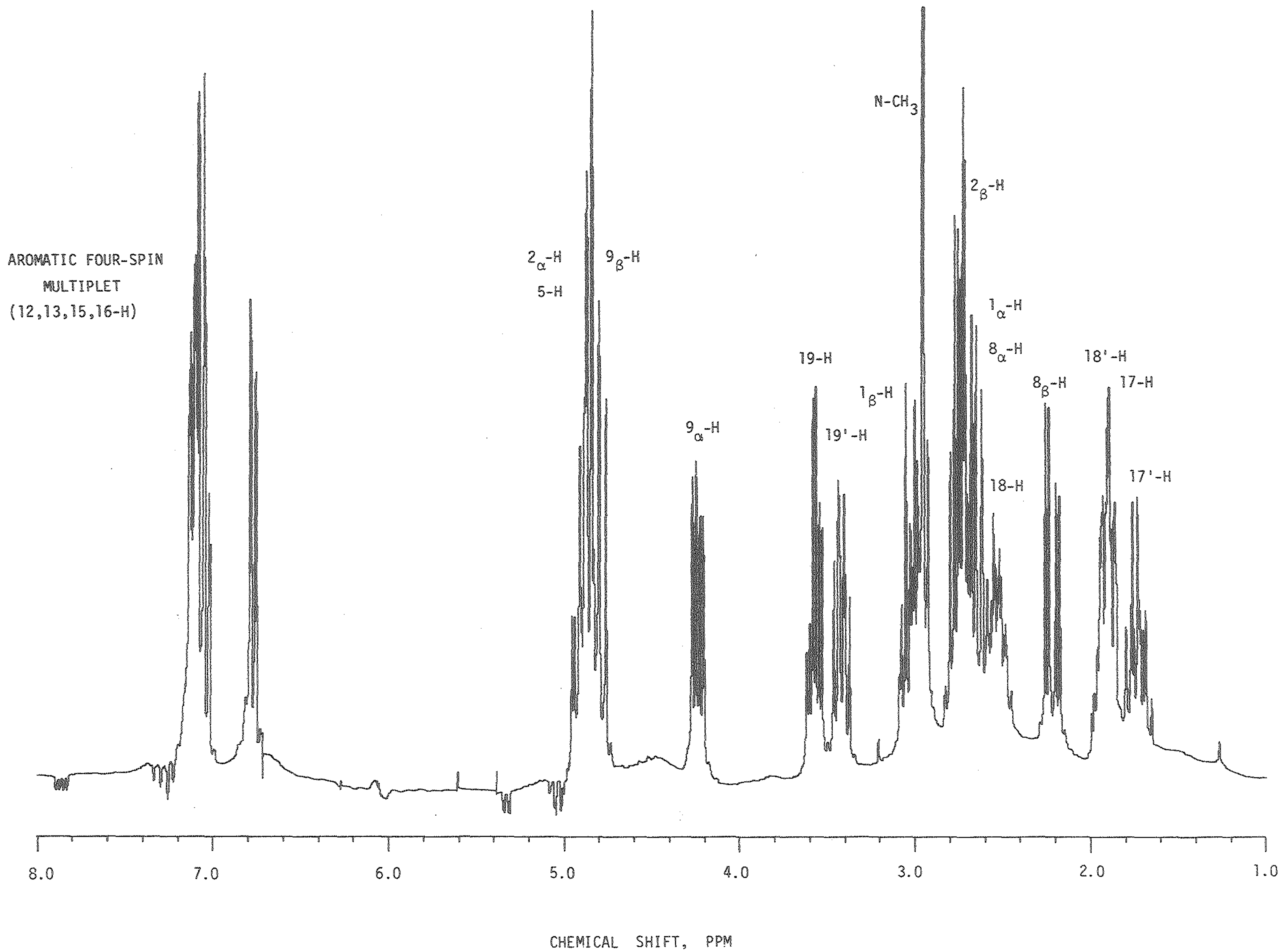

XBL 7910-12515

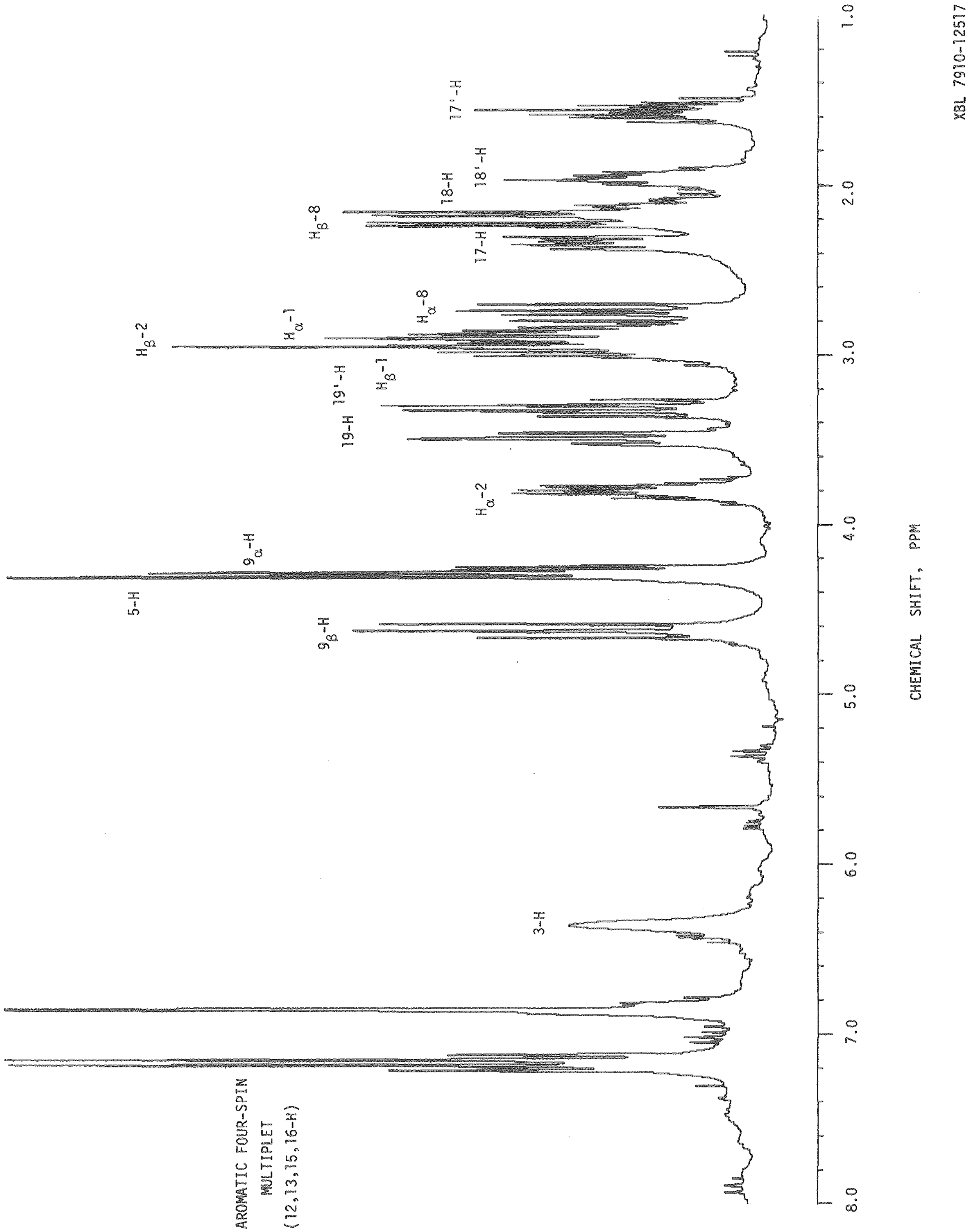
AROMATIC FOUR-SPIN
MULTIPLET
(12,13,15,16-H)
3-H
5-H
9_β-H
9_α-H
H_α-2
19-H
19'-H
H_β-1
H_β-2
H_α-1
H_α-8
H_β-8
17-H
18-H
18'-H
17'-H
8.0
7.0
6.0
5.0
4.0
3.0
2.0
1.0
CHEMICAL SHIFT, PPM
XBL 7910-12517

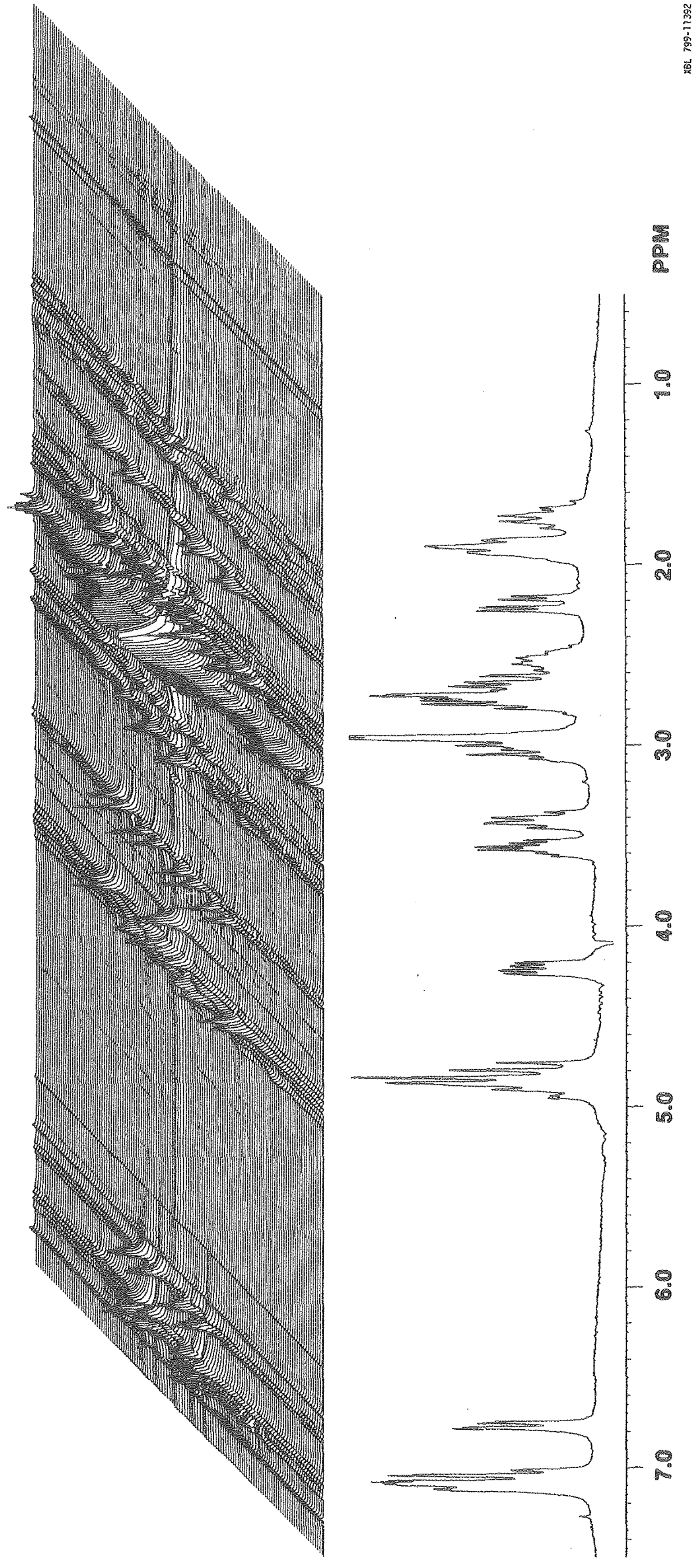
7.0
6.0
5.0
4.0
3.0
2.0
1.0
PPM
XBL 799-11392

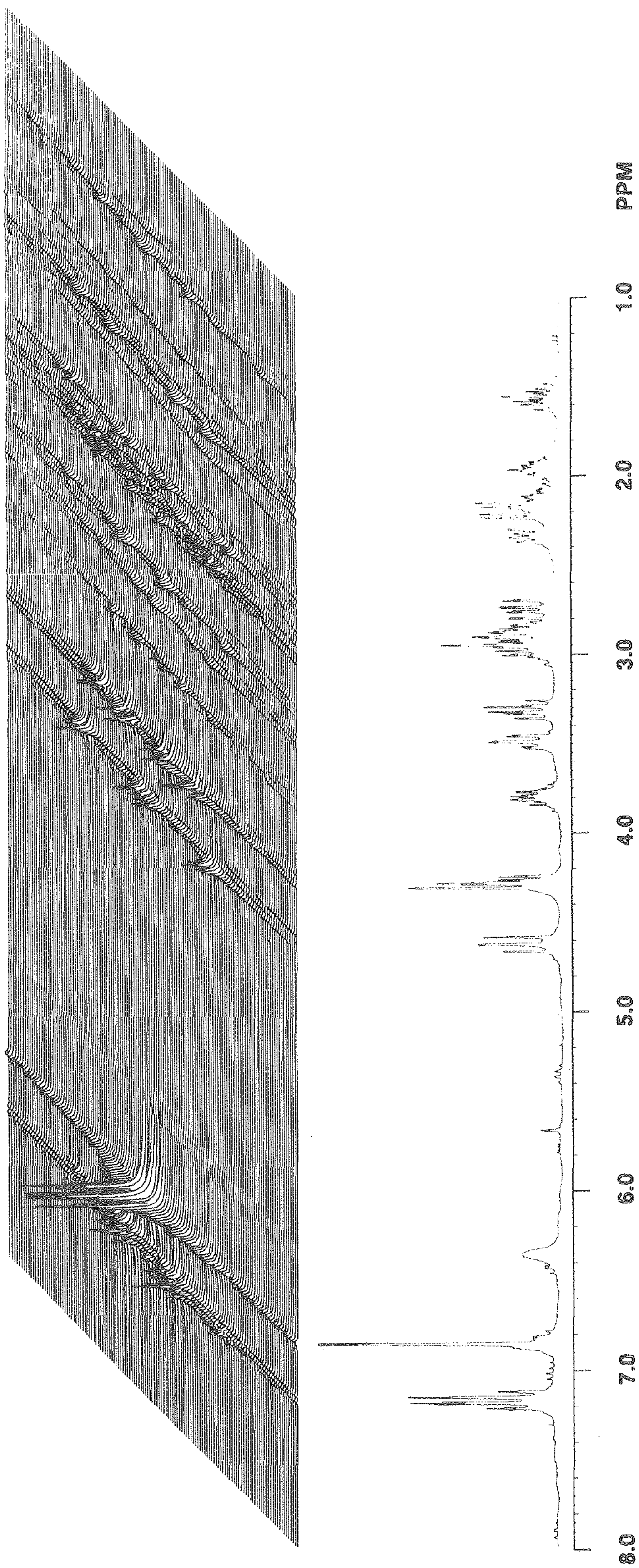

XBL 799-11852

two-dimensional frequency plane. It is also evident that line widths in the f_1 (J) dimension are narrower because the refocusing process eliminates the line broadening effect of field inhomogeneities.

Even when the 2-D spectra of Figures 1.11 and 1.12 are plotted on greatly enlarged scales, there is a great deal of complexity which is difficult to interpret. Nagayama, et al, have described the utility of cross-sections and projections in the presentation of 2-D data.[27] Two visualization schemes were used to aid in the interpretation of the 2-Ds; they are best illustrated with the enlarged 2-D of the 2.6 - 3.1 δ region of the N-H cyclopeptide **6b** (Figure 1.12). Figure 1.13 shows this enlargement with a corresponding 0° projection, and Figure 1.14 shows a contour map of exactly the same area. The doublet of doublets of doublets centered at 2.747 ppm is strikingly clear in both, but visualization of the complex non-first-order pattern at 2.82 - 3.03 δ is made much easier by the contour plot. Contour plots of the other spectral regions of **6a** and **6b** are shown in Figures 1.15 - 1.32. With the aid of these contour plots, a number of tentative assignments could be made (*e.g.* doublets of doublets of doublets were identified as being parts of particular four-spin patterns, based on the size of the couplings).

The full assignment of all lines in both spectra was completed with a series of homonuclear decoupling experiments that made use of the 2-D 45° projections. It has been pointed out that coupled multiplets are effectively rotated 45° into the 2-D frequency plane, thus coupled lines always appear on a 45° diagonal (frequency).[28] A 45° projection of a 2-D plot will align coupled multiplets as single lines, yielding what has been termed a proton decoupled proton spectrum.[29] 45° and 0°

projection sums of the cyclopeptide 2-D spectra (Figures 1.11 and 1.12) are shown in Figures 1.33 - 1.36, plotted above the respective normal spectra. The simplification that is seen in the proton decoupled proton spectra is quite dramatic; although intensity information is misleading, the collapse of all multiplets into single lines makes the selection of decoupling frequencies simple. Homonuclear decoupling experiments using the irradiation frequencies obtained in this manner led to the rapid, direct assignment of all lines in both normal spectra (6a and 6b). The tentative assignments are shown in Figures 1.9 and 1.10; line frequencies and relative intensities are tabulated in Tables 1.1 and 1.2.

B. Comparison of Assignments

1. Aromatic Four-Spin Multiplet

Although the four-spin patterns exhibited by the C_{12}-C_{13}-C_{15}-C_{16} aromatic protons would not be expected to change very much in going from the N-methyl cyclopeptide to the N-H case, they appear to be quite different (Figures 1.9 and 1.10). The reason for the difference is revealed by the 45° projections (Figures 1.33 and 1.35). The N-methyl case 6a has three protons that are closely spaced (7.0-7.2 δ) and a single different proton at higher field (6.85 δ), while the N-H case 6b has two protons at $\sim$ 7.2 δ and two at 6.85 δ. This is a rather striking change to result from simply adding a methyl group some distance away.

2. Proline Seven-Spin Systems

The proline C_5-C_{17}-C_{17}'-C_{18}-C_{18}'-C_{19}-C_{19}' seven-spin systems were assigned with the aid of published data on the *cyclo*-tri-L-prolyl system.[30] The two C_{19} protons were virtually identical in the N-H and N-methyl cases, but slight differences in chemical shift are noticeable for one of the C_{18} protons, and fairly pronounced differences are seen for the C_{17} and C_5 protons. Examination of models reveals that changes in these shifts are consistent with a reorientation of the C_4 carbonyl. A summary of differences is tabulated in Table 1.3

3. C_8 - C_9 Four-Spin System

The C_8-C_8'-C_9-C_9' four-spin patterns should be important indicators of ring conformation, as twisting about the C_8-C_9 axis should be reflected in changes in the vicinal coupling constants. Examination of these four-spin patterns shows minimal differences in the chemical shifts of the lines, but the line patterns are different -- reflecting changes in the coupling constants.

4. C_1 - C_2 Four-Spin System

As in the case of the C_8-C_9 four-spin system, the C_8-C_8'-C_9-C_9' four-spin pattern would be expected to reflect rotation about the C_1-C_2 bond axis. Examination of models reveals that inversion of the C_4 carbonyl should markedly change the C_1-C_2 proton dihedral angles and hence the vicinal coupling constants.

One of the C_2 protons moves upfield by 220 Hz in going from the

N-methyl case **6a** to the N-H cyclopeptide **6b**; otherwise the main difference is in the appearance of the multiplets. Analysis of this region is made difficult by the overlap with lines from other spin systems, and the closeness of the chemical shifts of the two C_1 and one C_2 protons, resulting in highly non-first-order patterns.

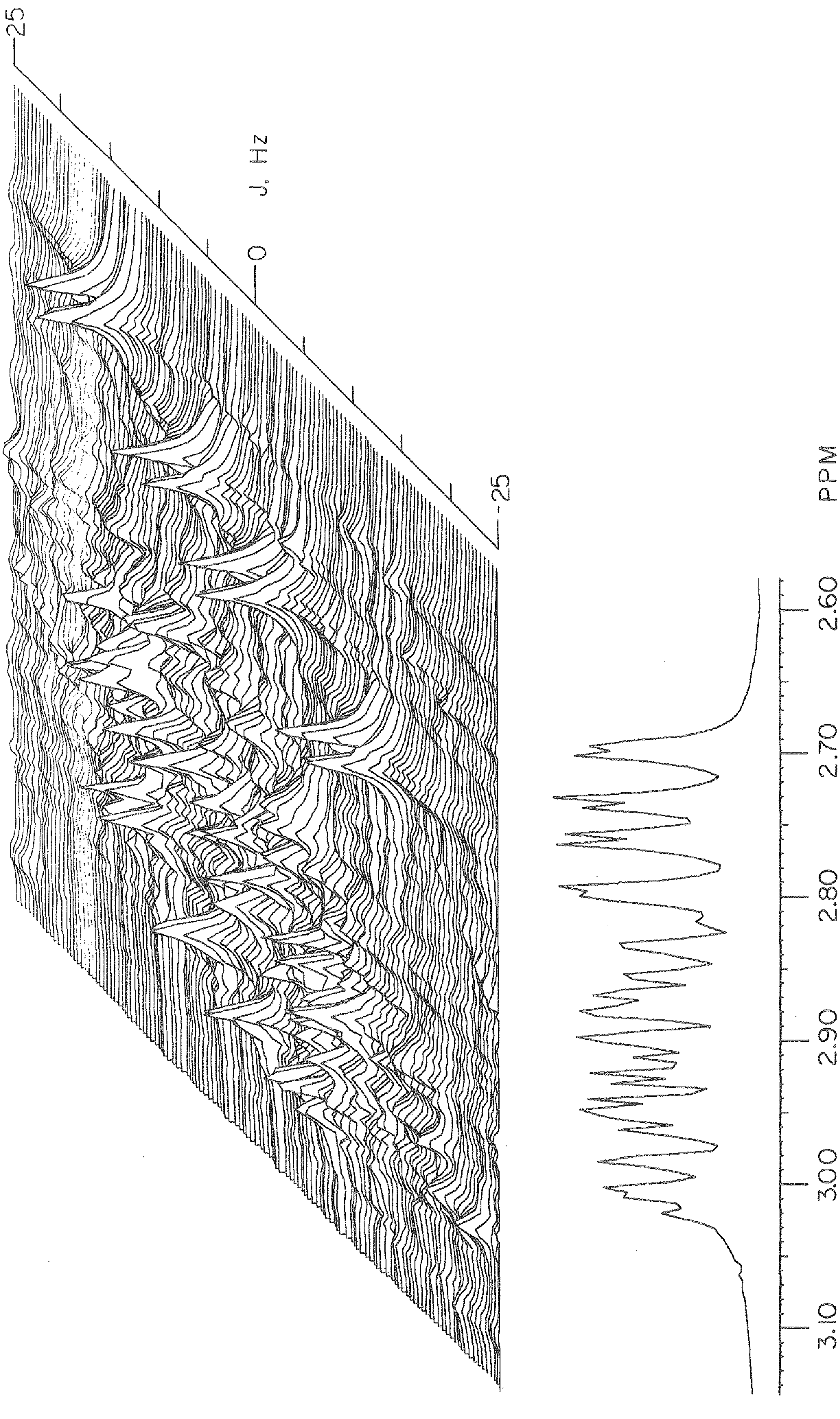

XBL 799-11391

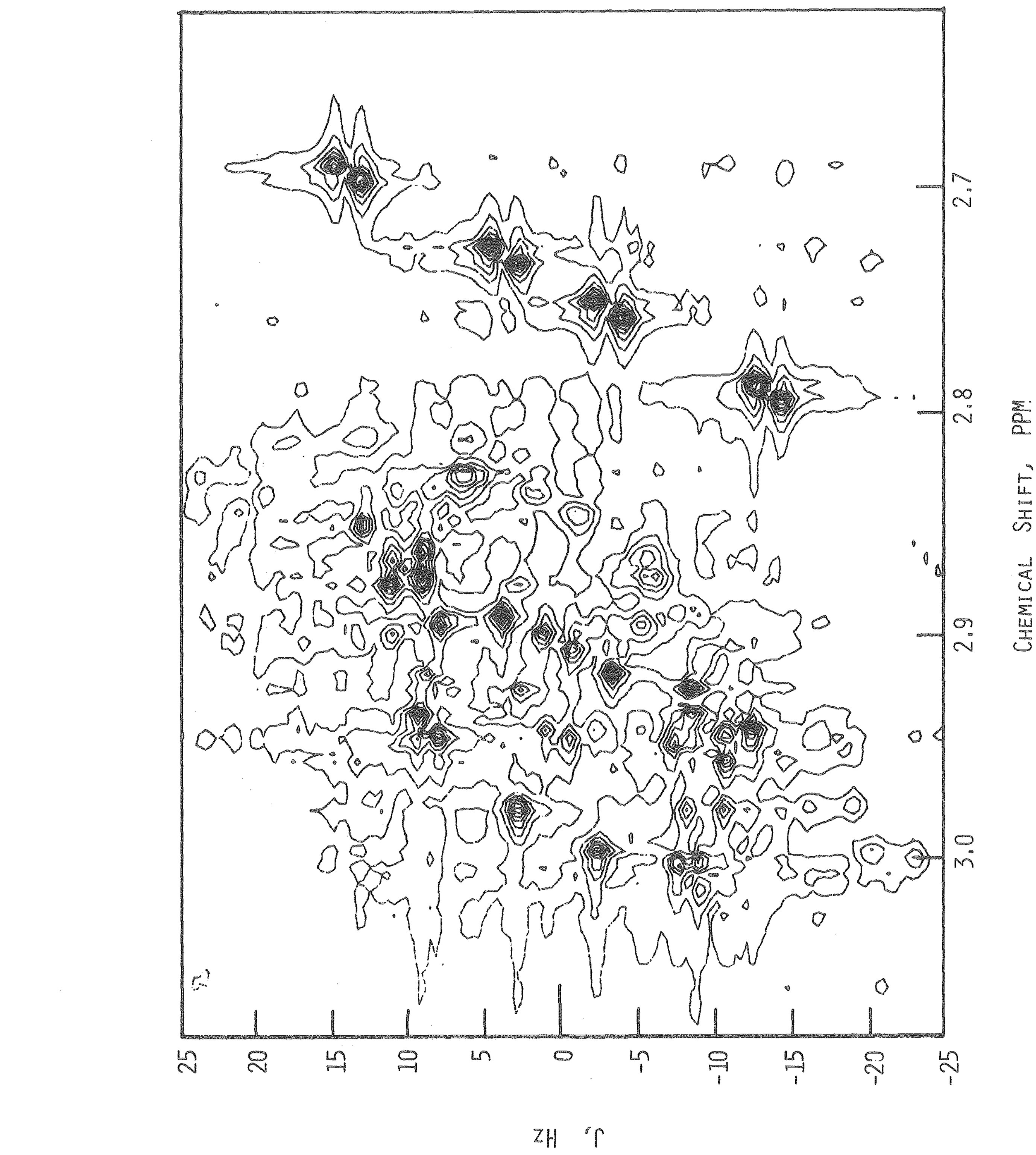

XBL 798-11152

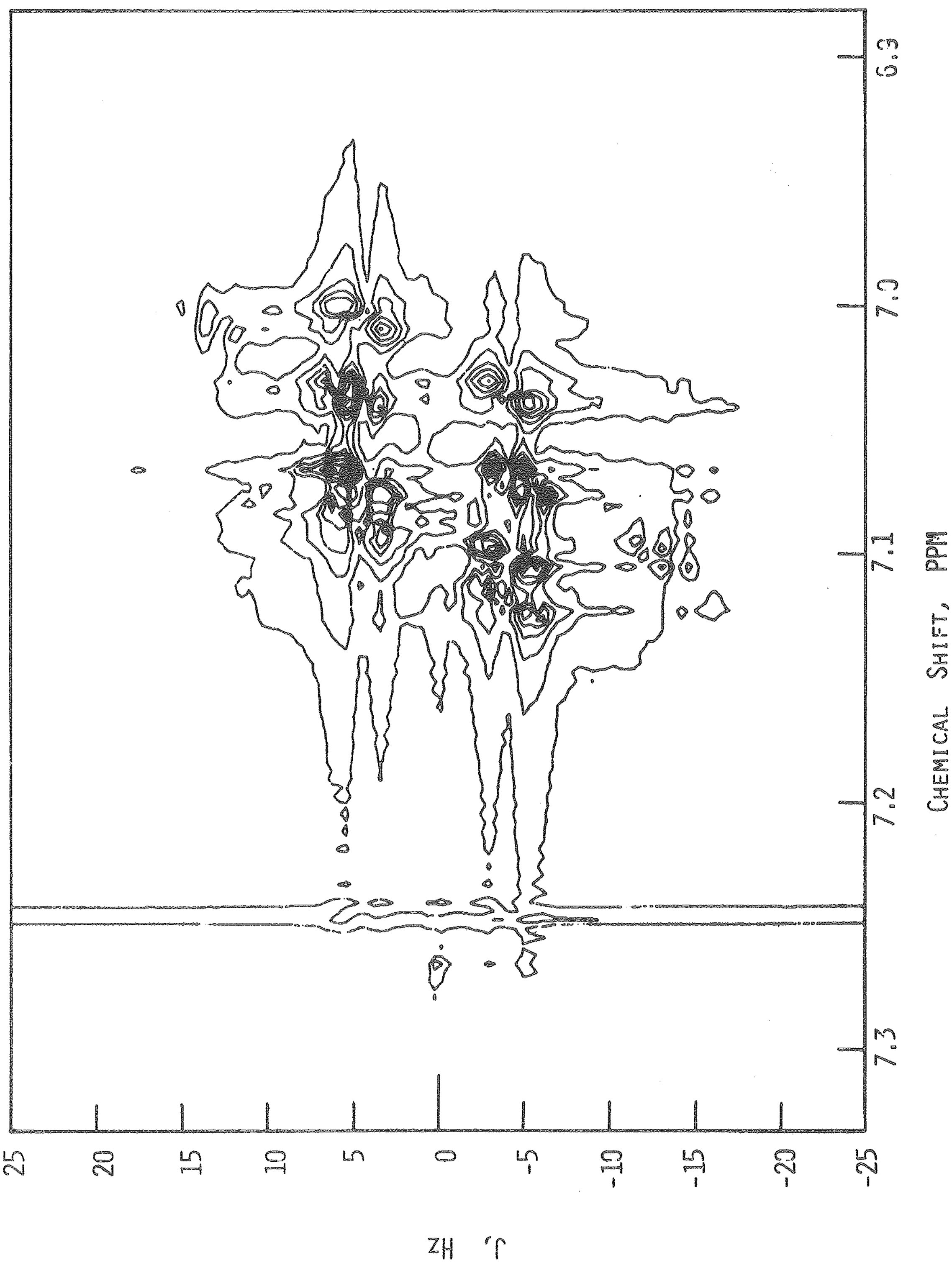

XBL 798-11167

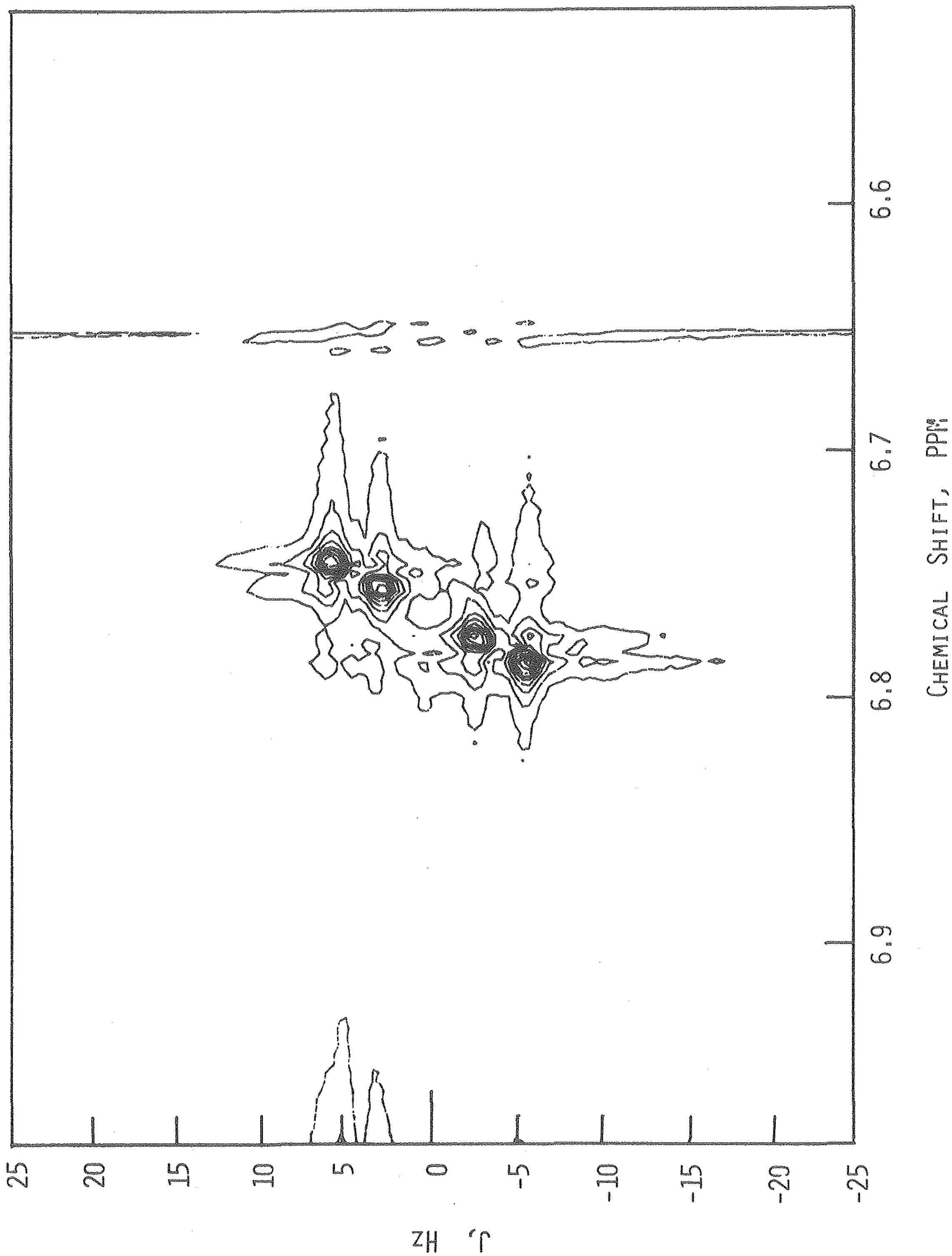

XBL 798-11166

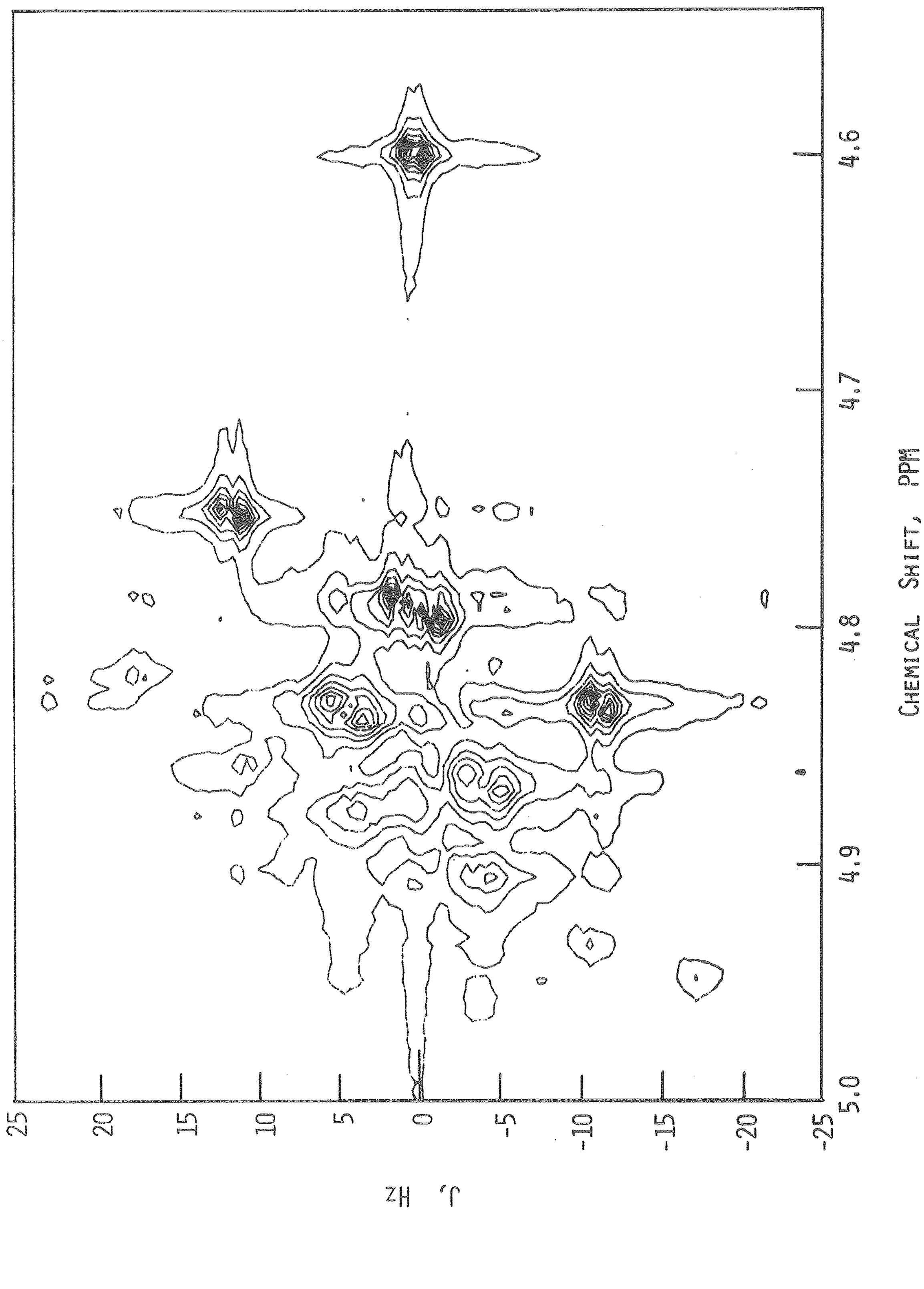

XBL 798-11165

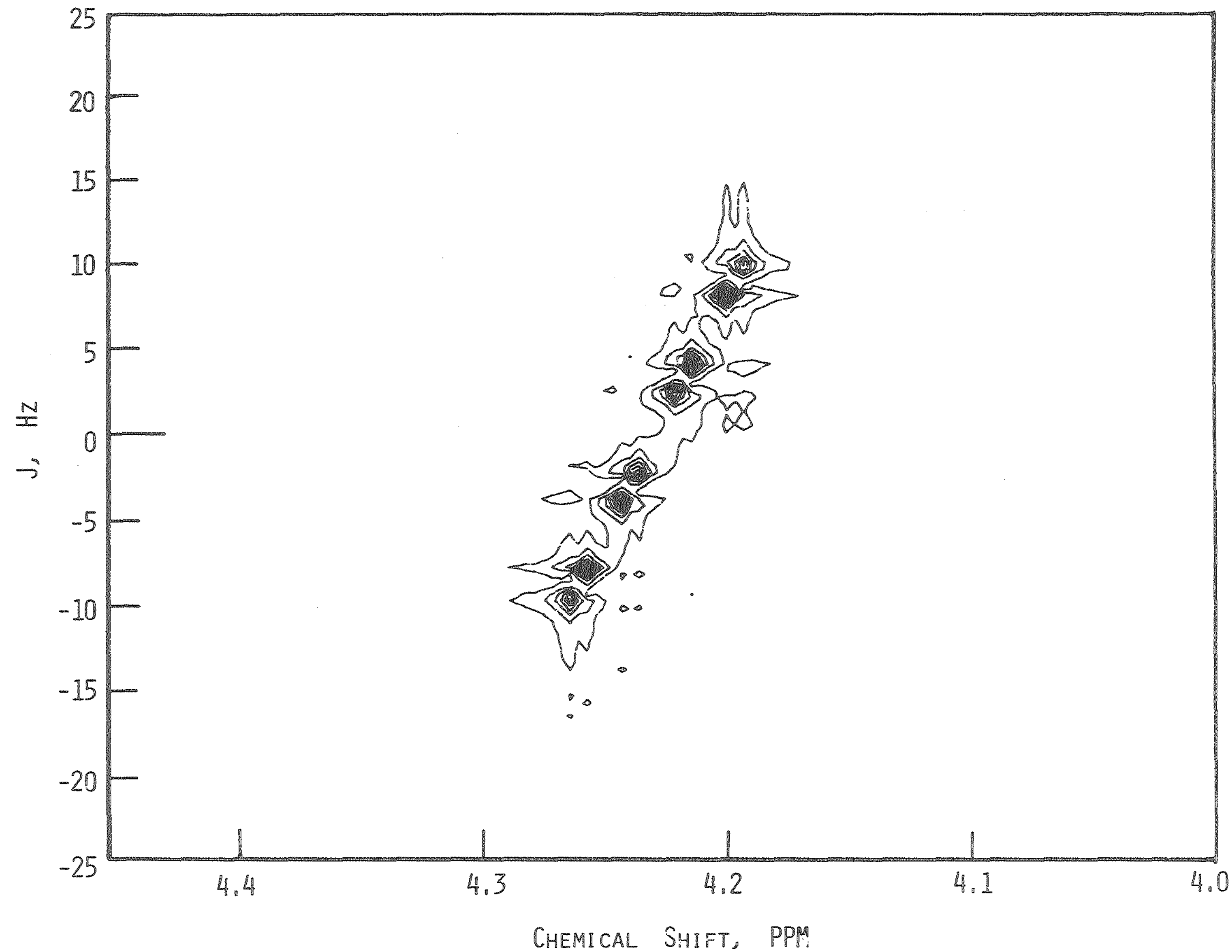

XBL 798-11164

Figure 1.19 Contour Plot of the 3.71 - 3.25 δ Spectral Region of the Two-dimensional Homonuclear J-Spectrum of the N-Methyl Cyclopeptide, 6a

Figure 1.20 Contour Plot of the 3.14 - 2.68 δ Spectral Region of the Two-dimensional Homonuclear J-Spectrum of the N-Methyl Cyclopeptide, 6a

Figure 1.21 Contour Plot of the 2.89 - 2.43 δ Spectral Region of the Two-dimensional Homonuclear J-Spectrum of the N-Methyl Cyclopeptide, 6a

Figure 1.22 Contour Plot of the 2.46 - 2.00 δ Spectral Region of the Two-dimensional Homonuclear J-Spectrum of the N-methyl Cyclopeptide, 6a

Figure 1.23 Contour Plot of the 2.06 - 1.60 δ Spectral Region of the Two-dimensional Homonuclear J-Spectrum of the N-Methyl Cyclopeptide, 6a

Figure 1.24 Contour Plot of the 7.38 - 6.92 δ Spectral Region of the Two-dimensional Homonuclear J-Spectrum of the N-H Cyclopeptide, 6b

Figure 1.25 Contour Plot of the 7.06 - 6.60 δ Spectral Region of the Two-dimensional Homonuclear J-Spectrum of the N-H Cyclopeptide, 6b

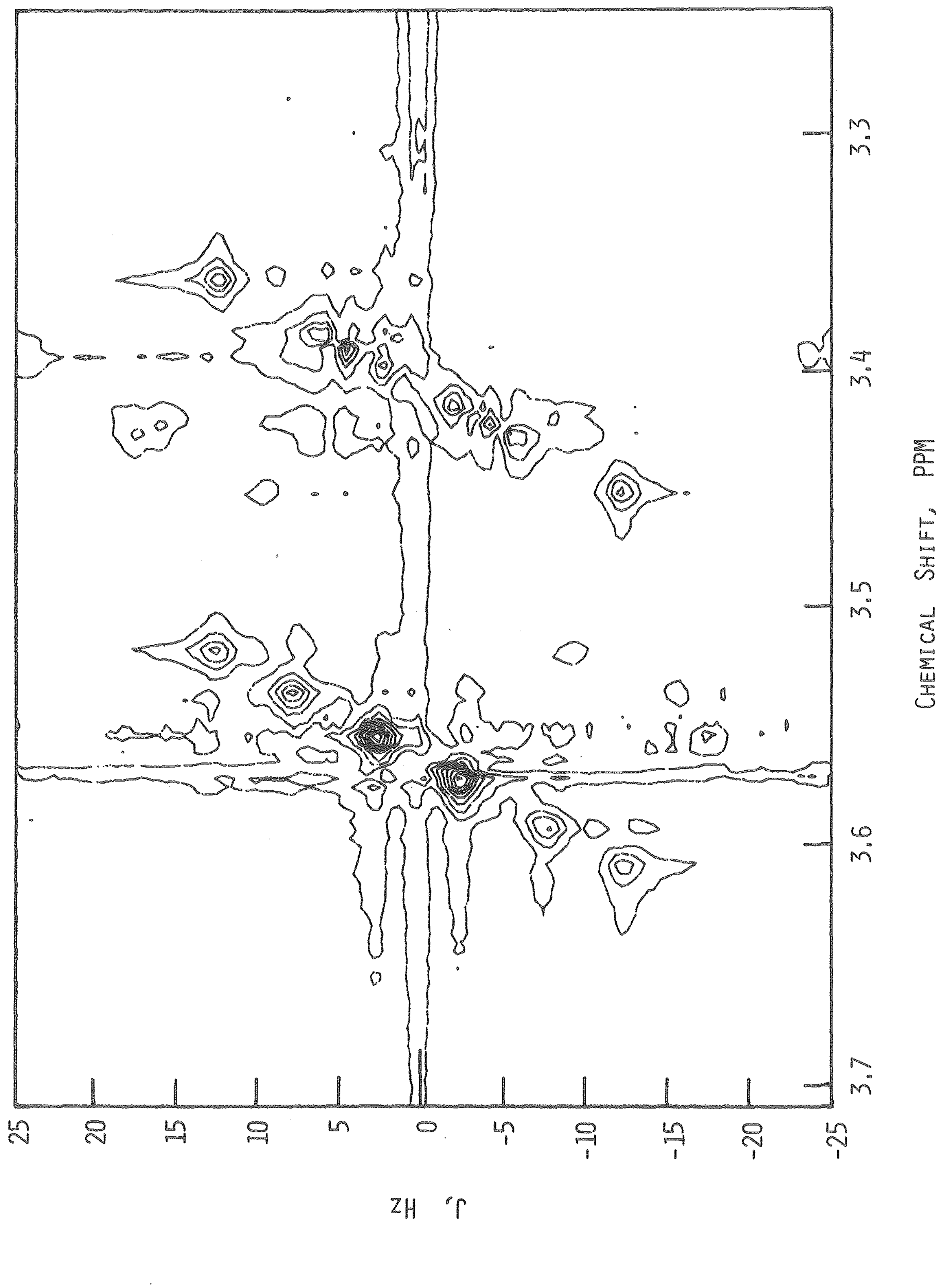

XBL 798-11163

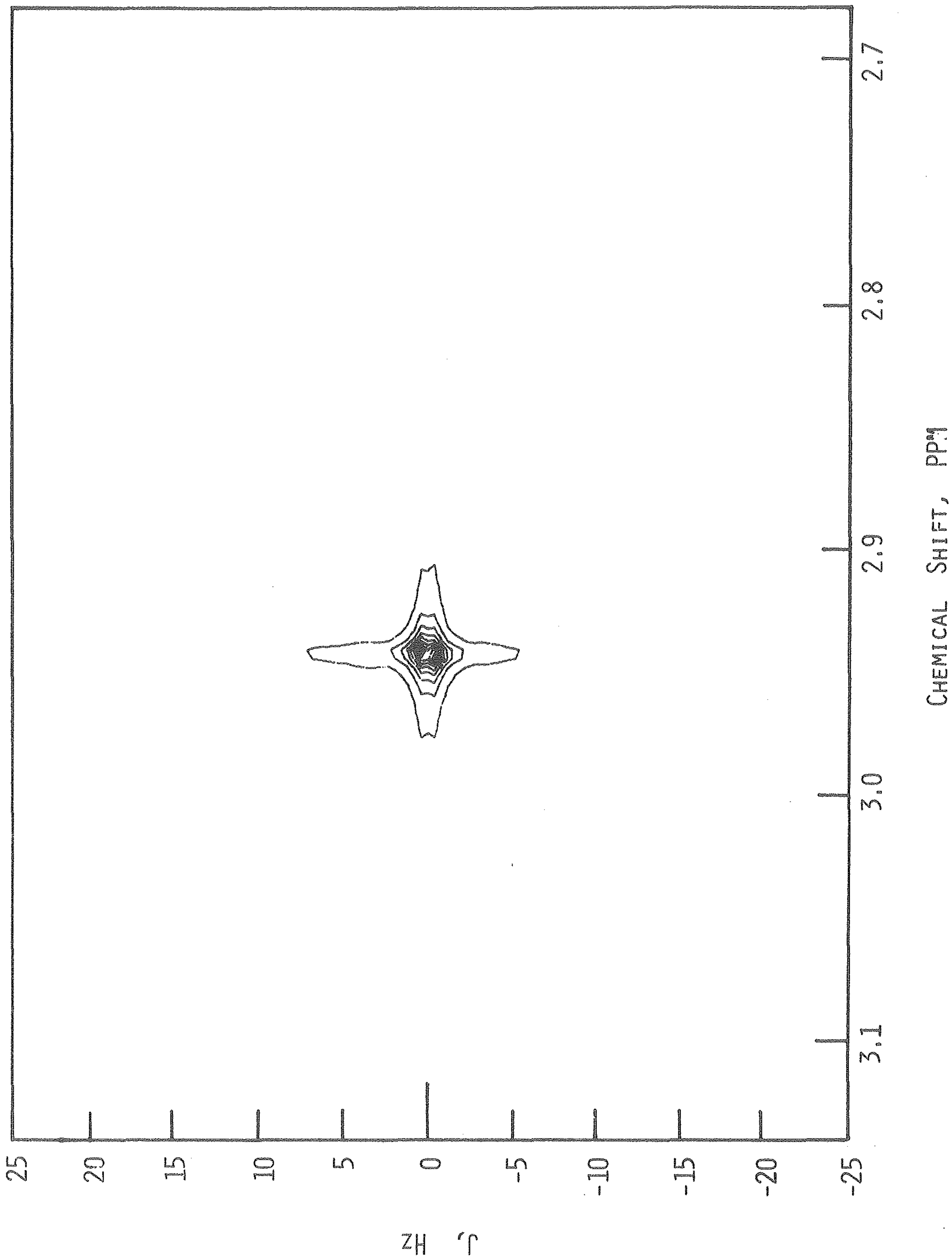

XBL 798-11162

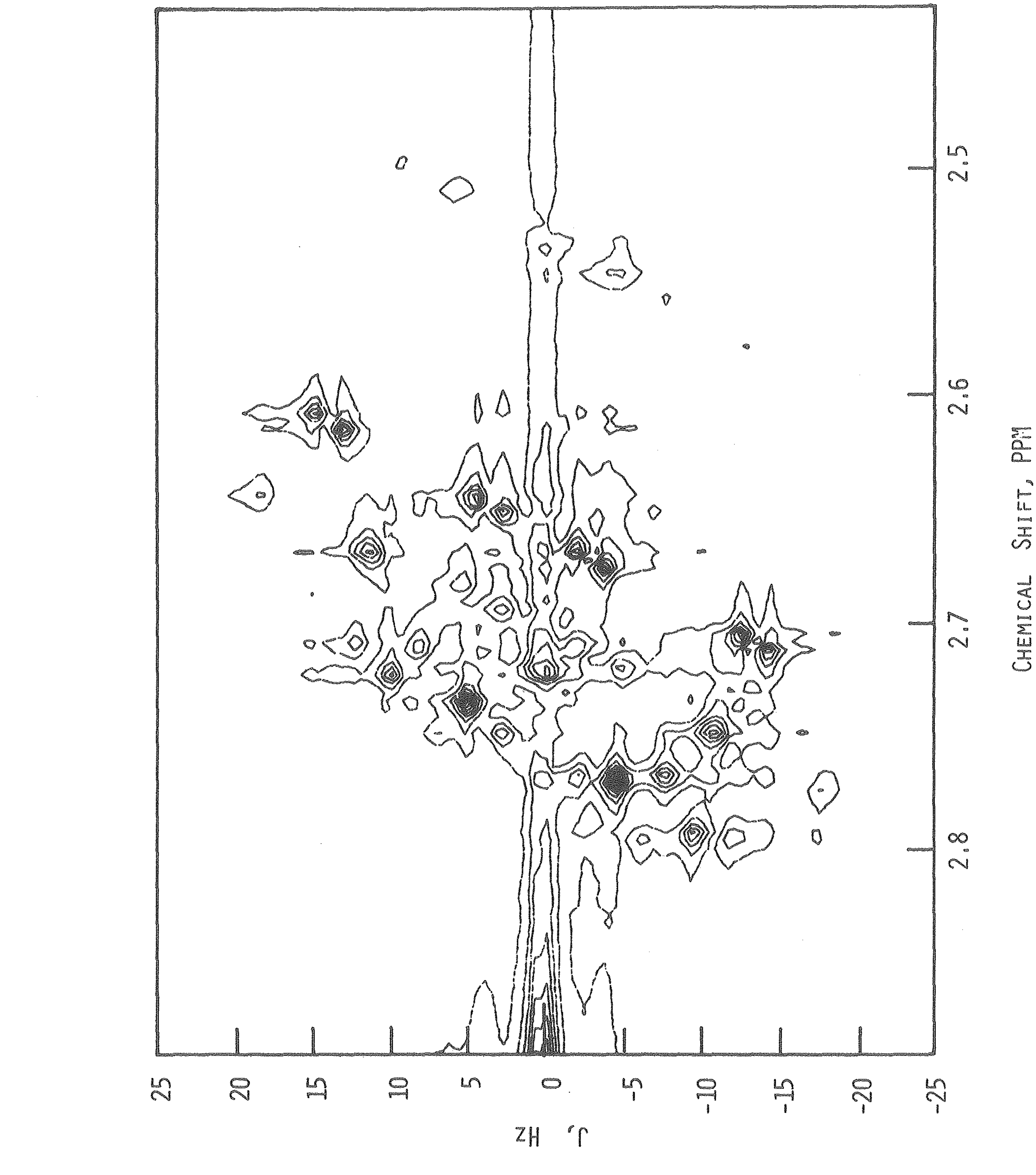

XBL 798-11161

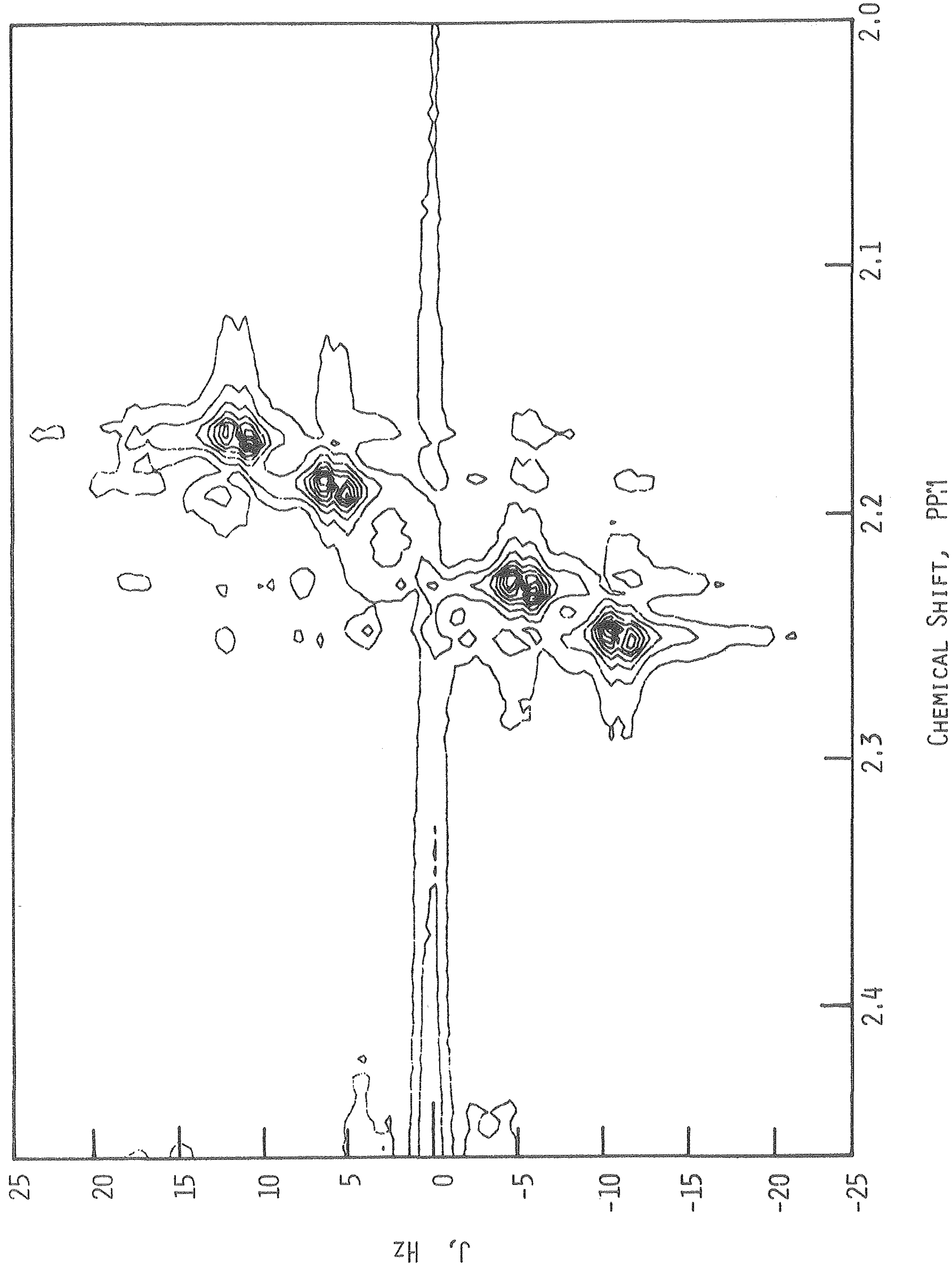

XBL 798-11154

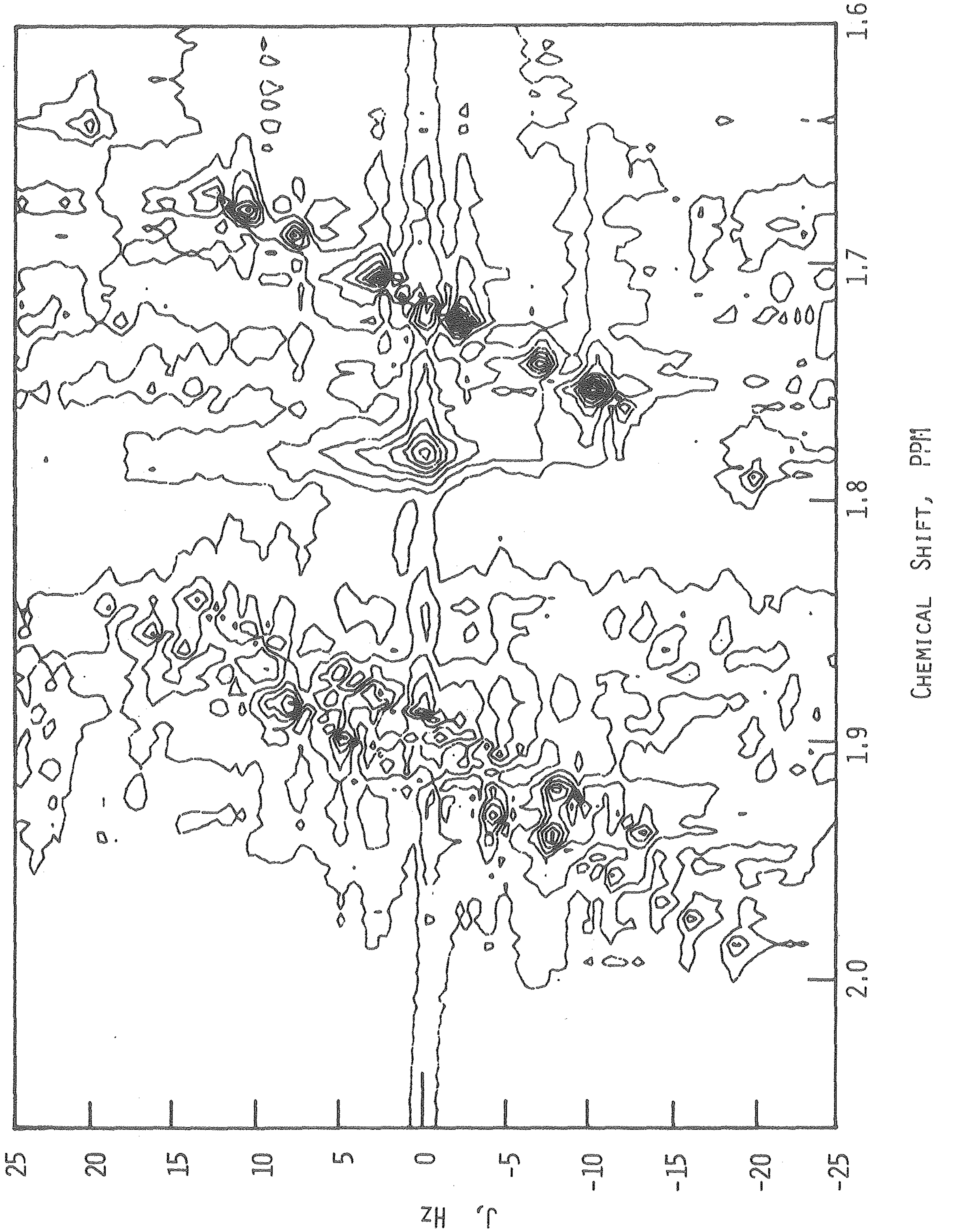

XBL 798-11160

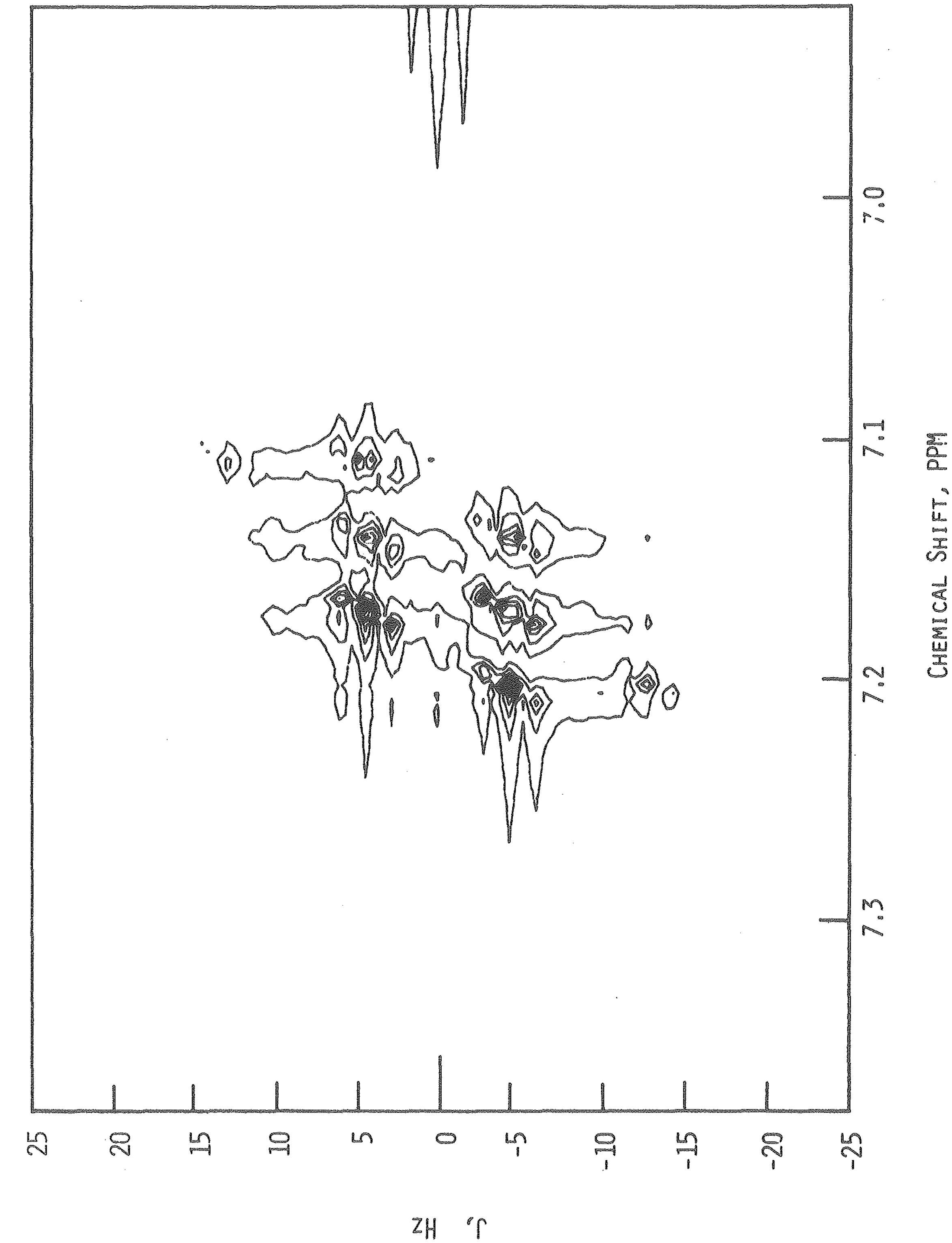

XBL 798-11158

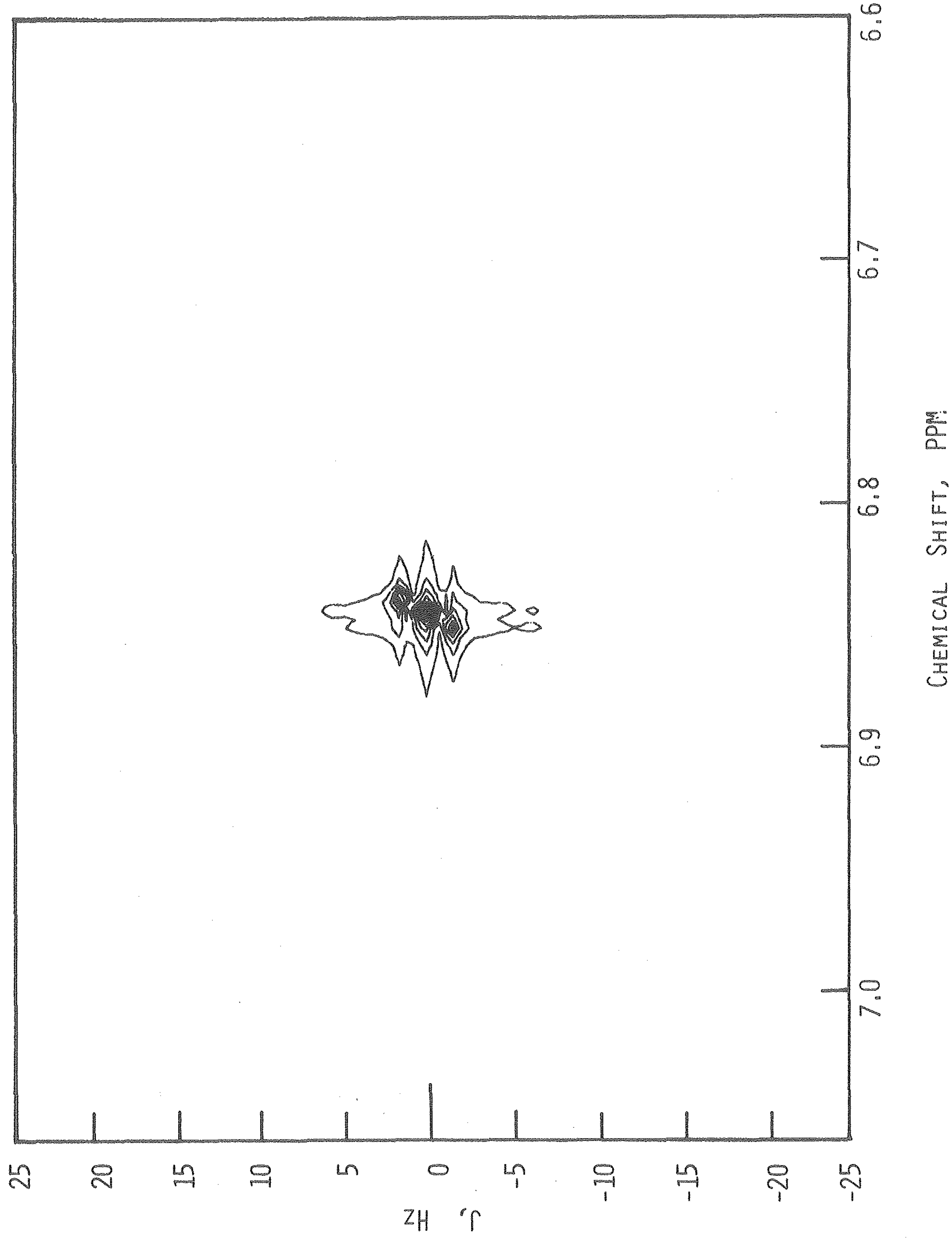

XBL 798-11159

Figure 1.26 Contour Plot of the 4.87 - 4.41 δ Spectral Region of the Two-dimensional Homonuclear J-Spectrum of the N-H Cyclopeptide, **6b**

Figure 1.27 Contour Plot of the 4.50 - 4.04 δ Spectral Region of the Two-dimensional Homonuclear J-Spectrum of the N-H Cyclopeptide, **6b**

Figure 1.28 Contour Plot of the 4.03 - 3.57 δ Spectral Region of the Two-dimensional Homonuclear J-Spectrum of the N-H Cyclopeptide, **6b**

Figure 1.29 Contour Plot of the 3.62 - 3.16 δ Spectral Region of the Two-dimensional Homonuclear J-Spectrum of the N-H Cyclopeptide, **6b**

Figure 1.30 Contour Plot of the 2.50 - 2.05 δ Spectral Region of the Two-dimensional Homonuclear J-Spectrum of the N-H Cyclopeptide, **6b**

Figure 1.31 Contour Plot of the 2.28 - 1.82 δ Spectral Region of the Two-dimensional Homonuclear J-Spectrum of the N-H Cyclopeptide, **6b**

Figure 1.32 Contour Plot of the 1.75 - 1.29 δ Spectral Region of the Two-dimensional Homonuclear J-Spectrum of the N-H Cyclopeptide, **6b**

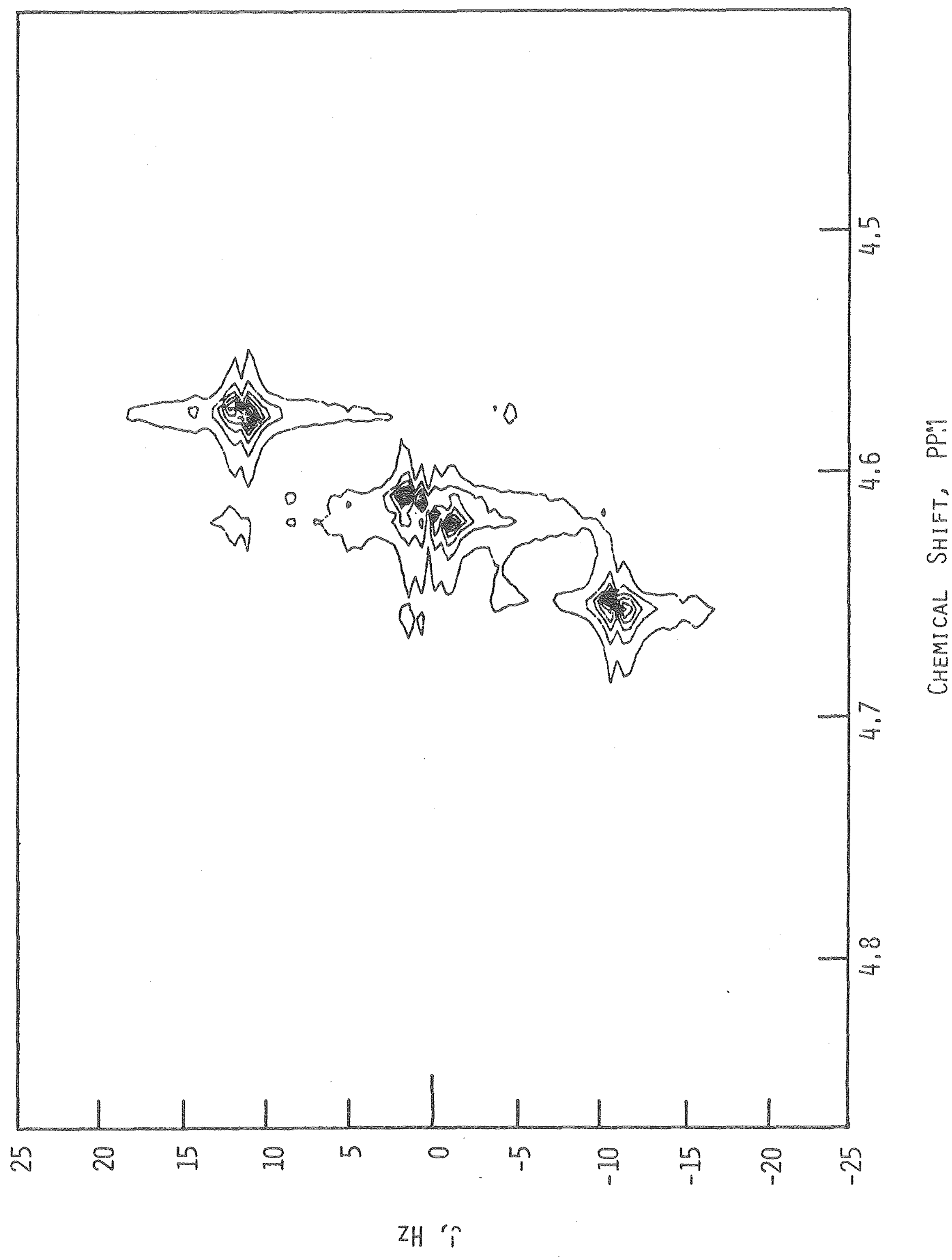

XBL 798-11157

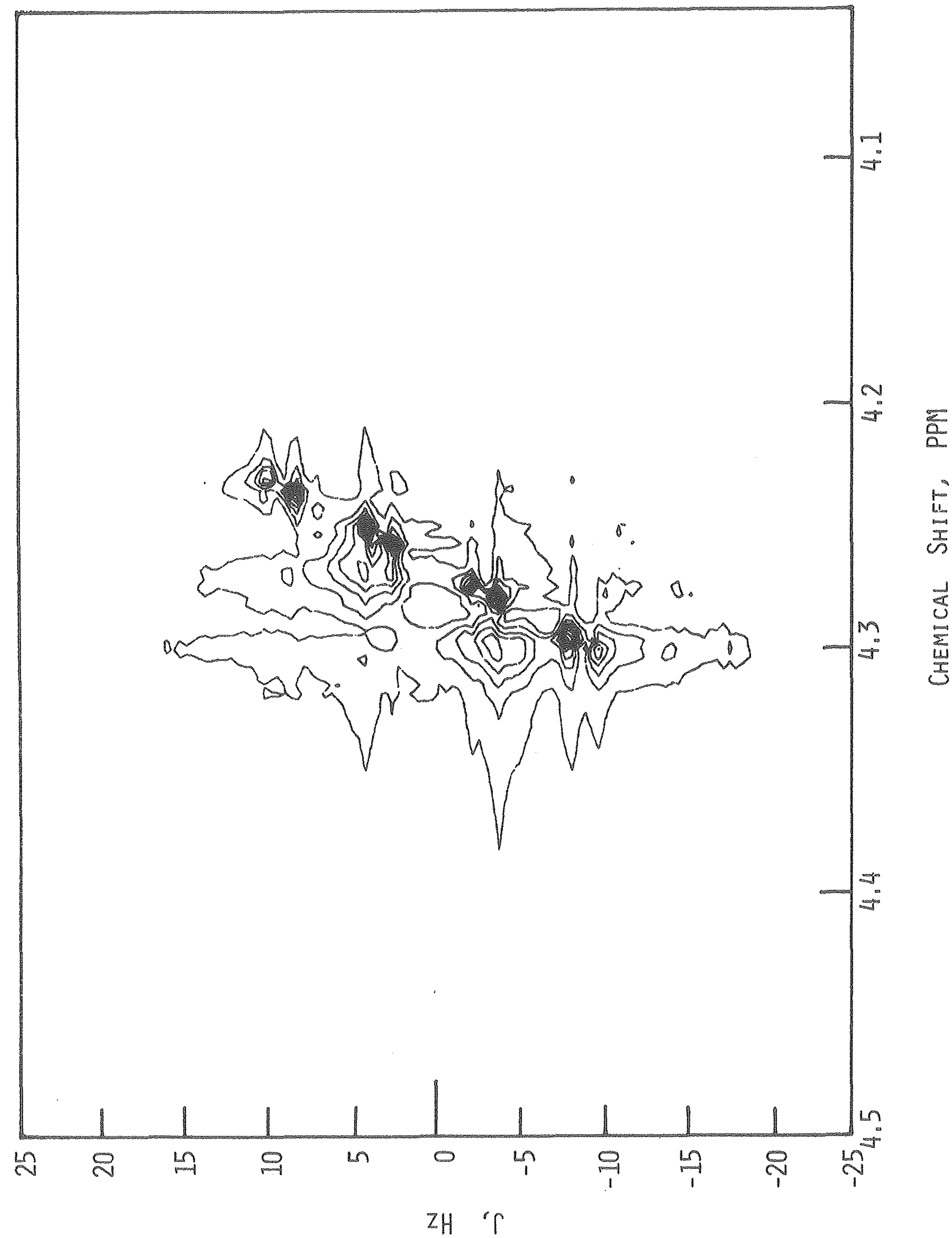

XBL 798-11153

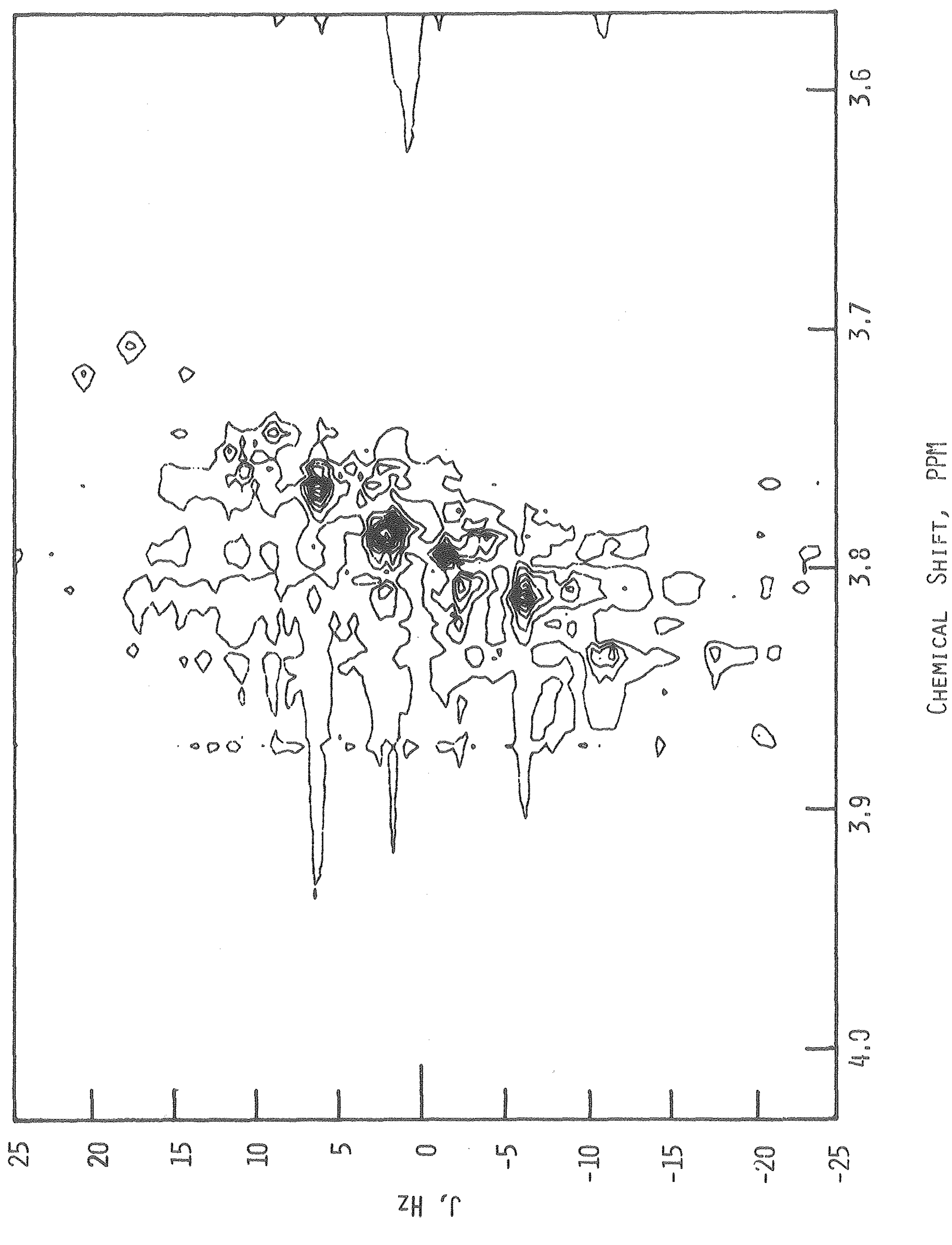

XBL 798-11156

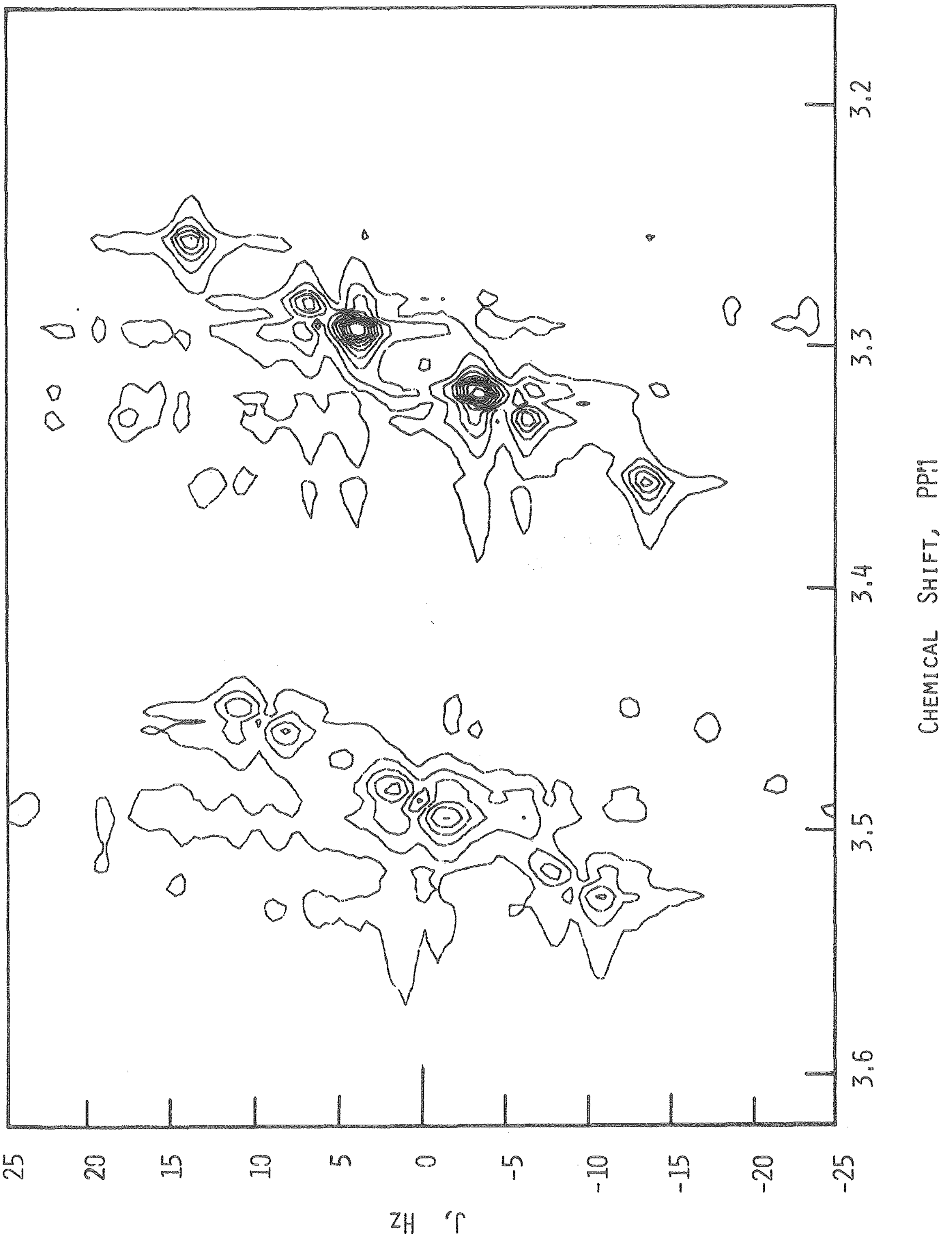

XBL 798-11155

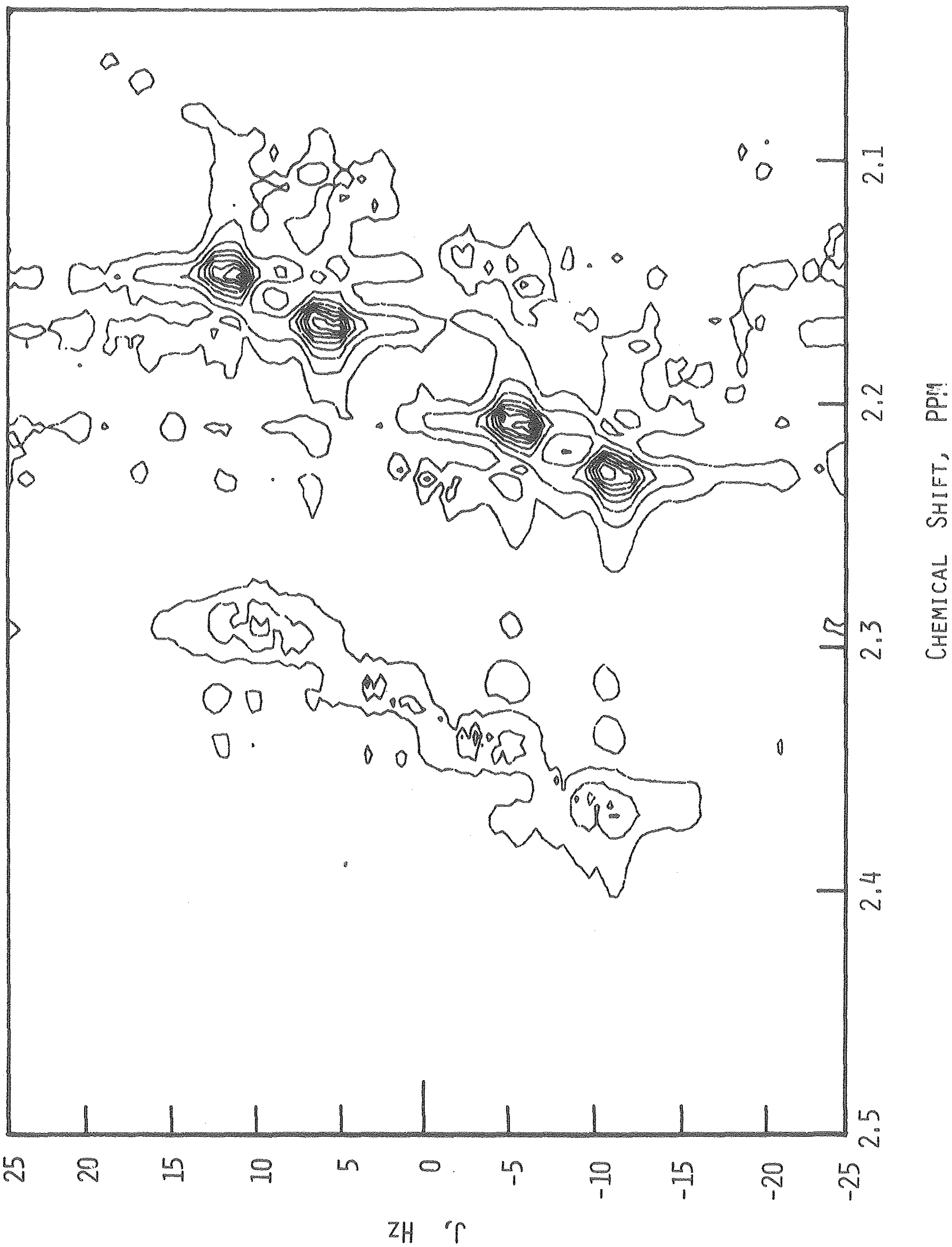

XBL 798-11168

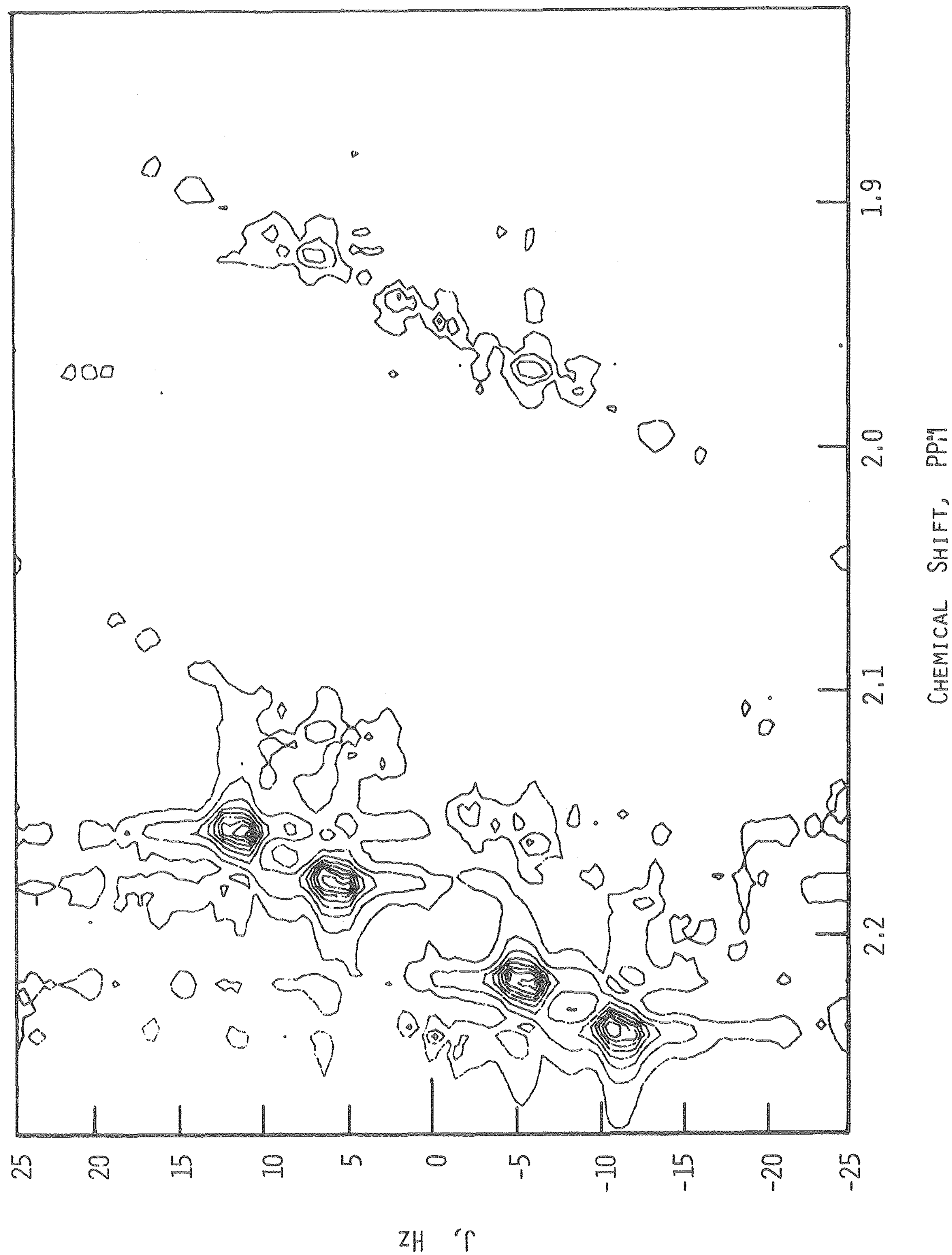

XBL 798-11169

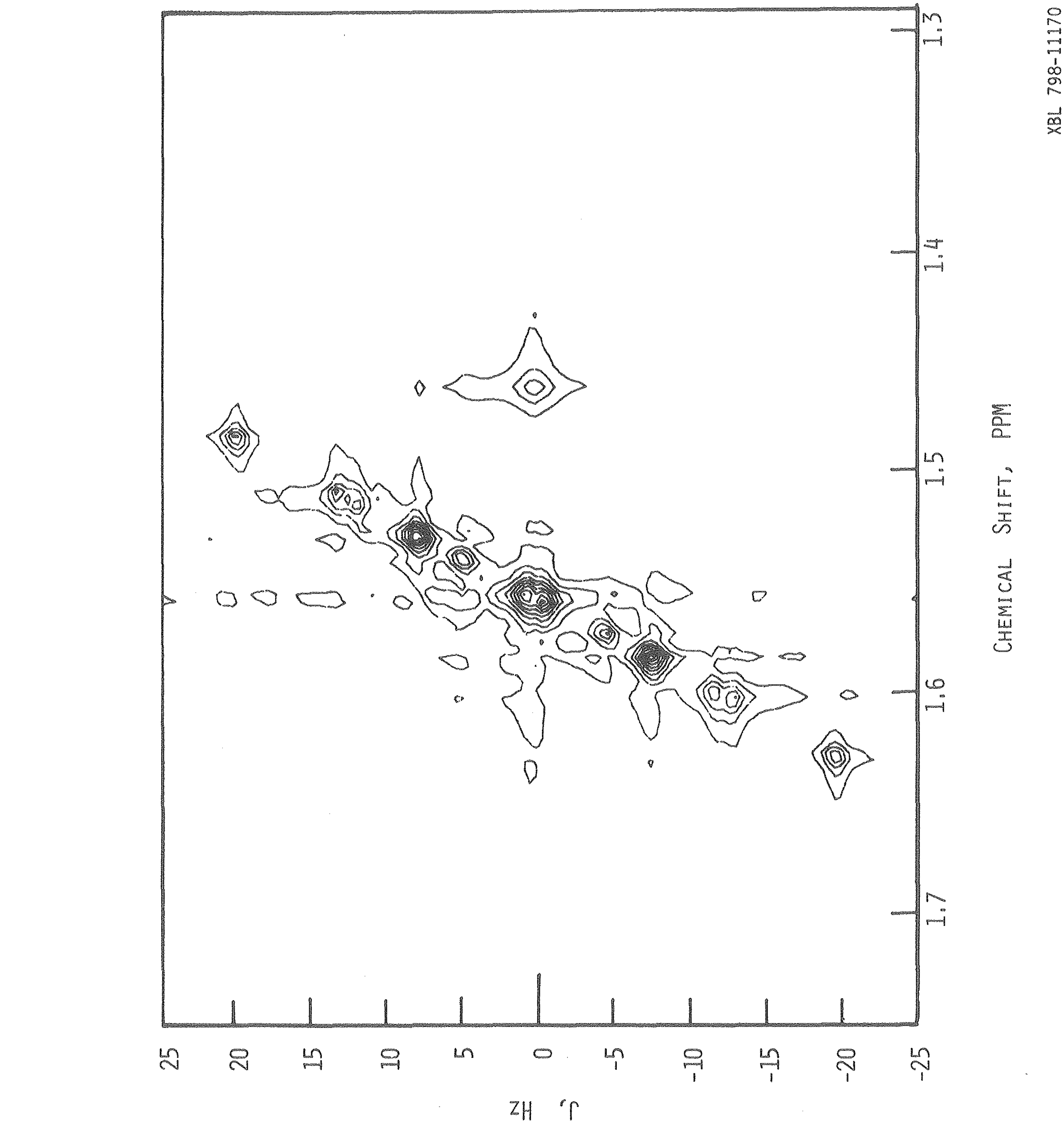
CHEMICAL SHIFT, PPM
1.3
1.4
1.5
1.6
1.7
J, Hz
25
20
15
10
5
0
-5
-10
-15
-20
-25
XBL 798-11170

Figure 1.33 270 MHz ^{1}H NMR Spectrum of *Cyclo*-[3-(4-β-N-methylamino-ethyl)phenyloxypropanoyl-L-prolyl], **6a**

Top: 0° Projection Sum of the 2-D Homonuclear J-Spectrum

Lower: Normal Spectrum

Figure 1.34 270 MHz ^{1}H NMR Spectrum of *Cyclo*-[3-(4-β-N-methylamino-ethyl)phenyloxypropanoyl-L-prolyl], **6a**

Top: 45° Projection Sum of the 2-D Homonuclear J-Spectrum

Lower: Normal Spectrum

Figure 1.35 270 MHz ^{1}H NMR Spectrum of *Cyclo*-[3-(4-β-aminoethyl) phenyloxypropanoyl-L-prolyl], **6b**

Top: 0° Projection Sum of the 2-D Homonuclear J-Spectrum

Lower: Normal Spectrum

Figure 1.36 270 MHz ^{1}H NMR Spectrum of *Cyclo*-[3-(4-β-aminoethyl) phenyloxypropanoyl-L-prolyl], **6b**

Top: 45° Projection Sum of the 2-D Homonuclear J-Spectrum

Lower: Normal Spectrum

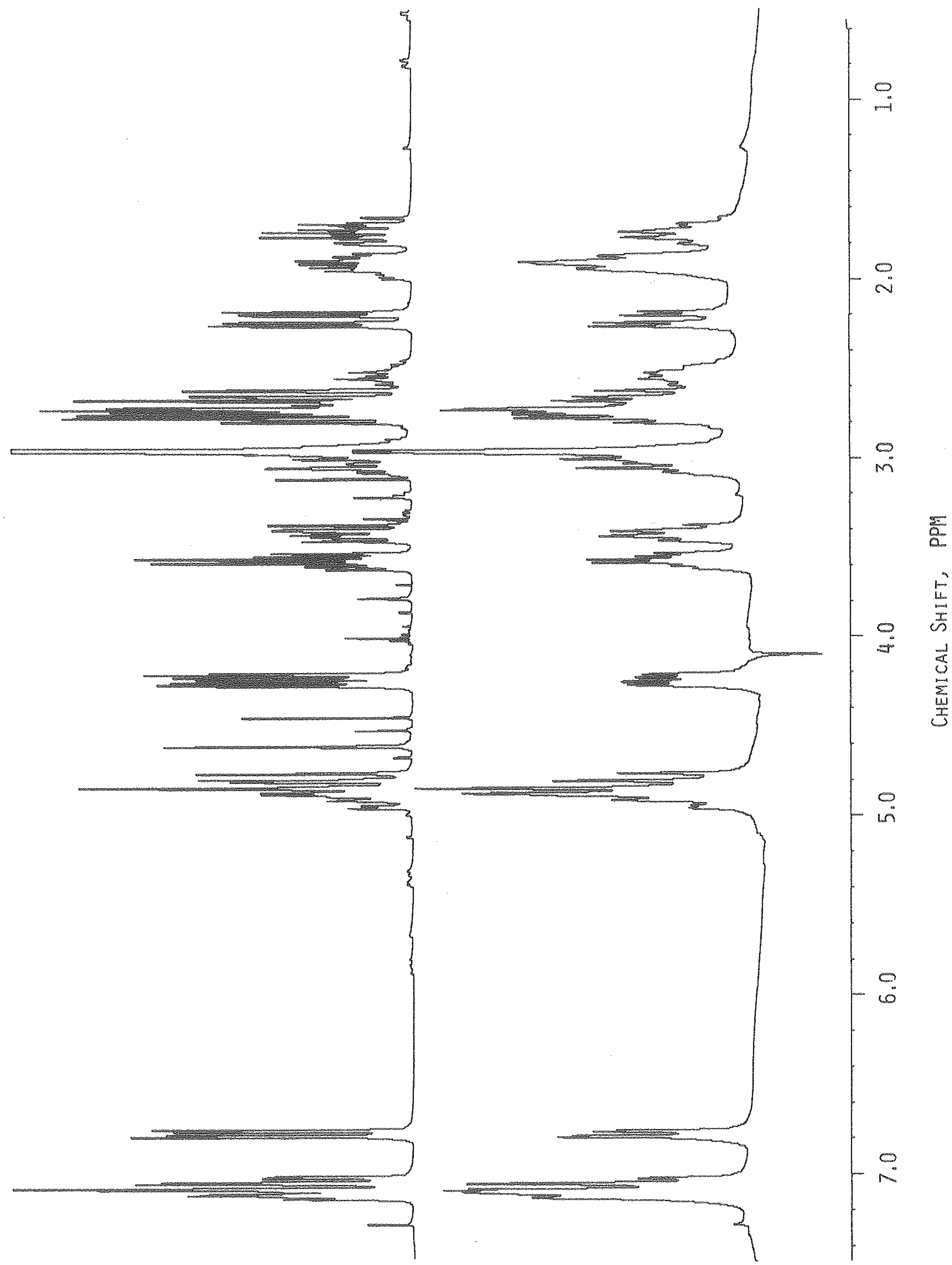

XBL 7910-12173

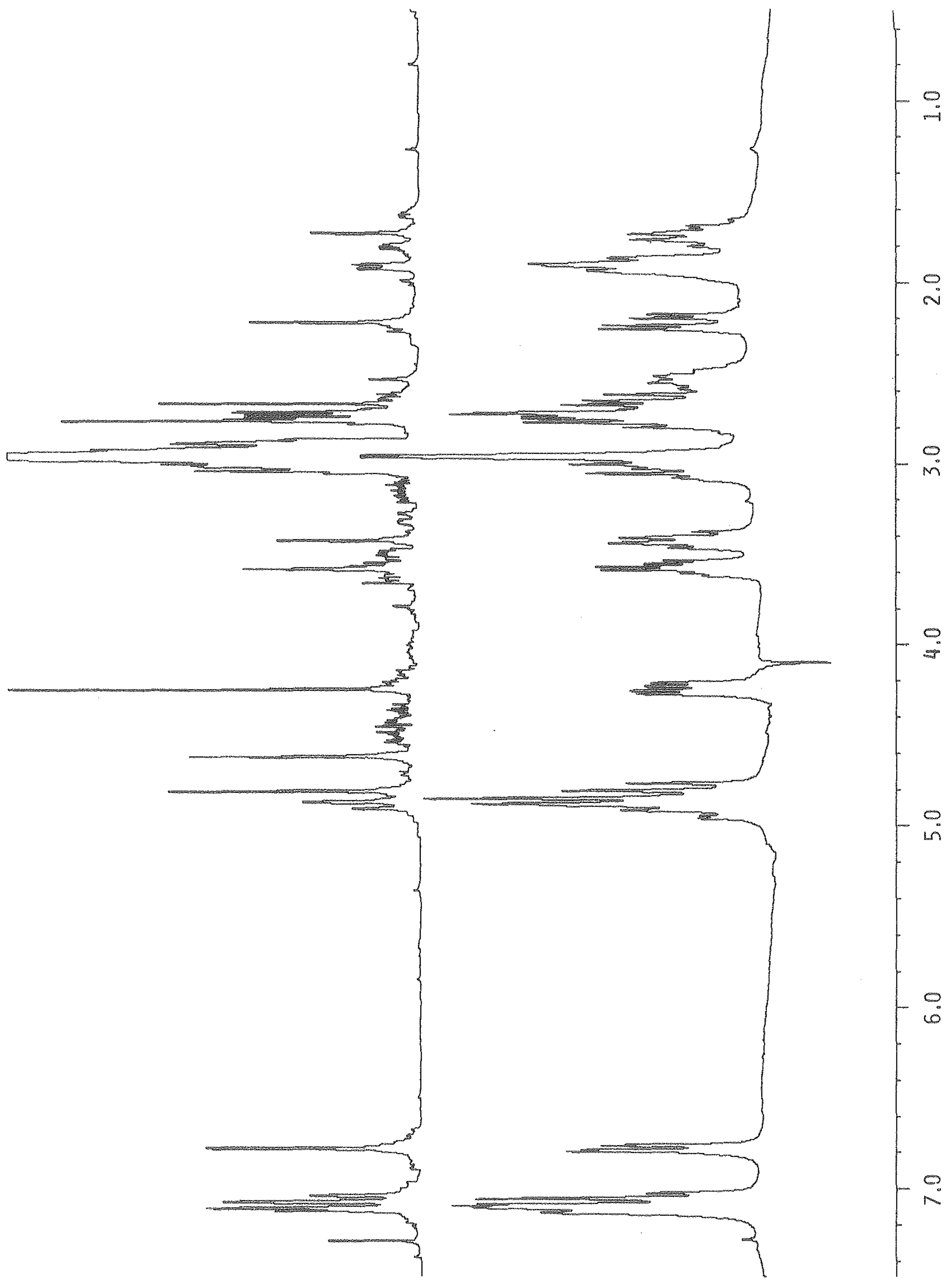

XBL 7910-12174

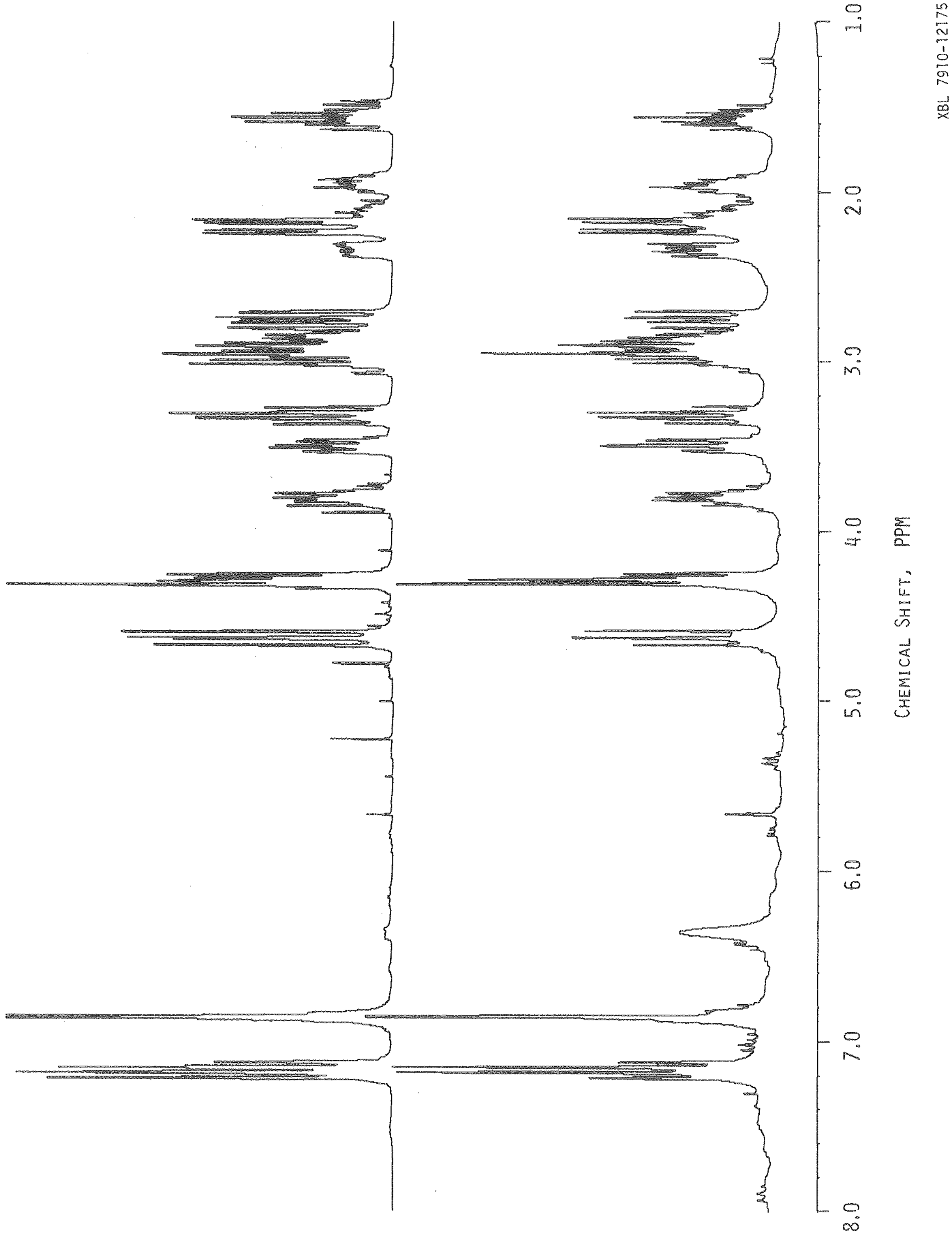
1.0
2.0
3.0
4.0
5.0
6.0
7.0
8.0
CHEMICAL SHIFT, PPM
XBL 7910-12175

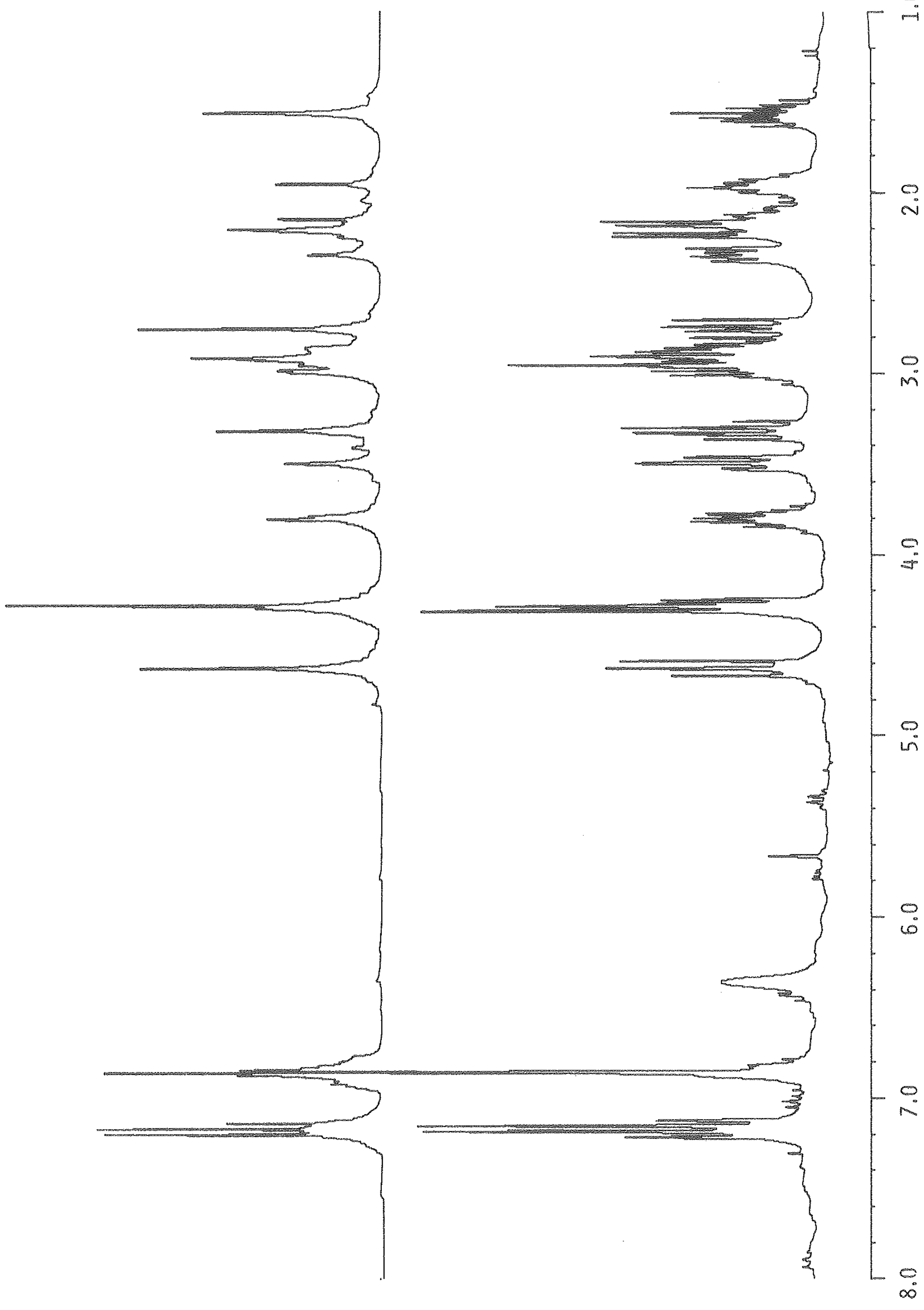

XBL 7910-12176

Table 1.1 NMR Line Assignments for *Cyclo*-[3-(4-β-N-methylamino-ethyl)phenyloxypropanoyl-L-prolyl], 6a

Frequency (Hz)	Height	Assignment
1923.64	508.22	
1921.47	463.05	Complex multiplet, part of aromatic (12,13,15,16-H) 4-spin pattern
1917.36	620.41	
1915.38	658.96	
1913.24	700.48	
1910.91	644.90	
1903.15	649.96	
1894.90	280.46	
1832.18	453.60	
1830.02	423.53	Apparent doublet of doublets, part of aromatic (12,13,15,16-H) 4-spin pattern
1824.04	378.73	
1821.78	326.85	
1336.69	171.70	
1333.04	164.82	Complex multiplet containing 5-H, 2-H, and 9-H
1324.71	336.52	
1314.12	656.58	
1306.44	757.58	
1295.19	463.07	
1289.29	123.70	
1284.18	324.52	
1151.93	282.38	
1150.95	301.42	Doublet of doublet of doublets, 9'-H, part of 8,8',9,9'-H 4-spin pattern
1146.69	316.43	
1145.40	305.38	
1140.32	282.62	
1139.09	282.42	
1134.95	268.73	
975.73	159.47	
971.29	204.94	19-H, part of prolyl 7-spin system (5,17,17',18,18',19,19'-H)
966.08	380.76	
961.47	387.09	
956.55	286.94	
951.95	242.31	
933.50	233.40	
926.91	360.32	19'-H, part of prolyl 7-spin system (5,17,17',18,18',19,19'-H)
926.08	359.37	
918.32	337.96	
912.77	119.18	
911.90	117.63	
909.41	180.71	

Table 1.1 [continuation]

Frequency (Hz)	Height	Assignment
832.38	164.56	
829.73	225.77	2-H, appearance approximates a doublet
823.28	411.21	of doublets
816.52	309.45	
809.35	443.47	
796.49	3645.98	N-CH_3
762.89	125.09	
754.51	329.52	1-H, 1'-H, complex multiplet, part of
747.59	546.43	1,1',2,2'-H 4-spin pattern
742.15	549.86	
738.64	546.70	
735.12	705.05	
732.47	650.02	
727.90	338.29	
721.07	464.09	8-H, appearance close to that of a
716.15	394.62	quartet, part of 8,8',9,9'-H 4-spin
714.83	417.29	pattern
710.84	187.78	
706.21	372.33	
697.45	210.56	
693.90	184.86	18-H, part of prolyl 7-spin system
690.90	216.57	(5,17,17',18,18',19,19'-H)
688.09	275.08	
685.31	246.56	
682.01	236.72	
678.92	263.70	
676.38	231.55	
672.84	171.87	
672.17	175.33	
669.50	176.27	
667.28	147.17	
661.00	106.62	
608.35	382.25	
602.90	372.36	8'-H, dominated by doublet of doublets,
597.90	372.36	part of 8,8',9,9'-H 4-spin pattern
596.81	117.27	
595.60	121.22	
591.92	315.41	
586.57	277.28	

Table 1.1 [continuation]

Frequency (Hz)	Height	Assignment
536.97	130.41	
536.16	132.42	18'-H, 17-H, broad multiplet, part of prolyl 7-spin system (5,17,17',18, 18',19,19'-H)
532.85	166.07	
532.21	168.35	
521.81	404.77	
520.53	405.84	
513.80	501.58	
511.05	532.25	
502.22	363.77	
484.66	190.89	
481.25	144.91	17'-H, complex multiplet, part of prolyl 7-spin system (5,17,17',18, 18',19,19'-H)
474.84	315.30	
471.83	225.74	
466.84	318.36	
462.74	226.13	
457.53	185.63	
454.22	192.06	
445.18	102.12	

Table 1.2 NMR Line Assignments for *Cyclo*-[3-(4-β-aminoethyl) phenyloxypropanoyl-L-prolyl], 6b

Frequency (Hz)	Height	Assignment
1948.33	237.39	
1946.94	344.27	(Triplet) Part of aromatic 4-spin (12,13,15,16-H) pattern
1945.53	253.01	
1939.91	613.11	
1938.37	781.76	(Triplet) Part of aromatic 4-spin (12,13,15,16-H) pattern
1937.15	569.86	
1929.90	756.86	Part of aromatic 4-spin (12,13,15,16-H) pattern
1922.36	218.17	Part of aromatic 4-spin (12,13,15,16-H) pattern
1857.78	174.86	
1855.99	203.35	Complex multiplet dominated by triplet, part of aromatic 4-spin (12,13,15, 16-H) pattern
1850.82	1574.15	
1849.48	1990.71	
1848.13	1298.90	
1843.33	101.10	
1841.81	103.99	
1841.17	102.99	
1838.58	108.40	
1716.71	159.18	(Broad) 3-H (N-H)
1258.74	255.34	9-H, part of 8,8',9,9'-H 4-spin pattern, has appearance of a doublet of doublets
1248.90	387.82	
1248.27	373.31	
1247.28	381.09	
1246.62	388.46	
1237.13	387.37	
1162.89	729.11	
1161.79	697.38	5-H and 9'-H; 5-H is part of the prolyl 7-spin system (5,17,17',18,18',19,19'), 9'-H is part of 8,8',9,9'-H 4-spin pattern
1157.36	462.87	
1151.24	284.61	
1149.77	271.15	
1145.61	276.19	
1144.15	189.60	
1037.37	120.49	
1033.86	91.38	2-H, part of 1,1',2,2'-H 4-spin pattern
1030.38	179.07	
1029.71	218.61	
1026.26	166.60	

Table 1.2 [continuation]

Frequency (Hz)	Height	Assignment
1024.70	210.73	(continued)
1023.19	156.68	2-H, part of 1,1',2,2'-H 4-spin pattern
1021.55	112.39	
1018.65	193.03	
1016.94	188.98	
1015.22	89.97	
952.53	139.01	19-H, part of 5,17,17',18,18',19,19'-H prolyl 7-spin system (doublet of triplets)
950.25	156.05	
943.30	322.82	
941.16	308.50	
934.26	231.16	
932.09	208.43	
907.08	191.66	19'-H, part of 5,17,17',18,18',19,19'-H prolyl 7-spin system (doublet of triplets)
899.84	254.45	
897.27	335.42	
890.07	351.39	
887.54	158.88	
880.35	139.36	
817.63	73.25	
814.27	124.63	
811.62	257.30	1-H, 2'-H, 1'-H
810.21	207.93	
805.01	294.11	Complex multiplet that includes the 1, 1', and 2-H protons of the 1,1',2,2'-H 4-spin pattern
799.27	300.12	
796.37	562.73	
794.15	343.18	
791.03	281.71	
788.88	260.84	
786.01	282.87	
784.30	357.82	
782.96	413.61	
782.19	355.95	
778.00	287.44	
776.83	322.34	
775.56	292.93	
774.12	244.95	
771.97	194.70	
770.96	266.65	
766.40	214.16	
764.97	195.23	
760.89	110.23	

Table 1.2 [continuation]

Frequency (Hz)	Height	Assignment
755.95	218.65	
754.50	209.76	
745.82	230.84	8-H, part of 8,8',9,9'-H 4-spin pattern
744.35	202.14	(quartet of doublets)
739.18	274.56	
737.72	261.76	
729.06	264.05	
727.60	196.77	
641.09	178.25	17-H, part of 5,17,17',18,18',19,19'-H
634.52	217.49	prolyl 7-spin system (broad quartet)
628.95	190.63	
622.27	224.67	
604.77	368.97	
602.90	135.02	
599.27	370.15	8'-H, part of 8,8',9,9'-H 4-spin pattern
595.81	115.08	(broad doublet of doublets)
592.68	148.84	
590.44	209.23	
588.05	357.49	
582.44	389.76	
578.39	126.60	
574.64	133.48	
573.92	133.87	18-H, part of 5,17,17',18,18',19,19'-H
571.83	155.04	prolyl 7-spin system (complex
569.61	107.49	multiplet)
568.74	95.17	
565.12	76.65	
562.84	76.14	
562.04	70.66	
540.47	87.59	
538.69	123.99	
536.60	90.08	18'-H, part of 5,17,17',18,18',19,19'-H
533.54	158.00	prolyl 7-spin system (complex
531.66	224.05	multiplet)
529.55	142.79	
526.44	149.24	
524.49	155.52	
521.75	110.92	
519.23	124.00	

Table 1.2 [continuation]

Frequency (Hz)	Height	Assignment
440.29	100.85	
432.81	160.03	17'-H, part of 5,17,17',18,18',19,19'-H prolyl 7-spin system (complex multiplet)
428.19	199.54	
425.21	119.30	
420.77	258.40	
416.10	97.19	
413.19	149.51	
408.84	84.37	

Table 1.3 Cyclopeptide Prolyl Seven-Spin Systems: Summary of Chemical Shift Differences Between N-Methyl (6a) and N-H (6b) Cases

Proton	N-Methyl Case Chemical Shift	N-H Case Chemical Shift
C_5	1310.30 Hz	1157.63 Hz
C_{17}	511.64 Hz	630.68 Hz
C_{17}'	464.70 Hz	420.13 Hz
C_{18}	683.37 Hz	577.92 Hz
C_{18}'	518.01 Hz	520.30 Hz
C_{19}	963.70 Hz	946.25 Hz
C_{19}'	921.48 Hz	893.37 Hz

1.5 Analysis of NMR Data

A. Summary of Approach

Non-first-order coupling patterns are best analyzed by comparison with calculated simulations. In the analysis of the cyclopeptide NMR data, the procedure used may be briefly outlined:

1. Approximate simulation -- Using frequencies derived from the 2-D 45° projections and coupling constants derived from the 2D contour plots, a first rough simulation was calculated. Coupling constants were then adjusted in successive simulations to produce the closest possible match to the actual spectrum. N-Methyl cyclopeptide **6a** calculations also employed the dihedral angle data available from the x-ray structure, along with Karplus relations to give relative magnitudes of vicinal couplings.
2. Transition assignment and iterative fit -- After a calculation produced a simulated spectrum that appeared to be close enough to the actual spectrum for transitions to be assigned, an iterative fit was performed using a version of the LAOCN3 program of Castellano and Bothner-By.[31] Both coupling constants and line frequencies were allowed to vary in the least-squares procedure.
3. Incorrect assignment of transitions -- If the iterative fit routine did not converge, it was assumed that incorrect assignment of some transitions had been made. A different simulation was calculated, and new transition assignments were made.

4. Convergence of iterative fit -- When the iterative fit routine converged and produced a low RMS error of fit, good values for coupling constants and chemical shifts were presumably obtained. The calculated chemical shifts and couplings were then used to generate a new simulated spectrum, which was plotted for comparison with the actual spectrum. Convergence does not insure that the correct assignments had been made, this is where there is a possibility of ambiguity. In highly non-first-order systems, conclusions are regarded as tentative. In systems approaching first-order (such as the C_8-C_8'-C_9-C_9' four-spin system), it is quite straightforward to make transition assignments, and greater confidence may be placed in the values of couplings so obtained.

B. C_8 - C_9 Four-Spin System

Dihedral angles for the protons of the C_8-C_8'-C_9-C_9' four-spin system of the N-methyl cyclopeptide are listed in Table 1.4. The Karplus relations (2) and (3), although not necessarily valid for a O-CH_2-CH_2-CO- configuration, were used to give order of magnitude estimates of the vicinal coupling constants. Combined with estimates of couplings derived from the contour plots of Figure 1.18, 1.21, and 1.22, a first approximate coupling pattern was derived for use in a simulation (Figure 1.37). Of the calculated transitions generated by this pattern, all but two were readily assigned (Table 1.5 lists these assignments). The calculated shifts and coupling constants (Figure 1.38) produced the simulated spectrum of Figure 1.39 (shown with the normal spectrum for comparison); the two are in excellent agreement.

The C_8-C_8'-C_9-C_9' four-spin system of the N-H cyclopeptide **6b** was analyzed in a similar fashion. The approximate values derived from the 2-D 45° projection and contour maps (Figure 1.40) were used to calculate transition frequencies (Table 1.6). All but three transitions were assigned, leading to an RMS error of fit of 0.200 Hz in the iterative solution. The calculated best-fit shifts and coupling constants (Figure 1.41) led to the simulated spectrum of Figure 1.42, again an excellent match to the actual spectrum.

Both bond angles and coupling constants were available for the N-methyl case, therefore different constants for the Karplus relations (1) - (3) could be calculated. These constants would then reflect the unique substitution patterns of the C_8-C_9 carbons in the cyclopeptides, and they would be directly applicable to the calculation of bond angles in the N-H case. Attempts were made to fit the J -- angle data to relationships such as:

$$^3J(\theta) = A \cos^2\theta + B \cos\theta + C \tag{8}$$

and

$$^3J(\theta) = A \cos^2\theta + B \cos\theta + C \sin\theta \tag{9}$$

but the best estimator of the vicinal coupling in this case turned out to be:

$$^3J(\theta) = 9.512 \cos^2\theta + 0.681 \tag{10}$$

Application of (10) to the N-H data gave the following bond angles:

Vicinal Coupling	Calculated J	Calculated Angle
H_α-8-9-H_α	1.457 Hz	73°
H_α-8-9-H_β	10.313 Hz	180°
H_β-8-9-H_α	5.903 Hz	42°
H_β-8-9-H_β	-0.053 Hz	90°

C. C_1 - C_2 Four-Spin System

The exact same method of analysis used for the C_8-C_8'-C_9-C_9' four-spin system was applied to the analysis of the C_1-C_1'-C_2-C_2' four-spin system. Approximate coupling patterns (Figures 1.43 and 1.46) were derived partly with the aid of 360 MHz ^1H spectra, because of the overlap with interfering lines at 270 MHz. Calculated transition frequencies were considerably more difficult to assign in these cases (Tables 1.7 and 1.8), but the calculated simulations (Figures 1.45 and 1.48) are not unreasonable approximations of the observed spectra.

Consideration of the exact couplings derived from the calculations for the N-methyl case (Figure 1.44) led to an expression for ^3J in this case:

$$^3J(\theta) = 13.78 \cos^2\theta - 1.14 \qquad (11)$$

Application to the calculated couplings for the N-H case (Figure 1.47) led to the following bond angles:

Vicinal Coupling	Calculated J	Calculated Angle
H_{α}-1-2-H_{α}	4.999	48°
H_{α}-1-2-H_{β}	4.296	51°
H_{β}-1-2-H_{α}	4.261	51°
H_{β}-1-2-H_{β}	15.341	0°

D. Proline Seven-Spin Systems

The structural rigidity of the five-membered ring proline accounts for the similarity of appearance in the seven-spin patterns of the two cyclopeptides. Using chemical shift frequencies derived from the 2-D 45° projections and published coupling constants (Figure 1.49),[30] the simulated spectrum of Figure 1.50 was generated. While not an exact match, it was sufficiently close to the actual spectrum that an iterative solution was deemed not worthwhile (because of the large number of transition assignments that would have been necessary).

E. Aromatic Four-Spin Systems

The same procedure outlined above was applied to the analysis of the C_{12}-C_{13}-C_{15}-C_{16} aromatic four-spin systems. Approximate values (Figures 1.51 and 1.54) used for an iterative fit yielded calculated values and spectra (Figure 1.52 - 1.56, Tables 1.9, 1.10).

Despite the availability of x-ray data for the N-methyl cyclopeptide, it was not possible to unambiguously assign any of the aromatic resonances. The patterns are quite unusual though, and a significant change occurs in chemical shifts in going from the N-methyl cyclopeptide to the N-H case.

F. Analysis of Spectral Data of *Cyclo*-[3-(4-β-aminoethyl)phenyloxy-4-methylpentanoyl-L-prolyl], **6c**

No mention has been made yet of the 9-isopropyl substituted N-H cyclopeptide **6c**. Examination of the normal and the two-dimensional homonuclear J-spectra and projections reveal a great deal of similarity to the N-H case **6c** (Figures 1.57 - 1.60). Coupling patterns and chemical shifts are virtually identical except for the substitution of an isopropyl group for the 9-α-H. Thus the configuration at C_9 appears to be the same as in the natural product Ceanothine-B, **4**. The NMR spectrum indicates that the cyclization that produced **6c** resulted in the predominant formation of this isomer (essentially the only isomer by NMR). This is significant from a synthetic standpoint because no resolution of isomers was done prior to the cyclization; only the desired product was formed.

G. Metal Affinity of N-Methyl Cyclopeptide

The NMR data presented above clearly demonstrate a marked difference in conformation between the N-H cyclopeptide **6b** and the N-methyl case **6a**. It was hypothesized that the arrangement of the C_4 and C_7 carbonyls might be a key factor in metal binding, and that because the carbonyls face opposite sides of the ring in the N-methyl case, distinctly different metal affinities would be displayed.

The circular dichroism spectrum of the N-methyl cyclopeptide in the presence of Na^+ and Mg^{2+} is shown in Figure 1.61. Clearly there is a negligible change in the CD upon the addition of Na^+, and there is a slight change upon the addition of Mg^{2+}. As expected then, the N-methyl case **6a** exhibits only slight affinity for the divalent Mg^{2+} in comparison to the N-H case **6b** (Figure 1.7). This is consistent with the proposal that the C_4-C_7 carbonyls face the same side of the ring in the N-H cyclopeptide.

Table 1.4 N-Methyl Cyclopeptide -- Dihedral Angles from X-ray Data

Atoms	Angle	$8.5\cos^2\phi - 0.28$ (0-90°) $9.5\cos^2\phi - 0.28$ (90-180°)
H_α-9-8-H_α	84.3°	-0.2
H_α-9-8-H_β	33.8°	5.589
H_β-9-8-H_α	-157.6°	7.840
H_β-9-8-H_β	84.4°	-0.199
H_α-1-2-H_α	-42.5°	4.340
H_α-1-2-H_β	76.0°	0.217
H_β-1-2-H_α	-160.7°	8.182
H_β-1-2-H_β	-42.5°	4.340

Figure 1.37 Approximate Chemical Shift and Coupling Constant Pattern of the C_8-C_8'-C_9-C_9' Four-Spin Pattern, N-Methyl Cyclopeptide (6a), Used in Simulation Calculations

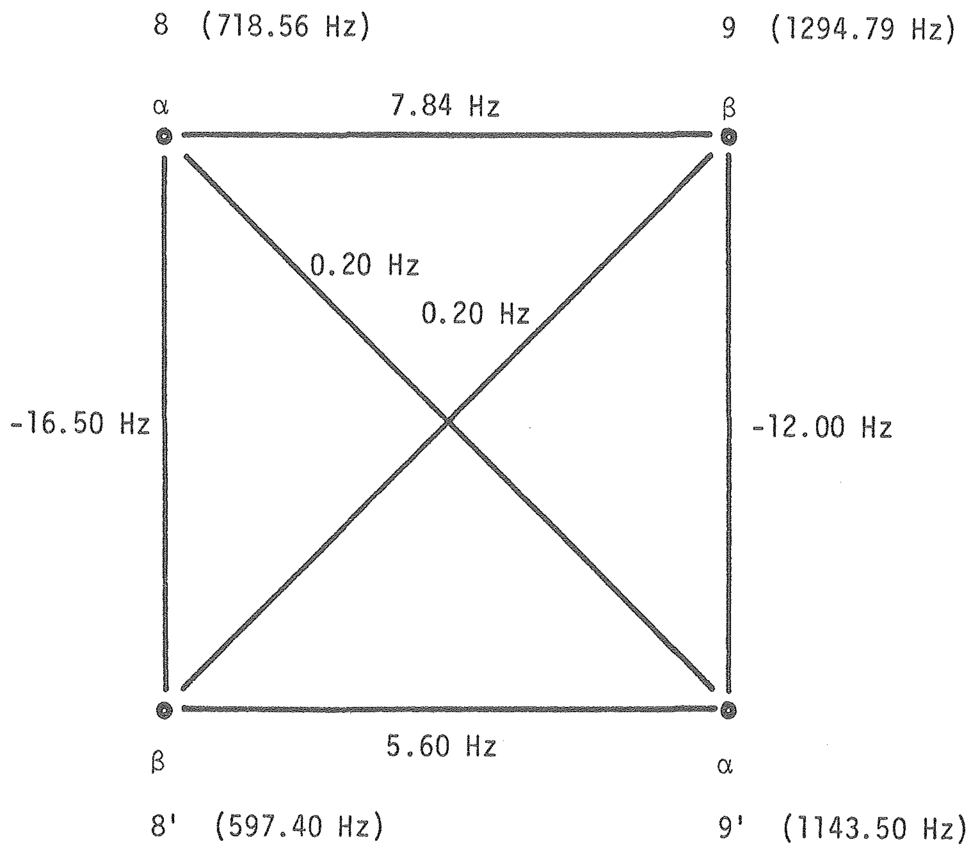
8 (718.56 Hz)
9 (1294.79 Hz)
α
7.84 Hz
β
0.20 Hz
0.20 Hz
-16.50 Hz
-12.00 Hz
β
5.60 Hz
α
8' (597.40 Hz)
9' (1143.50 Hz)

Table 1.5 Calculated Transition Frequencies and Assignment of Observed Lines for the Simulation of the C_8-C_8'-C_9-C_9' Four-Spin System, N-Methyl Cyclopeptide

Transition From	To	Calculated Frequency	Calculated Intensity	Observed Frequency	Obs-Calc Error
10	15	586.270	.853	586.560	.289
5	11	586.576	.862	586.560	-.016
3	9	591.738	.866	591.820	.081
1	4	592.046	.876	591.820	-.226
13	16	602.624	1.126	602.770	.145
8	14	602.931	1.118	602.770	-.161
6	12	608.091	1.152	608.190	.098
2	7	608.400	1.144	608.190	-.210
10	13	704.336	1.115	704.350	.013
3	6	705.998	1.129	706.090	.091
5	8	714.506	1.141	714.340	-.166
1	2	716.165	1.155	716.100	-.065
15	16	720.690	.841	720.830	.139
9	12	722.351	.843	722.340	-.011
11	14	730.861	.885		
4	7	732.519	.887		
7	14	1133.140	.934	1133.060	-.080
4	11	1134.798	.932	1134.680	-.118
2	8	1138.609	.912	1138.690	.080
1	5	1140.268	.910	1140.370	.101
12	16	1144.944	1.093	1144.900	-.044
9	15	1146.604	1.079	1146.590	-.014
6	13	1150.411	1.075	1150.470	.058
3	10	1152.072	1.061	1152.090	.017
7	12	1284.014	1.097	1283.900	-.114
2	6	1284.324	1.098	1284.290	-.033
4	9	1294.182	1.056	1294.050	-.132
1	3	1294.491	1.057	1294.790	.298
14	16	1295.818	.938	1295.610	-.208
8	13	1296.125	.935	1296.250	.124
11	15	1305.989	.909	1305.830	-.159
5	10	1306.294	.906	1306.520	.225

Figure 1.38 Calculated Chemical Shift and Coupling Constant Pattern of the C_8-C_8'-C_9-C_9' Four-Spin Pattern, N-Methyl Cyclopeptide (6a)

Figure 1.39 Top: Calculated Spectrum for the C_8-C_8'-C_9-C_9' Four-Spin Pattern, N-Methyl Cyclopeptide (6a)

Lower: Normal Spectrum

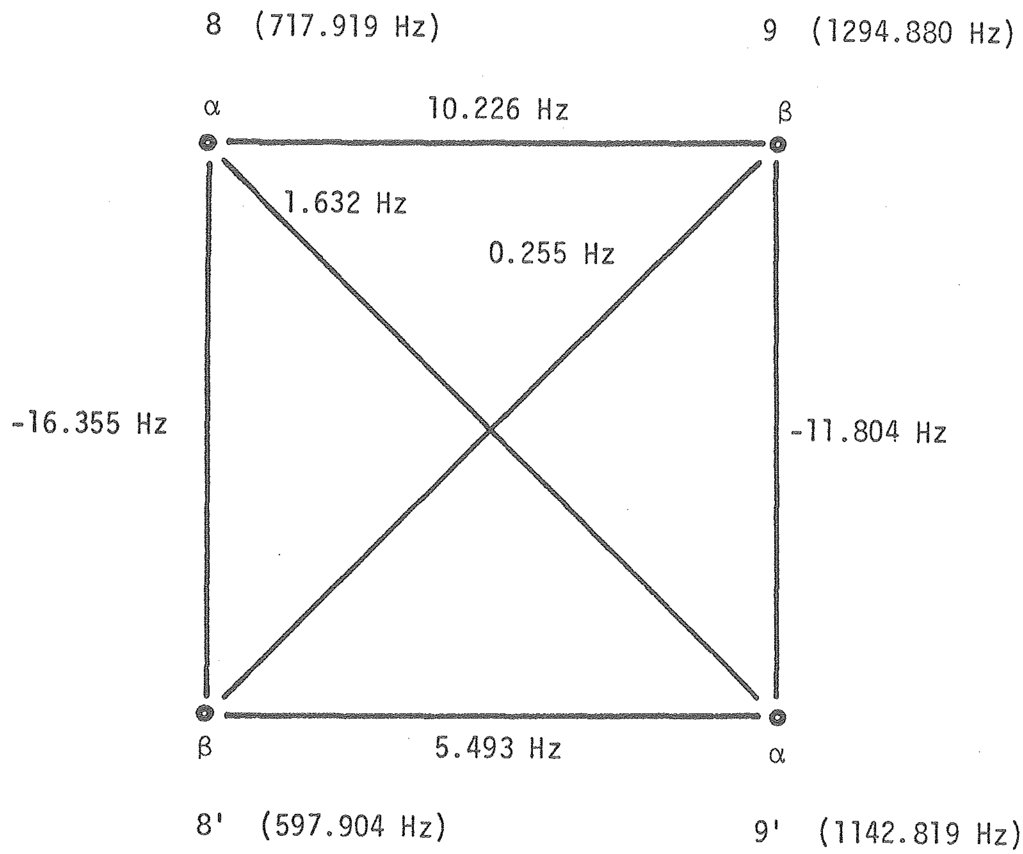
8 (717.919 Hz)
9 (1294.880 Hz)
α
10.226 Hz
β
1.632 Hz
0.255 Hz
-16.355 Hz
-11.804 Hz
β
5.493 Hz
α
8' (597.904 Hz)
9' (1142.819 Hz)

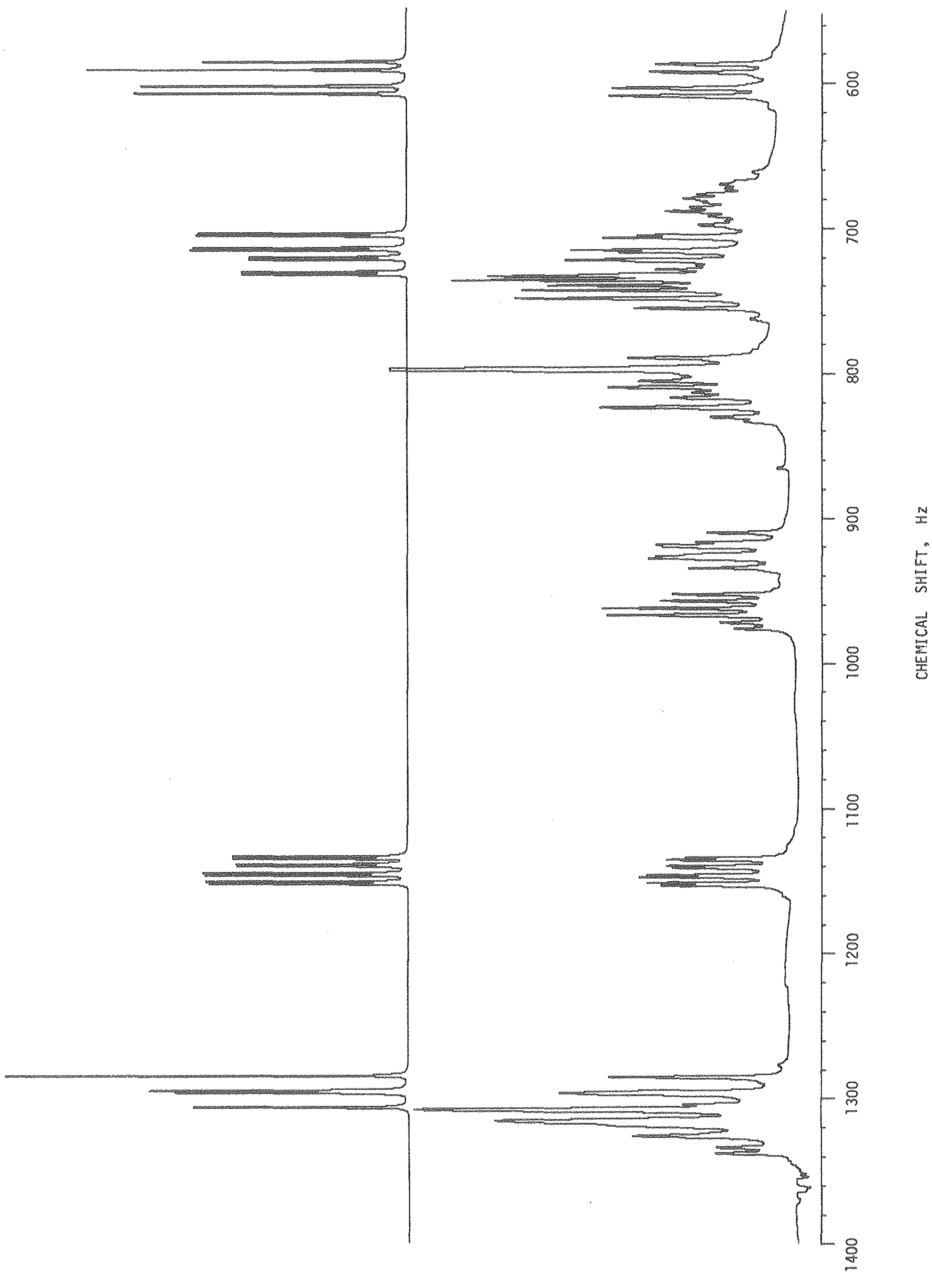

XBL 7910-12568

Figure 1.40 Approximate Chemical Shift and Coupling Constant Pattern of the C_8-C_8'-C_9-C_9' Four-Spin Pattern, N-H Cyclopeptide (6b), Used in Simulation Calculations

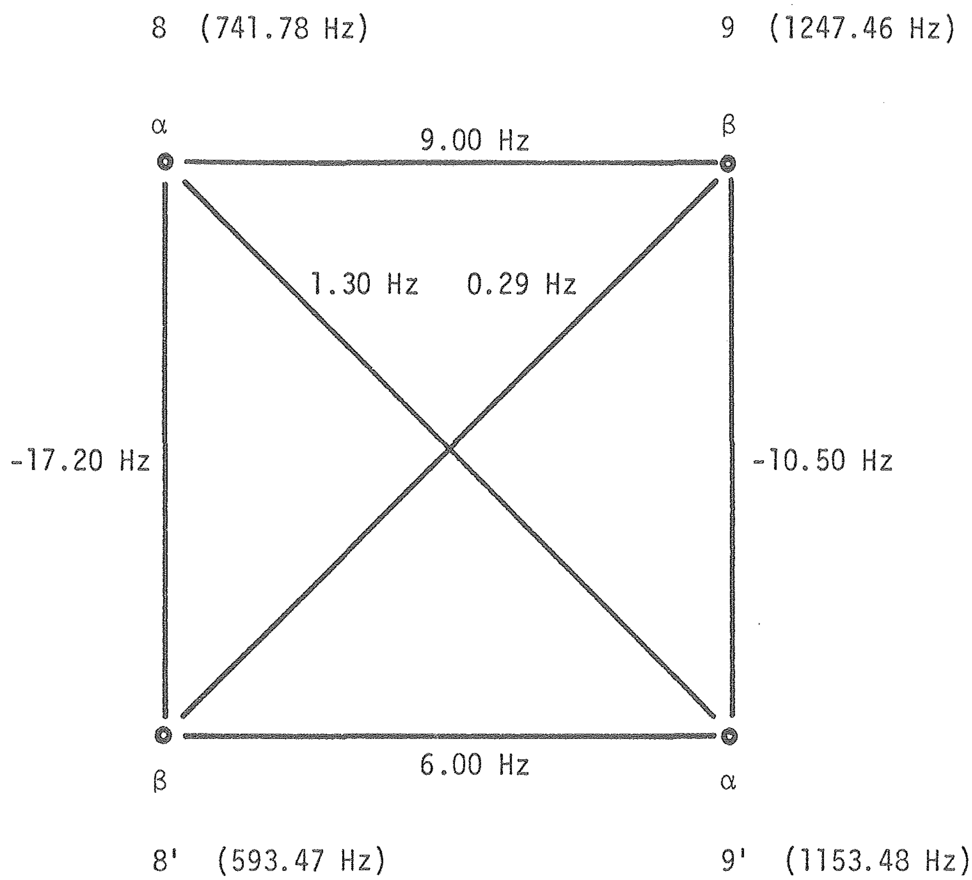

8 (741.78 Hz)
9 (1247.46 Hz)
α
β
9.00 Hz
1.30 Hz
0.29 Hz
-17.20 Hz
-10.50 Hz
β
6.00 Hz
α
8' (593.47 Hz)
9' (1153.48 Hz)

Table 1.6 Calculated Transition Frequencies and Assignment of Observed Lines for the Simulation of the C_8-C_8'-C_9-C_9' Four-Spin System, N-H Cyclopeptide

Transition From	To	Calculated Frequency	Calculated Intensity	Observed Frequency	Obs-Calc Error
5	11	582.354	.881	582.490	.135
10	15	582.358	.875	582.490	.131
1	4	588.226	.897	588.080	-.146
3	9	588.228	.891	588.080	-.148
13	16	599.104	1.103	599.270	.165
8	14	599.104	1.097	599.270	.165
6	12	604.970	1.129	604.820	-.150
2	7	604.972	1.123	604.820	-.152
10	13	727.237	1.090	727.350	.112
3	6	728.740	1.102	728.740	-.000
5	8	737.487	1.124	737.490	.002
1	2	738.987	1.136	738.900	-.087
15	16	743.983	.862	744.040	.056
9	12	745.482	.864	745.530	.047
11	14	754.236	.908	754.220	-.016
4	7	755.733	.911	755.620	-.113
7	14	1143.721	.890	1143.879	.158
4	11	1145.218	.896	1145.300	.081
2	8	1149.589	.862	1149.600	.010
1	5	1151.090	.869	1151.050	-.040
12	16	1155.078	1.137	1154.240	-.838
9	15	1156.577	1.117		
6	13	1160.944	1.123	1161.460	.515
3	10	1162.447	1.102	1162.560	.112
7	12	1237.032	1.144	1236.940	-.092
2	6	1237.034	1.150	1236.940	-.094
1	3	1247.281	1.095		
4	9	1247.283	1.090	1247.260	-.023
14	16	1248.389	.896		
8	13	1248.389	.889	1248.360	-.029
5	10	1258.638	.863	1258.760	.121
11	15	1258.642	.869	1258.760	.117

Figure 1.41 Calculated Chemical Shift and Coupling Constant Pattern of the C_8-C_8'-C_9-C_9' Four-Spin Pattern, N-H Cyclopeptide (**6b**)

Figure 1.42 Top: Calculated Spectrum for the C_8-C_8'-C_9-C_9' Four-Spin Pattern, N-H Cyclopeptide (**6b**)

Lower: Normal Spectrum

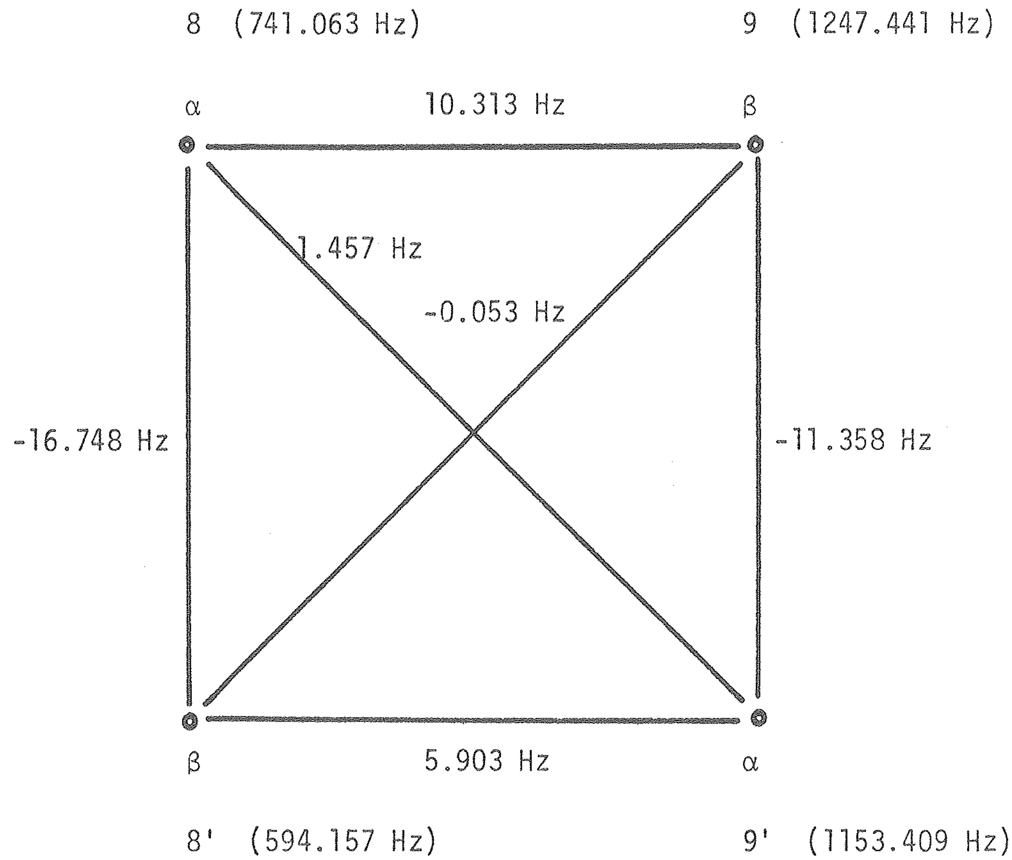
8 (741.063 Hz)
9 (1247.441 Hz)
α
10.313 Hz
β
1.457 Hz
-0.053 Hz
-16.748 Hz
-11.358 Hz
β
5.903 Hz
α
8' (594.157 Hz)
9' (1153.409 Hz)

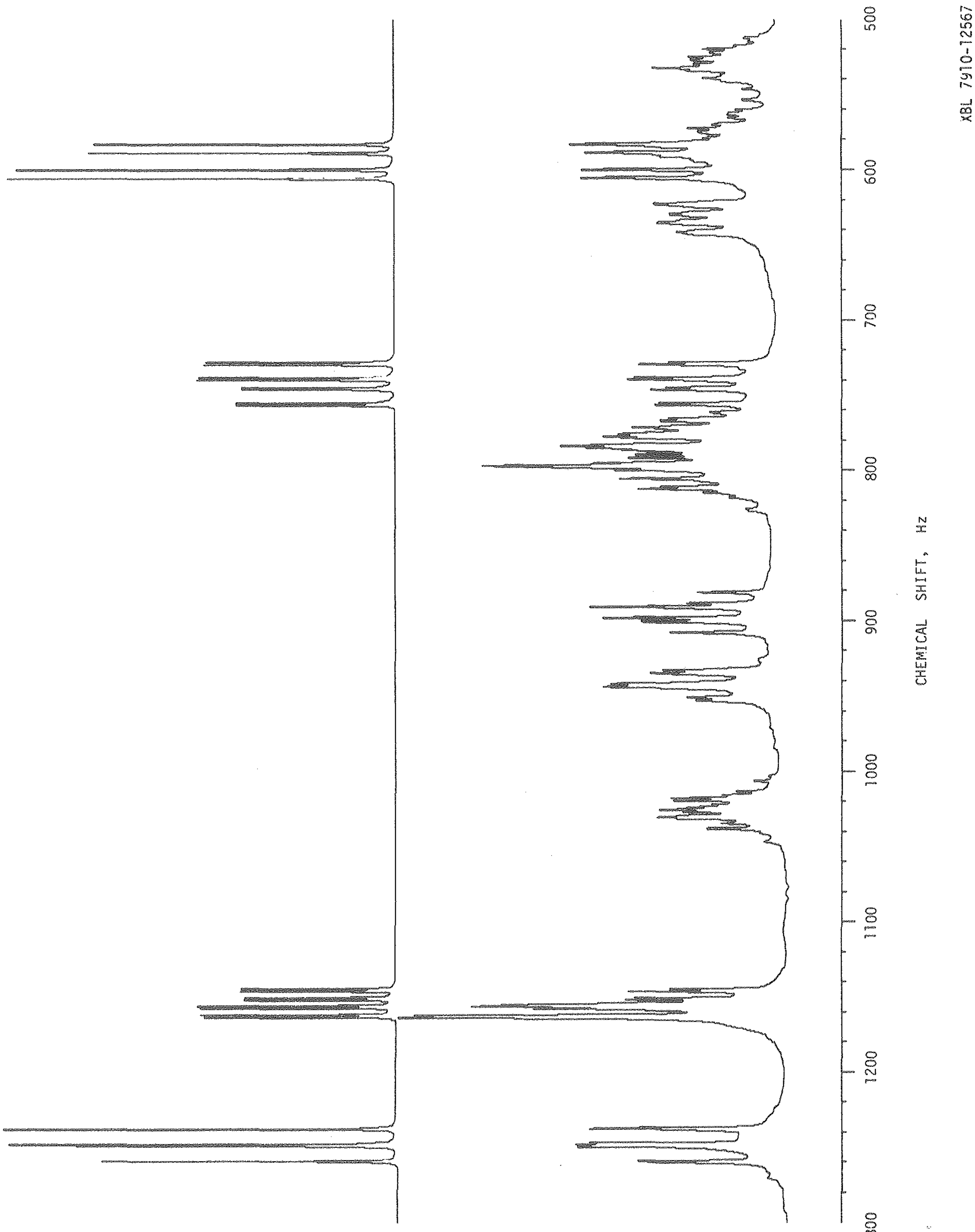
500
600
700
800
900
1000
1100
1200
1300
CHEMICAL SHIFT, Hz
XBL 7910-12567

Figure 1.43 Approximate Chemical Shift and Coupling Constant Pattern of the C_1-C_1'-C_2-C_2' Four-Spin Pattern, N-Methyl Cyclopeptide (6a), Used in Simulation Calculations

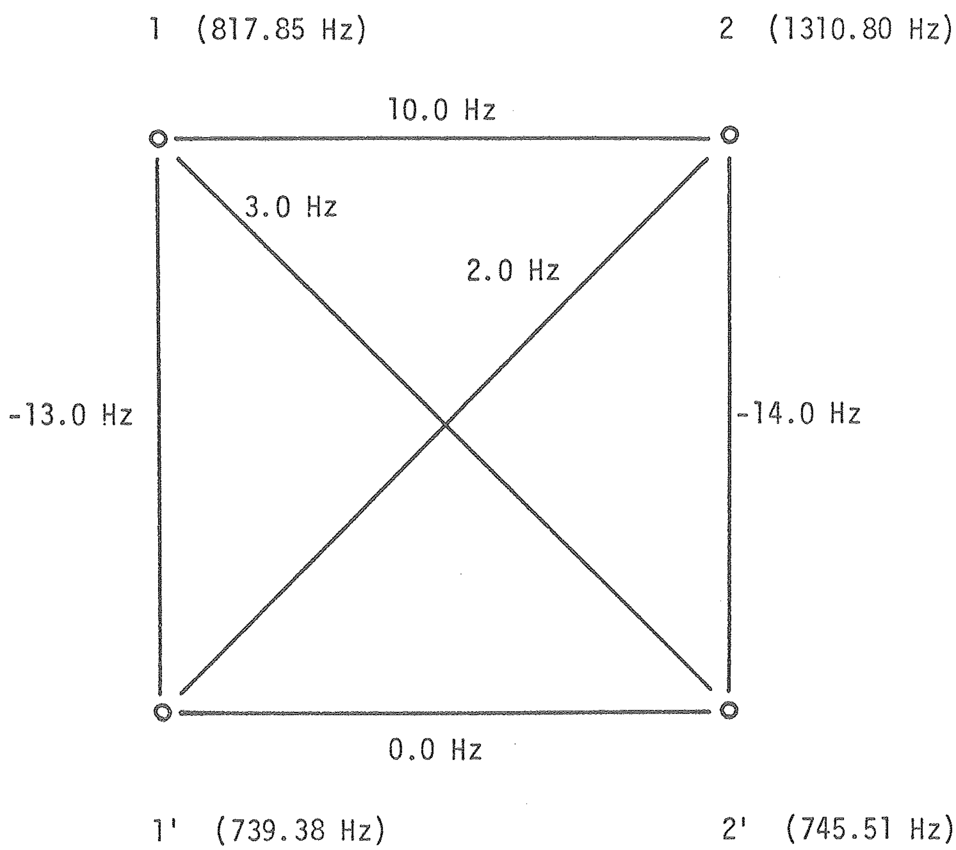
1 (817.85 Hz)
2 (1310.80 Hz)
10.0 Hz
3.0 Hz
2.0 Hz
-13.0 Hz
-14.0 Hz
0.0 Hz
1' (739.38 Hz)
2' (745.51 Hz)

Table 1.7 Calculated Transition Frequencies and Assignment of Observed Lines for the Simulation of the C_1-C_1'-C_2-C_2' Four-Spin System, N-Methyl Cyclopeptide

Transition From	To	Calculated Frequency	Calculated Intensity	Observed Frequency	Obs-Calc Error
3	9	726.879	.849		
10	15	726.886	.864		
7	14	727.061	.883		
2	8	727.071	.907		
5	11	732.107	1.164	732.320	.212
1	4	732.117	.603	732.320	.202
4	11	733.746	.735	735.110	1.363
1	5	733.756	1.323	735.110	1.353
6	12	737.833	1.174	738.650	.816
13	16	737.840	1.072	738.650	.809
8	14	743.130	1.160	742.180	-.950
2	7	743.140	1.111	742.180	-.960
6	13	748.314	.850	747.400	-.914
12	16	748.322	.999	747.400	-.922
3	10	754.949	1.179	754.460	-.489
9	15	754.956	1.119	754.460	-.496
10	13	805.057	1.245		
3	6	811.692	.973		
15	16	816.012	.933		
5	8	816.477	1.205		
9	12	822.646	.751		
1	2	823.162	1.070	822.850	-.312
11	14	827.499	.950	829.300	1.800
4	7	834.185	.824	832.670	-1.515
7	12	1297.486	1.069		
2	6	1302.793	1.050		
4	9	1309.024	1.000	1306.520	-2.504
1	3	1314.263	1.003	1313.920	-.343
14	16	1318.747	.993	1318.130	-.617
8	13	1324.036	.974	1324.970	.933
11	15	1330.235	.949	1331.720	1.484
5	10	1335.456	.913	1336.510	1.053

Figure 1.44 Calculated Chemical Shift and Coupling Constant Pattern of the C_1-C_1'-C_2-C_2' Four-Spin Pattern, N-Methyl Cyclopeptide (6a)

Figure 1.45 Top: Calculated Spectrum for the C_1-C_1'-C_2-C_2' Four-Spin Pattern, N-Methyl Cyclopeptide (6a)

Lower: Normal Spectrum

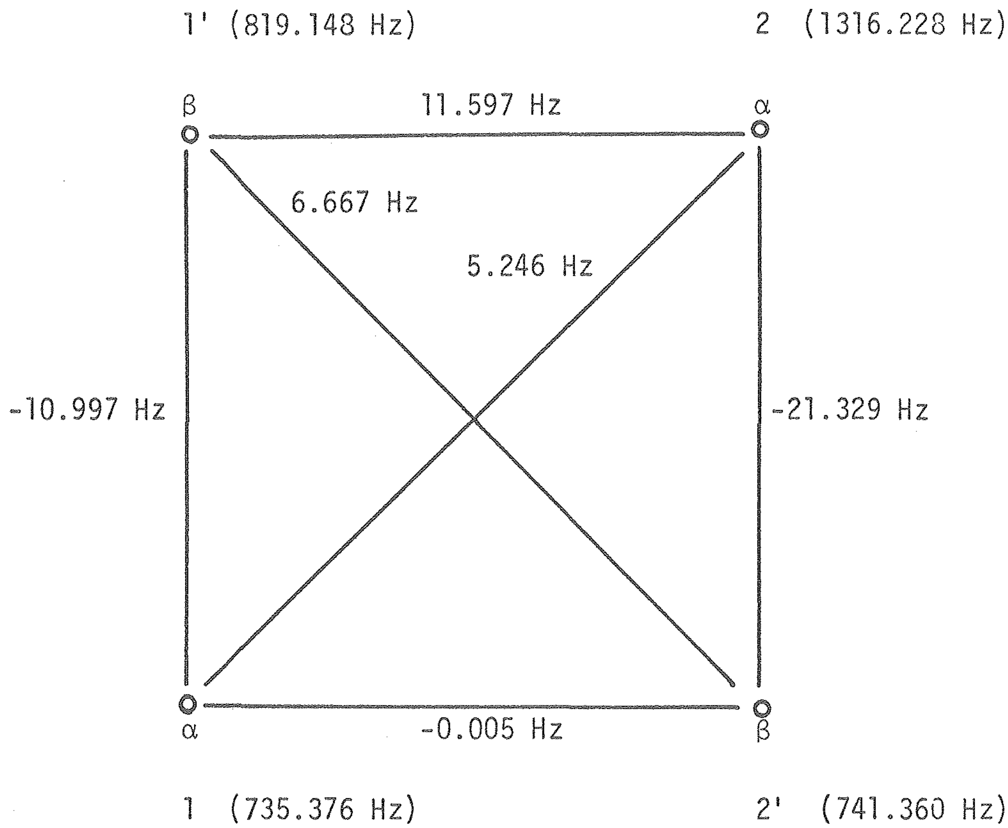

1' (819.148 Hz)
2 (1316.228 Hz)
β
11.597 Hz
α
6.667 Hz
5.246 Hz
-10.997 Hz
-21.329 Hz
α
-0.005 Hz
β
1 (735.376 Hz)
2' (741.360 Hz)

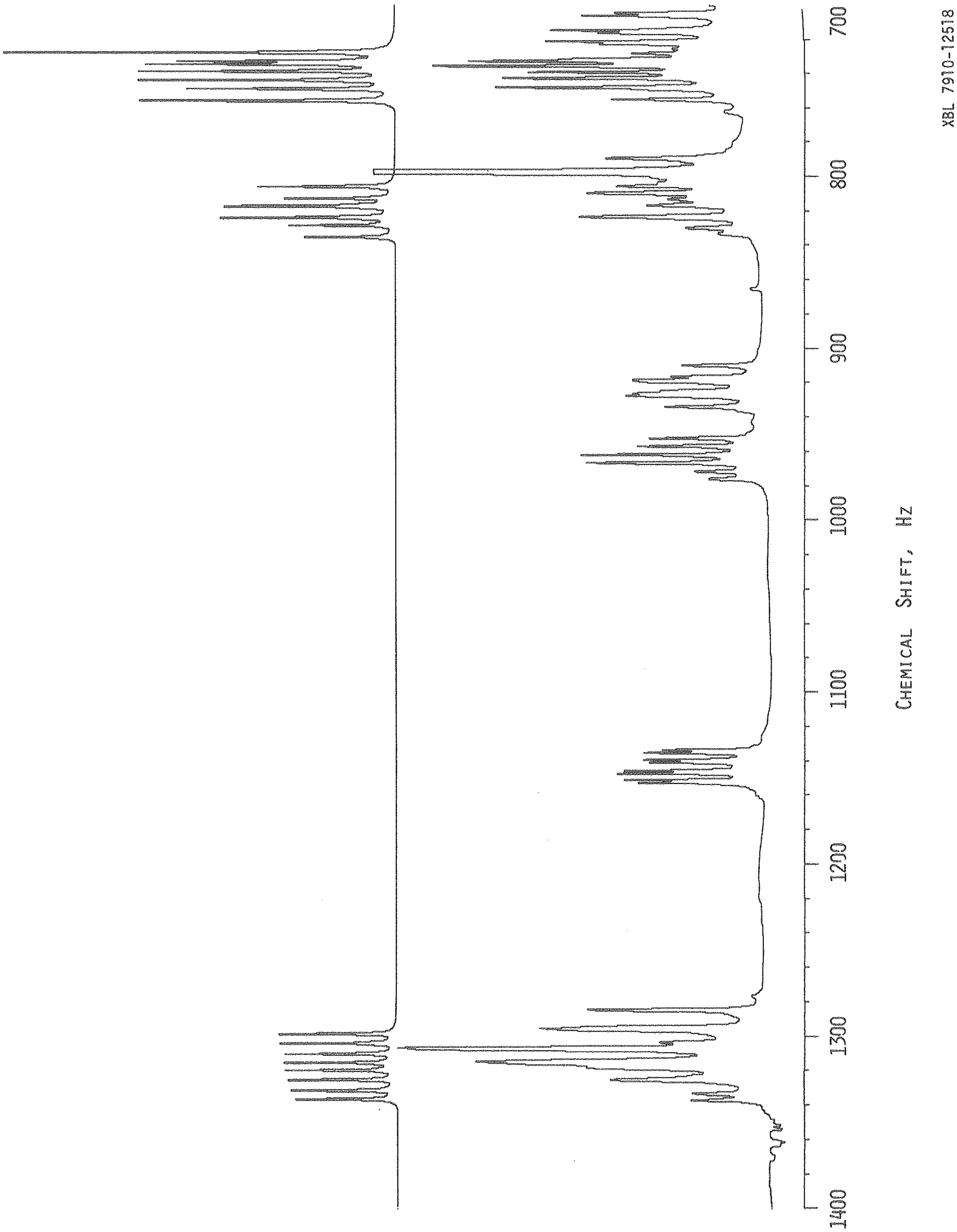
700
800
900
1000
1100
1200
1300
1400
CHEMICAL SHIFT, Hz
XBL 7910-12518

Figure 1.46 Approximate Chemical Shift and Coupling Constant Pattern of the C_1-C_1'-C_2-C_2' Four-Spin Pattern, N-H Cyclopeptide (6b), Used in Simulation Calculations

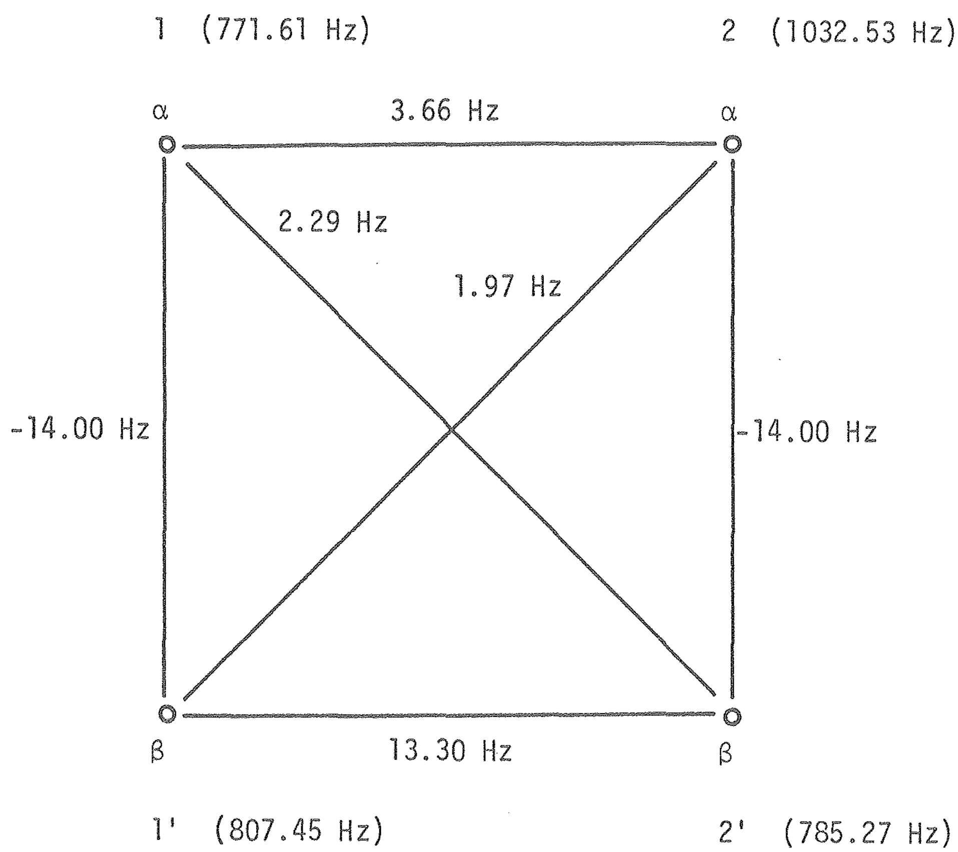
1 (771.61 Hz)
2 (1032.53 Hz)
α
3.66 Hz
α
2.29 Hz
1.97 Hz
-14.00 Hz
-14.00 Hz
β
13.30 Hz
β
1' (807.45 Hz)
2' (785.27 Hz)

Table 1.8 Calculated Transition Frequencies and Assignment of Observed Lines for the Simulation of the C_1-C_1'-C_2-C_2' Four-Spin System, N-H Cyclopeptide

Transition From	To	Calculated Frequency	Calculated Intensity	Observed Frequency	Obs-Calc Error
9	13	745.004	.041		
10	13	761.800	.548		
3	6	762.644	.697		
5	8	764.239	.524		
7	14	764.854	.202		
1	2	767.629	.755		
4	11	768.244	.762		
15	16	770.222	.486	772.170	1.947
9	12	771.066	.962	772.170	1.103
11	14	778.202	1.937	775.710	-2.492
12	16	779.849	1.488		
9	15	780.693	.106		
2	8	780.896	1.262		
4	7	781.591	.874		
1	5	784.286	1.550	783.630	-.656
10	12	787.862	1.237		
6	13	792.897	1.493	793.170	.272
3	10	793.741	2.204	794.770	1.028
5	11	795.457	2.053	794.770	-.687
10	15	797.488	1.380	797.470	-.018
13	16	805.911	1.041	804.240	-1.671
5	7	808.804	.048		
8	14	809.419	.842	810.690	1.270
3	9	810.537	.108	810.690	.152
1	4	811.499	.682	810.690	-.809
2	11	812.113	.080		
6	12	818.959	.228		
2	7	825.460	.359		
4	10	1001.967	.118		
7	12	1008.238	.590		
2	6	1014.739	1.052		
7	15	1017.864	.476		
4	9	1018.762	.920	1019.620	.857
1	3	1019.724	1.010	1019.620	-.104
11	12	1021.585	.461		
14	16	1023.232	.983	1021.310	-1.922
8	13	1026.740	.942	1025.940	-.800
5	10	1029.179	.842	1029.880	.700
11	15	1031.211	.494	1032.490	1.278
5	9	1045.975	.081		

Figure 1.47 Calculated Chemical Shift and Coupling Constant Pattern of the C_1-C_1'-C_2-C_2' Four-Spin Pattern, N-H Cyclopeptide (6b)

Figure 1.48 Top: Calculated Spectrum for the C_1-C_1'-C_2-C_2' Four-Spin Pattern, N-H Cyclopeptide (6b)

Lower: Normal Spectrum

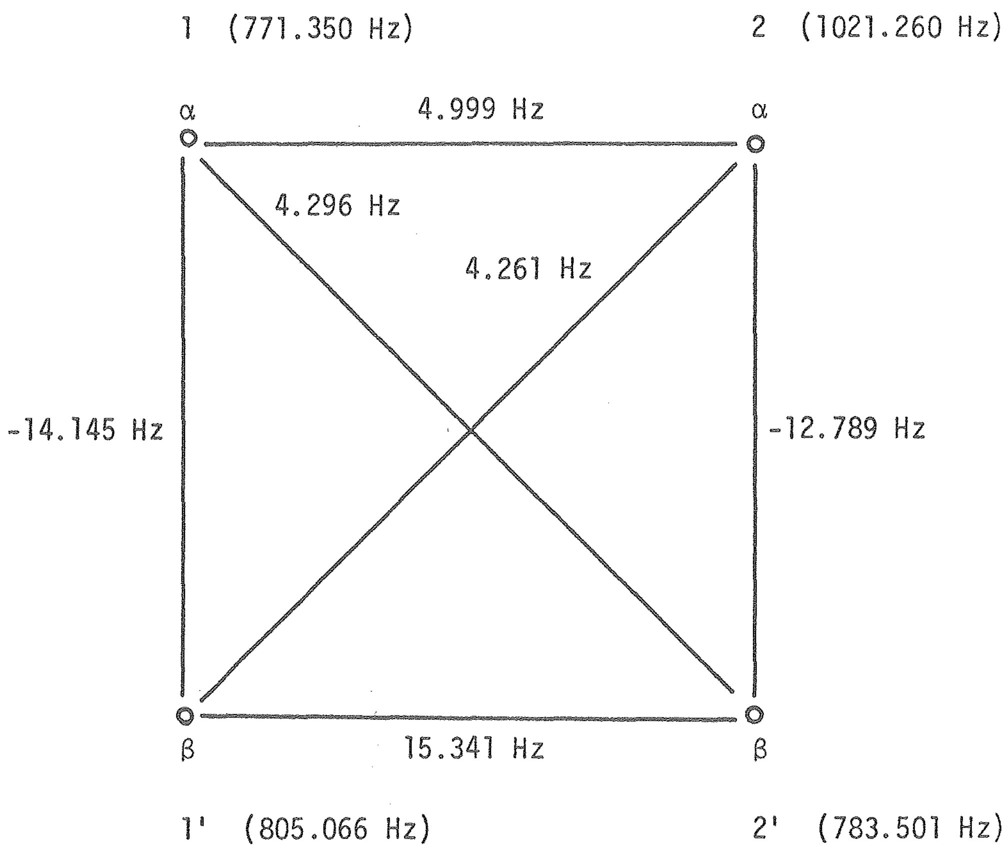
1 (771.350 Hz)
2 (1021.260 Hz)
α
4.999 Hz
α
4.296 Hz
4.261 Hz
-14.145 Hz
-12.789 Hz
β
15.341 Hz
β
1' (805.066 Hz)
2' (783.501 Hz)

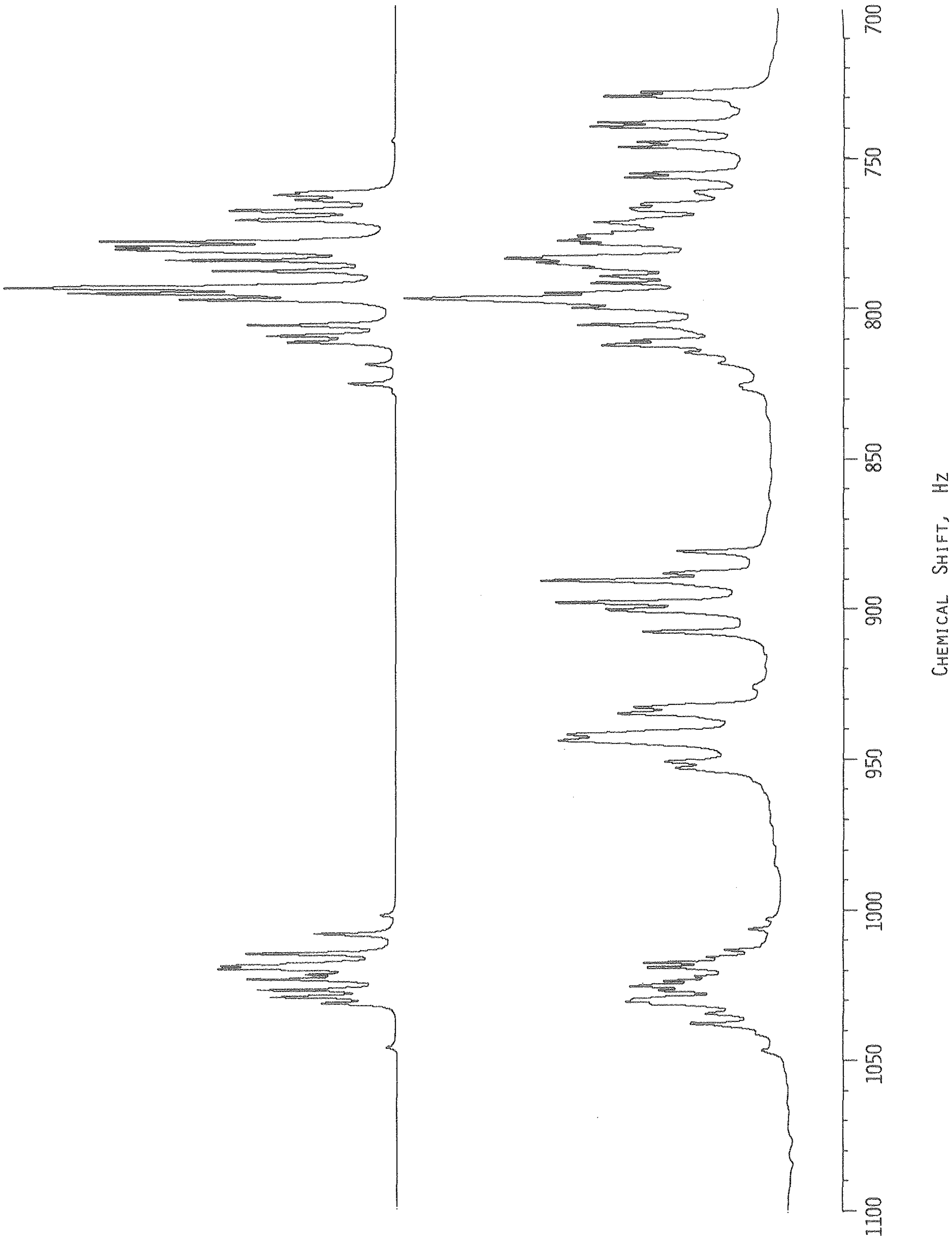

XBL 7910-12519

Figure 1.49 Approximate Chemical Shift and Coupling Constant Pattern of the C_5-C_{17}-C_{17}'-C_{18}-C_{18}'-C_{19}-C_{19}' Seven-Spin Prolyl Pattern, N-Methyl Cyclopeptide (6a), Used in Simulation Calculations

Figure 1.50 Top: Approximate Calculated Spectrum for the C_5-C_{17}-C_{17}'-C_{18}-C_{18}'-C_{19}-C_{19}' Seven-Spin Prolyl Pattern, N-Methyl Cyclopeptide (6a) Using Values from Figure 1.49

Lower: Normal Spectrum

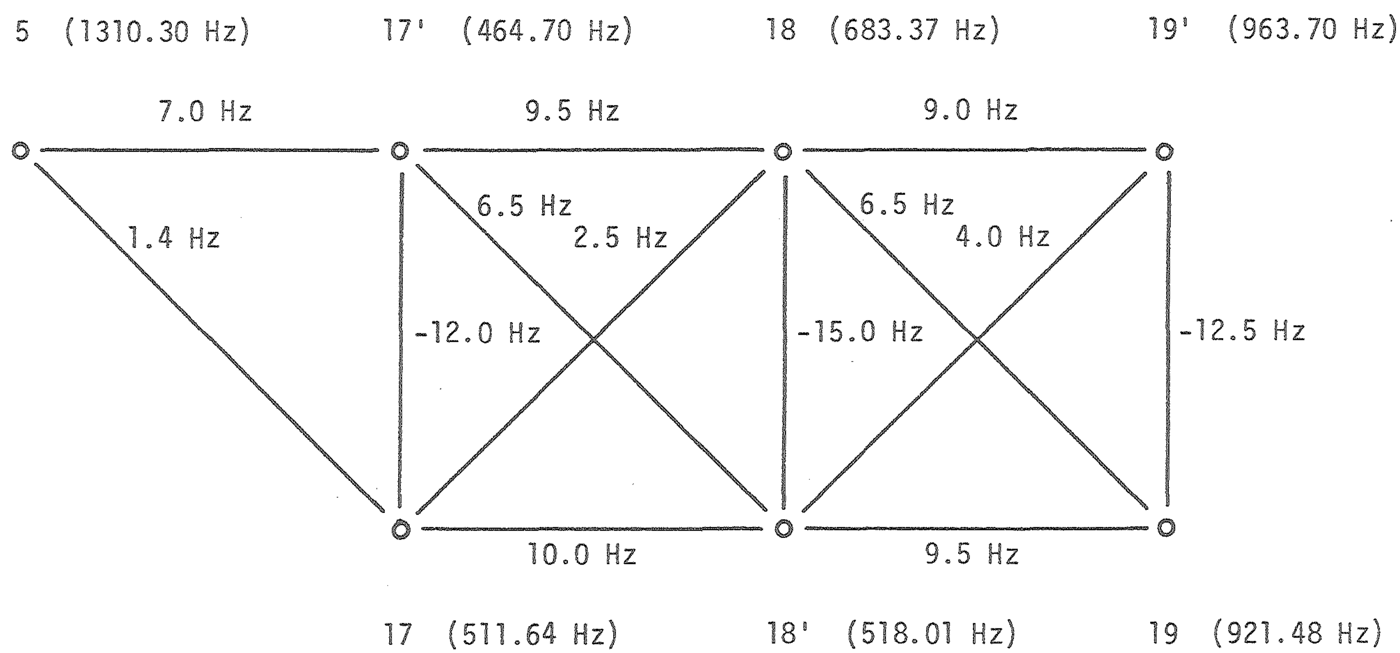
5 (1310.30 Hz)
17' (464.70 Hz)
18 (683.37 Hz)
19' (963.70 Hz)
7.0 Hz
9.5 Hz
9.0 Hz
1.4 Hz
6.5 Hz
2.5 Hz
6.5 Hz
4.0 Hz
-12.0 Hz
-15.0 Hz
-12.5 Hz
10.0 Hz
9.5 Hz
17 (511.64 Hz)
18' (518.01 Hz)
19 (921.48 Hz)

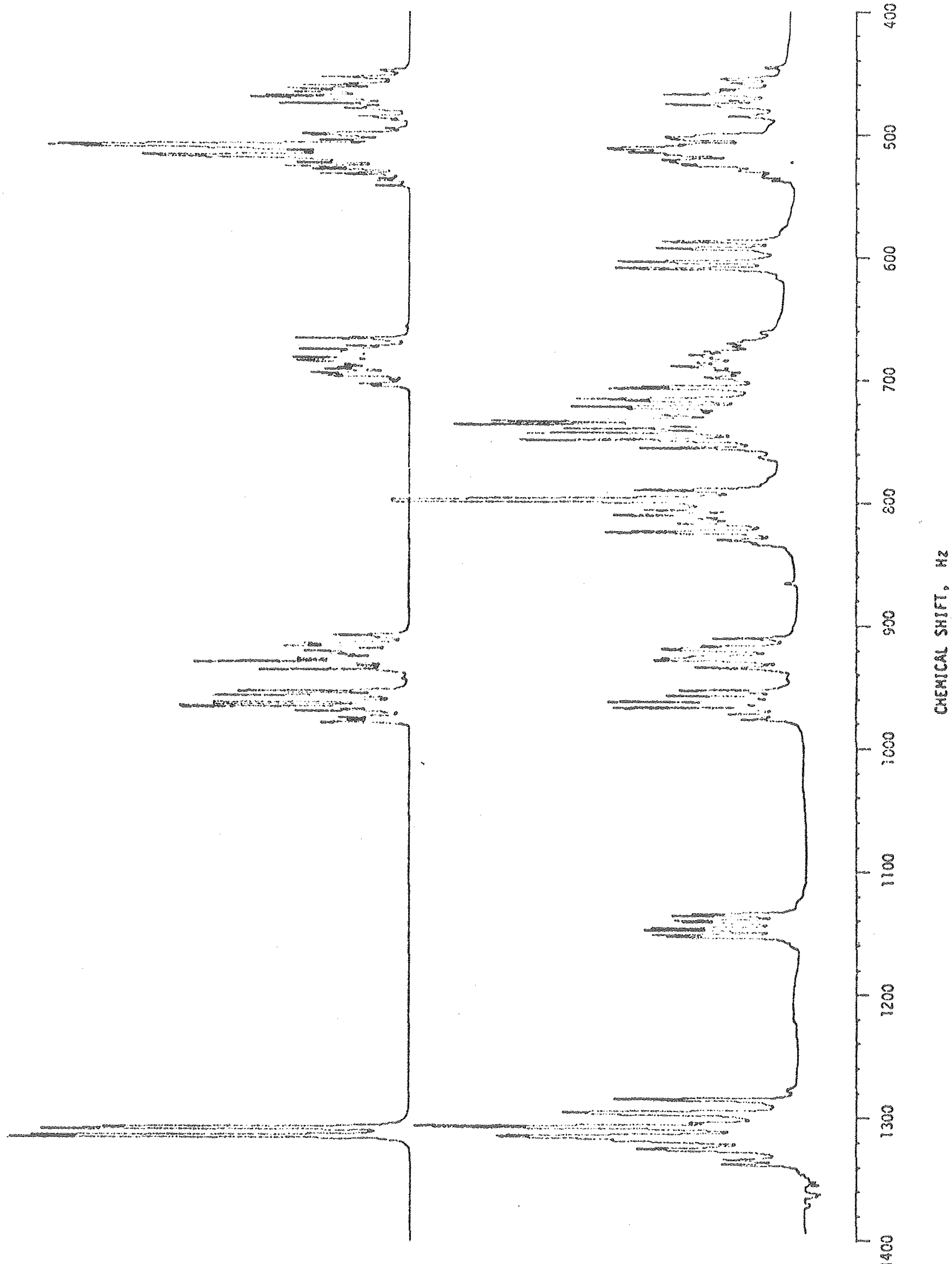

CHEMICAL SHIFT, Hz
400
500
600
700
800
900
1000
1100
1200
1300
1400

Figure 1.51 Approximate Chemical Shift and Coupling Constant Pattern of the C_{12}-C_{13}-C_{15}-C_{16} Four-Spin Aromatic Pattern, N-Methyl Cyclopeptide (6a), Used in Simulation Calculations

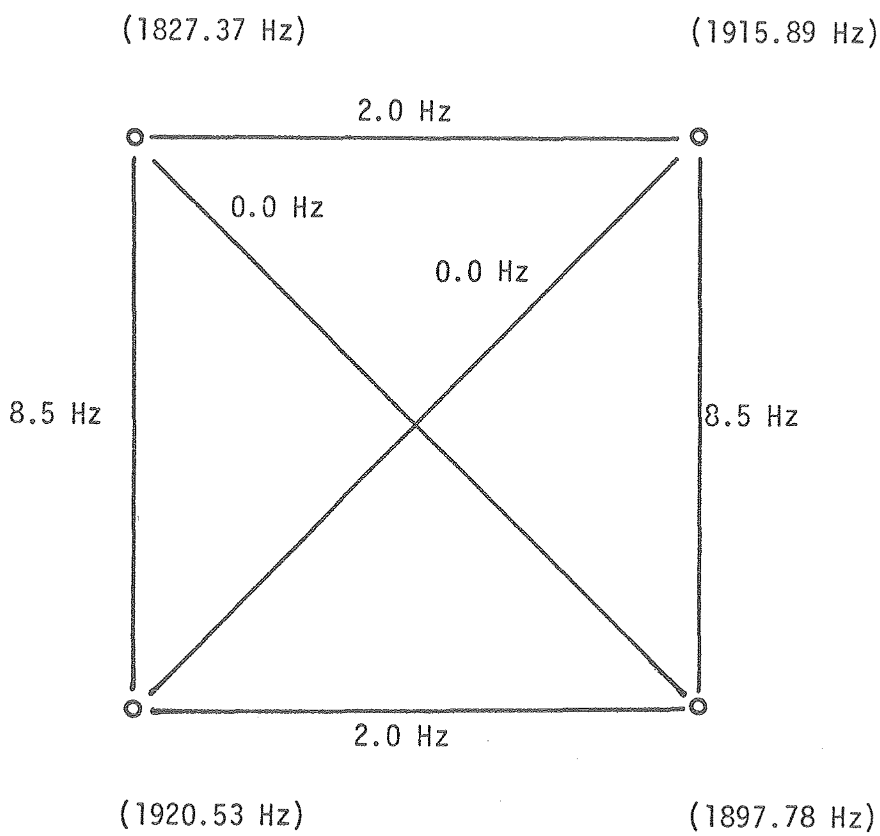
(1827.37 Hz)
(1915.89 Hz)
2.0 Hz
0.0 Hz
0.0 Hz
8.5 Hz
8.5 Hz
2.0 Hz
(1920.53 Hz)
(1897.78 Hz)

Table 1.9 Calculated Transition Frequencies and Assignment of Observed Lines for the C_{12}-C_{13}-C_{15}-C_{16} Four-Spin Aromatic System, N-Methyl Cyclopeptide

Transition From	To	Calculated Frequency	Calculated Intensity	Observed Frequency	Obs-Calc Error
9	12	1821.265	.884	1821.380	.114
15	16	1821.292	.887	1821.380	.087
4	7	1823.746	.838	1823.810	.063
11	14	1823.867	.935	1823.810	-.057
4	6	1824.945	.097		
3	7	1828.468	.106		
10	13	1829.544	1.053	1829.590	.045
3	6	1829.668	.946	1829.590	-.078
5	8	1832.063	1.117	1831.990	-.073
1	2	1832.092	1.120	1831.990	-.102
9	15	1892.901	.553	1892.800	-.101
12	16	1892.928	.460	1892.800	-.128
6	13	1894.810	.502	1894.860	.049
3	10	1894.933	.608	1894.860	-.073
6	14	1899.897	.043		
4	11	1900.975	1.287	1901.020	.044
7	14	1901.097	1.254	1901.020	-.077
2	8	1902.978	1.709	1903.140	.161
1	5	1903.007	1.538	1903.140	.132
14	16	1910.411	1.364	1910.590	.178
8	13	1910.472	1.699	1910.590	.117
11	15	1912.986	1.349	1912.970	-.016
5	10	1912.991	1.430	1912.970	-.021
13	16	1915.498	1.287	1915.610	.111
8	14	1915.559	1.128	1915.610	.050
6	12	1917.380	1.347	1917.230	-.150
2	7	1917.441	.565	1917.230	-.211
7	12	1918.579	.225	1918.340	-.239
2	6	1918.640	.846	1918.340	-.300
4	9	1921.060	.683	1921.190	.129
1	3	1921.065	.430	1921.190	.124
10	15	1923.750	.984	1923.800	.049
5	11	1923.755	.987	1923.800	.044
3	9	1925.783	.754	1925.850	.066
1	4	1925.787	.909	1925.850	.062

Figure 1.52 Calculated Chemical Shift and Coupling Constant Pattern of the C_{12}-C_{13}-C_{15}-C_{16} Four-Spin Aromatic Pattern, N-Methyl Cyclopeptide (6a)

Figure 1.53 Top: Calculated Spectrum for the C_{12}-C_{13}-C_{15}-C_{16} Four-Spin Aromatic Pattern, N-Methyl Cyclopeptide (6a)

Lower: Normal Spectrum

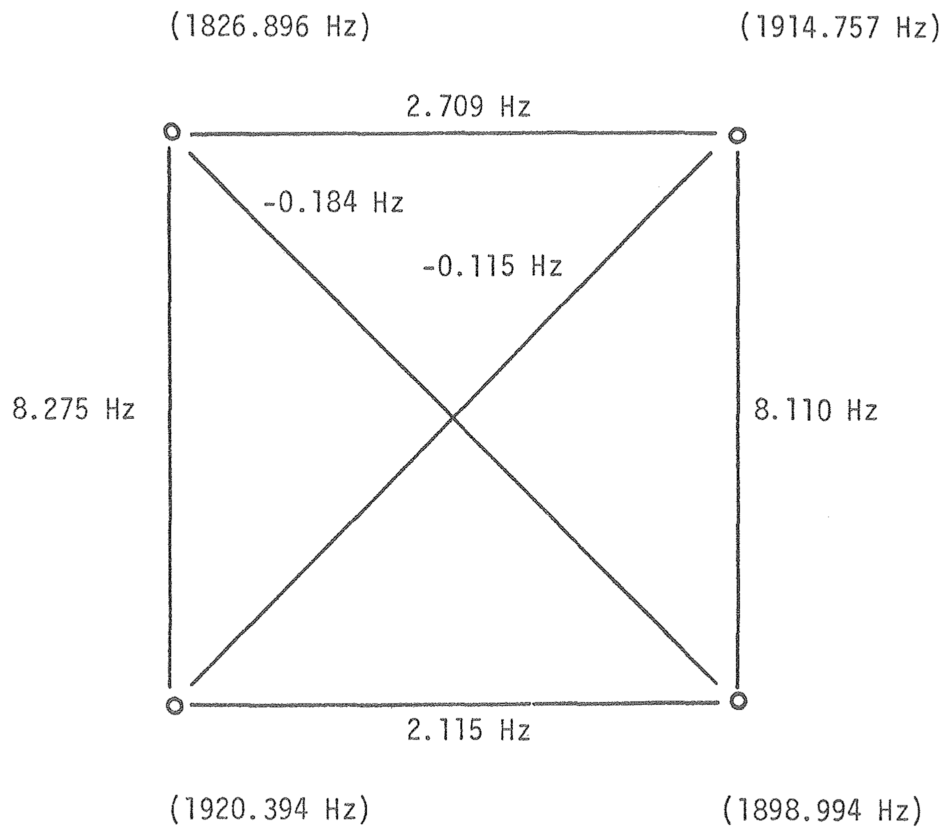

(1826.896 Hz)
(1914.757 Hz)
2.709 Hz
-0.184 Hz
-0.115 Hz
8.275 Hz
8.110 Hz
2.115 Hz
(1920.394 Hz)
(1898.994 Hz)

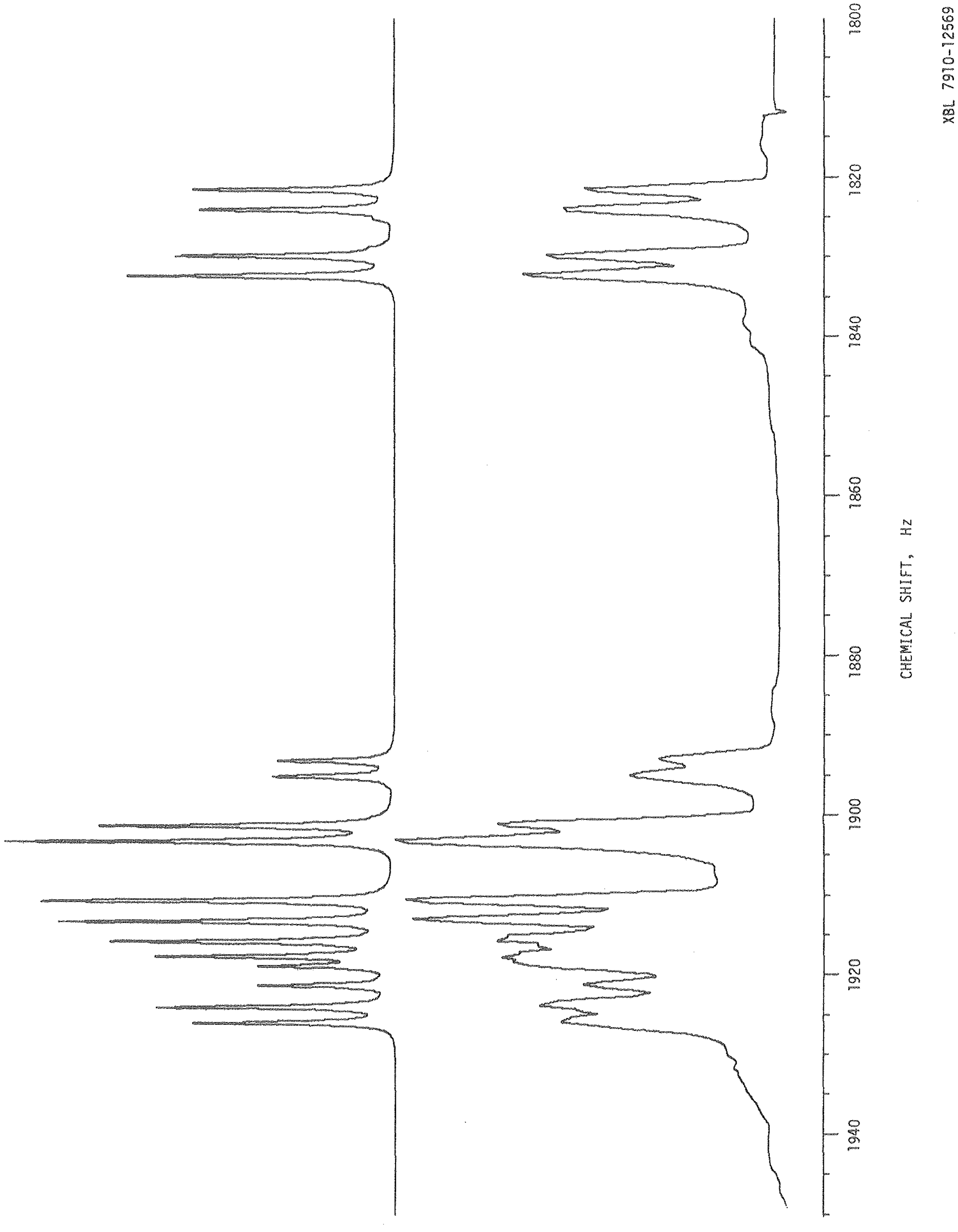
1800
1820
1840
1860
1880
1900
1920
1940
CHEMICAL SHIFT, Hz
XBL 7910-12569

Figure 1.54 Approximate Chemical Shift and Coupling Constant Pattern of the C_{12}-C_{13}-C_{15}-C_{16} Four-Spin Aromatic Pattern, N-H Cyclopeptide (6b), Used in Simulation Calculations

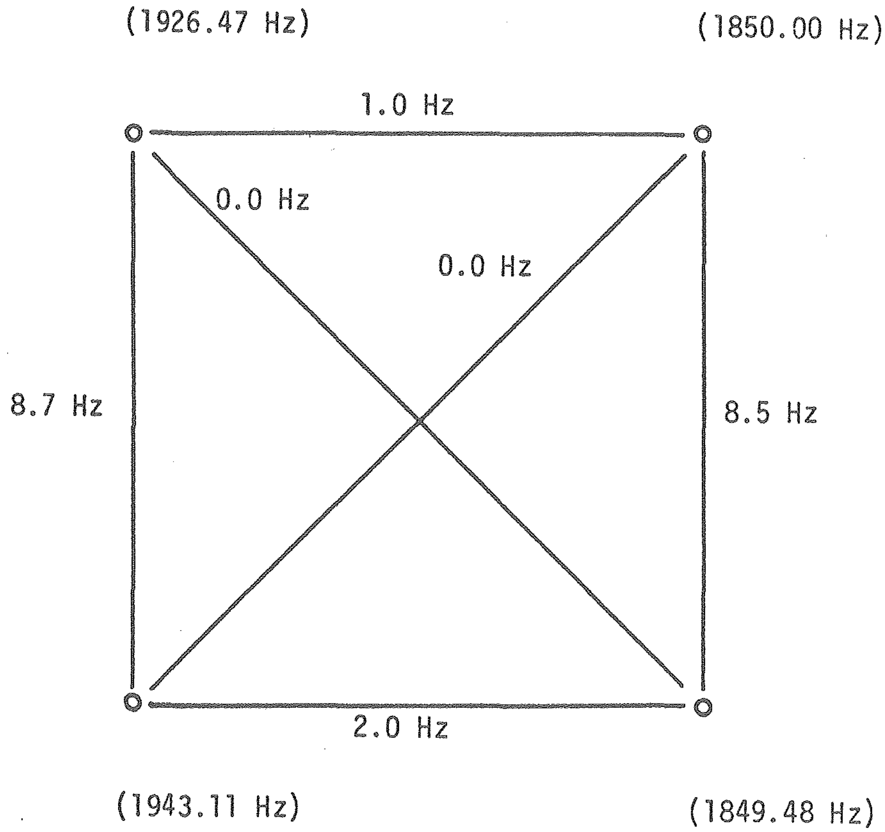
(1926.47 Hz)
(1850.00 Hz)
1.0 Hz
0.0 Hz
0.0 Hz
8.7 Hz
8.5 Hz
2.0 Hz
(1943.11 Hz)
(1849.48 Hz)

Table 1.10 Calculated Transition Frequencies and Assignment of Observed Lines for the C_{12}-C_{13}-C_{15}-C_{16} Four-Spin Aromatic System, N-H Cyclopeptide

Transition From	To	Calculated Frequency	Calculated Intensity	Observed Frequency	Obs-Calc Error
12	16	1848.592	1.941	1848.290	-.302
7	12	1848.727	1.947	1848.290	-.436
11	15	1848.998	1.962	1849.480	.481
4	11	1849.133	1.970	1849.480	.346
6	13	1849.871	1.991	1849.480	-.391
2	6	1849.974	1.995	1849.480	-.494
5	10	1850.276	2.020	1850.720	.443
1	5	1850.382	2.027	1850.720	.337
15	16	1920.499	.473	1920.940	.440
9	14	1920.891	.484	1920.940	.048
11	12	1920.905	.485	1920.940	.034
4	7	1921.311	.525	1920.940	-.371
5	8	1921.810	.051		
10	13	1928.961	1.545	1929.390	.428
3	8	1929.355	1.449	1929.390	.034
5	6	1929.366	1.447	1929.390	.023
1	2	1929.774	1.453	1929.390	-.384
13	16	1936.626	1.563	1936.640	.013
3	6	1936.911	.053		
8	14	1937.889	1.493	1937.860	-.029
6	12	1937.906	1.504	1937.860	-.046
2	7	1939.153	1.436	1939.080	-.073
10	15	1945.088	.492	1944.960	-.128
3	9	1946.353	.490	1946.350	-.003
5	11	1946.367	.505	1946.350	-.017
1	4	1947.616	.507	1947.680	.063

Figure 1.55 Calculated Chemical Shift and Coupling Constant Pattern of the C_{12}-C_{13}-C_{15}-C_{16} Four-Spin Aromatic Pattern, N-H Cyclopeptide (6b)

Figure 1.56 Top: Calculated Spectrum for the C_{12}-C_{13}-C_{15}-C_{16} Four-Spin Aromatic Pattern, N-H Cyclopeptide (6b)

Lower: Normal Spectrum

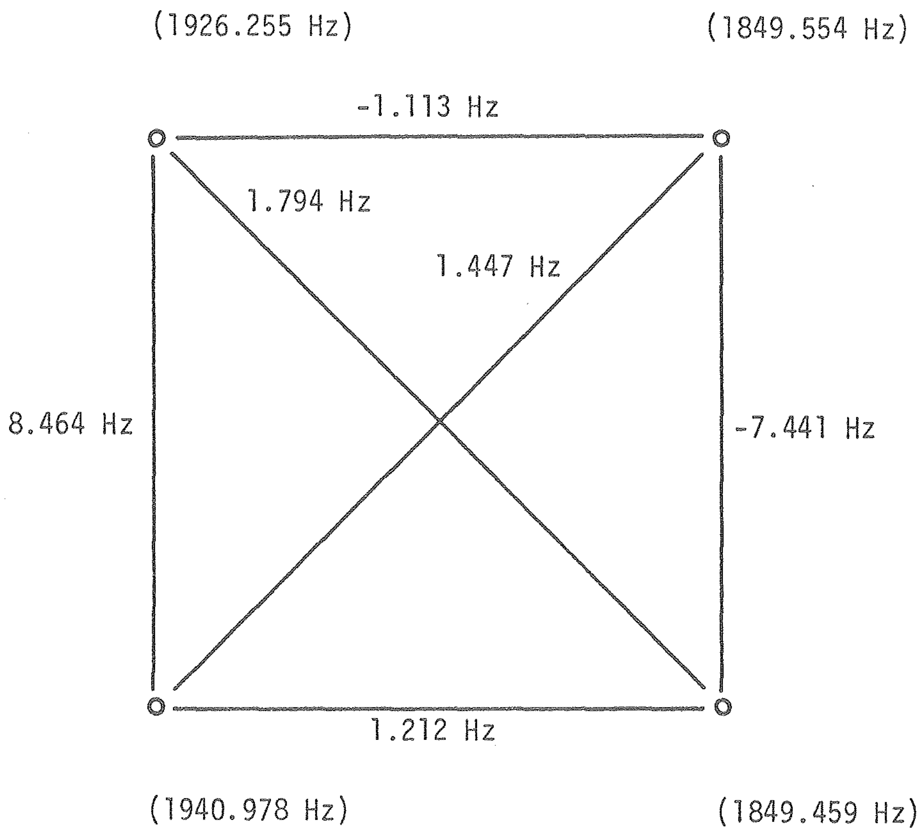
(1926.255 Hz)
(1849.554 Hz)
-1.113 Hz
1.794 Hz
1.447 Hz
8.464 Hz
-7.441 Hz
1.212 Hz
(1940.978 Hz)
(1849.459 Hz)

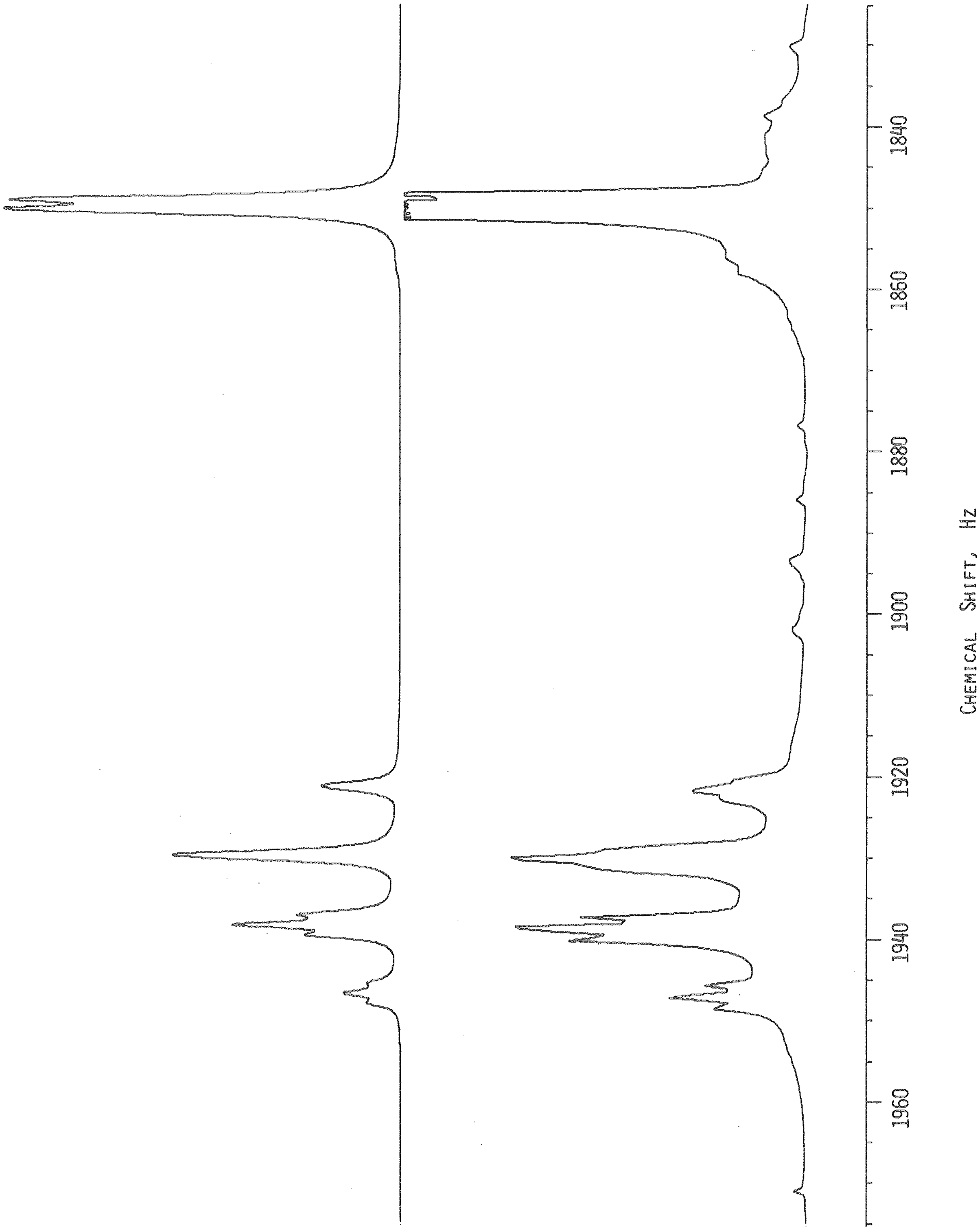

XBL 7910-12520

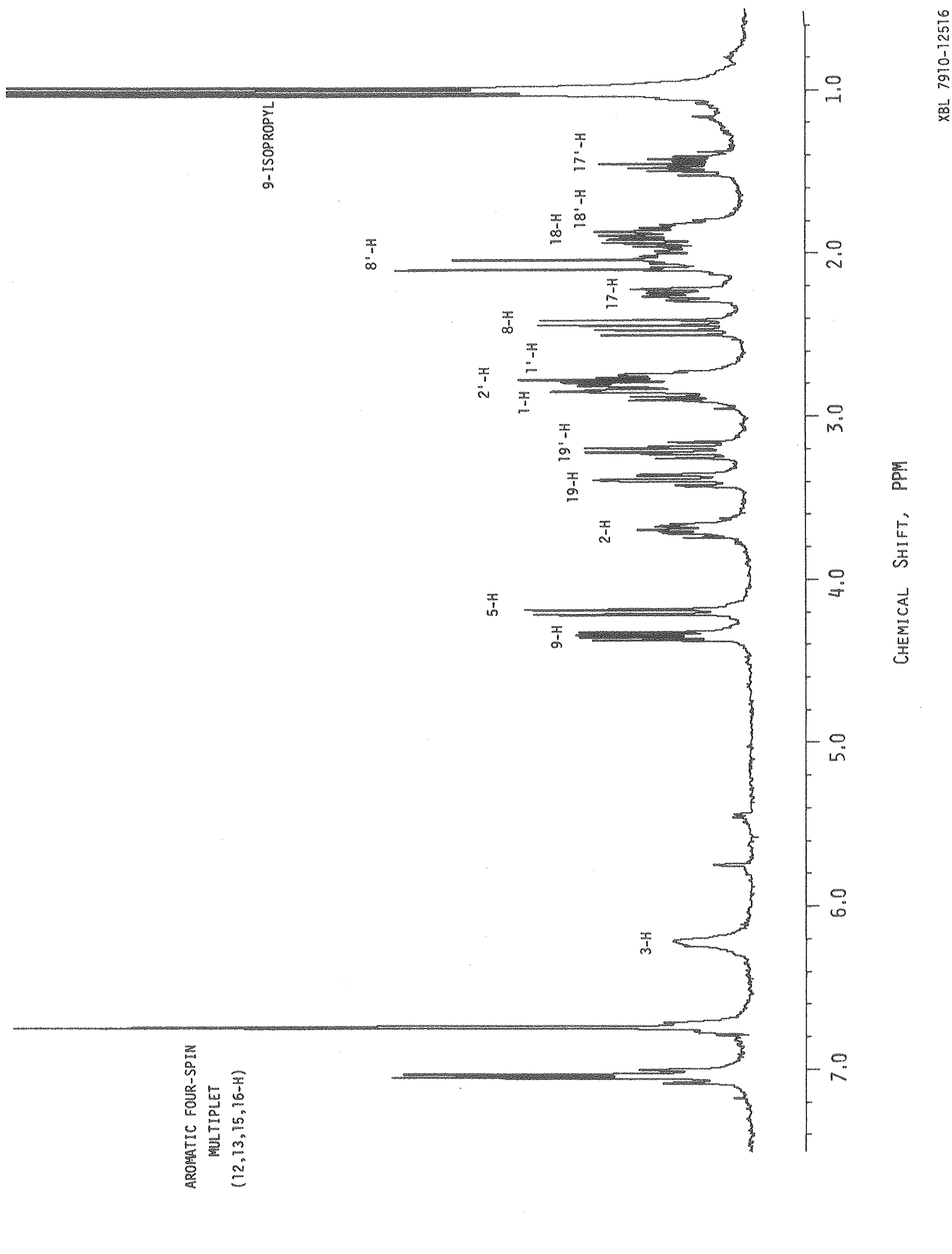
9-ISOPROPYL
8'-H
18-H
18'-H
17'-H
17-H
8-H
1'-H
2'-H
1-H
19'-H
19-H
2-H
5-H
9-H
3-H
AROMATIC FOUR-SPIN
MULTIPLET
(12,13,15,16-H)
1.0
2.0
3.0
4.0
5.0
6.0
7.0
CHEMICAL SHIFT, PPM
XBL 7910-12516

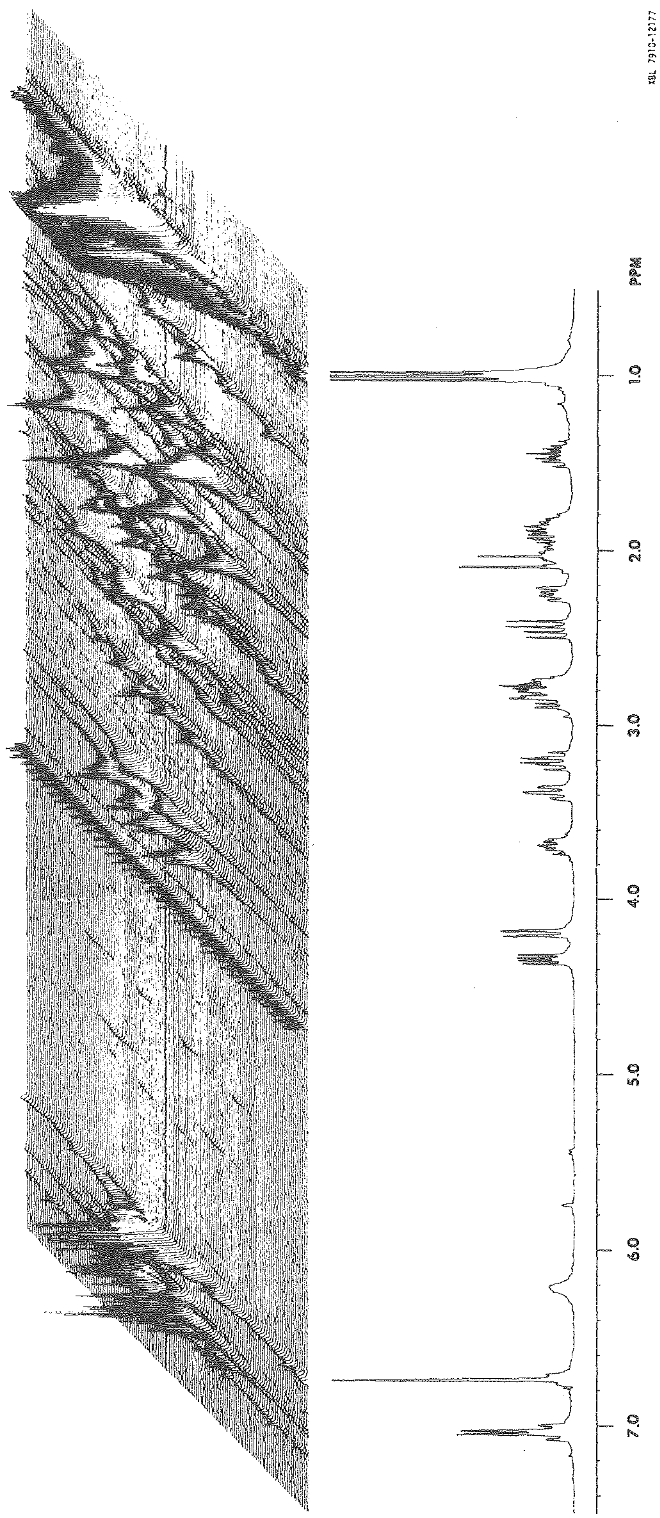
XBL 7910-12177
PPM
1.0
2.0
3.0
4.0
5.0
6.0
7.0

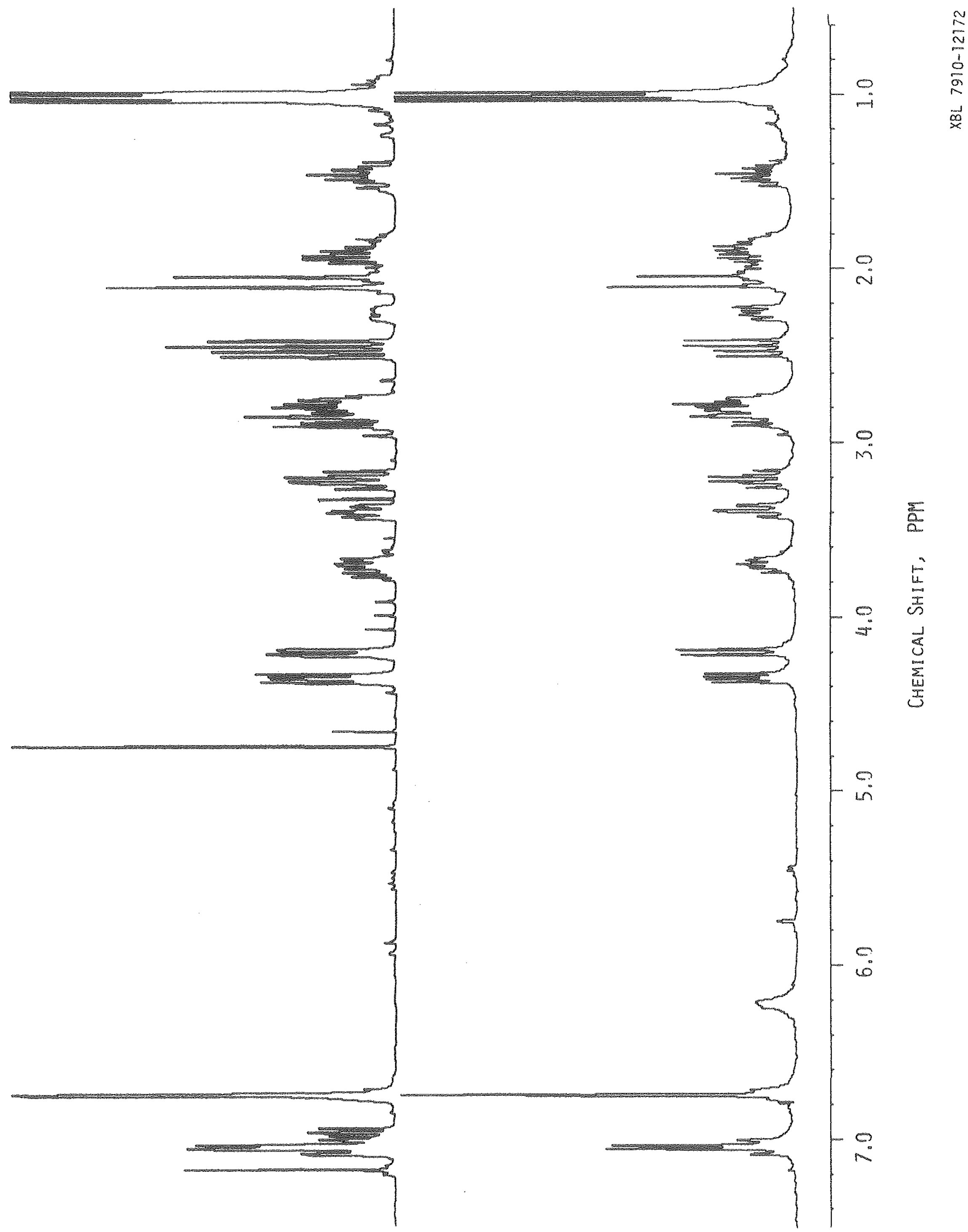
1.0
2.0
3.0
4.0
5.0
6.0
7.0
CHEMICAL SHIFT, PPM
XBL 7910-12172

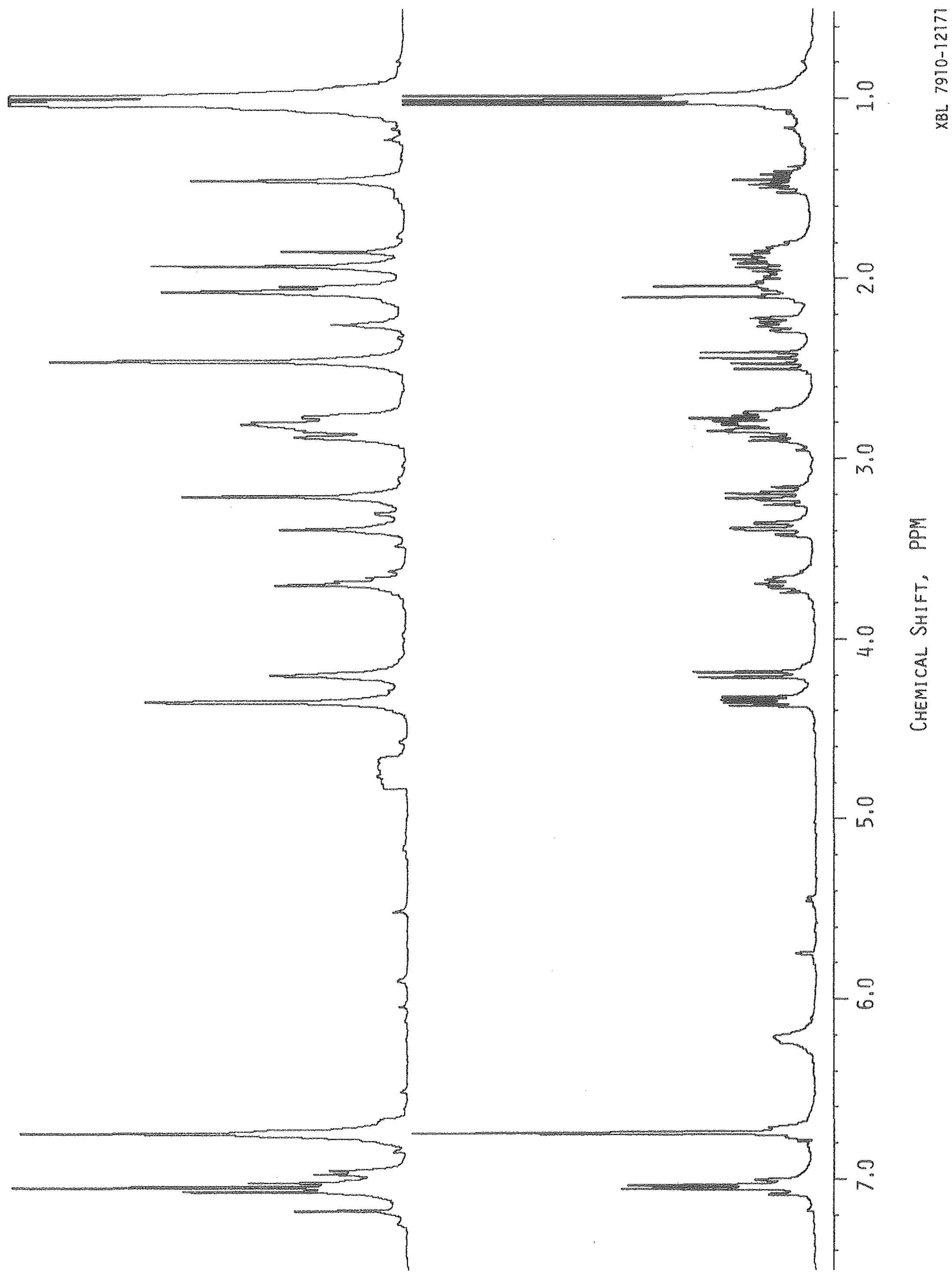
1.0
2.0
3.0
4.0
5.0
6.0
7.0
CHEMICAL SHIFT, PPM
XBL 7910-12171

Figure 1.61 Metal Binding Behavior of *Cyclo*-[3-(4-β-N-methylaminoethyl)phenyloxypropanoyl-L-prolyl], 6a, as shown by Circular Dichroism

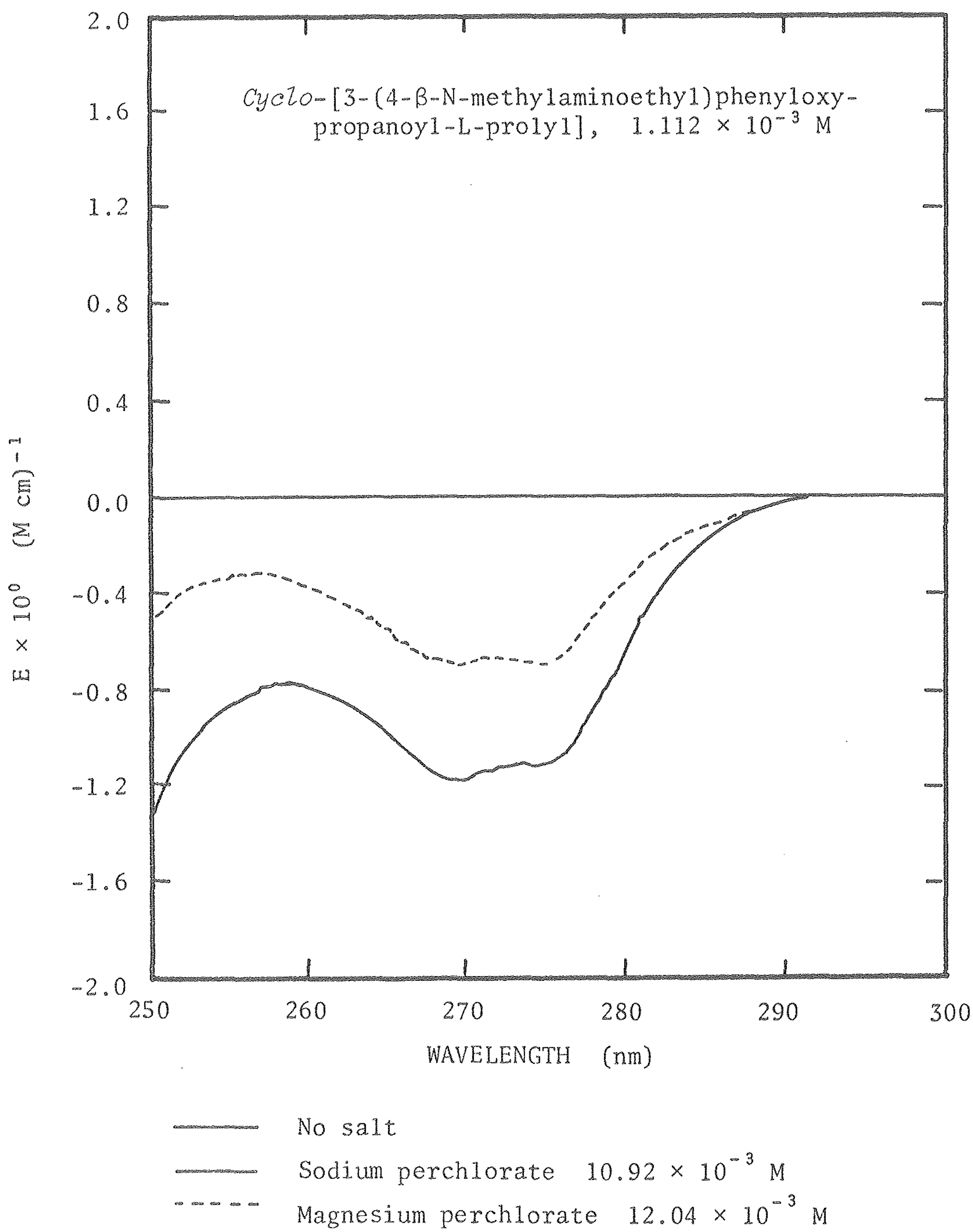

Cyclo-[3-(4-β-N-methylaminoethyl)phenyloxy-propanoyl-L-prolyl], 1.112 × 10⁻³ M
2.0
1.6
1.2
0.8
0.4
0.0
-0.4
-0.8
-1.2
-1.6
-2.0
E × 10⁰ (M cm)⁻¹
250
260
270
280
290
300
WAVELENGTH (nm)
No salt
Sodium perchlorate 10.92 × 10⁻³ M
Magnesium perchlorate 12.04 × 10⁻³ M

1.6 Summary

A. Cyclopeptide Alkaloid Model Systems Conformations

The employment of the technique for obtaining two-dimensional homonuclear J-spectra has led to conformational data on model systems for the cyclopeptides. NMR data has shown that the solution conformations of *cyclo*-[3-(4-β-N-methylaminoethyl)phenyloxypropanoyl-L-prolyl] **6a** and *cyclo*-[3-(4-β-aminoethyl)phenyloxypropanoyl-L-prolyl] **6b** differ markedly, and the change in bond angles as reflected by the vicinal coupling constants are consistent with a major difference in the orientation of the C_4 carbonyl. This difference in conformation accounts for the contrasting metal affinities of the two compounds.

The differences in bond angles are summarized in Table 1.11. The approximate nature of these calculations is reflected by the less than desired internal consistency of the changes. In the absence of large changes in the geminal couplings, it would be expected that H_α-H_α angles and H_β-H_β angles would change in the same direction. When changes in the geminal couplings are observed, however, it becomes more difficult to draw conclusions.

B. Methodology

The utility of 2-D homonuclear J-spectra in conformational analysis has been demonstrated for small polypeptides that have relatively few discrete conformational possibilities. The approach that has been used may be briefly reviewed:

1. If a series of compounds is to be studied, it is beneficial to have an x-ray crystal structure for at least one member of the group. The availability of both bond angles and coupling constants allows the derivation of $J - \theta$ relations that reflect the local substituent pattern.

2. Acquire the normal and the 2-D homonuclear J-spectrum.

3. Construct 45° projections of the 2-D spectrum, and plot contour maps of the spectral regions of interest.

4. Use the frequencies derived from the 45° projection for comprehensive homonuclear decoupling experiments to make all assignments.

5. Simulate spin systems where changes in orientation are likely to be reflected by changes in vicinal coupling constants.

6. Using the accurate coupling constant data with angle information from the x-ray, develop predictors for the vicinal coupling constants. This permits the calculation of dihedral angles where the x-ray is not available.

Table 1.11 Comparison of Bond Angles -- N-Methyl Cyclopeptide (X-Ray Data) and N-H Cyclopeptide (Calculated)

Dihedral Angle	N-Methyl Case 6a	N-H Case 6b
H_α-8-9-H_α	84.3°	73°
H_α-8-9-H_β	-157.6°	180°
H_β-8-9-H_α	33.8°	42°
H_β-8-9-H_β	84.4°	90°
H_α-1-2-H_α	-42.5°	48°
H_α-1-2-H_β	76.0°	51°
H_β-1-2-H_α	-160.7°	51°
H_β-1-2-H_β	-42.5°	0°

1.7 Experimental Section

Cyclopeptide model compounds **6a** - **6c** were purified by chromatography on Sephadex LH-20 followed by sublimination at *ca.* 100° C at < 100 μ pressure. NMR samples were prepared with nitric acid washed pipettes and sample tubes (Wilmad 528-PP) using Aldrich "100.00%" (99.9985 atom % D) $CDCl_3$. Samples were prepared in a Vacuum Atmospheres argon filled glove box, and were filtered through acid washed pipettes with glass wool plugs.

NMR spectra were acquired on the 270 MHz spectrometer system described in Part II. Prior to the acquisition of a 2-D file, the 90° pulse length was measured. This was found to vary from 4.95 - 6.00 μsec. Acquired spectral widths ranged from ±1400 Hz to ±2500 Hz (quadrature detection). The waiting time between the 90° and the 180° pulse was incremented by 10 msec, corresponding to a J spectral width of ±25 Hz.

Homonuclear decoupling experiments were run as described in Section 2.3.4. In some instances a wider than normal spectral width was used because of the spectrum offset resulting from using one frequency synthesizer to drive both the observe and the decouple transmitters. The decoupler was normally run at a 4 - 20% duty cycle at a pulse delay from the DCLOCK adjusted to minimize DC offsets in the detected signal.

1.8 References

1. W.A. Thomas in "Annual Reports on NMR Spectroscopy," Vol. 6B, E.F. Mooney, Ed., Academic Press, New York, NY., 1976, pp 1-41

2. F.A. Bovey, A.I. Brewster, D.J. Patel, A.E. Tonelli, D.A. Torchia, *Accounts Chem. Res.*, 5, 193 (1972)

3. D.W. Urry and M. Ohnishi in "Spectroscopic Approaches to Biomolecular Conformation," D.W. Urry, Ed., American Medical Association Press, Chicago, IL., 1970, pp 263 ff

4. F.A. Bovey in "Chemistry and Biology of Peptides, Proceedings of the Third American Peptide Symposium," J. Meienhofer, Ed., Ann Arbor Science Publishers, Ann Arbor, MI., 1972, pp 3 ff

5. G.N. Ramachandran and V. Sasisekharan in "Advances in Protein Chemistry," Vol. 23, C.F. Afinson, Ed., Academic Press, New York, NY, 1968, pp 284 ff

6. M. Karplus, *J. Chem. Phys.*, 30, 11 (1959)

7. M. Karplus, *J. Amer. Chem. Soc.*, 85, 2870 (1963)

8. G.N. Ramachandran and R. Chandrasekaran, *Biopolymers*, 10, 935 (1971)

9. G.N. Ramachandran, R. Chandrasekaran, and K.D. Kopple, *Biopolymers*, 10, 2113 (1971)

10. J. Jeener, presented at Ampère International Summer School, Basko Polje, Yugoslavia, 1971, unpublished

11. W.P. Aue, E. Bartholdi, and R.R. Ernst, *J. Chem. Phys.*, 64, 2229 (1976)

12. A. Kumar, D. Welti, and R.R. Ernst, *J. Mag. Resonance*, 18, 69 (1975)

13. L. Müller, A. Kumar, and R.R. Ernst, *J. Chem. Phys.*, 63,5490(1975)

14. G. Bodenhausen, R. Freeman, R. Niedermeyer, and D. Turner, *J. Mag. Resonance*, 26, 133 (1977)

15. R. Freeman and G. Morris, *Bull. Mag. Resonance*, 1, 5 (1979)

16. K. Wüthrich, K. Nagayama, and R.R. Ernst, *Trends Biol. Sci.*, 178 (1979)

17. E.L. Hahn and D.E. Maxwell, *Phys. Rev.*, 88, 1070 (1952)

18. M. Païs, X. Monseur, X. Lusinchi, and R. Goutarel, *Bull. Soc. Chim. France*, (1964) 817

19. E.W. Warnhoff, *Fortschr. Chem. Org. Naturst.*, 28, 162 (1970)

20. R. Tschesche and E.V. Kaussman, in "The Alkaloids," Vol. XV, R.H.F. Manske, Ed., Academic Press, New York, NY, 1975, pp 165-203

21. E. Haslinger, *Tetrahedron*, 34, 685 (1978)

22. J.C. Lagarias, R.A. Houghten, and H. Rapoport, *J. Amer. Chem. Soc.*, 100, 8202 (1978)

23. Y. Ogihara, *Experientia*, 33, 1454 (1977)

24. T. Wieland in "Chemistry and Biology of Peptides," J. Meienhofer, Ed., Ann Arbor Science Publishers, Ann Arbor, MI., 1972, p. 377

25. V. Madison, M. Atreyl, C.M. Deber, and E.R. Blout, *J. Amer. Chem. Soc.*, 96, 6725 (1974)

26. F.K. Klein and H. Rapoport, *J. Amer. Chem. Soc.*, 90, 3576 (1968)

27. K. Nagayama, P. Bachmann, K. Wuthrich, and R.R. Ernst, *J. Mag. Resonance*, 31, 133 (1978)

28. 2-D plots do not always appear to deploy multiplets along 45° diagonals because of the difference in plot scaling (Hz/cm) that is usually used.

29. W.P. Aue, J. Karhan, and R.R. Ernst, *J. Chem. Phys.*, 64, 4226 (1976)

30. C.M. Deber, D.A. Torchia, and E.R. Blout, *J. Amer. Chem. Soc.*, 93, 4893 (1971)

31. S. Castellano and A.A. Bothner-By, *J. Chem. Phys.*, 41, 3863 (1964)

II. Multinuclear NMR Spectrometer for the Study of Biological Systems

"The reasonable man adapts himself to the world; the unreasonable one persists in trying to adapt the world to himself. Therefore all progress depends on the unreasonable man."

- George Bernard Shaw

2.1 Introduction

In recent years, nuclear magnetic resonance has been applied to the study of a wide range of biological problems. With the advent of commercially available pulsed Fourier transform spectrometer systems operating at ever higher magnetic field strengths, problems of great complexity have become addressable. It is the purpose of this section to describe the design principles and some of the construction details of a broadband multinuclear NMR spectrometer system that was built in this laboratory. The spectrometer had as a design objective the inclusion of features that would make it especially suited to working with biological systems.

The text that follows will describe particular aspects of the 8 - 270 MHz multinuclear NMR spectrometer at the Chemical Biodynamics Laboratory at Berkeley. The system was used for the majority of the work described in Part 1. What follows may be classified into three categories:

- Overall system design and description of major functional blocks.
- Test and characterization procedures.
- Detailed description of original design work. Parts fabricated at the Electronics Research and Development Group, Lawrence Berkeley Laboratory, are included in functional descriptions but detailed information is not provided. The same applies to commercial equipment.

Most original designs and most significant modifications to commercial equipment have been assigned Lawrence Berkeley Laboratory (LBL) print numbers (16X series for fabrication done at LCB). All original drawings are on permanent file at the LBL Electronics Engineering Print Room.

2.2 System Design Considerations

When the construction of the 8 - 270 MHz spectrometer system was initiated, the goal was the implementation of a number of specific capabilities:

1. Multiple pulse experiments -- The system had to be capable of generating precisely timed sequences of radio frequency excitation pulses. Different pulses in the sequence might also have different relative phase shifts. This capability would be useful for proton-enhanced, spin-locking, and a variety of other experiments.

2. Broadband observe -- It was desirable to be able to observe a wide range of nuclei using the same frequency generation and observe system. The goal was to construct a system that could observe at any frequency (within the range dictated by the magnetic field strength) while decoupling at any second frequency and optionally locking at a third frequency. The only limitation on frequency (nuclei) combinations would be the availability of an appropriate probe.

3. Flexible decoupling -- for many of the proton experiments that were to be done, an efficient homonuclear decoupling capability would be essential. For high resolution and proton-enhanced ^{13}C and ^{15}N experiments, broadband noise-modulated low and high power proton decoupling would be necessary.

4. Simple structure for generating new pulse sequences -- it was desired that new pulse sequences should be generated via software microprograms rather than hardwired connection of timers. This would permit rapid reconfiguration of experiments and a degree of automation not otherwise possible.

Frequency generation on the 8 - 270 MHz spectrometer system follows the widely used scheme described by Ellett, et al.[1] Observe, decouple, and lock frequencies are generated by single sideband mixing of a 30 MHz intermediate frequency (IF) with local oscillator frequencies supplied by frequency synthesizers (Figure 2.1). Lower sidebands are selected in all three channels, and the actual single sideband conversion is realized by a term-by-term implementation of the trigonometric identity

$$\cos(\omega_1 - \omega_2) = \cos\omega_1 \cos\omega_2 + \sin\omega_1 \sin\omega_2 \tag{1}$$

using quadrature hybrids to perform Hilbert Transforms and power combiners to perform summing operations (Figure 2.2).

On the transmitter side of the spectrometer system, the use of an intermediate frequency makes the generation of pulses with different relative phases quite straightforward. Phase shifting is done at the 30 MHz IF using narrowband 30 MHz quadripole networks; these phase shifts are then frequency translated in the course of single sideband mixing. This circumvents the need for wide bandwidth phase shifters.

The use of an IF considerably simplifies the task of building a sensitive and selective receiver, as the design is just that of a

Figure 2.1 8 - 270 MHz Spectrometer System Block Diagram

Figure 2.2 Phase Shift Modulator Scheme for Single Sideband Frequency Conversion

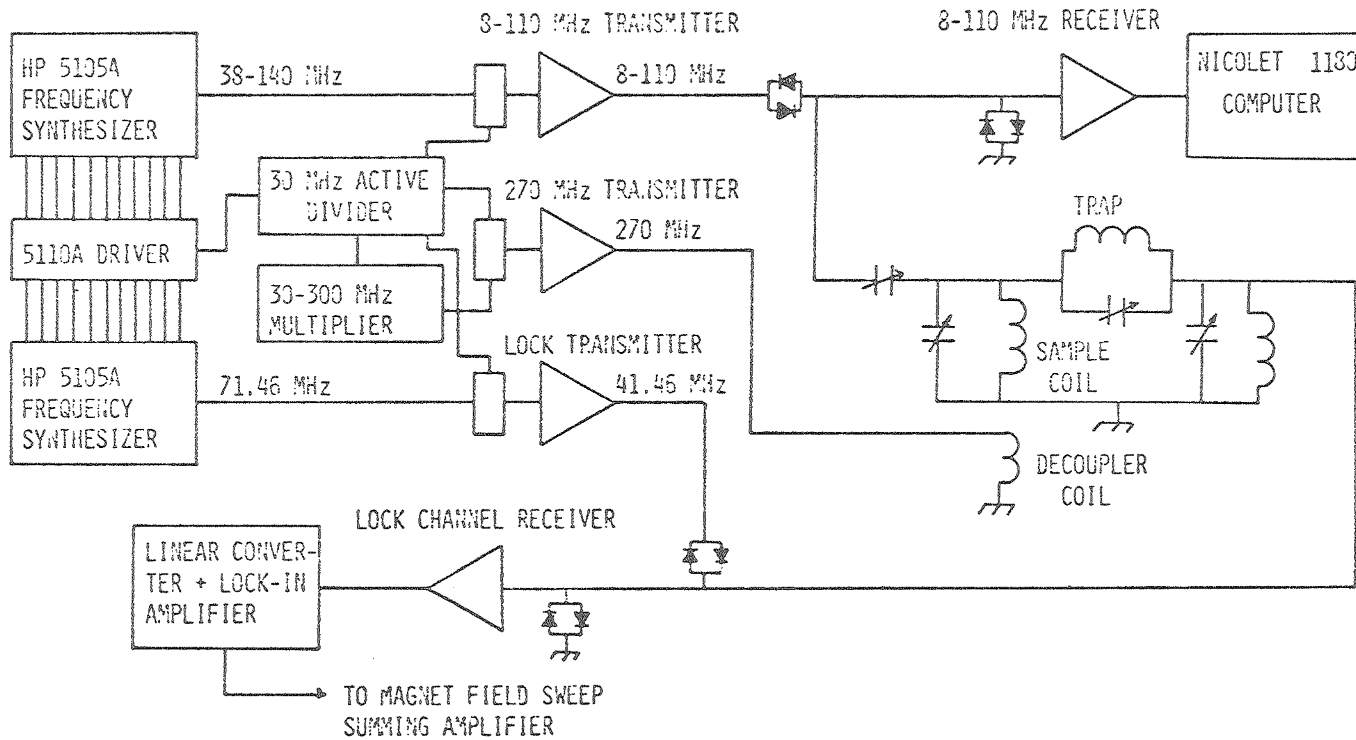
8-110 MHz TRANSMITTER
8-110 MHz RECEIVER
HP 5105A FREQUENCY SYNTHESIZER
38-140 MHz
8-110 MHz
NICOLET 1180 COMPUTER
30 MHz ACTIVE DIVIDER
270 MHz TRANSMITTER
270 MHz
TRAP
5110A DRIVER
30-300 MHz MULTIPLIER
SAMPLE COIL
LOCK TRANSMITTER
HP 5105A FREQUENCY SYNTHESIZER
71.46 MHz
41.46 MHz
DECOUPLER COIL
LOCK CHANNEL RECEIVER
LINEAR CONVER-TER + LOCK-IN AMPLIFIER
TO MAGNET FIELD SWEEP SUMMING AMPLIFIER

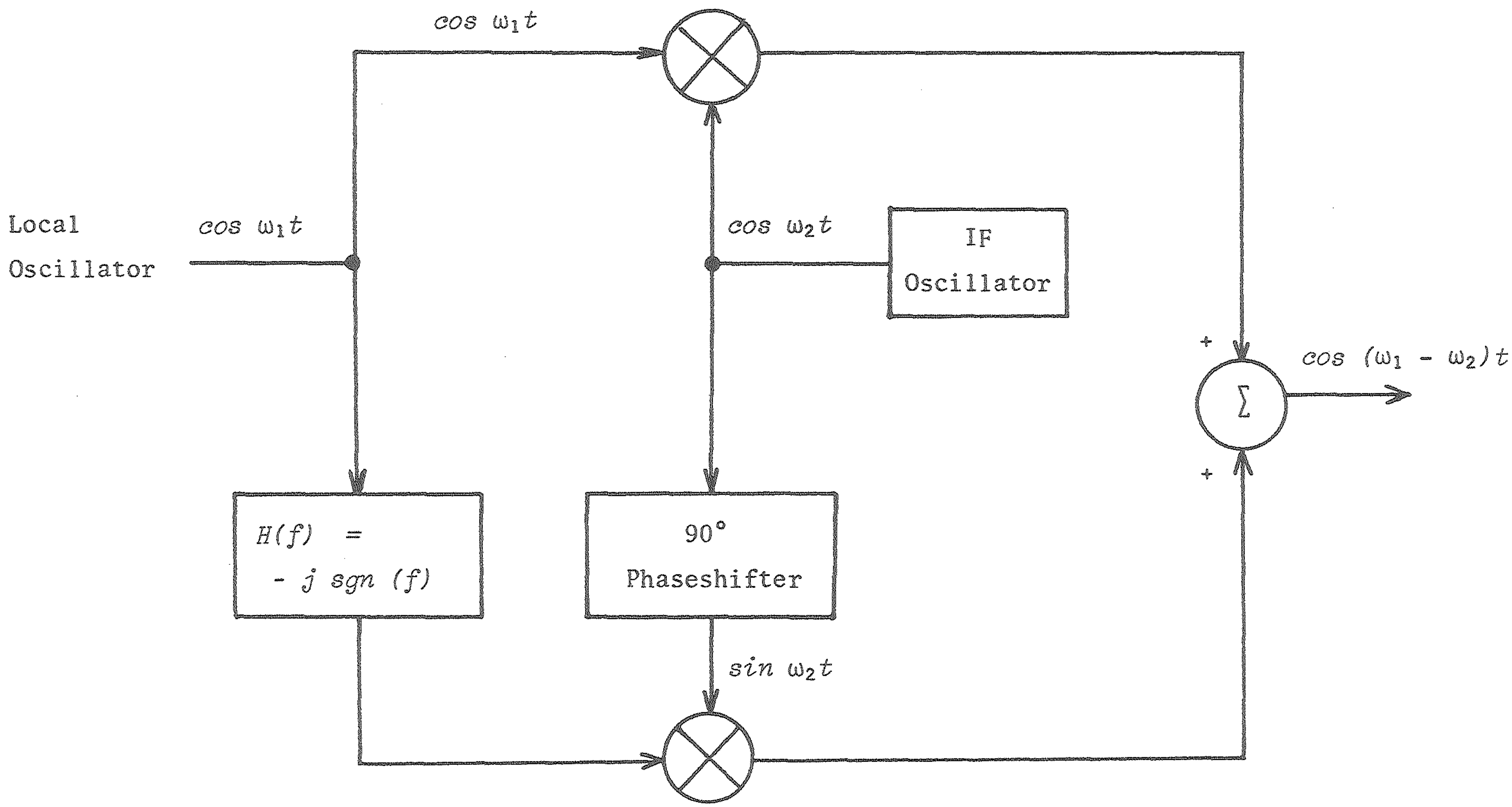
cos ω₁t
Local
Oscillator
cos ω₁t
cos ω₂t
IF
Oscillator
+
cos (ω₁ - ω₂)t
Σ
+
H(f) =
- j sgn (f)
90°
Phaseshifter
sin ω₂t

superheterodyne receiver. A superheterodyne receiver has good sensitivity and selectivity because the IF filter provides most of the predetection filtering. Since this filter need not be tunable, it can be relatively complex. The same local oscillator frequency used in the transmitter is used to tune the receiver (Figure 2.3). Image frequency $(\omega_{obs} \pm 2\omega_{IF})$ rejection may be accomplished either by single sideband mixing (expensive because of the need for two broadband quadrature hybrids for the signal and the local oscillator) or by suitable Rf pre-filtering prior to mixing.

Figure 2.3 Superheterodyne Receiver Structure

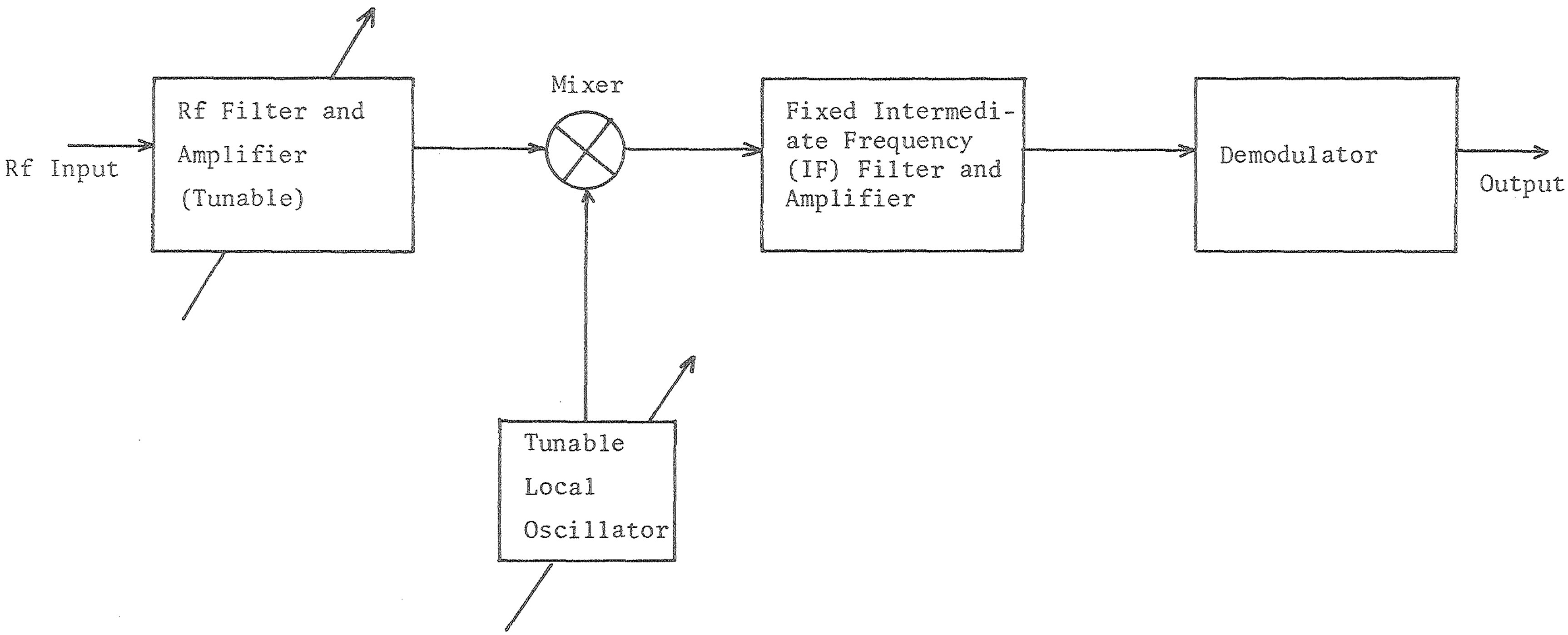
Rf Input
Rf Filter and Amplifier (Tunable)
Mixer
Fixed Intermediate Frequency (IF) Filter and Amplifier
Demodulator
Output
Tunable Local Oscillator

2.3 Major Subsystems

2.3.1 Magnet

The spectrometer system is based on a commercial Bruker Instruments 63.5 kGauss superconducting solenoid with a 5 cm room temperature bore. When the room temperature shim coils are installed, 4 cm remains for the probes. Operation at this field strength implies the NMR frequencies listed in Table 2.1.

The magnet system was used with some modification to the room temperature shim control system, the H_0 field sweep amplifiers, and the shim reference voltage supplies. These modifications are described in detail below.

2.3.2 Observe Channel Transmitter

The observe channel transmitter is outlined in Figure 2.4. The 30 MHz IF is derived from a 30 MHz Active Power Divider (10X223) which in turn receives 30 MHz from the Hewlett-Packard 5110A frequency synthesizer driver, which serves as the master frequency reference for the whole system. Phase shifts of 0°, 90°, 180°, or 270° may be imposed on the 30 MHz IF by the 10X209 Four Phase Generator, which operates under the control of the 16X892 data processor interface. Phase shifts are produced by gated selection of one of the four outputs of a Merrimac 18134 quadripole network.

The phase-shifted 30 MHz output is single sideband converted to the desired NMR frequency in the 10X206 Single Sideband Generator, using a local oscillator frequency supplied by one of the HP5105A

Table 2.1 8 - 270 MHz Spectrometer System, Principal Operating Frequencies

Isotope	Natural Abundance	NMR Frequency at 63.42 KGauss	Relative Sensitivity
^{1}H	99.9844%	269.9982 MHz	1.000
^{31}P	100.0 %	109.297 MHz	0.0664
^{13}C	1.108 %	67.8975 MHz	0.0159
^{15}N	0.365 %	27.360 MHz	0.0010
^{2}H	0.0156%	41.4513 MHz	0.0097

Figure 2.4 8 - 270 MHz Spectrometer System, Observe Channel Transmitter Interconnect [16X9673-B3]

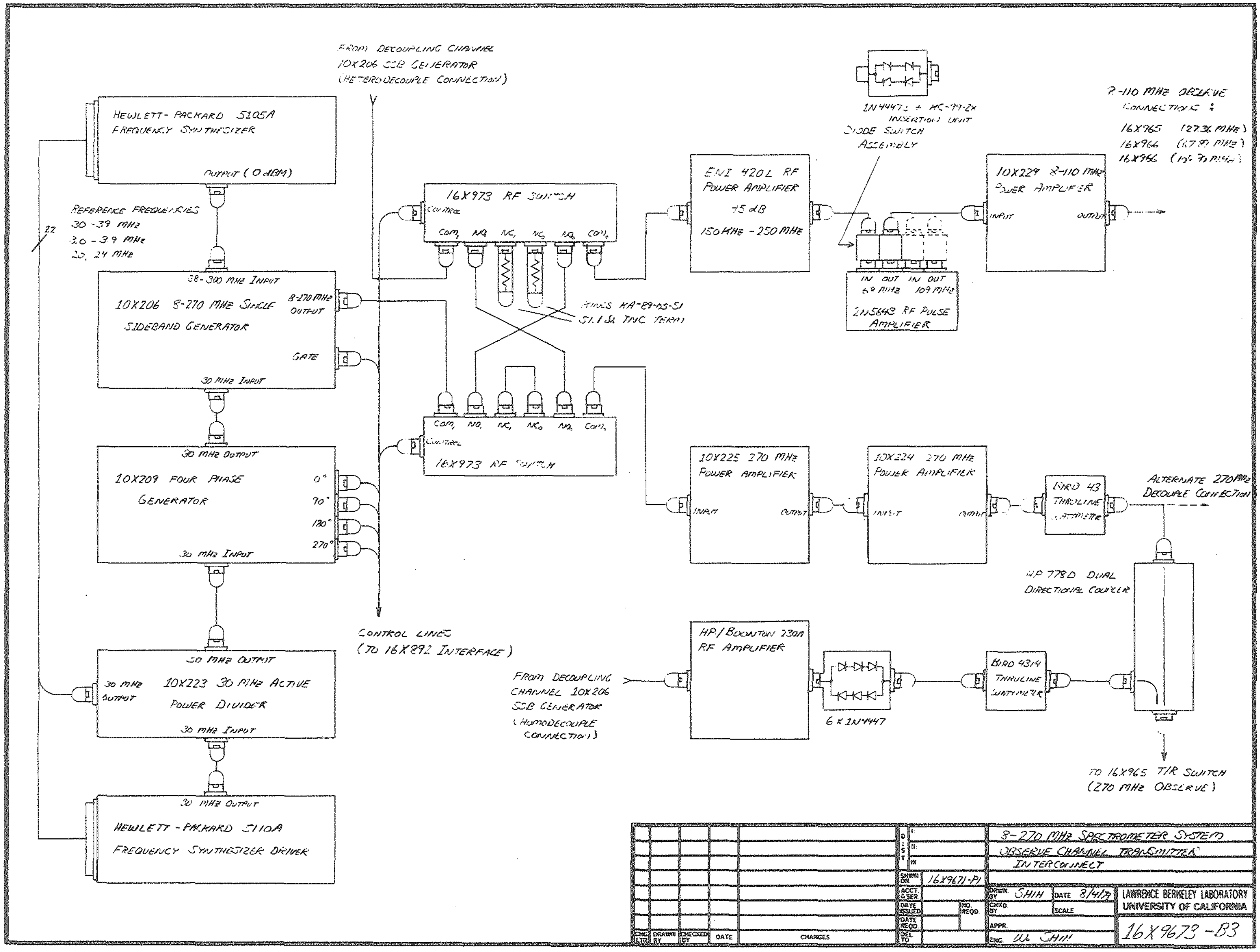
FROM DECOUPLING CHANNEL 10X206 SSB GENERATOR (HETERODECOUPLE CONNECTION)
HEWLETT-PACKARD 5105A FREQUENCY SYNTHESIZER
OUTPUT (0 dBM)
REFERENCE FREQUENCIES 30 - 39 MHz 3.0 - 3.9 MHz 20, 24 MHz
22
38-300 MHz INPUT
10X206 8-270 MHz SINGLE SIDEBAND GENERATOR
8-270 MHz OUTPUT
GATE
30 MHz INPUT
30 MHz OUTPUT
10X209 FOUR PHASE GENERATOR
0° 90° 180° 270°
30 MHz INPUT
30 MHz OUTPUT
10X223 30 MHz ACTIVE POWER DIVIDER
30 MHz OUTPUT
30 MHz INPUT
30 MHz OUTPUT
HEWLETT-PACKARD 5110A FREQUENCY SYNTHESIZER DRIVER
16X973 RF SWITCH
CONTROL
COM, NO, NC, NC, NO, COM,
KINGS KA-89-05-51 51.1 Ω TNC TERM
16X973 RF SWITCH
CONTROL LINES (TO 16X892 INTERFACE)
ENI 420L RF POWER AMPLIFIER
45 dB
150 KHz - 250 MHz
1N4447 + KC-79-2X INSERTION UNIT
DIODE SWITCH ASSEMBLY
IN OUT IN OUT
69 MHz 109 MHz
2N5643 RF PULSE AMPLIFIER
10X229 8-110 MHz POWER AMPLIFIER
INPUT
OUTPUT
8-110 MHz OBSERVE CONNECTIONS :
16X965 (27.36 MHz)
16X964 (67.97 MHz)
16X966 (109.70 MHz)
10X225 270 MHz POWER AMPLIFIER
INPUT
OUTPUT
10X224 270 MHz POWER AMPLIFIER
INPUT
OUTPUT
BIRD 43 THRULINE WATTMETER
ALTERNATE 270 MHz DECOUPLE CONNECTION
HP 778D DUAL DIRECTIONAL COUPLER
HP / BOONTON 230A RF AMPLIFIER
FROM DECOUPLING CHANNEL 10X206 SSB GENERATOR (HOMODECOUPLE CONNECTION)
6 x 1N4447
BIRD 4314 THRULINE WATTMETER
TO 16X965 T/R SWITCH (270 MHz OBSERVE)
8-270 MHz SPECTROMETER SYSTEM
OBSERVE CHANNEL TRANSMITTER INTERCONNECT
16X9671-P1
DRAWN BY SHIH
DATE 8/4/77
LAWRENCE BERKELEY LABORATORY
UNIVERSITY OF CALIFORNIA
ENG. W. SHIH
16X9673-B3
CHANGES

frequency synthesizers. Bandwidth limitations of components in the single sideband generator restrict the NMR operating frequency range to 8 - 270 MHz. Pulse gating is also done in the single sideband generator, again under data processor control via the 16X892 interface.

Pulse amplification to a suitable power level is accomplished with either of two sets of Rf power amplifiers, depending on the frequency. $^{1}H/^{19}F$ observe pulses are amplified by the 10X225 270 MHz solid state power amplifier employing cascaded 2N5641/42/43 common emitter stages. The output of this unit is fed to the 10X224 270 MHz Power Amplifier. This amplifier employs an Eimac 8877 (3CX1500A7) high-mu power triode. Final stage maximum output is approximately 1.2 kW PEP at 1% duty cycle.

Rf power amplification in the frequency range of 8 - 110 MHz uses an ENI 420L broadband linear power amplifier as a first stage driver (45 dB gain, 150 kHz - 250 MHz power bandwidth). The output of this amplifier is routed to the 10X229 8-110 MHz Power Amplifier for final stage gain. Optionally, 2N5643 common-emitter Rf amplifiers may be used at 68 or 109 MHz to provide higher drive levels. The 10X229 amplifier again employs an Eimac 8877 power triode, but this time the output is tunable over the specified operating range.

Transmitter signal routing is via two 16X973 Rf switches connected in a cross-bar arrangement, controlled by 50 Ω TTL level control lines. Transmitter outputs are routed to transmit/receive (T/R) switches (duplexers) that are designed for specific operating frequencies. The 16X965 T/R switch is used for 27.36 MHz (^{15}N) and 270 MHz (^{1}H), and the 16X966 T/R switch is used for 67.90 MHz (^{13}C) and 109.30 MHz (^{31}P). These switches isolate the receivers from the probe and transmitter during Rf pulse transmission, and they isolate the probe and receiver from transmitter noise during the balance of the operating cycle. Design details of both T/R switch units are described below.

270 MHz (^1H) signals are also routed through a Hewlett-Packard 778D directional coupler. A low power transmitter may be attached to one of the coupled ports for homonuclear proton decoupling, solvent suppression by presaturation, or other experiments requiring concurrent use of both a high power and a low power Rf amplifier.

2.3.3 Observe Channel Receiver

The observe channel receiver is a superheterodyne receiver employing synchronous detection (Figure 2.5). Initial Rf preamplification and band limiting is done by amplifiers contained in the T/R switch assemblies, 16X965 (270 MHz and 27.36 MHz) and 16X966 (67.90 MHz and 109.30 MHz). Rf amplifier bandwidths and gains are summarized in Table 2.2. In all cases, the image frequency is far enough removed so that image noise should not be a problem.

The appropriate preamplifier output is routed to the down-converter via a step attenuator. Frequency conversion to the 30 MHz IF is done in the 10X210 8-270 MHz to 30 MHz Linear Converter using a standard output level HP 10514A double-balanced mixer running with a saturated local oscillator signal supplied by the 10X206 Single Sideband Generator. Varying degrees of signal attenuation may be required in the case of strong signals (^1H) to minimize intermodulation distortion that will increase drastically as the signal level approaches the 1 dB compression point. Similarly, as signals approach 2 to 5 dB below the mixer's conversion compression level, Rf desensitization by large signals

Figure 2.5 8 - 270 MHz Spectrometer System Observe Channel Receiver Interconnect [16X9673-B4]

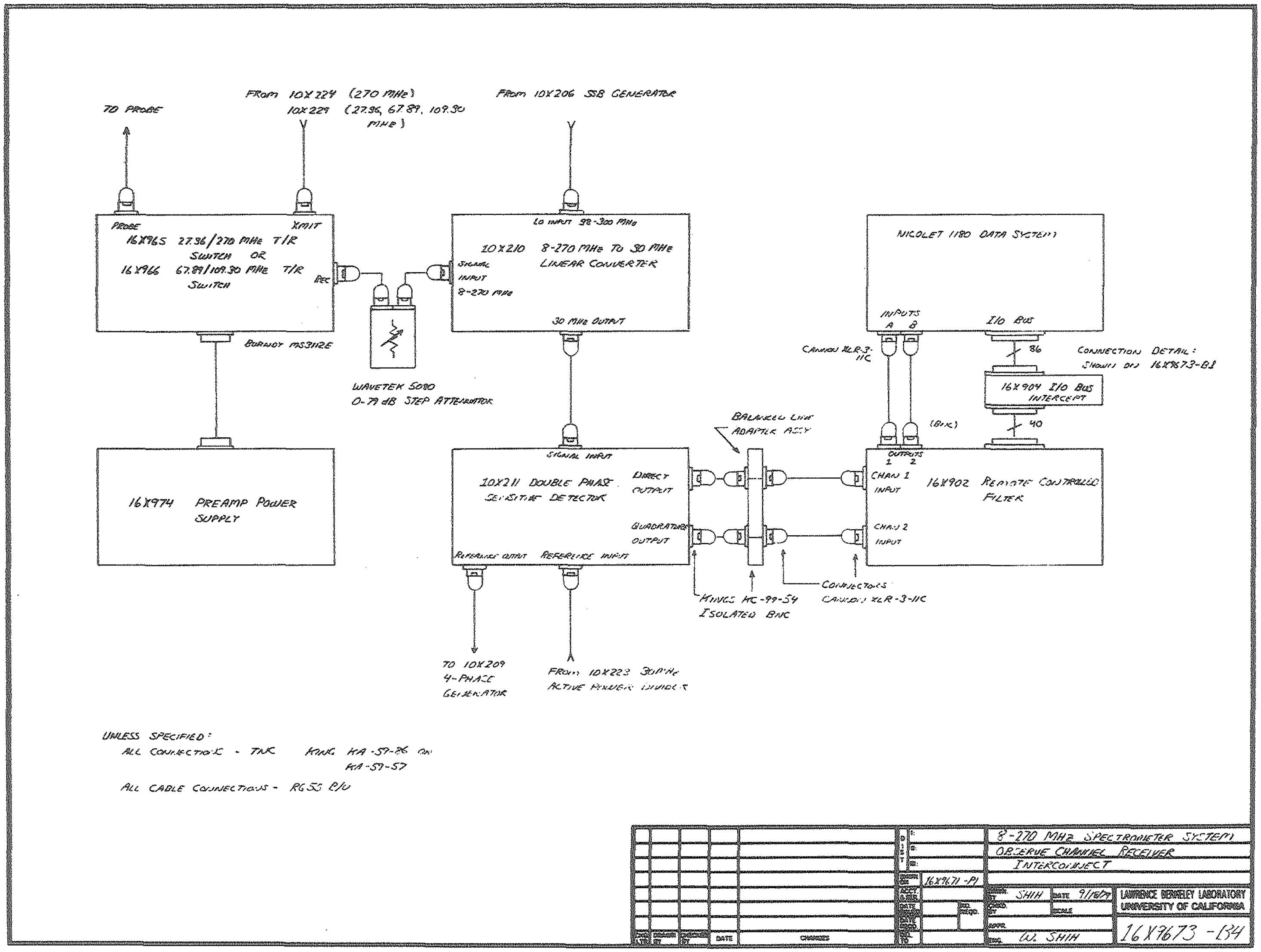
TO PROBE
FROM 10X224 (270 MHz)
10X229 (27.36, 67.89, 109.30 MHz)
FROM 10X206 SSB GENERATOR
PROBE
XMIT
16X965 27.36/270 MHz T/R SWITCH OR
16X966 67.89/109.30 MHz T/R SWITCH
REC
BURNDY MS3112E
WAVETEK 5080
0-79 dB STEP ATTENUATOR
LO INPUT 38-300 MHz
10X210 8-270 MHz TO 30 MHz LINEAR CONVERTER
SIGNAL INPUT 8-270 MHz
30 MHz OUTPUT
NICOLET 1180 DATA SYSTEM
INPUTS A B
I/O BUS
CANNON XLR-3-11C
86
CONNECTION DETAIL: SHOWN ON 16X9673-B1
16X904 I/O BUS INTERCEPT
40
(BIX)
OUTPUTS 1 2
16X974 PREAMP POWER SUPPLY
SIGNAL INPUT
10X211 DOUBLE PHASE SENSITIVE DETECTOR
DIRECT OUTPUT
QUADRATURE OUTPUT
REFERENCE OUTPUT
REFERENCE INPUT
BALANCED LINE ADAPTER ASSY
CHAN 1 INPUT
CHAN 2 INPUT
16X902 REMOTE CONTROLLED FILTER
KINGS KC-99-54 ISOLATED BNC
CONNECTORS CANNON XLR-3-11C
TO 10X209 4-PHASE GENERATOR
FROM 10X223 30 MHz ACTIVE POWER DIVIDER
UNLESS SPECIFIED:
ALL CONNECTIONS - TNC KING KA-59-26 OR KA-59-57
ALL CABLE CONNECTIONS - RG55 B/U
8-270 MHz SPECTROMETER SYSTEM
OBSERVE CHANNEL RECEIVER
INTERCONNECT
16X9671-P1
SHIH
DATE 9/16/79
W. SHIH
LAWRENCE BERKELEY LABORATORY
UNIVERSITY OF CALIFORNIA
16X9673-B4
DATE
CHANGES

Table 2.2 Observe Channel Receiver Characteristics

NUCLEUS	*RECEIVER CENTER FREQUENCY*	*RECEIVER RF BANDWIDTH*	*RF AMPLIFIER GAIN*
^{1}H	269.9985 MHz	40 MHz	36 dB
^{2}H	41.4513 MHz	3 MHz	18 dB
^{13}C	70.0000 MHz	30 MHz	30 dB
^{31}P	120.0000 MHz	40 MHz	30 dB
^{15}N	27.3600 MHz	3 MHz	36 dB

may cause increased small signal conversion loss.

A saturating local oscillator drive level is used to drive the mixer diodes into the linear regions of the I-V curve and reduce the percentage of time spent in the nonlinear region about V = 0. Such a mode of operation improves odd order harmonic suppression and two-tone third order suppression. Use of a higher level mixer that incorporates series diodes could in principle further improve the receiver dynamic range, but at the expense of requiring a higher local oscillator drive level.

After conversion to the 30 MHz IF, the signal is amplified by up to 80 dB and is pre-detection filtered. The IF amplifier output is routed to another step attenuator so that the output level to the synchronous detector can be adjusted, again to minimize odd order harmonic distortion and effects caused by excessive signal levels.

Synchronous detection is performed in the 10X211 Double Phase Sensitive Detector using a 30 MHz reference from the 10X223 30 MHz Active Power Divider. The reference 30 MHz is split into quadrature components with a quadrature hybrid, and the incoming signal is phase detected twice using these two references. The two resulting signals (in phase quadrature) are low-pass filtered and amplified by up to 40 dB by the 16X902 Remote Controlled Filter. After this anti-aliasing filter (4-pole Butterworth characteristic), the two signals are digitized and signal averaged by a Nicolet Instruments Corp. Model 1180 Data System.

2.3.4 Decouple Channel Transmitter

The decouple channel transmitter is structured in the same fashion as the observe channel transmitter. Two interconnection drawings show the configurations for homonuclear ^{1}H decoupling (Figure 2.6) and heteronuclear noise-modulated proton decoupling for ^{13}C, ^{31}P, or ^{15}N observation (Figure 2.7).

Efficient homonuclear proton decoupling utilizes a pulsed Rf irradiation at the decoupling frequency that is gated at the sampling rate of the digitizer (of the data acquisition system) as set by the acquisition spectral width (software set). The timing of this pulse train is synchronized with the sampling window of the sample and hold on the digitizer input so that decoupling pulses occur only during the null time between samples. Pulse width and delay relative to the sampling window are set using a pulse generator (Hewlett-Packard 8013A or equivalent) triggered by the D CLOCK signal (dwell clock) available on the 1180 data system rear panel after suitable modification to the sweep control board (board 13) of the processor. Sweep control board modifications are summarized on Print 16X983.

At present, there are two Hewlett-Packard 5105A frequency synthesizers in the spectrometer system. One is normally used to supply the observe channel local oscillator, and the other is used for the lock channel local oscillator. The need for a third synthesizer for homonuclear decoupling is circumvented by using the observe channel local oscillator to also drive the decoupler. This requires that decoupling always take place at the center of a spectrum when quadrature phase detection is employed. This is generally not a problem for proton

Figure 2.6 8 - 270 MHz Spectrometer System Decouple Channel Transmitter Interconnect for Homonuclear Decoupling (^{1}H) [16X9673-B7]

Figure 2.7 8 - 270 MHz Spectrometer System Decouple Channel Transmitter Interconnect for Heteronuclear Proton Decoupling [16X9673-B8]

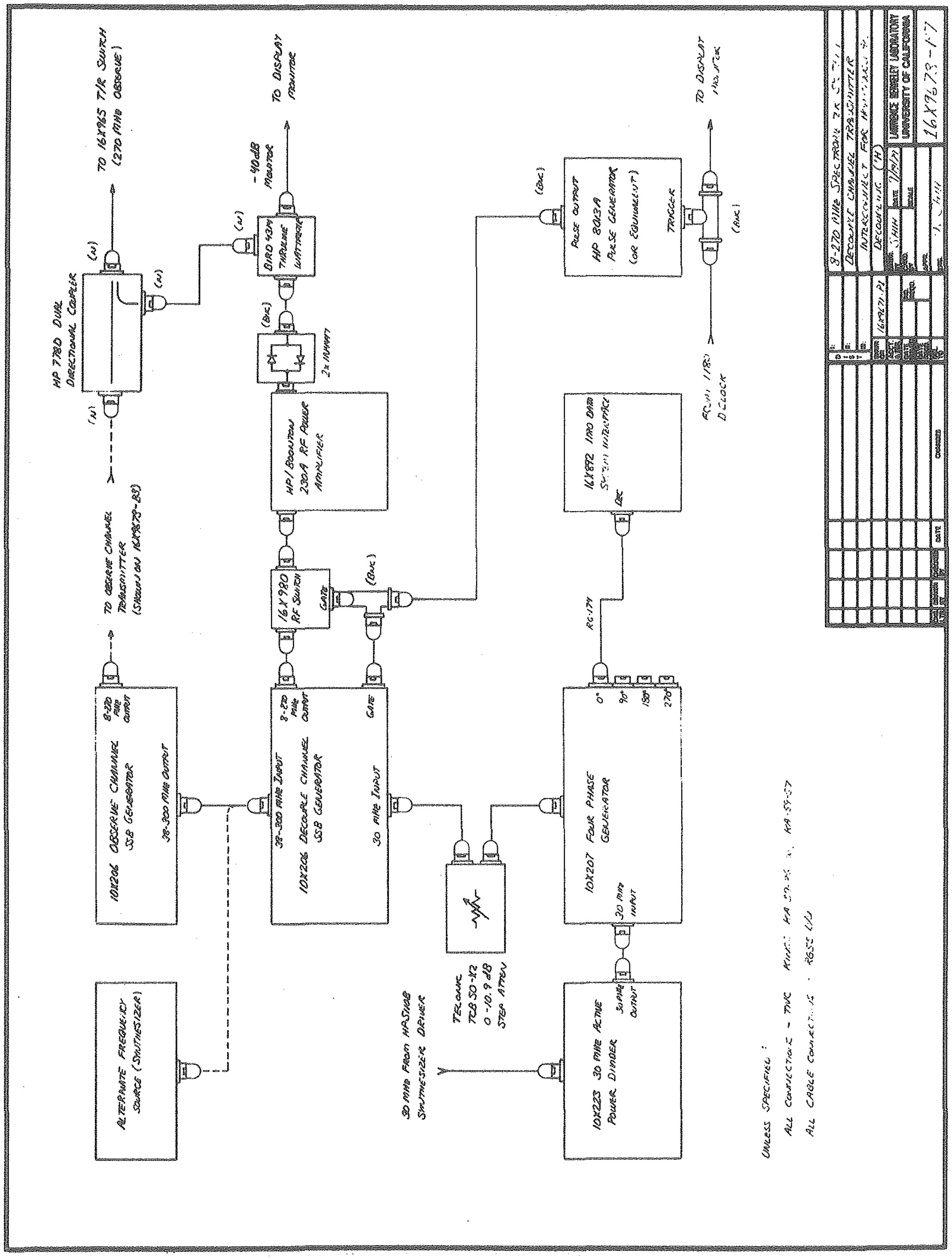

ALTERNATE FREQUENCY SOURCE (SYNTHESIZER)
10X206 OBSERVE CHANNEL SSB GENERATOR
38-300 MHz OUTPUT
8-270 MHz OUTPUT
TO OBSERVE CHANNEL TRANSMITTER (SHOWN ON 16X8673-83)
HP 778D DUAL DIRECTIONAL COUPLER
TO 16X965 T/R SWITCH (270 MHz OBSERVE)
10X206 DECOUPLE CHANNEL SSB GENERATOR
38-300 MHz INPUT
8-270 MHz OUTPUT
30 MHz INPUT
GATE
16X920 RF SWITCH
HP/BOONTON 230A RF POWER AMPLIFIER
2W IMPACT
BIRD 43 THRULINE WATTMETER
-40dB MONITOR
TO DISPLAY MONITOR
HP 8013A PULSE GENERATOR (OR EQUIVALENT)
PULSE OUTPUT
TRIGGER
TO DISPLAY
FROM 1180 CLOCK
10X207 FOUR PHASE GENERATOR
30 MHz INPUT
0°
90°
180°
270°
RG-174
16X872
10X223 30 MHz ACTIVE POWER DIVIDER
30 MHz OUTPUT
30 MHz FROM HP5105B SYNTHESIZER DRIVER
TELONIC TCB 30-1/2 0-10.9 dB STEP ATTEN
UNLESS SPECIFIED:
ALL CONNECTORS - TNC
LAWRENCE BERKELEY LABORATORY
UNIVERSITY OF CALIFORNIA
8-270 MHz SPECTROMETER
DECOUPLE CHANNEL TRANSMITTER
16X7673-17

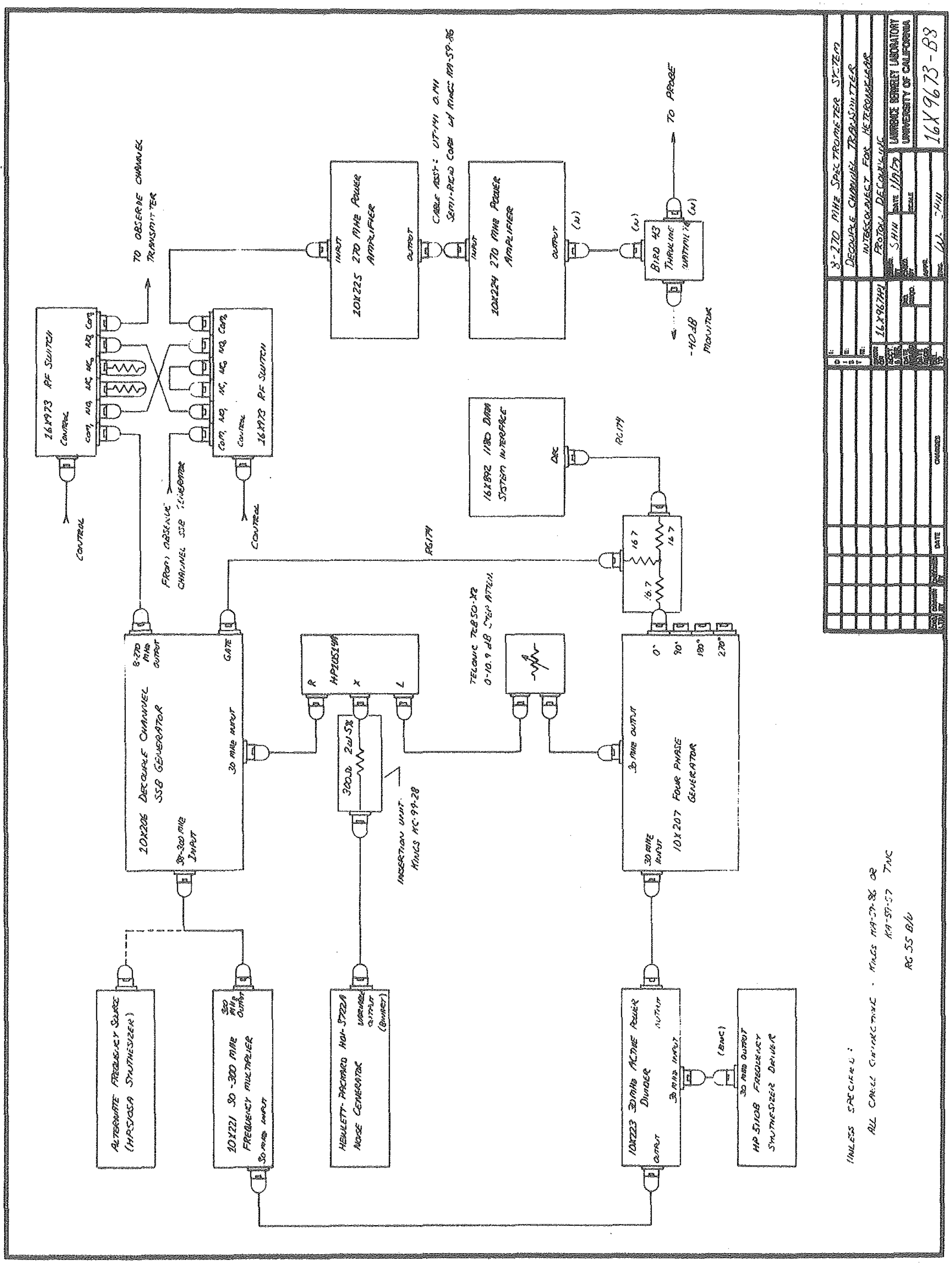
ALTERNATE FREQUENCY SOURCE (HP5105A SYNTHESIZER)
10X221 30-300 MHz FREQUENCY MULTIPLIER
30 MHz INPUT
300 MHz OUTPUT
HEWLETT-PACKARD HOI-3722A NOISE GENERATOR
VARIABLE OUTPUT (BINARY)
10X223 30MHz ACTIVE POWER DIVIDER
OUTPUT
30 MHz INPUT
(BNC)
30 MHz OUTPUT
HP 5110B FREQUENCY SYNTHESIZER DRIVER
20X206 DECOUPLE CHANNEL SSB GENERATOR
8-270 MHz OUTPUT
38-300 MHz INPUT
30 MHz INPUT
GATE
HP10514A
R
X
L
300Ω 2W 5%
INSERTION UNIT KINGS KC-99-28
TELONIC TCB50-X2 0-10.9 dB STEP ATTEN.
30 MHz OUTPUT
30 MHz INPUT
10X207 FOUR PHASE GENERATOR
0°
90°
180°
270°
16.7
RG174
16X892 1180 DATA SYSTEM INTERFACE
DEC
16X973 RF SWITCH
CONTROL
COM, NO, NC, NC, NO, COM
FROM OBSERVE CHANNEL SSB GENERATOR
TO OBSERVE CHANNEL TRANSMITTER
INPUT
20X225 270 MHz POWER AMPLIFIER
OUTPUT
CABLE ASSY: UT-141 0.141 SEMI-RIGID CORE W/ KINGS KA-59-86
20X224 270 MHz POWER AMPLIFIER
(N)
BIRD 43 THRULINE WATTMETER
TO PROBE
-40 dB MONITOR
UNLESS SPECIFIED:
ALL CABLE CONNECTORS - KINGS KA-59-86 OR KA-59-57 TNC
RG 55 B/U
8-270 MHz SPECTROMETER SYSTEM
DECOUPLE CHANNEL TRANSMITTER
INTERCONNECT FOR HETERONUCLEAR
PROTON DECOUPLING
16X967HP1
SHIH
1/19/79
W. SHIH
LAWRENCE BERKELEY LABORATORY
UNIVERSITY OF CALIFORNIA
16X9673-B3
CHANGES
DATE

spectra when a wide spectral width and enough data points can be used.

The observe channel local oscillator is obtained from the "pass-through" 38 - 300 MHz LO output of the observe channel 10X206 Single Sideband Generator. The 30 MHz IF is gated by the decouple channel 10X207 Four Phase Generator, and it is then passed through a 0 - 10.9 dB (0.1 dB step) attenuator for fine power regulation. After single sideband conversion in the 10X206 Single Sideband Generator, the gated signal is passed through a 16X980 high isolation Rf switch (90 dB on/off ratio) prior to amplification by a Hewlett-Packard/ Boonton Radio 230A tuned Rf power amplifier.

The low power homodecoupling Rf pulse train is duplexed with the high power observe channel pulses using a Hewlett-Packard 778D Dual Directional Coupler. This coupler isolates the output stages of the two transmitters, preventing adverse interactions. The 778D coupler has produced excellent results for proton homodecoupling, yielding spectra that are surprisingly free of spurious lines.

The heteronuclear proton decoupling connection shown in Figure 2.7 uses primarily the 10X221 30 - 300 MHz Frequency Multiplier as a local oscillator source. This requires that the magnetic field, as adjusted by the coarse H_0 field sweep amplifier (part of the 16X935 63 kG Magnet Shim Control) be adjusted so that the center of the decoupling bandwidth will occur in the desired part of the proton spectrum. The observe and lock local oscillator frequencies are then adjusted accordingly. Alternatively, the lock channel may be disabled and the lock synthesizer used to supply the decoupling center frequency.

For noise-modulated proton decoupling, the 30 MHz IF is 0/180°

phase modulated using a Hewlett-Packard 10514A double-balanced mixer as a modulator. A Hewlett-Packard 3722A shift register type pseudo-random noise generator is used to provide a binary pulse string to drive the modulator. Modulation bandwidth is adjusted by varying the clock period; the radiated power spectral density may be checked with a spectrum analyzer operating at either the 30 MHz intermediate frequency (looking at the output immediately after the modulator) or at the 270 MHz decoupling frequency (looking at the signal before the 10X225 270 MHz Power Amplifier or at the probe connection using a dummy load and -40 dB pick-off). Again the 0.1 dB step attenuator inserted into the 30 MHz line after the 10X209 Four Phase Generator is used for fine power control. Decoupling power is monitored with a Bird Thru-Line Rf directional wattmeter with either a standard plug-in element or a -40 dB directional coupler element. Decoupler power levels of < 10 watts RMS are normally sufficient for high resolution heteronuclear proton decoupling experiments.

2.3.5 Lock Channel

Although superconducting magnets have extremely stable fields, it has been found that some form of internal locking (*i.e.* H_0 field stabilization based on a resonance internal to the sample) is of great utility. Any nucleus may be selected for locking; deuterium is the choice in most high resolution work because of the pervasive use of deuterated solvents in NMR sample preparation. The principal benefits of operating in an internal locked mode are:

- Minimization of field drift during long term signal averaging that is required for experiments such as 2D data acquisition.

• A combination of monitoring the lock channel signal amplitude and viewing the lock signal lineshape and ringing pattern provides a convenient method of optimizing the H_0 field homogeneity.

The lock channel block diagram is shown in Figure 2.8. The channel may be subdivided into several functional units:

1. Lock channel transmitter -- operating under gating control of the 16X894 Lock Channel Control. The lock channel transmitter is very similar to the observe channel transmitter (2.3.2) except that the output power level is far lower. Frequency generation is again via single sideband mixing with a synthesizer supplied local oscillator.

2. Lock channel receiver -- is also similar to the observe channel receiver. After conversion to the 30 MHz intermediate frequency and predetection filtering, the lock signal is phase detected and supplied to the 16X894 control unit.

3. Lock channel control -- detects the lock signal and generates an error signal that is applied to the H_0 field sweep amplifier that is incorporated in the room temperature shim system controller (16X935).

4. Magnet shim control -- contains the H_0 field sweep amplifier to which error signals are applied. This unit also handles the display functions associated with field homogeneity adjustments.

Figure 2.8 8 - 270 MHz Spectrometer System ^{2}H Lock System Interconnect [16X9673-B6]

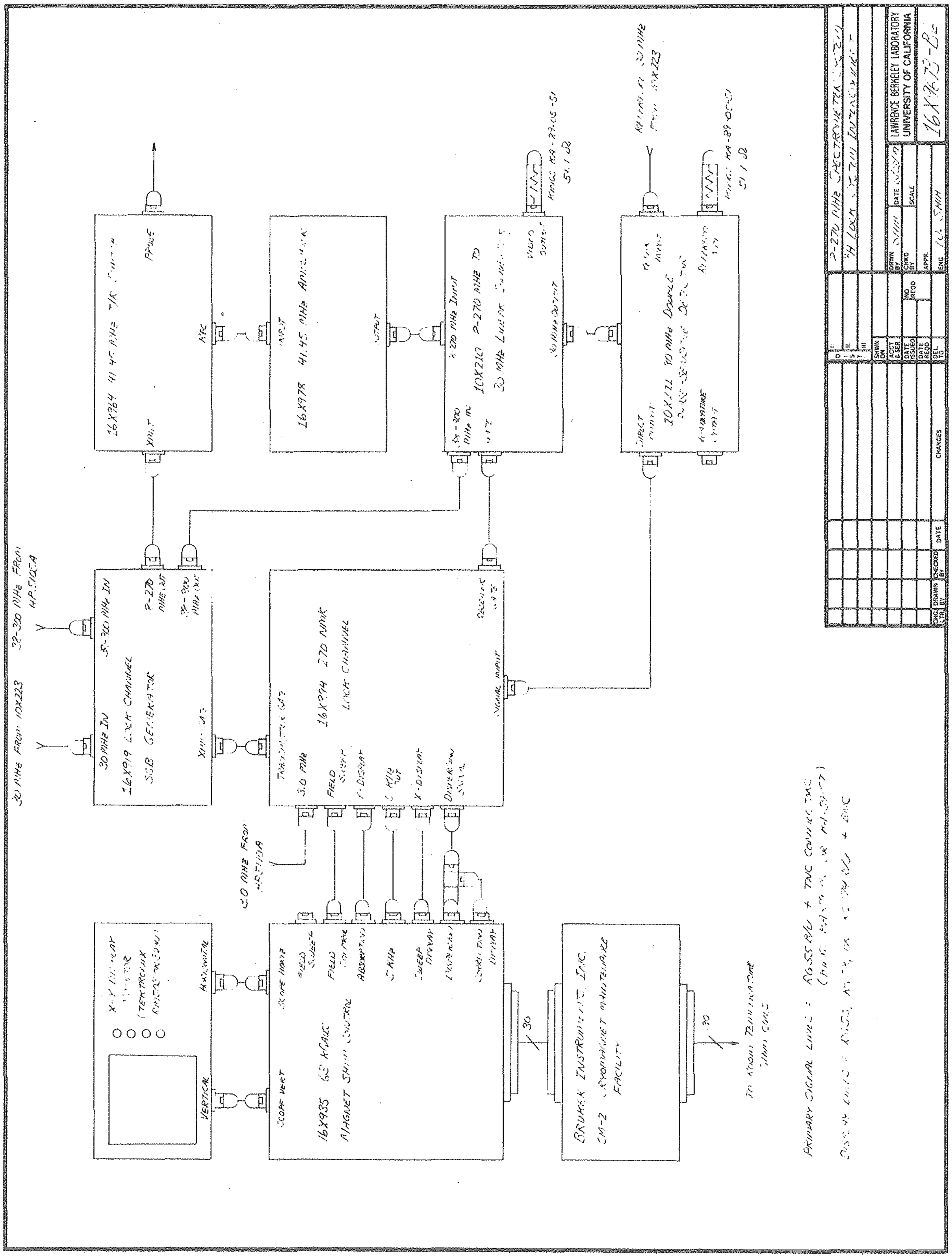
LAWRENCE BERKELEY LABORATORY
UNIVERSITY OF CALIFORNIA

The lock channel operates in the pulsed time-shared mode, with a gating frequency of 1.25 KHz. This implies that the lock nucleus is resonated at 1.25 KHz below the actual Larmor frequency, using the lower modulation sideband. The 1.25 KHz is derived in the 16X894 Lock Channel Control from a 3.0 MHz reference (from the HP 5110A frequency synthesizer driver) by direct digital division. Quadrature 5 KHz reference frequencies are also derived for use later in detection.

The 1.25 KHz pulse train (with adjustable delay and duty cycle) gates the 16X919 Lock Channel Single Sideband Generator. This unit is functionally equivalent to the 10X206 Single Sideband Generator used in the observe and decouple channels except that a phase-amplitude trim network is set to optimize conversion (harmonic suppression) at an output operating frequency of 41.451 MHz (the normal deuterium frequency).

Transmit/receive switching is handled by the 16X964 T/R Switch assembly. This unit differs from the T/R switches used for observation because of the difference in power levels. A 3 dB resistive pad is used for transmitter isolation; most of the noise blanking is performed by the final high isolation Rf switch in the 16X919 SSB generator. Diode switches were used originally in the T/R switch, but they were found to result in extreme non-linear behavior of the signal DC offset when the transmitter power level was varied.

The lock receiver is identical to the observe channel receiver; a 16X978 41.45 MHz amplifier is cascaded before the linear converter to provide 0 - 80 dB (adjustable) additional Rf gain. The 10X211 phase detector output is a low-pass signal whose amplitude is proportional to the lock signal strength.

The low-pass lock signal is bandpass filtered in the 16X894 lock control unit, and then it is phase detected at 5 KHz. Detection is done at four times the transmitter gating frequency to increase the efficiency of transmitter blanking. Because of a large amount of transmitter leakage, detection at 1.25 KHz would lead to large DC offsets in the detected output.[4] Detection at four times the gating frequency has the added advantage that both absorption and dispersion mode signals may be conveniently generated; the dispersion signal is used to generate the actual control signal and the absorption signal is used for display purposes.

Proportional plus integral control action is used. The control signal that is fed to the H_0 field sweep amplifier, m(t), is generated from the detected dispersion signal, e(t), in a form such as

$$m(t) = K_p\, e(t) + \frac{K_p}{T_i} \int_0^t e(t)\, dt \qquad (2)$$

K_p, the proportional sensitivity, is the controller gain; it may be adjusted at a number of points in the control loop. T_i is the integral time, it may also be internally adjusted. Proportional plus integral control action is used because pure porportional control leads to steady-state errors which may be eliminated by addition of the integral term.

2.3.6 Probes

Probes are key elements of the 8 - 270 MHz spectrometer system. Their function of course is to couple radiofrequency excitations to the sample and detect the resulting behavior of the nuclear magnetizations. Most high resolution probes provide at least the following capabilities:

- Observation at either a single frequency or over a set bandwidth.
- Proton decoupling for the observation of ^{13}C, ^{31}P, ^{15}N, etc.
- Provision for heteronuclear internal locking, usually on deuterium.
- Monitoring of sample temperature, with provision for heating or cooling.

The observation and locking functions are usually fulfilled by one coil, and decoupling is done with a second orthogonal coil. The solenoid configuration of a superconducting magnet imposes another constraint: if probes are to remain in place when samples are interchanged, the samples must be removed axially. Since the Rf coils must generate fields orthogonal to the H_0 field direction, this dictates the use of Helmholtz style coils rather than solenoids.

Factors influencing probe design have been discussed extensively in the literature.[5-9] The typical arrangement consists of a parallel resonant circuit with elements R, L, and C. The sample is contained in the coil, L, and the capacitance C is used to set the resonance frequency:

$$\omega_0 = 1/\sqrt{LC} \tag{3}$$

Losses are modeled by the parallel resistance R, and the figure of merit is defined by

$$Q = R/\omega_0 L = R\omega_0 C = R\sqrt{C/L} \tag{4}$$

To maximize power transfer from the transmitter to the resonant circuit (and conversely from the sample to the receiver), a passive (loss-less) two-port network may be used to effect an impedance transformation (Figure 2.9). Synthesis of these two port networks and general probe design principles have been described elsewhere.[9-13]

Five probes presently exist for the LCB 8 - 270 MHz spectrometer system. Associated sample tube sizes and operating frequencies are listed in Table 2.3. Circuit configurations are summarized in Figures 2.10 - 2.18. The 5 mm ^{1}H, 10 mm ^{13}C, 10 mm ^{31}P, and 15 mm ^{15}N probes represent reconstructions of commercial Bruker Instruments, Inc. probes. Reconstruction generally involved replacement of one or both coils, replacement of all tunable capacitors, and the repositioning of several key capacitors to make remote tuning possible. The 10 mm $^{1}H/^{3}H/^{13}C/^{2}H$ probe was fabricated using Bruker probe housings; the balance of the probe consisted of locally fabricated parts. Remote tuning capabilities were included for all frequencies. Figures 2.19 and 2.20 show two views of this probe.

As is apparent from the drawings, tapped parallel tuned circuits (or a variation) were used in all cases. It was found that the parallel tuning capacitor could be used to adjust the resonant frequency with minimal changes to the probe input impedance, therefore when remote tuning capabilities were included, this was the capacitor that was made adjustable.

The relationship of coil geometry to performance has been discussed in detail by Hoult and Richards.[14] Helmholtz coils of a geometry prescribed by Lyddane and Ruark,[15] and others,[16,17] were used for low frequencies (< 100 MHz). Above 100 MHz, coils of a design similar

Table 2.3 8 - 270 MHz Spectrometer System: Sample Probe Specifications

PROBE	*SAMPLE TUBE SIZE*	*OPERATING FREQUENCIES*		*REMOTE TUNING CAPABILITY*
^{1}H	5 mm	^{1}H	269.9985 MHz	
		^{2}H	41.4513 MHz	
^{13}C	10 mm	^{13}C	67.8975 MHz	
		^{1}H	269.9985 MHz	×
		^{2}H	41.4513 MHz	
^{31}P	10 mm	^{31}P	109.2970 MHz	
		^{1}H	269.9985 MHz	×
		^{2}H	41.4513 MHz	
^{15}N	15 mm	^{15}N	27.3600 MHz	×
		^{1}H	269.9985 MHz	×
		^{2}H	41.4513 MHz	
$^{13}C/^{1}H/^{3}H$	10 mm	^{13}C	67.8975 MHz	×
		^{1}H	269.9985 MHz	Wide range tuning
		^{2}H	41.4513 MHz	×

Figure 2.9 Matching of a Parallel Resonant Circuit with a Passive Lossless Two-port

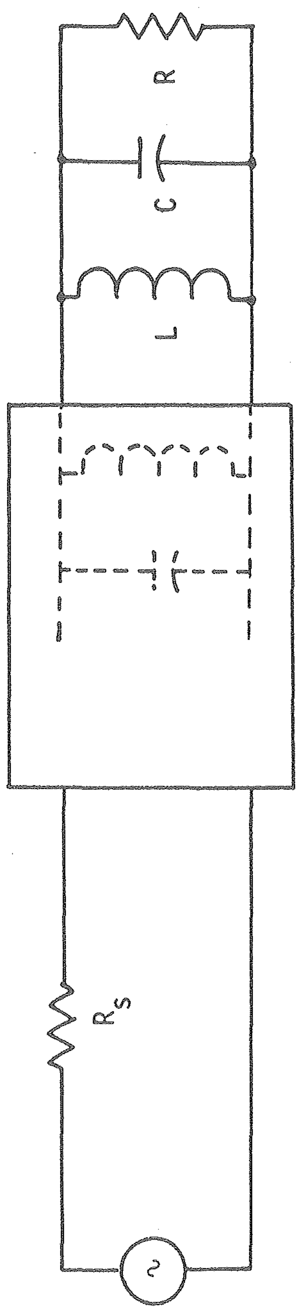
R
C
L
R_S

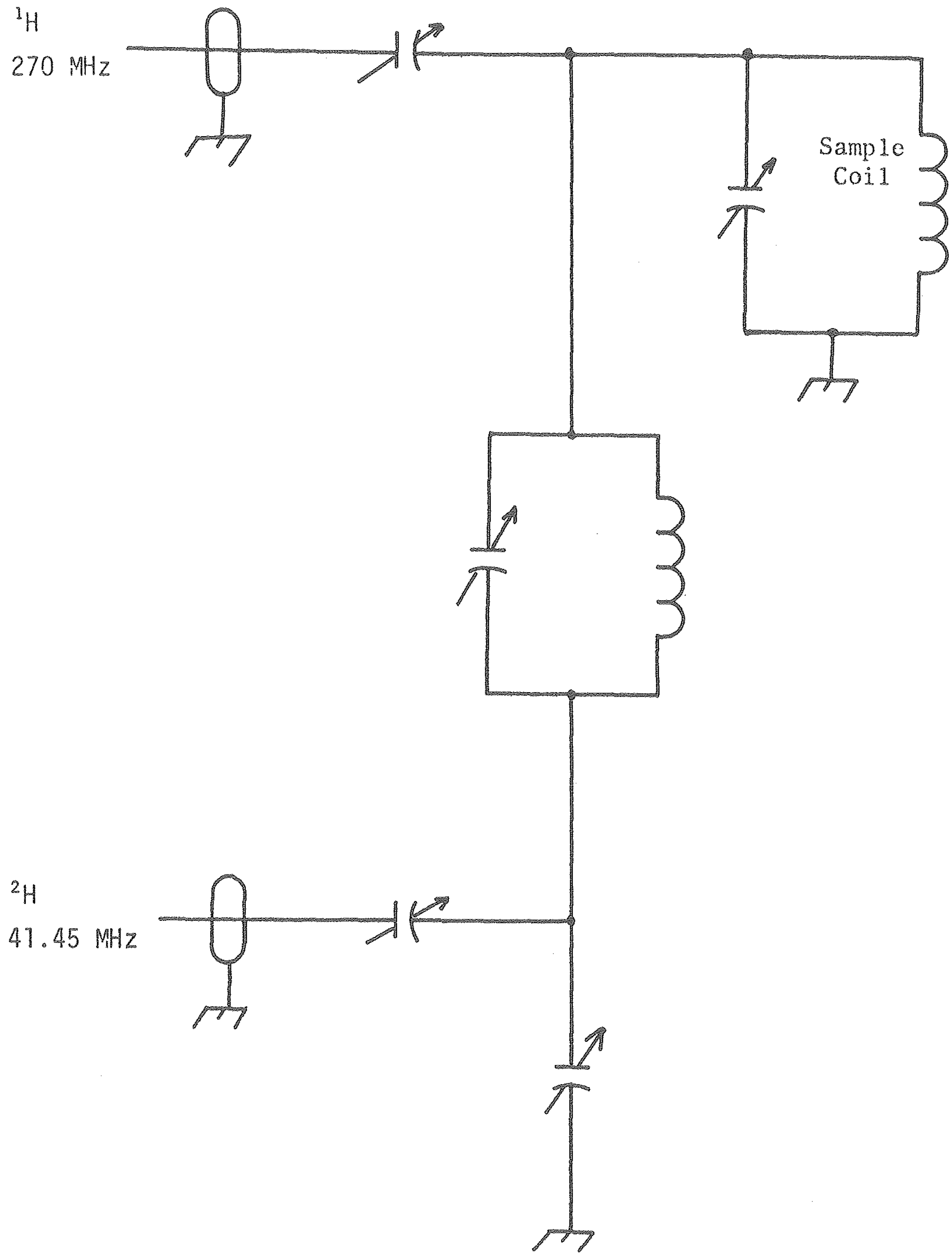

All variable capacitors: Johanson 5761 paralleled with appropriate value ATC 100B series porcelain chip capacitors

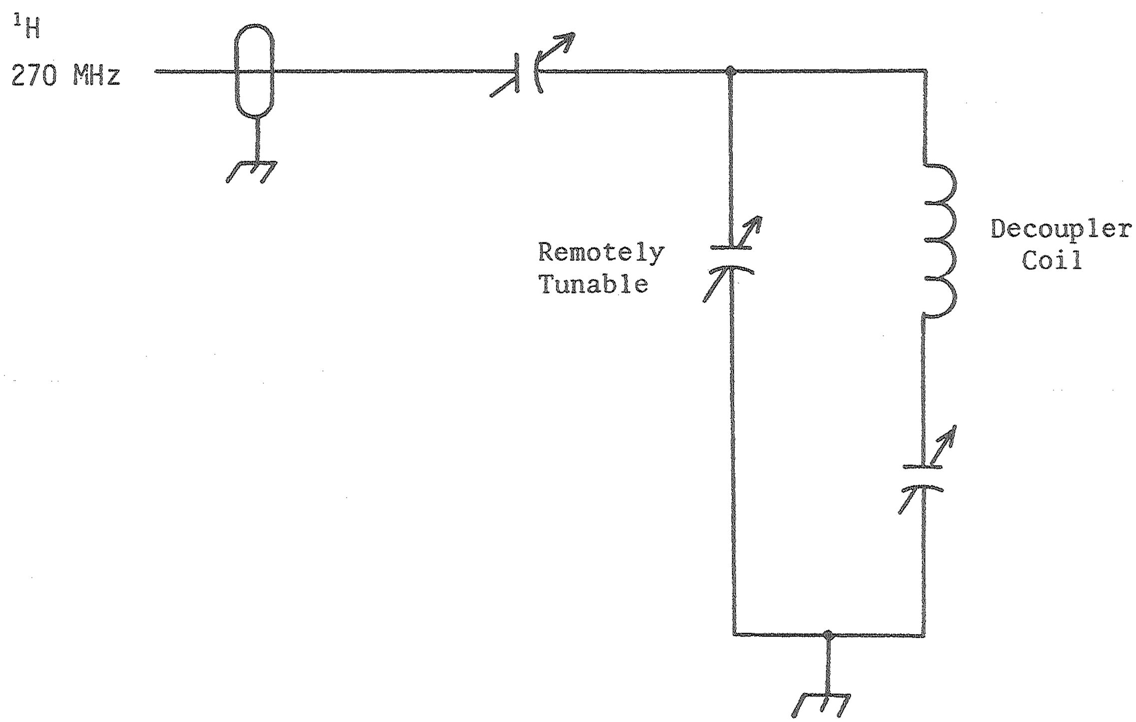

All variable capacitors: Johanson 5761 paralleled with appropriate value ATC 100B series porcelain chip capacitors

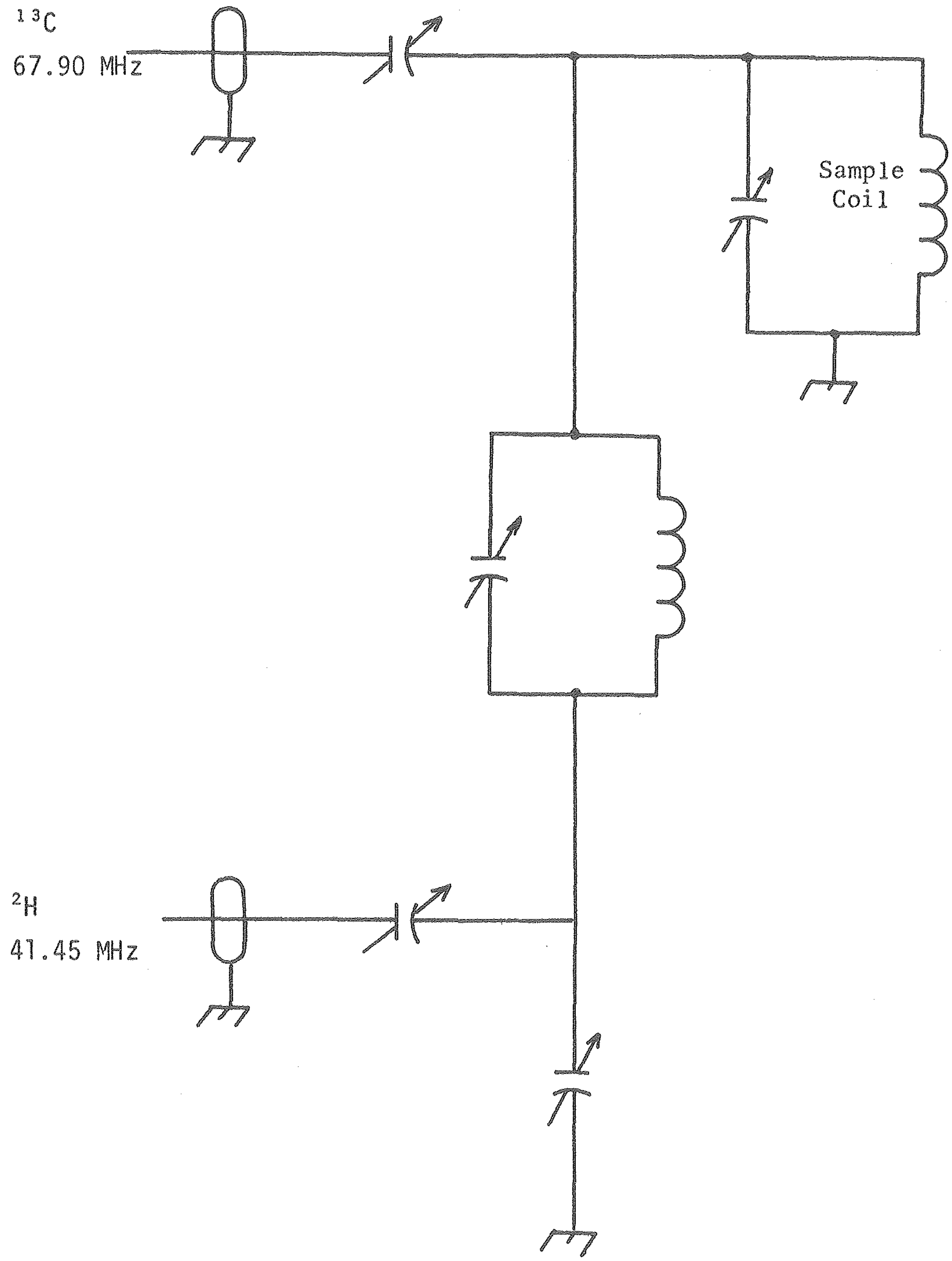

All variable capacitors: Johanson 5761 paralleled with appropriate value ATC 100B series porcelain chip capcaitors

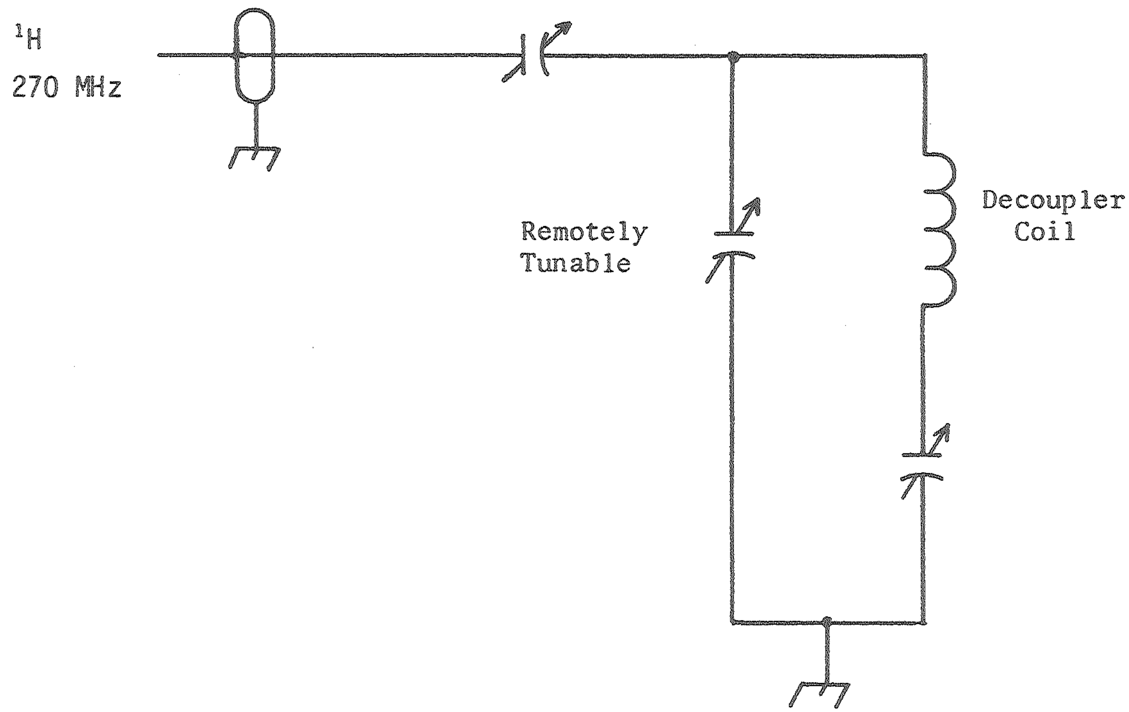

All variable capacitors: Johanson 5761 paralleled with appropriate value ATC 100B series porcelain chip capacitor

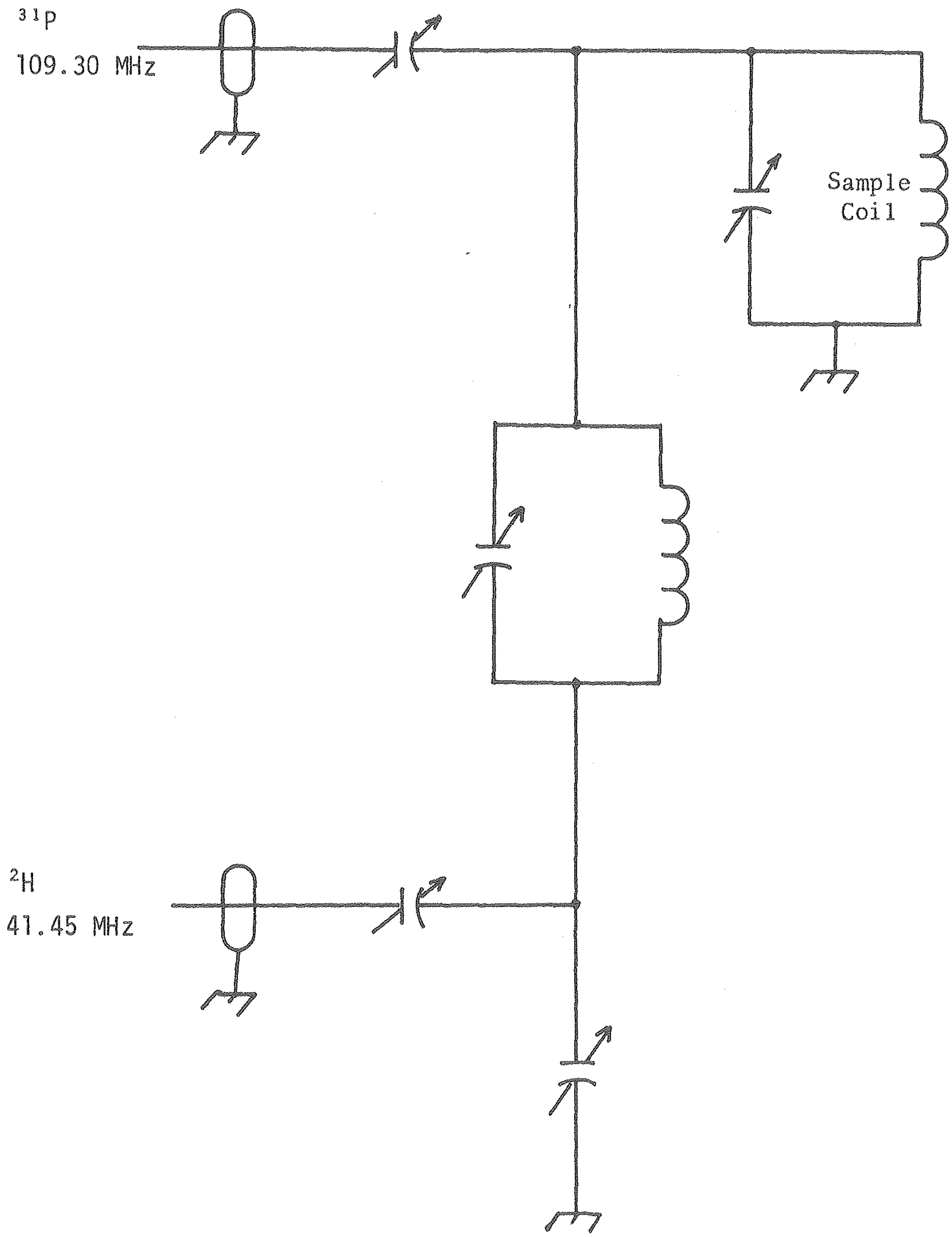

All variable capacitors: Johanson 5761 paralleled with appropriate value ATC 100B series porcelain chip capacitors

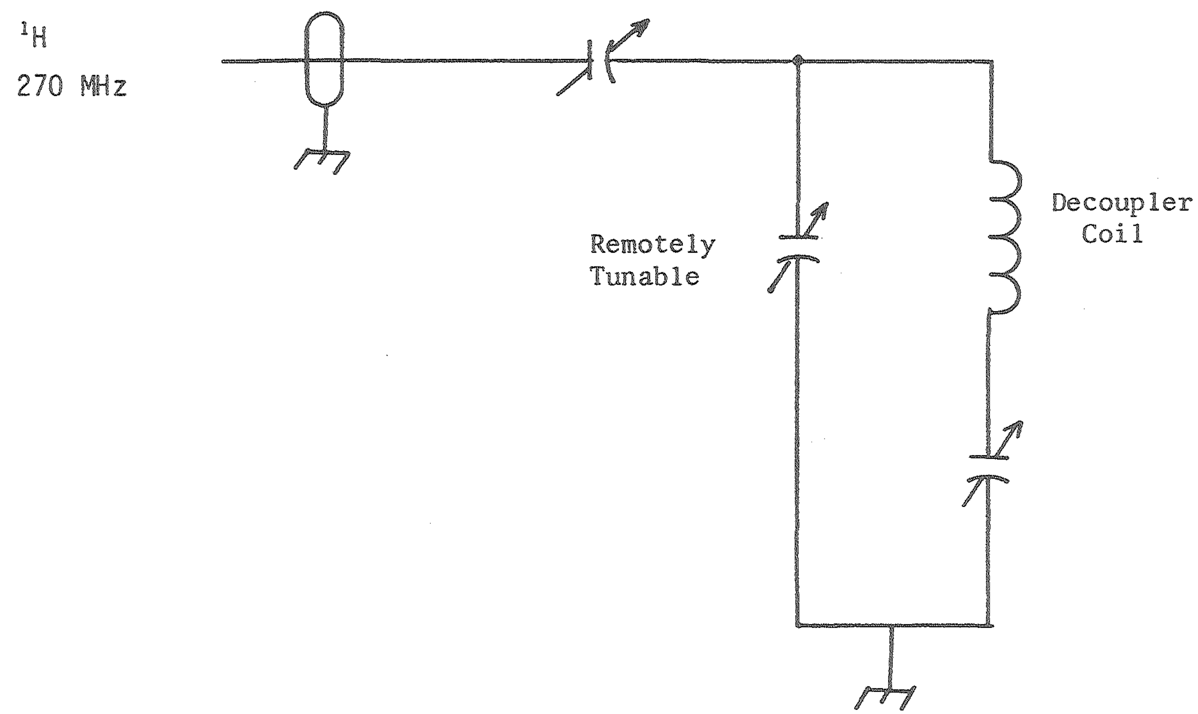

All variable capacitors: Johanson 5761 or equivalent, paralleled with appropriate value ATC100B series porcelain chip capacitors

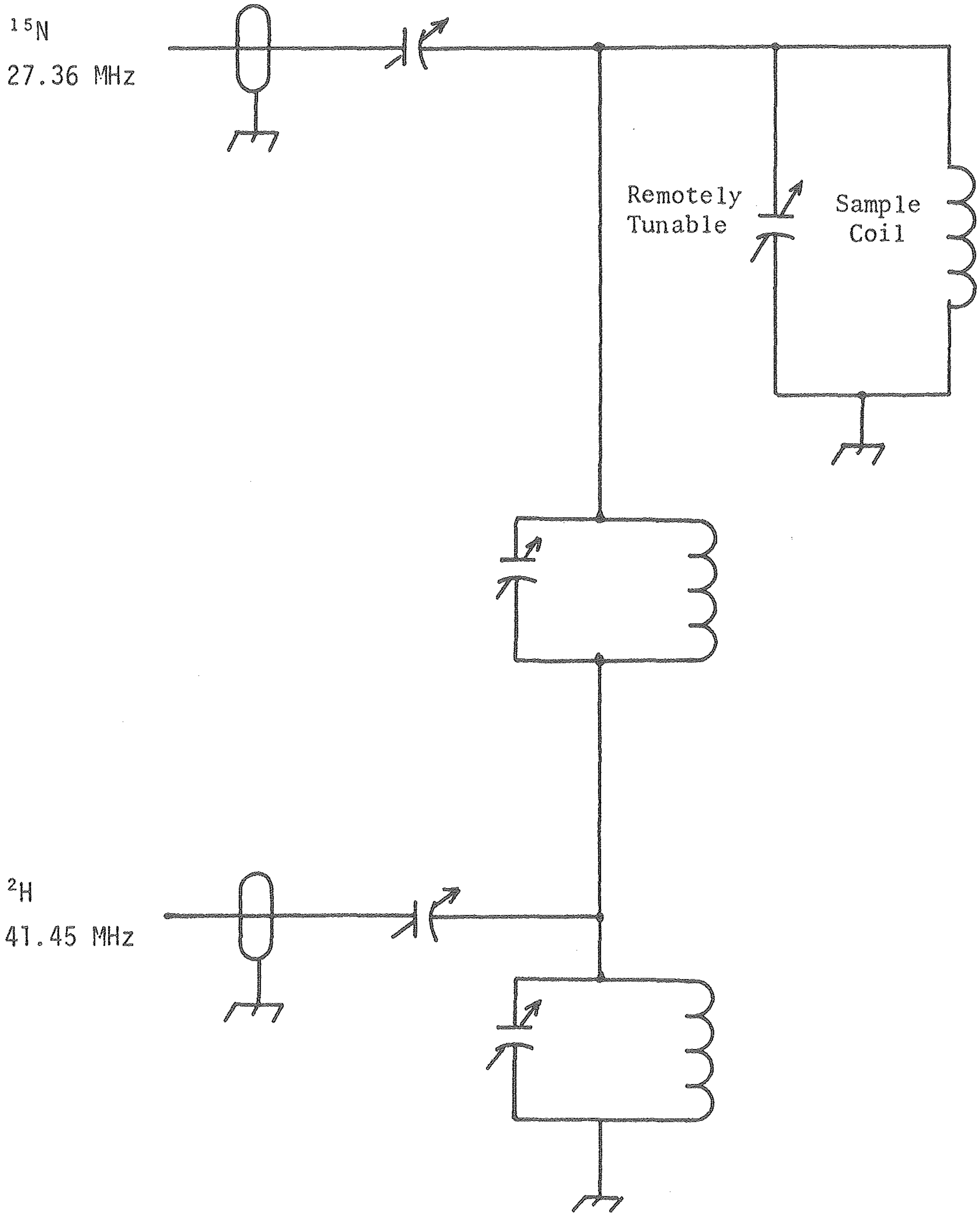

All variable capacitors: Johanson 5761 or equivalent, paralleled with appropriate value ATC 100B series porcelain chip capacitors

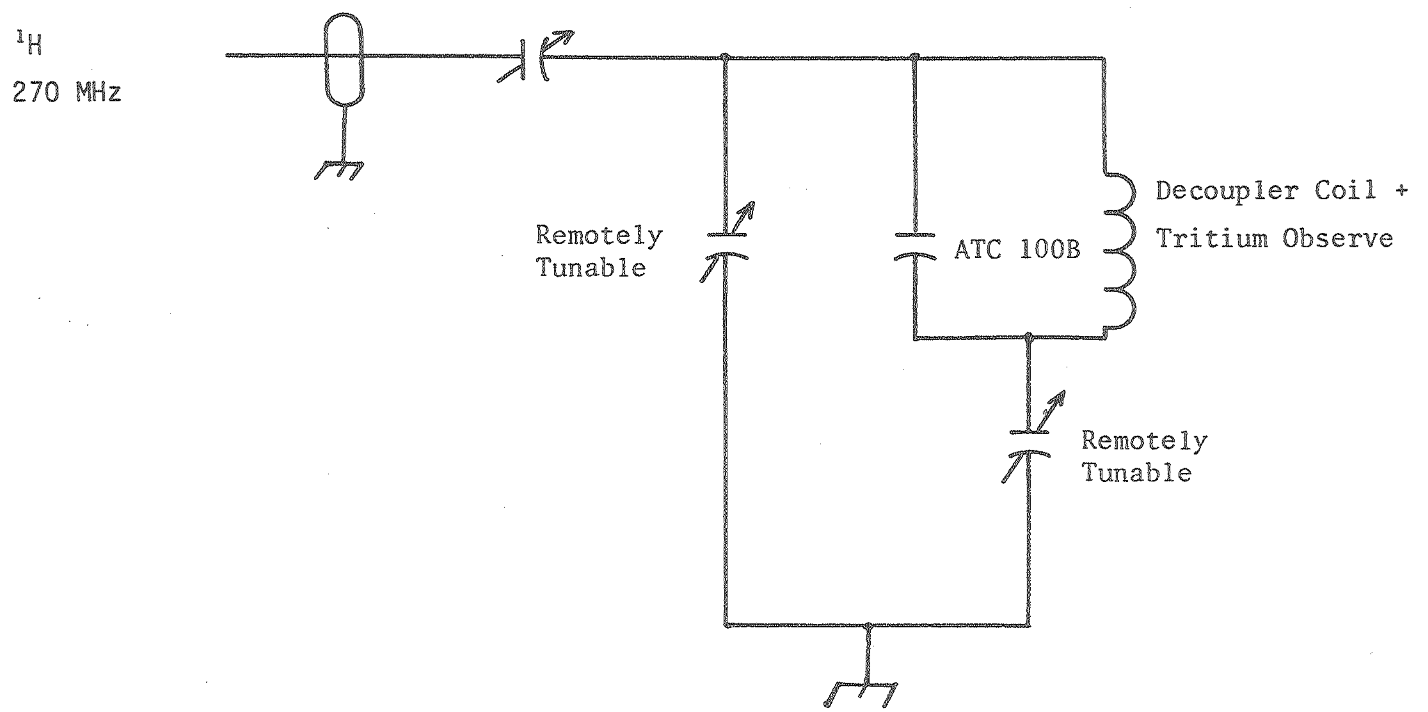

All variable capacitors: Johanson 5341 0.8 - 10 pF variable, paralleled with appropriate value ATC 100B series porcelain chip capacitor

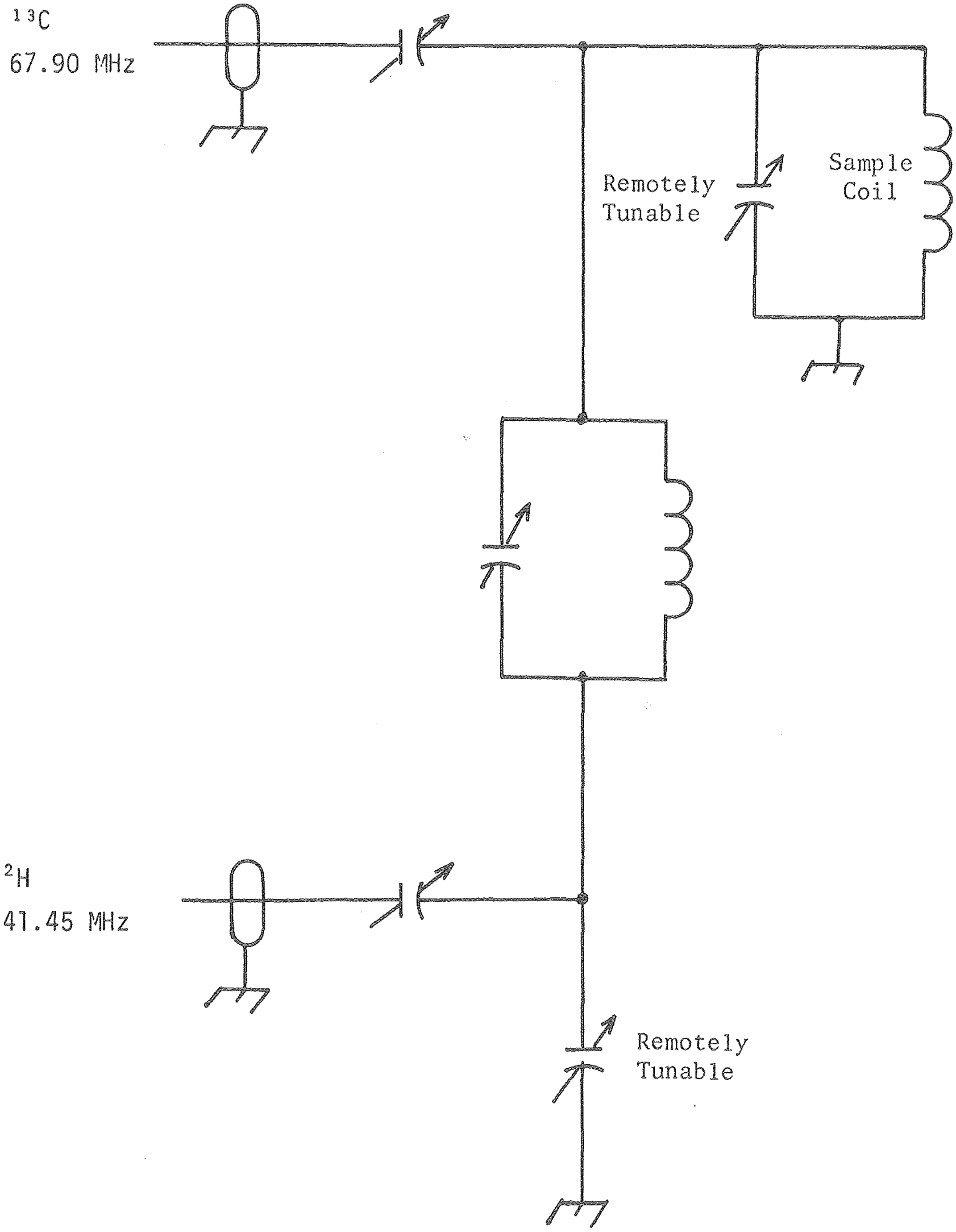

All variable capacitors: Johanson 5341 0.8 - 10 pF variable, paralleled with appropriate value ATC 100B series porcelain chip capacitors

Figure 2.19 $^{1}H/^{3}H/^{13}C/^{2}H$ 10 mm Probe, Insert Detail and 67.89 MHz/ 41.45 MHz Matching Network Detail (Cover removed)

Figure 2.20 $^{1}H/^{3}H/^{13}C/^{2}H$ 10 mm Probe, Insert Detail and 270 MHz Matching Network Detail (Cover removed)

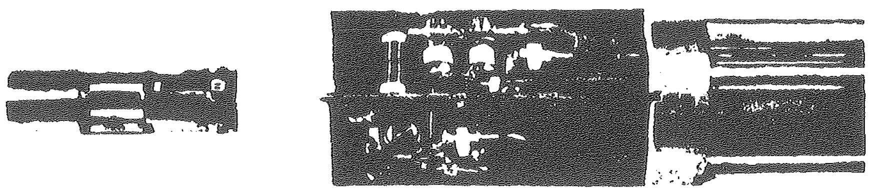

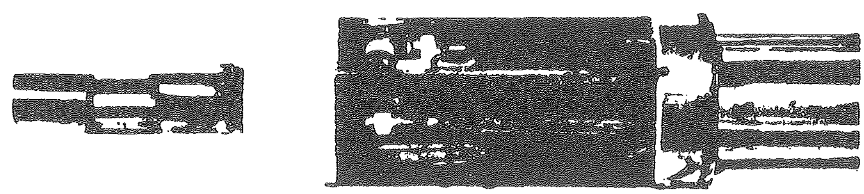

Figure 2.21 Typical High Frequency Coil Cutting Pattern, Dimensions Shown for Placement on the Inside of a 13 mm O.D. Insert

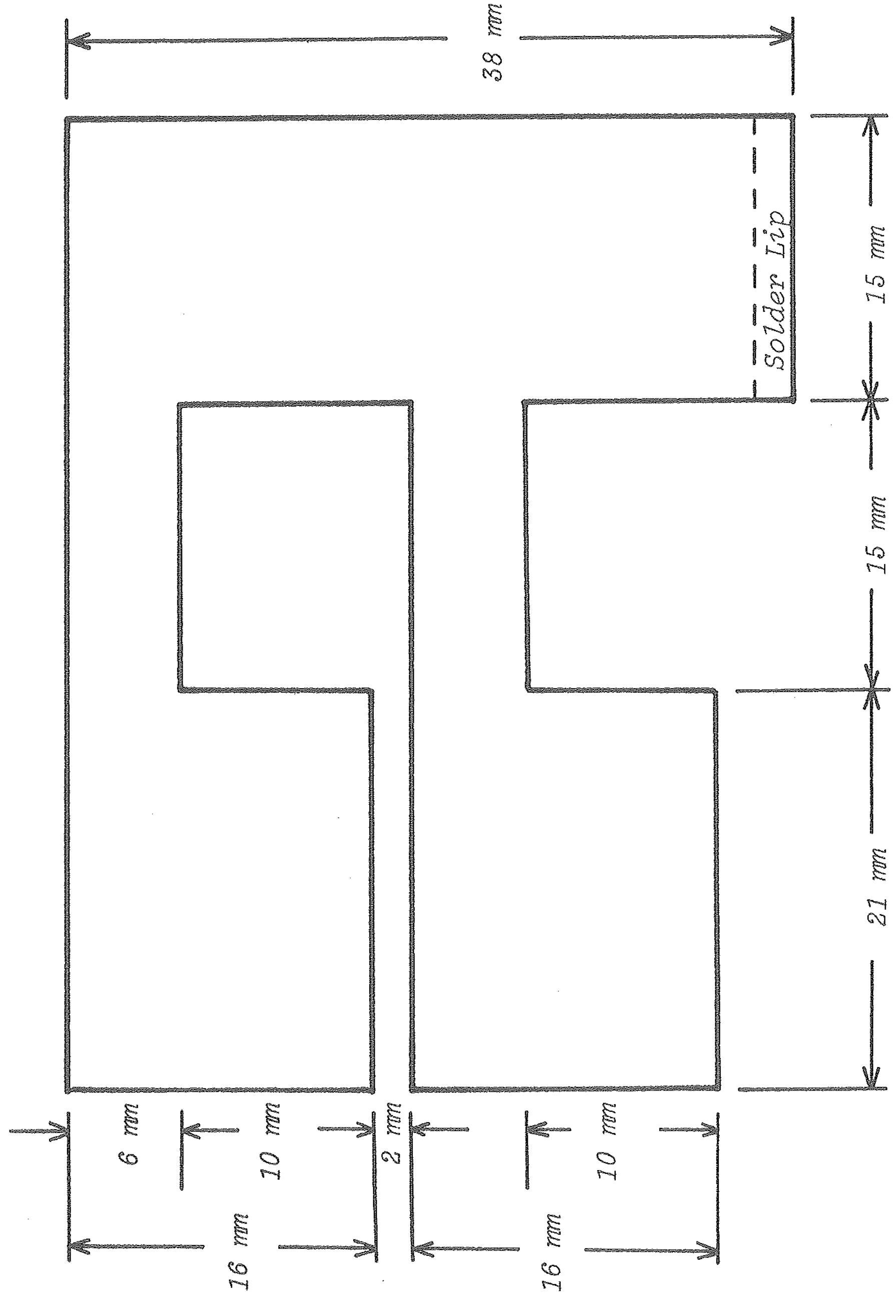
38 mm
Solder Lip
15 mm
15 mm
21 mm
6 mm
10 mm
2 mm
10 mm
16 mm
16 mm

to one of Dadok were used (visible in Figures 2.19 and 2.20). These were cut from 0.001" OFHC copper foil (Electronic Space Products, Los Angeles, CA) in a pattern such as is shown in Figure 2.21. The principal advantages of this configuration are:

1. Once the coil is soldered together, it is self-supporting and no adhesives are required to fasten it to the insert glass.
2. Reduced sensitivity to bulk susceptibility changes in the sample were noticed; the reason is not known.
3. Vastly improved heat dissipation when the coils were used for broadband noise-modulated decoupling, because of increased surface area and a consequent increase in heat transfer efficiency to the cooling gas stream.
4. Lower distributed inductance made the attainment of higher operating frequencies easier; also higher Q's were attained.

The most significant problem with this design coil was that the large surface area resulted in significant capacitive coupling to the other coil (if one was present). Probe design, construction, and tuning were done with the aid of the three network analysis methods described in Section 2.4.1.

2.3.7 Data Processing and Control

A Nicolet Instruments Corp. Model 1180 Data Processor is one of the key elements of the LCB 8 - 270 MHz spectrometer system. Operating under a Nicolet Technology Corp. supplied software package (NTCFT-1180), this unit handles all data acquisition and control functions. This section will outline the digital interconnections between peripheral devices and the processor. Connections may be subdivided into four categories:

1. High speed mass I/O
2. Low speed I/O and display drivers
3. Direct I/O bus connections
4. Nicolet 293A Programmable Pulser I/O connections

All digital interconnections are shown in Figure 2.22. The first two categories are covered in detail in the Nicolet 1180 Service Manual,[18] and only brief mention of connections is made. The third category includes devices connected via the 16X904 I/O Bus Intercept; among these are the 16X950 Temperature Control, the 16X956 CalComp 565 Interface, and the 16X902 Remote Controlled Low-Pass Filter. Devices in the last category include the 16X892 System Control Logic, and devices driven by the 293A digital-to-analog converters (DACs).

.1 High Speed Mass I/O

Two types of disk memory systems may be used with the 1180 -- a dual platter Diablo Model 44 drive using IBM 5440 type media, or a single platter (removable) Diablo Model 31 drive with IBM 2315 type media. The LCB system uses the latter; both drives share a common interface board with only minor timing variations.

When using Diablo 31 drives, bits 14 and 13 of the sector register specify the drive unit number. Up to four drives may be connected in daisy-chain fashion, using ribbon cables with integral ground planes.

Figure 2.22 8 - 270 MHz Spectrometer System Digital Interconnect [16X9673-B1]

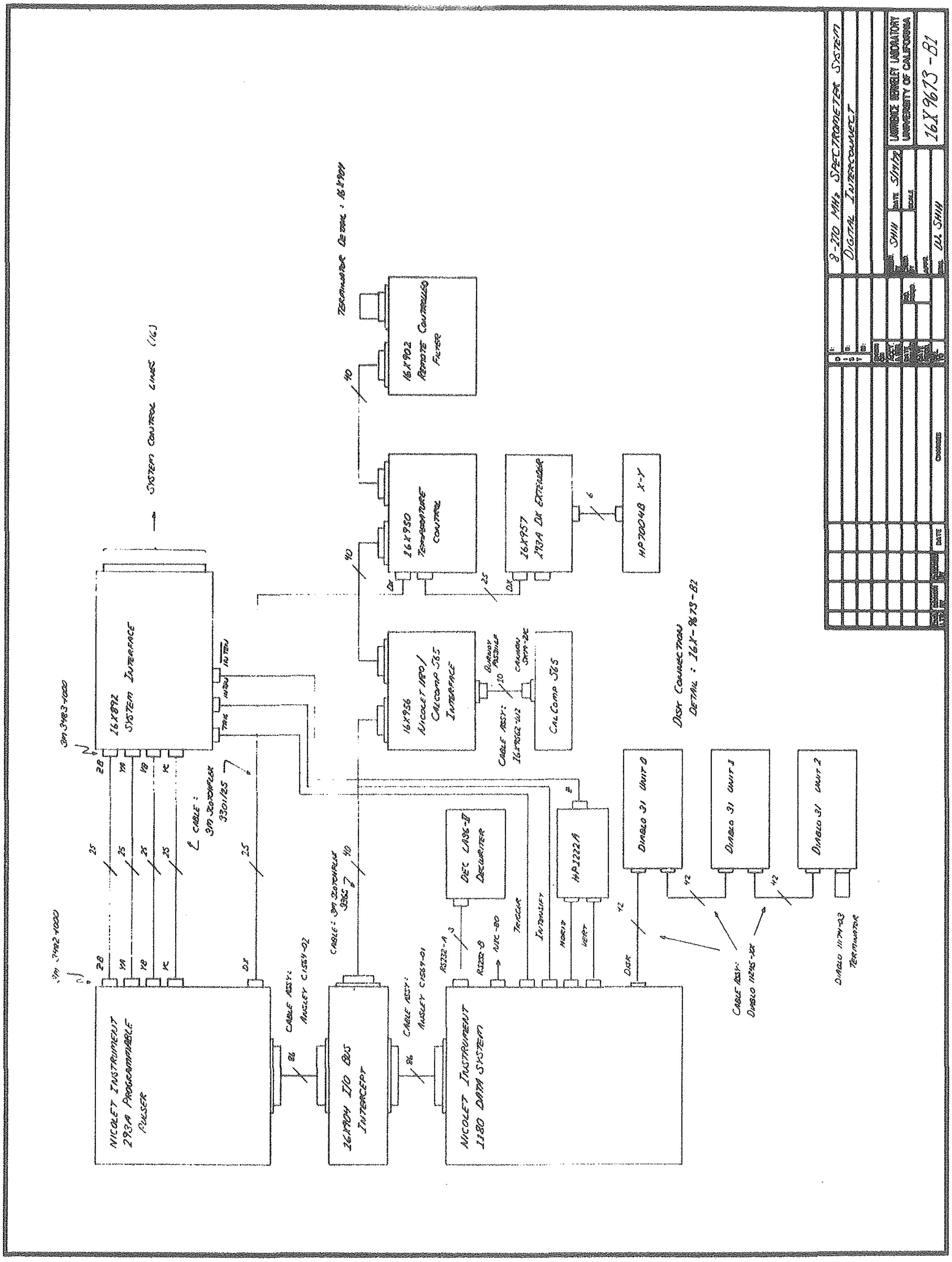

8-200 MHz SPECTROMETER SYSTEM
DIGITAL INTERCONNECT
LAWRENCE BERKELEY LABORATORY
UNIVERSITY OF CALIFORNIA
16X9673-B1
NICOLET INSTRUMENT 293A PROGRAMMABLE PULSER
16X904 I/O BUS INTERCEPT
NICOLET INSTRUMENT 1180 DATA SYSTEM
16X892 SYSTEM INTERFACE
SYSTEM CONTROL LINES (16)
16X936 NICOLET 1180/ CALCOMP 565 INTERFACE
CALCOMP 565
16X950 TEMPERATURE CONTROL
16X957 293A DX EXTENDER
HP7004B X-Y
16X902 REMOTE CONTROLLED FILTER
DEC LA36-II DECWRITER
HP1222A
DIABLO 31 UNIT 0
DIABLO 31 UNIT 1
DIABLO 31 UNIT 2
DISK CONNECTION DETAIL : 16X-9673-B2
DIABLO 1174-03 TERMINATOR

Each drive has jumper pins on its motherboard that select the unit number that it will recognize, therefore drives may be chained in any order.

Only one of the drives was originally delivered with the 1180; this was assigned Unit 0. Drives 1 and 2 were obtained used; after reconditioning, they were installed with locally modified power supplies (described by print 16X9673-B2).

.2 Low Speed I/O and Display Drivers

The 1180 Slow I/O board is used to interface low speed serial data format peripherals such as terminals. Serial I/O is handled by universal asynchronous receiver/transmitter chips (UARTs); two are provided (Channels A and B). The Channel A UART was connected to a Digital Equipment Corp. LA36 Decwriter II terminal, while the channel B UART was replaced with a high speed IM6402CPD (Harris 6402) UART which permitted operation at 38.4 KBaud. Channel B was connected to either a VAX 11/780 or to a Nicolet NIC-80 processor. Discussion of these connections is in Appendix 1.

The other type of slow I/O goes via the Display Board. Display board DACs are used to drive an X-Y-Z display (Hewlett-Packard 1222A) for the display of memory contents (spectra, etc.).

.3 Direct I/O Bus Connections

Locally designed 1180 peripherals that require 20 bit parallel I/O are connected directly to the 1180 I/O Bus by way of the 16X904 I/O Bus Intercept. This implies that the device must be assigned a unique address (that is not used internally by the 1180), and access to the device is via newly defined I/O instructions that incorporate this address. The three devices presently attached to the bus in this fashion were assigned the same device addresses that Nicolet Technology Corp. assigns to similar peripherals, thus minimal software changes were necessary. Details of each device will be provided in Section 2.5.

.4 Nicolet 293A I/O Connections

The bulk of the 293A I/O connections are for the 16X892 System Control Logic. The 16X892 print set and associated descriptions in Section 2.5 cover this subject thoroughly.

The other type of device connected to the 293A utilizes the DAC board in the 293A. These devices and their functional relationships are:

1. 16X950 Temperature Control -- uses DAC2 as part of the control loop; DAC2 drives the programmable power supply that powers the variable temperature gas heater.
2. 16X957 293A DX Extender -- provides for multiple connections to the 293A DX connector.
3. Hewlett-Packard 7004B recorder -- is used for generating plots when the CalComp 565 Incremental Plotter is not connected. DAC0 (DX-2) drives the X-axis, and DAC1 (DX-3) drives the Y-axis.

2.4 Test and Characterization Procedures

2.4.1 Complex Impedance, Reflection Coefficients, and VSWR

Sample probes for the 8 - 270 MHz spectrometer system were characterized by measuring the complex impedance of the various ports as a function of frequency. Three overlapping techniques were used; applicability was determined by the frequency range of interest, and by whether a swept frequency display was preferred or if it was necessary to get complete phase information at a single frequency.

When a transmission line is terminated with a load that is not identical to the characteristic line impedance, a standing wave pattern is set up along that line. This pattern is composed of an incident voltage wave E_i and a reflected wave E_r. The ratio of these two is the reflection coefficient, $\overline{\rho}$, which is a vector quantity that includes the relative phase between the two (Figure 2.23)

$$\overline{\rho} = \rho \angle \theta_\rho = \frac{E_r}{E_i} \tag{5}$$

The angle θ_ρ varies as the distance along the line from the load. The reflection coefficient is determined by the impedance of the load (Z) and the characteristic impedance of the line (Z_0):

$$\frac{Z}{Z_0} = \frac{1 + \overline{\rho}}{1 - \overline{\rho}} \tag{6}$$

The voltage standing wave ratio (VSWR) and return loss don't carry phase information:

$$\text{VSWR} = \frac{1 + |\overline{\rho}|}{1 - |\overline{\rho}|} \tag{7}$$

$$\text{Return Loss} = -20\ log\ |\overline{\rho}| \tag{8}$$

Reference points are an open circuit ($\rho = 1 \underline{/\ 0°}$) or a short circuit ($\rho = 1 \underline{/\ 180°}$).

2.4.2 Measurement Techniques

A. Complex Impedance, 500 KHz to 109 MHz

Impedance measurements in this frequency range were made with a Hewlett-Packard 4815A Vector Impedance Meter. This device measures the Rf current flowing through a device for a given low excitation voltage, and converts this information to a complex impedance reading (magnitude and phase angle).

B. Complex Impedance, 100 MHz to 1 GHz

Impedance measurements in this frequency range were made using a Hewlett-Packard 8405A Vector Voltmeter in conjunction with a Hewlett-Packard 778D Dual Directional Coupler in the test arrangement of Figure 2.24. The directional coupler is used to provide accurate samples of the incident and reflected wave amplitudes, and the phase angle between the two. Prior to making measurements, a short ($\rho = 1 \underline{/\ 180°}$) is placed at the end of the coupler, and a phase reference of 180° is set on the vector voltmeter using the phase offset and by stretching the sliding line.

The measured reflection coefficient is readily converted to complex impedance using a Smith chart. Alternatively, a short BASIC program was written to perform this conversion (Appendix 2).

C. VSWR, 1 MHz to 1 GHz

Voltage standing wave ratio measurements were made in a swept frequency mode using a Wiltron Model 610B swept frequency generator and an Anzac RB-3-50 VSWR Bridge. The test setup is illustrated in Figure 2.25. Since the VSWR does not contain phase information, this method was most useful when the network was already fairly well characterized; it was extremely useful for final probe tuning adjustments where the impedance match was already quite close.

Figure 2.23 Angle θ and Magnitude E_r/E_i of Incident and Reflected Waves as Determined by Load Impedance

Figure 2.24 Complex Impedance Measurement Using HP 8405A Vector Voltmeter and HP 778D Dual Directional Coupler

Figure 2.25 Swept Frequency VSWR Measurement Using Wiltron 610B Frequency Sweeper and VSWR Bridge

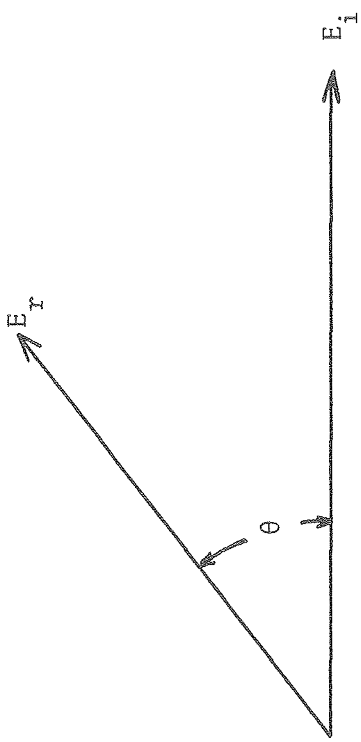

$$\frac{E_r}{E_i} = \bar{\rho}$$

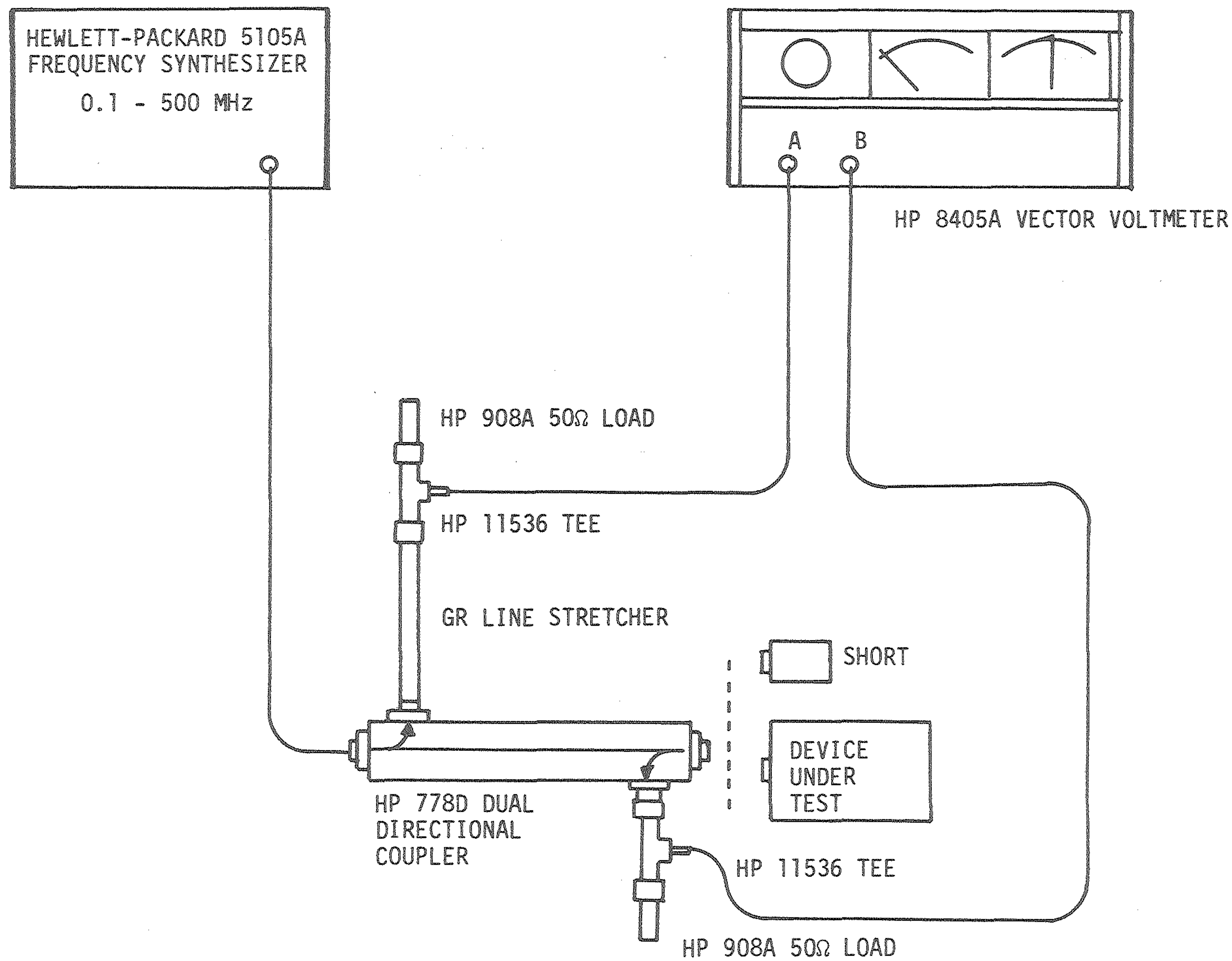

COMPLEX IMPEDANCE MEASUREMENT TEST SET-UP USING DIRECTIONAL COUPLER

XBL 7910-12483

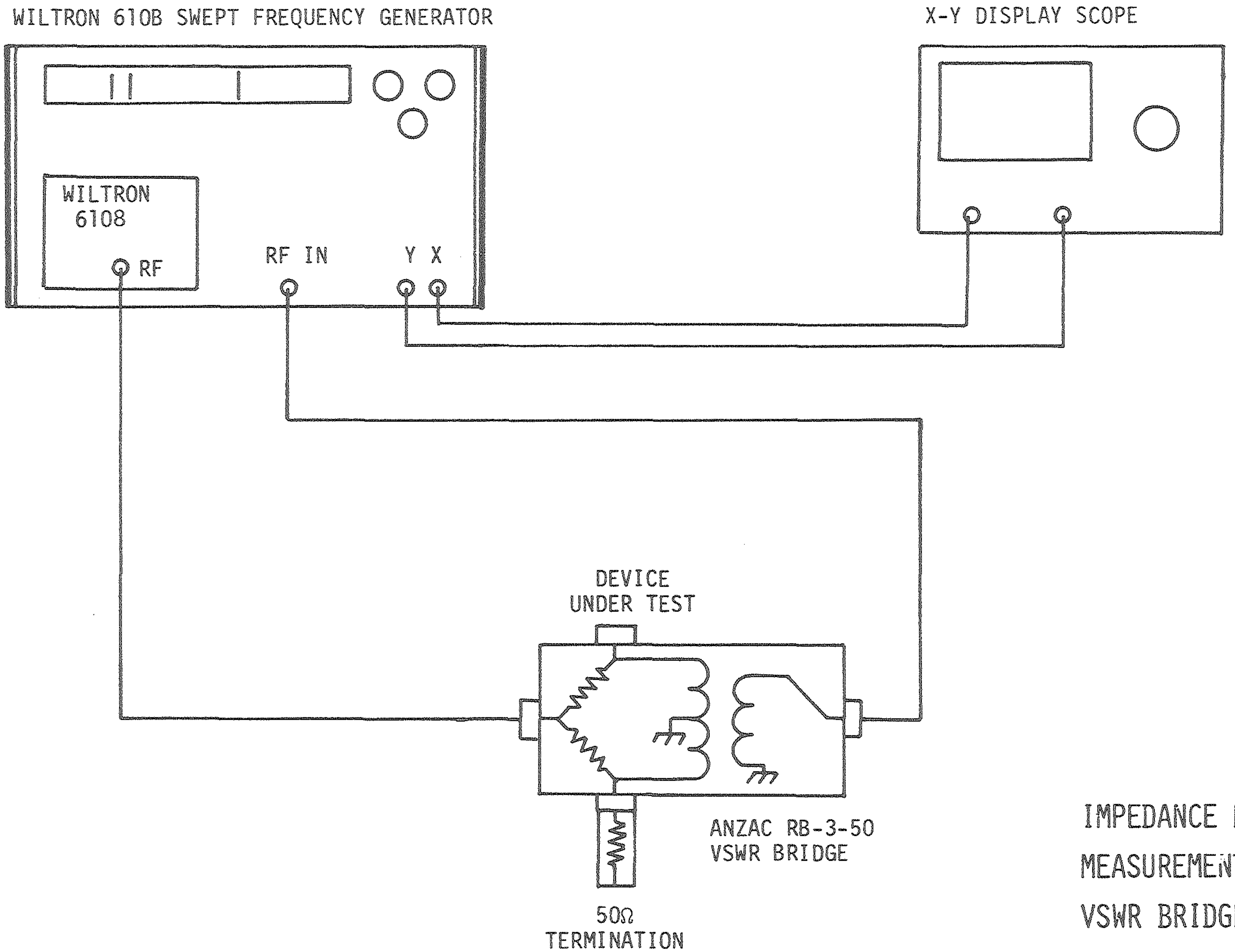

IMPEDANCE MISMATCH
MEASUREMENTS USING
VSWR BRIDGE

XBL 7910-12481

2.4.3 Evaluation of System Noise Performance

The usual form of the signal-to-noise ratio after a 90° pulse is given by Abragam:[19]

$$\frac{v_s}{v_n} = K\eta M_0 \left(\mu_0 Q\omega_0 V_c/4FkT_c\ \Delta f\right)^{1/2} \qquad (9)$$

where K is a numerical factor ($\simeq 1$) related to coil geometry; η is the "filling factor," *i.e.* the fraction of the coil volume occupied by sample; V_c is the coil volume; M_0 is the nuclear magnetization; Q is the quality factor of the coil; ω_0 is the Larmor frequency; μ_0 is the permeability of free space; F is the receiver noise figure at bandwidth Δf (Hz); k is Boltzmanns constant; and T_c is the probe temperature. It has been pointed out by several authors that this is not a fundamental equation, but is useful for order of magnitude calculations.[14,19,20]

Of the four unknowns in equation (9), K, η, Q, and F, only the latter two are easily measurable. This section is devoted to discussion of the last factor -- receiver noise performance, and other system noise contributions.

One of the traditional measures of spectrometer system performance has been the one-shot signal-to-noise ratios for certain standard samples. The difficulty with this approach is that it does not discriminate between the effects of magnetic field inhomogeneity and receiver noise performance. These effects were separated during the construction of the 8 - 270 MHz spectrometer system by making separate noise figure measurements on receiver system components, both individually and in cascade.

2.4.4 Noise Sources

Noise at an NMR receiver input may be attributed to two primary sources:

- Thermal noise in the probe, and radiative pick-up
- Transmitter noise

The probe is an RLC one-port network, therefore the mean square noise voltage at its output is given by Nyquist's formula:

$$\langle v_n^2(t)\rangle = 2\,kT_c\int_{-\infty}^{\infty} R(f)\,df \tag{10}$$

where R(f) is the real part of the complex impedance seen looking into the port. Thus for a narrow-band tuned probe, the principal contribution is thermal noise.

The nature of the output stages of the Eimac 8877 power triode amplifiers used for the transmitters suggests that transmitter noise is a combination of hot thermal noise and shot noise. The normal isolation procedure is to minimize current flow due to this noise voltage by using series crossed diodes. Since the current flow is related to the voltage drop V across each diode by

$$I = I_s\left(\exp\left(\frac{eV}{kT}\right) - 1\right) \tag{11}$$

where I_s is the reverse saturation current, enough diodes are used in series so that the drop across each is relatively small and I is accordingly small. Further discussion is included with the description of the transmit/receive switches (16X964, 16X965, 16X966).

2.4.5 Noise Figures

The most useful measure of a device's noise performance is the noise figure, F. For the ℓth device in the cascade of Figure 2.26, the noise figure F_ℓ is

$$\left(\frac{S}{N}\right)_\ell = \frac{1}{F_\ell}\left(\frac{S}{N}\right)_{\ell-1} \tag{12}$$

or in terms of decibels:

$$F_{dB} = 10 \, \ell og_{10} \, F_{ratio} \tag{13}$$

For an ideal device that introduces no noise, $F_\ell = 1$ (0 dB). It can be shown that if the available internal noise power of the device is P_{int},

$$F_\ell = 1 + \frac{P_{int}}{G_a k T_s B} \tag{14}$$

where G_a is the gain of the device, T_s the internal noise source temperature, and B the input noise source bandwidth. Thus increasing the gain tends to diminish the importance of the internal noise contribution, driving the F_ℓ towards unity.

The noise figure of a cascade of devices is given by Friis' formula:

Figure 2.26 Cascade of Subsystems Making Up a System, with Signal--to-Noise Ratios Defined at Each Point

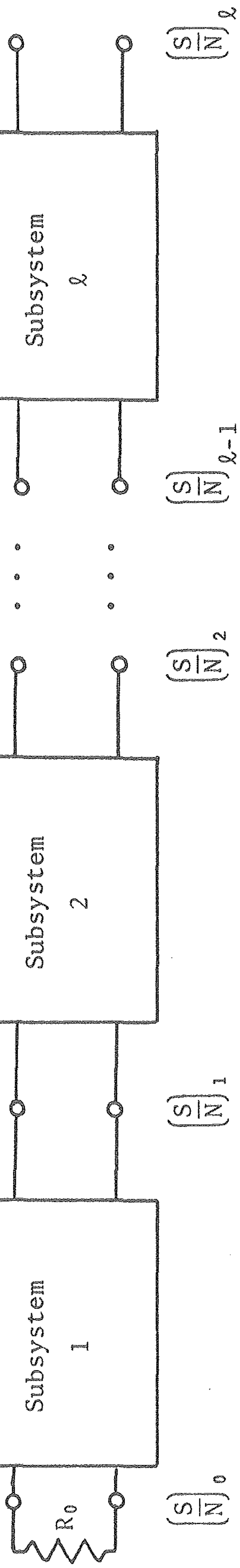

R_0
$\left(\frac{S}{N}\right)_0$
Subsystem 1
$\left(\frac{S}{N}\right)_1$
Subsystem 2
$\left(\frac{S}{N}\right)_2$
$\left(\frac{S}{N}\right)_{\ell-1}$
Subsystem ℓ
$\left(\frac{S}{N}\right)_\ell$

$$F = F_1 + \frac{F_2 - 1}{G_{a_1}} + \frac{F_3 - 1}{G_{a_1} G_{a_2}} + \cdots \tag{15}$$

where F_i is the noise figure of stage i and G_{a_i} is the corresponding gain of that stage. Passive devices such as mixers have insertion loss, *i.e.* a fractional gain < 1.

Inspection of the superheterodyne receiver structure of Figure 2.3 illustrates some of the important concerns with regard to the design of the observe channel receiver (Figure 2.5) for optimum noise performance. The Rf preamplifier noise figure (F_1 in this instance) will be the dominant term in the system noise figure, and the higher its gain G_{a_1}, the less important the noise figure of the mixer (which is typically 9 dB for the Hewlett-Packard 10514A units used in the 10X210 8 - 270 MHz to 30 MHz Linear Converters). The IF amplifier noise figure F_3 is still a crucial factor because G_{a_2} represents a fractional gain (HP 10514A single sideband conversion loss is typically 9 dB).

2.4.6 Noise Figure Measurement Procedure

Noise figure measurements were made with either an Ailtech Noise Figure Meter or a Hewlett-Packard 160 Noise Figure Meter. Both are equipped with broadband calibrated noise sources that are attached to the input of the receiver under test.

The 30 MHz IF output of the 10X210 8 - 270 MHz to 30 MHz Linear Converter is returned to the 30 MHz input on the noise figure meter, and a direct reading of cascaded system noise figure may be made. Receiver absolute performance was measured with the transmitter physically disconnected. Transmitter noise isolation was then measured by reconnecting the powered on/gated off transmitter and observing the degradation in system noise figure (if any).

Table 2.4 Observe Channel System Noise Performance

NUCLEUS	*LOCAL OSCILLATOR FREQUENCY*	*IF AMPLIFIER GAIN*	*NOISE FIGURE*
^{1}H	299.9985000 MHz	60 dB	2.3 dB
^{31}P	139.2970000 MHz	60 dB	2.2 dB
^{13}C	97.8975000 MHz	80 dB	2.3 dB
^{2}H	71.4513500 MHz	60 dB	5.0 dB
^{15}N	57.3600000 MHz	80 dB	1.5 dB

2.5 System Components

This section provides design summaries and operating characteristics of major components of the LCB 8 - 270 MHz spectrometer system. Only significant original designs are included.

2.5.1 16X892 System Control Logic

The LCB 8 - 270 MHz spectrometer system has as a key element a Nicolet Instruments Corp. Model 1180 Data System. This system includes a Model 293A Programmable Pulser, a unit that includes seven software settable timers with 32 nsec resolution, four digital-to-analog converters (DACs) with 12 bit resolution, programmable levels, and sense lines. When the 1180 system is used with a 293A and one or more disk memory subsystems, a large body of Nicolet supplied software that is applicable to NMR may be used. In particular, Nicolet Technology Corp. supplies a software package called NTCFT-1180, which will provide all of the control signals normally required to operate an NMR spectrometer system, in addition to handling data acquisition and reduction. Since the NTCFT software package is designed for use with NTC supplied spectrometer systems, there existed a large number of incompatibilities that had to be resolved before this package could be used on the LCB 8 - 270 MHz system.

The function of the 16X892 system control logic is to make the LCB 8 - 270 MHz system look like an NTC system. This approach was taken in preferrence to making software modifications for several reasons:

- Major software packages such as NTCFT tend to evolve over a period of years. The release of new software versions would necessitate local modification of each version as it is released.
- Software modification is a task that is perhaps an order of magnitude more difficult than designing compatible hardware.

Changing selected areas of large programs tends to be difficult, since it is hard to predict the global effects of these changes.

- After a large number of NTC systems are shipped, NTC will be obliged to insure compatibility of new software with existing hardware, therefore future hardware changes are likely to be minimal because of the cost of retrofitting.

Design Summary

The NTCFT -1180 software package running on the 1180/293A makes use of the 293A inputs and outputs that are listed in Table 2.5. The hardware implementation is shown in Figure 2.27.

The 8 - 270 MHz spectrometer system uses 10X209 Four-Phase Generators to produce phase shifts in the observing frequency. This unit has four gate control lines for 0°, 90°, 180°, and 270°; these lines drive Rf switches on the four outputs of a Merrimac quadripole network. Since NTCFT and the 293A signal changes in the phase rather than producing gate control signals that are high for the duration of the desired phase, a simple four-state machine was used as an interface.

The state diagram for this machine is shown in Figure 2.28. State definitions are as follows:

State (Q1,Q0)	Condition
0 0	0° phase shift on
0 1	90° phase shift on
1 0	180° phase shift on
1 1	270° phase shift on

Table 2.5 Summary of 1180/293A I/O Functions

293A Timer Outputs

Output	Function	293A Connection(GND)
SP0	Observe Rf on	ZB-5 (ZB-18)
SP1	Programmable via NX command	ZB-2 (ZB-15)
SP2	Programmable via NX command	ZB-6 (ZB-19)
SP3	Programmable via NX command	ZB-3 (ZB-16)
SP4	Programmable via NX command	ZB-4 (ZB-17)
SP5	1180 ADC trigger	ZB-1 (zb-14)

293A Programmable Levels

Level	Function	293A Connection
LEV0	Decoded by 16X892 logic	YC-17
LEV1	Decoded by 16X892 logic	YC-16
LEV2	Decoded by 16X892 logic	YC-14
LEV3	Decoded by 16X892 logic	YC-15
LEV4	Decoupler off	YC-4
LEV5	Aux. logic trigger to 16X892	YC-3
LEV6	Step plotter left (unused)	YC-2
LEV7	Release plotter x (unused)	YC-21
LEV8	Delay flag	YC-7
LEV9	Decoupler CW	YC-6
LEV10	unused	YC-5
LEV11	Step plotter right	YC-8
LEV12	Tune mode on (unused)	YA-2
LEV13	Decoupler level 2 (unused)	YA-3
LEV14	Used by NTCCOR	YA-1
LEV15	Release plotter y (unused)	YA-4
PENLIFT	Lower pen	DX-7

Table 2.5 (Continued)

293A DACs

DAC	Function	293A Connection(GND)
DAC0	Recorder X-axis	DX-2 (DX-15)
DAC1	Recorder Y-axis	DX-3 (DX-16)
DAC2	16X950 Temperature Control	DX-4 (DX-17)
DAC3	16X950 Temperature Control monitor	DX-5 (DX-18)

293A Sense Lines

Sense	Function	293A Connection
SENSE0	Plotter off left limit	YB-15
SENSE1	Plotter off right limit	YB-5
SENSE2	Lock on signal from 16X892	YB-20
SENSE3	External add/subtract flag	YB-3
SENSE4	Spinner rate (unused)	
SENSE5	Spinner rate (unused)	

Decoding of LEV0 - LEV3 by 16X892 logic

Levels (3210)	Function
0 0 0 0	Turn 90° phase shift off
0 0 0 1	Turn 90° phase shift on
0 0 1 0	Turn 180° phase shift off
0 0 1 1	Turn 180° phase shift on
0 1 0 0	No-op
1 0 1 0	Select FT mode
1 1 0 0	Low power FT mode

Figure 2.27 270 MHz Spectrometer System/Nicolet Instrument 293A Interface

Figure 2.28 270 MHz Spectrometer System/Nicolet Instrument 293A Interface, State Diagram and Transition Table

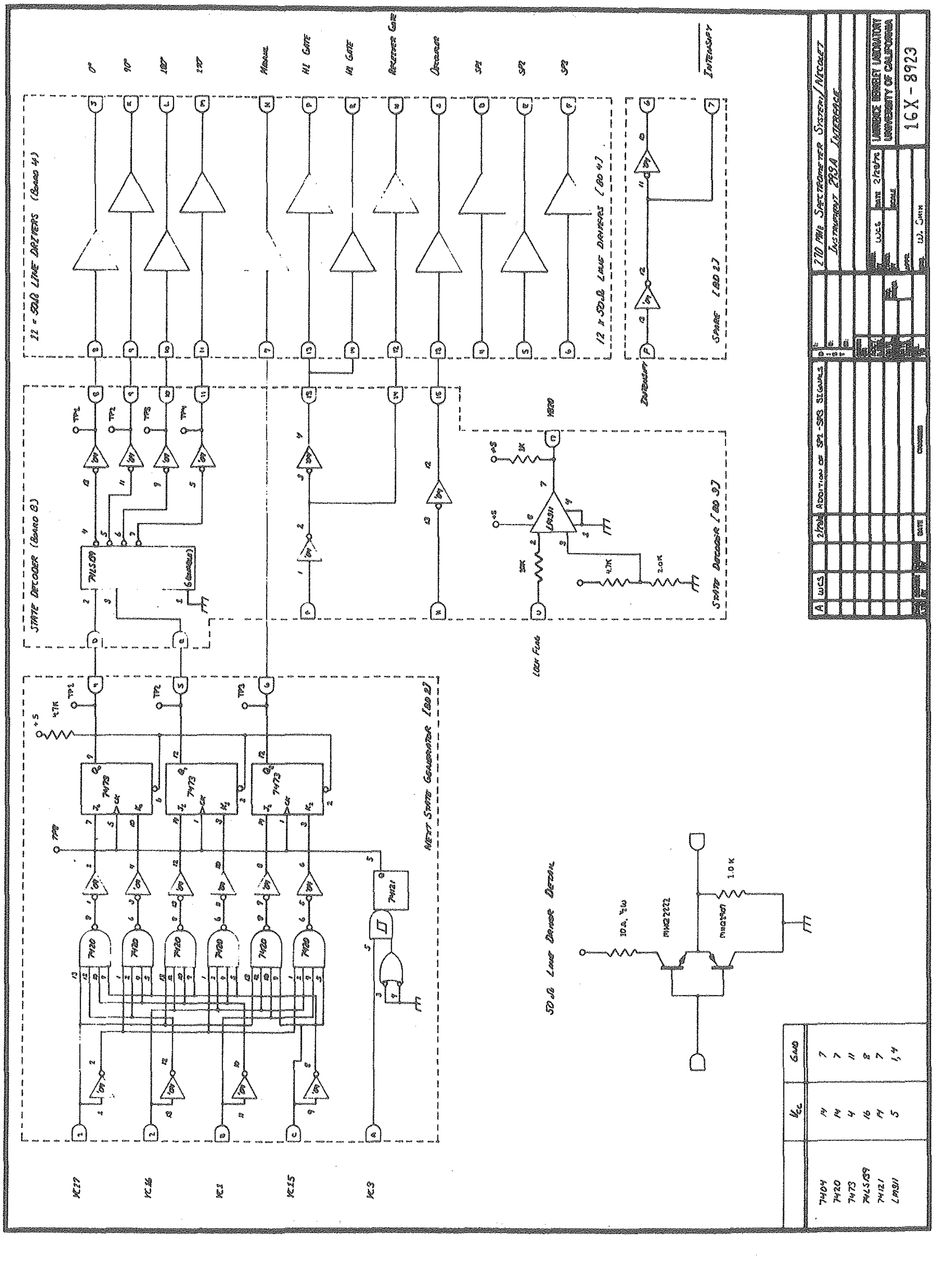
LAWRENCE BERKELEY LABORATORY
UNIVERSITY OF CALIFORNIA
16X-8923

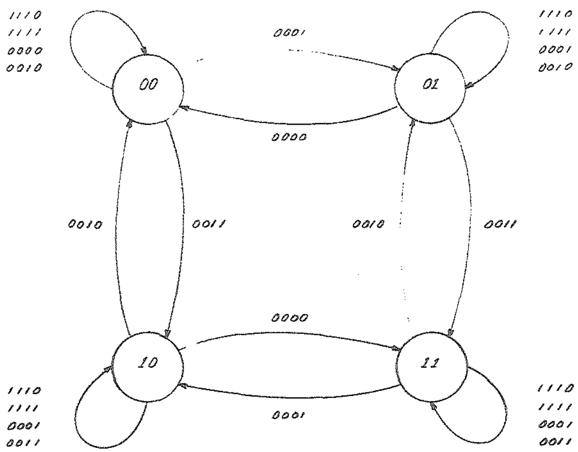

TRANSITION TABLE

PRESENT STATE		NEXT STATE		INPUTS				J-K IMPLEMENTATION CONNECTIONS			
Q_1	Q_0	Q_1	Q_0	L_3	L_2	L_1	L_0	J_1	K_1	J_0	K_0
0	0	0	0	0	0	0	0	0	X	0	X
0	0	0	1	0	0	0	1	0	X	1	X
0	0	0	0	0	0	1	0	0	X	0	X
0	0	1	0	0	0	1	1	1	X	0	X
0	0	0	0	1	1	X	X	0	X	0	X
0	1	0	0	0	0	0	0	0	X	X	1
0	1	0	1	0	0	0	1	0	X	X	0
0	1	0	1	0	0	1	0	0	X	X	0
0	1	1	1	0	0	1	1	1	X	X	0
0	1	0	1	1	1	X	X	0	X	X	0
1	0	1	0	0	0	0	0	X	0	0	X
1	0	1	1	0	0	0	1	X	0	1	X
1	0	0	0	0	0	1	0	X	1	0	X
1	0	1	0	0	0	1	1	X	0	0	X
1	0	1	0	1	1	X	X	X	0	0	X
1	1	1	0	0	0	0	0	X	0	X	1
1	1	1	1	0	0	0	1	X	0	X	0
1	1	0	1	0	0	1	0	X	1	X	0
1	1	1	1	0	0	1	1	X	0	X	0
1	1	1	1	1	1	X	X	X	0	X	0

STATE DEFINITIONS:

00 = 0° PHASE
01 = 90° PHASE
10 = 180° PHASE
11 = 270° PHASE

INPUT DEFINITIONS:

PROG LVL (293A) → 3	2	1	0	
0	0	0	0	90° ϕ SHIFT OFF
0	0	0	1	90° ϕ SHIFT ON
0	0	1	0	180° ϕ SHIFT OFF
0	0	1	1	180° ϕ SHIFT ON
1	1	1	0	DISABLE MANUAL PW CONTROL
1	1	1	1	ENABLE MANUAL PW CONTROL

270 MHz SPECTROMETER SYSTEM / NICOLET
INSTRUMENT 293A INTERFACE
STATE DIAGRAM AND TRANSITION TABLE

SHIH DATE 2/20/72
APPD. SHIH

LAWRENCE BERKELEY LABORATORY
UNIVERSITY OF CALIFORNIA

16X8923-H1

DATE CHANGES

The transition table (Table 2.6) shows programmable levels LEV3, LEV2, LEV1, and LEV0 as inputs, and LEV5 provides a trigger to clock the state transitions. The transition table shows an implementation with J-K flip-flops; Karnaugh maps and minimum implementations are shown in Figures 2.29 through 2.32.

Hardware implementation

A. Next State Generator (Board 2)

The next state generator board contains the two J-K flip-flops that hold the current phase state (7473s, Q0 and Q1), plus a third J-K flip-flop whose output is high when the manual pulse width control is enabled. Gating for manual pulse width control has not been installed. Combinatorial logic is implemented with 7420 NANDs, and a buffered LEV5 is used to clock transitions.

B. State Decoder (Board 3)

The current phase state is decoded by a 2-to-4 line decoder (74LS139); the decoder outputs are fed to the line driver board. All external control logic lines are buffered. The state decoder board also contains a comparator (LM311) that senses the presence or absence of LOCK from the 16X894 Lock Channel Control. This is used for a software interlock in NTCFT-1180.

C. Line Driver Board (Board 4)

The line driver board uses 12 standard 50 ohm complementary emitter-follower line drivers. All control lines on the system are

Table 2.6 16X892 Transition Table

Present State Q1	Present State Q0	Next State Q1	Next State Q0	Inputs LEV3	Inputs LEV2	Inputs LEV1	Inputs LEV0	J-K Implementation J1	J-K Implementation K1	J-K Implementation J0	J-K Implementation K0
0	0	0	0	0	0	0	0	0	X	0	X
0	0	0	1	0	0	0	1	0	X	1	X
0	0	0	0	0	0	1	0	0	X	0	X
0	0	1	0	0	0	1	1	1	X	0	X
0	0	0	0	1	1	X	X	0	X	0	X
0	1	0	0	0	0	0	0	0	X	X	1
0	1	0	1	0	0	0	1	0	X	X	0
0	1	0	1	0	0	1	0	0	X	X	0
0	1	1	1	0	0	1	1	1	X	X	0
0	1	0	1	1	1	X	X	0	X	X	0
1	0	1	0	0	0	0	0	X	0	0	X
1	0	1	1	0	0	0	1	X	0	1	X
1	0	0	0	0	0	1	0	X	1	0	X
1	0	1	0	0	0	1	1	X	0	0	X
1	0	1	0	1	1	X	X	X	0	0	X
1	1	1	0	0	0	0	0	X	0	X	1
1	1	1	1	0	0	0	1	X	0	X	0
1	1	0	1	0	0	1	0	X	1	X	0
1	1	1	1	0	0	1	1	X	0	X	0
1	1	1	1	1	1	X	X	X	0	X	0

Figure 2.29 J1 Karnaugh Map

L3 L2 = 0 0

L1 L0 \ Q1 Q0	00	01	11	10
00	0	0	X	X
01	0	0	X	X
11	1	1	X	X
10	0	0	X	X

L3 L2 = 1 0
0 1
1 1

L1 L0 \ Q1 Q0	00	01	11	10
00	0	0	X	X
01	0	0	X	X
11	0	0	X	X
10	0	0	X	X

Minimum implementation: $J1 = L0\ L1\ \overline{L2}\ \overline{L3}$

Figure 2.30 K1 Karnaugh Map

L3 L2 = 0 0

L1 L0 \ Q1 Q0	00	01	11	10
00	X	X	0	0
01	X	X	0	0
11	X	X	0	0
10	X	X	1	1

L3 L2 = 1 0
0 1
1 1

L1 L0 \ Q1 Q0	00	01	11	10
00	X	X	0	0
01	X	X	0	0
11	X	X	0	0
10	X	X	0	0

Minimum implementation: $K1 = \overline{L0}\ L1\ \overline{L2}\ \overline{L3}$

Figure 2.31 J0 Karnaugh Map

L3 L2 = 0 0

L1 L0 \ Q1 Q0	00	01	11	10
00	0	X	X	0
01	1	X	X	1
11	0	X	X	0
10	0	X	X	0

L3 L2 = 1 0
0 1
1 1

L1 L0 \ Q1 Q0	00	01	11	10
00	0	X	X	0
01	0	X	X	0
11	0	X	X	0
10	0	X	X	0

Minimum implementation: $J0 = L0\,\overline{L1}\,\overline{L2}\,\overline{L3}$

Figure 2.32 K0 Karnaugh Map

L3 L2 = 0 0

L1 L0 \ Q1 Q0	00	01	11	10
00	X	1	1	X
01	X	0	0	X
11	X	0	0	X
10	X	0	0	X

L3 L2 = 1 0
0 1
1 1

L1 L0 \ Q1 Q0	00	01	11	10
00	X	0	0	X
01	X	0	0	X
11	X	0	0	X
10	X	0	0	X

Minimum implementation: $K0 = \overline{L0}\ \overline{L1}\ \overline{L2}\ \overline{L3}$

50 ohm coaxial cable, and all gate inputs are 50 ohm terminations. The use of low impedance transmission lines insures that long cable runs may be used without excessive noise pickup or reflection problems. The transistors used in the drivers are MHQ2222 or MHQ2907 quad NPN and PNP arrays.

2.5.2 16X894 Lock Channel Control Unit

The 16X894 Lock Channel Control provides the control signals and the lock-in detection necessary for the implementation of a pulsed time-shared heteronuclear lock system. The unit is used in conjunction with a Hewlett-Packard 5110A Frequency Synthesizer Driver (reference frequency source), and it provides control signals to the 16X919 Lock Channel SSB Generator, the 10X210 8-270 MHz to 30 MHz Linear Converter, and the 16X935 63 KG Magnet Shim Control.

The unit gates the observing transmitter at 1.25 KHz, and lock-in detection is performed at 5 KHz. This scheme permits dual detection of a pair of signals that are in phase quadrature, and allows the simultaneous generation of both an absorption mode signal (for display purposes) and a dispersion mode signal (for field correction).

Front panel controls permit adjustment of transmitter duty cycle, audio phase, field sweep rate, field sweep width, and lock threshold. The lock threshold detector is used to communicate the presence or absence of lock to the Nicolet 1180 data system via the 16X892 interface and the Nicolet 293A.

Design Summary

A. Frequency Generation and Control Signals (Figure 2.33)

The 1.25 KHz transmitter gating rate is derived from a buffered 3.0 MHz from the HP 5110A synthesizer driver. The 5110A is designed to drive one 50 ohm line per output, thus the 3.0 MHz input is buffered with an emitter-follower to increase the input impedance. This

Figure 2.33 270 MHz Spectrometer System, Lock Channel 5 KHz Four Phase Generator (Board 1), Gate Generator (Board 2)

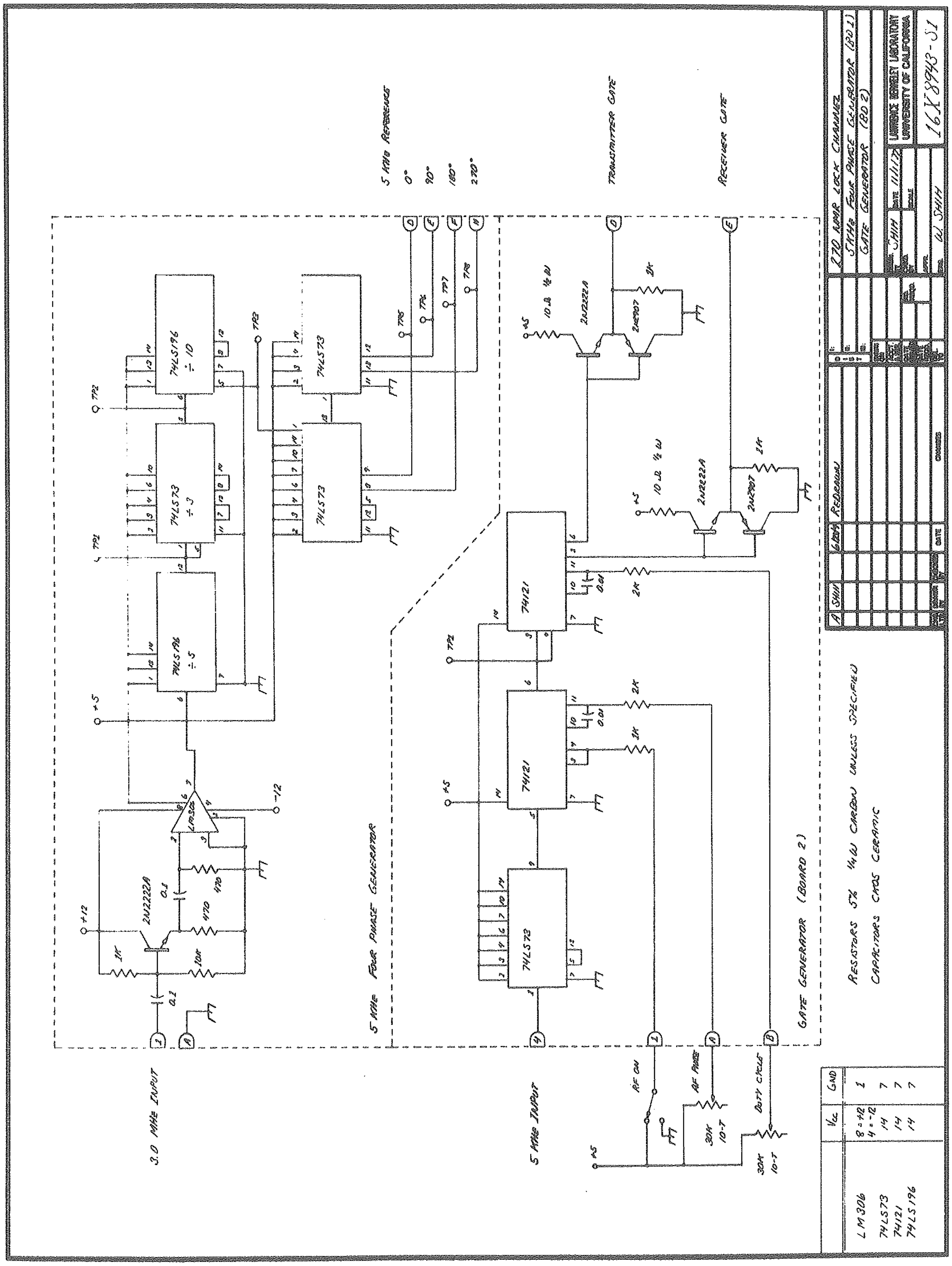
270 AMPR LOCK CHANNEL
5KHz FOUR PHASE GENERATOR (BD 1)
GATE GENERATOR (BD 2)
LAWRENCE BERKELEY LABORATORY
UNIVERSITY OF CALIFORNIA
16X8943-S1
W. SHIH
REDRAWN
5 KHz FOUR PHASE GENERATOR
GATE GENERATOR (BOARD 2)
RESISTORS 5% 1/4W CARBON UNLESS SPECIFIED
CAPACITORS CMOS CERAMIC
3.0 MHz INPUT
5 KHz INPUT
5 KHz REFERENCE
0°
90°
180°
270°
TRANSMITTER GATE
RECEIVER GATE
RF ON
RF PHASE
DUTY CYCLE
74LS196
74LS73
74121
LM306
2N2222A
2N2907

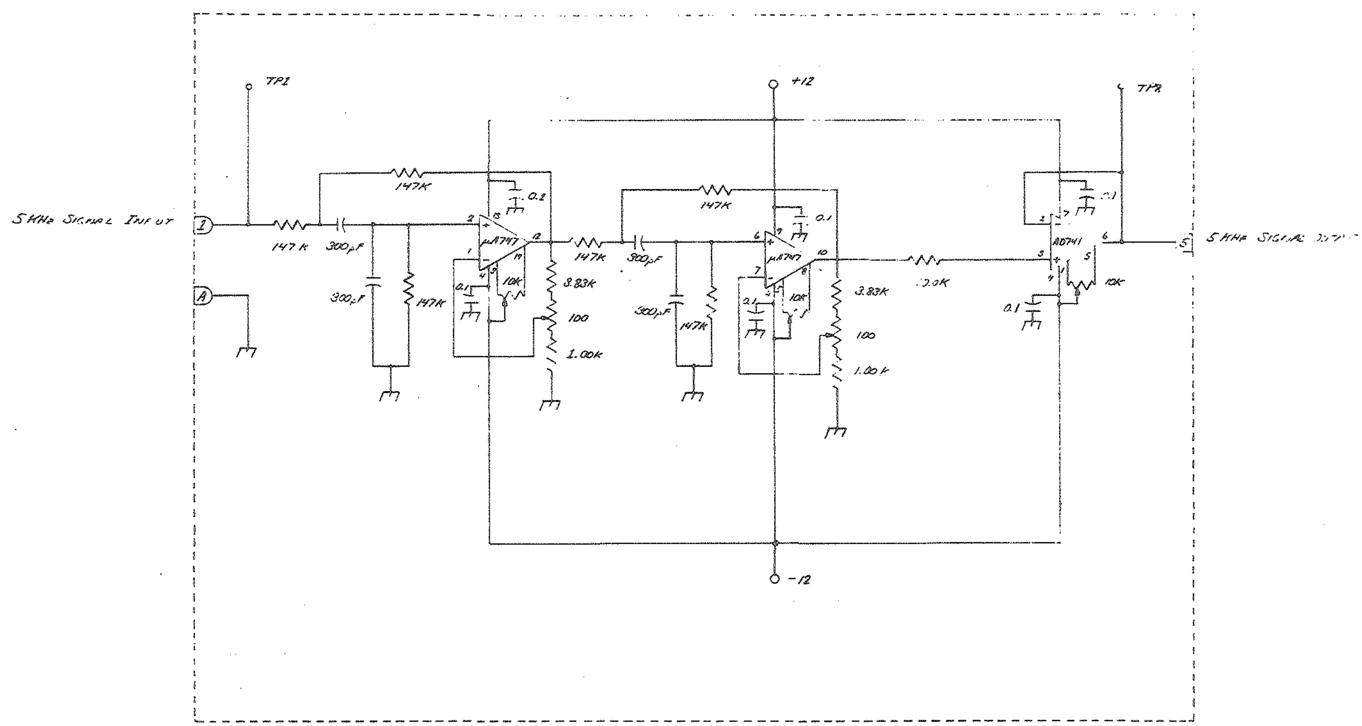

ALL RESISTORS 1% METAL FILM
CAPACITORS: SILVER MICA (300 pF) OR CMOS (0.1)
ALL TRIMPOT: CERMET

A	SHIH	8/1/81	REDRAWN

270 NMR LOCK CHANNEL
5 KHz BANDPASS FILTER
(BOARD 3)

SHIH DATE 11/1/77
W. SHIH

LAWRENCE BERKELEY LABORATORY
UNIVERSITY OF CALIFORNIA

16X2745-S2

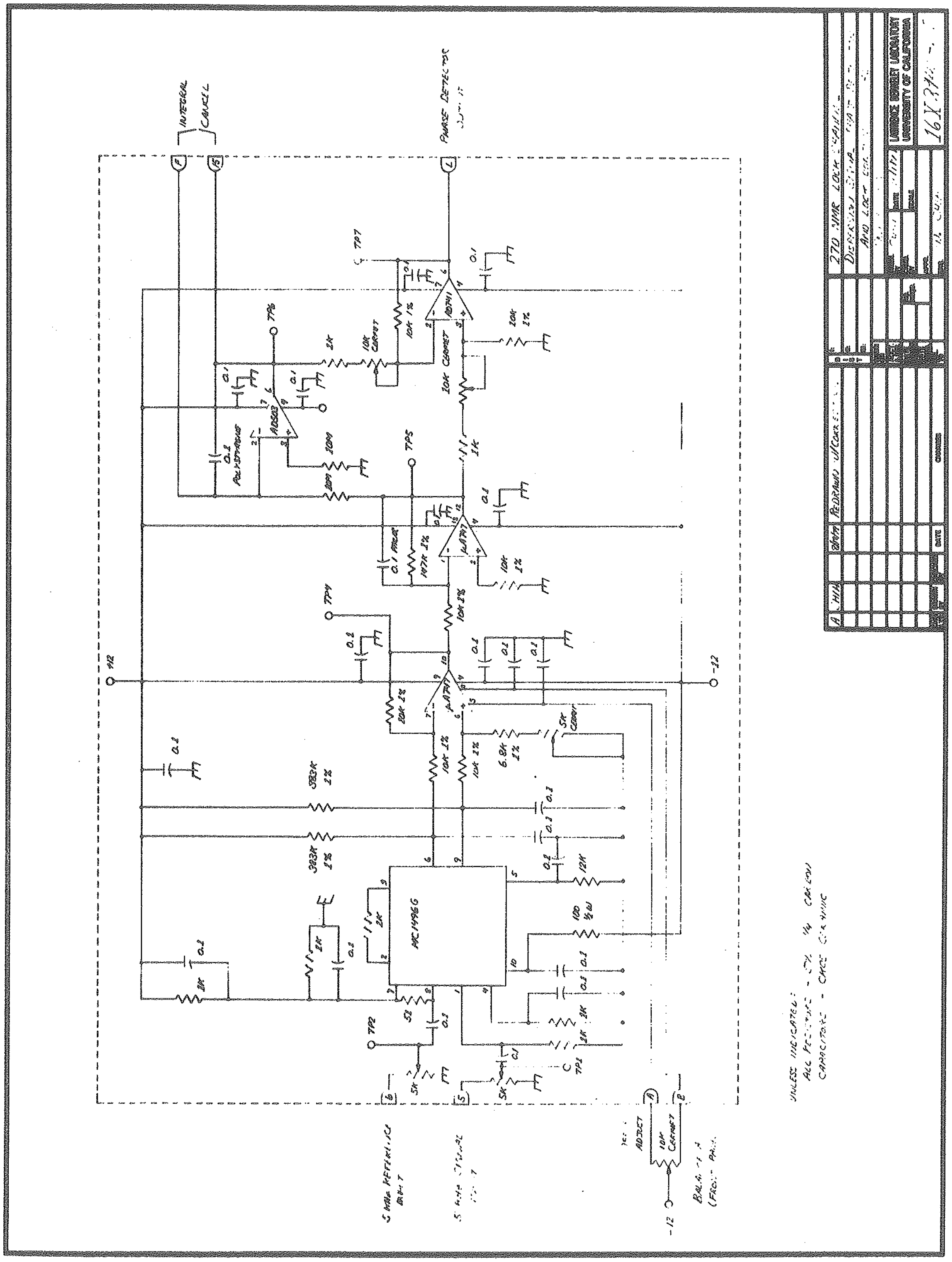
MC1496G
AD503
AD741
TP2
TP4
TP5
TP6
TP7
PHASE DETECTOR
INTEGRAL
CANCEL
LAWRENCE BERKELEY LABORATORY
UNIVERSITY OF CALIFORNIA

buffered signal is converted into a TTL pulse train by the LM306 comparator, and the pulse train is divided by 150 to yield 20 KHz. The 20 KHz is routed to four successive T flip-flops to produce four square waves with relative phases of 0°, 90°, 180°, and 270°. The 0° signal is fed to two successive monostables (74121); the first is used to generate an adjustable time delay for audio phase shifting, and the second is used to vary the pulse width of the transmit gate for duty cycle control. The resultant pulse train is buffered by a complementary emitter-follower, and the signal is fed to the rear panel XMIT GATE for the 16X919 Lock Channel SSB Generator. The complementary output from the last monostable is also buffered and fed to the 10X210 Linear Converter for use as a receiver gate.

B. 5 KHz Signal Active Bandpass Filter (Figure 2.34)

The signal from the 10X211 Double Phase Sensitive Detector is fed via a rear panel BNC to board 3. On this board are two identical voltage controlled voltage source (VCVS) active filters with a center frequency of 5 KHz. The last stage is an AD741 voltage follower that provides buffering.

C. Dispersion Signal Phase Detector (Figure 2.35)

Both the dispersion and the absorption signal phase detectors are based on MC1496/1596 series monolithic balanced modulators. The MC1496 consists of a differential amplifier driving a dual differential amplifier; operation of the device is based on the ability to deliver the product of two input voltages when the magnitudes of these voltages are within the limits of linear operation.

In this application, the dual differential amplifier is driven into saturation by the reference 5 KHz signal; the 5 KHz lock signal is fed via a trimpot to the differential amplifier, and the input amplitude is adjusted so that the device operates in the center of the linear region. The differential output is converted to a single-ended signal by a 747 differential amplifier, and the signal is then low-pass filtered (1-pole) with a 747-based active filter.

The control algorithm used for field control is the position form of the proportional plus integral control. The proportional term is taken directly from the low-pass filter output, and the integral term is generated with an AD503 FET-input operational amplifier connected as an integrator. The two terms are summed with an AD741 connected as a summing amplifier; trimpots are provided for the adjustment of the relative weightings of the proportional and integral terms. In addition, an offset adjustment pot is brought to the front panel so that DC offsets may be conveniently bucked.

D. Absorption Signal Phase Detector (Figure 2.36)

The absorption signal phase detector board is identical to the dispersion signal board, except there is no integrator and no summing amplifier. In addition, the low-pass filter bandwith is larger (pole at a higher frequency) to make ringing easier to observe. Again, an offset adjustment is brought to the front panel to allow for the bucking of DC components.

E. Sweep Control Logic (Figure 2.37)

The sweep control logic board provides for the front panel

Figure 2.36 270 MHz Spectrometer System, Lock Channel Absorption Signal Phase Detector (Board 5)

Figure 2.37 270 MHz Spectrometer System, Lock Channel Sweep Control Logic (Board 7)

Figure 2.38 270 MHz Spectrometer System, Lock Channel Analog Buffer (Board 6) and Sweep Generator (Board 9)

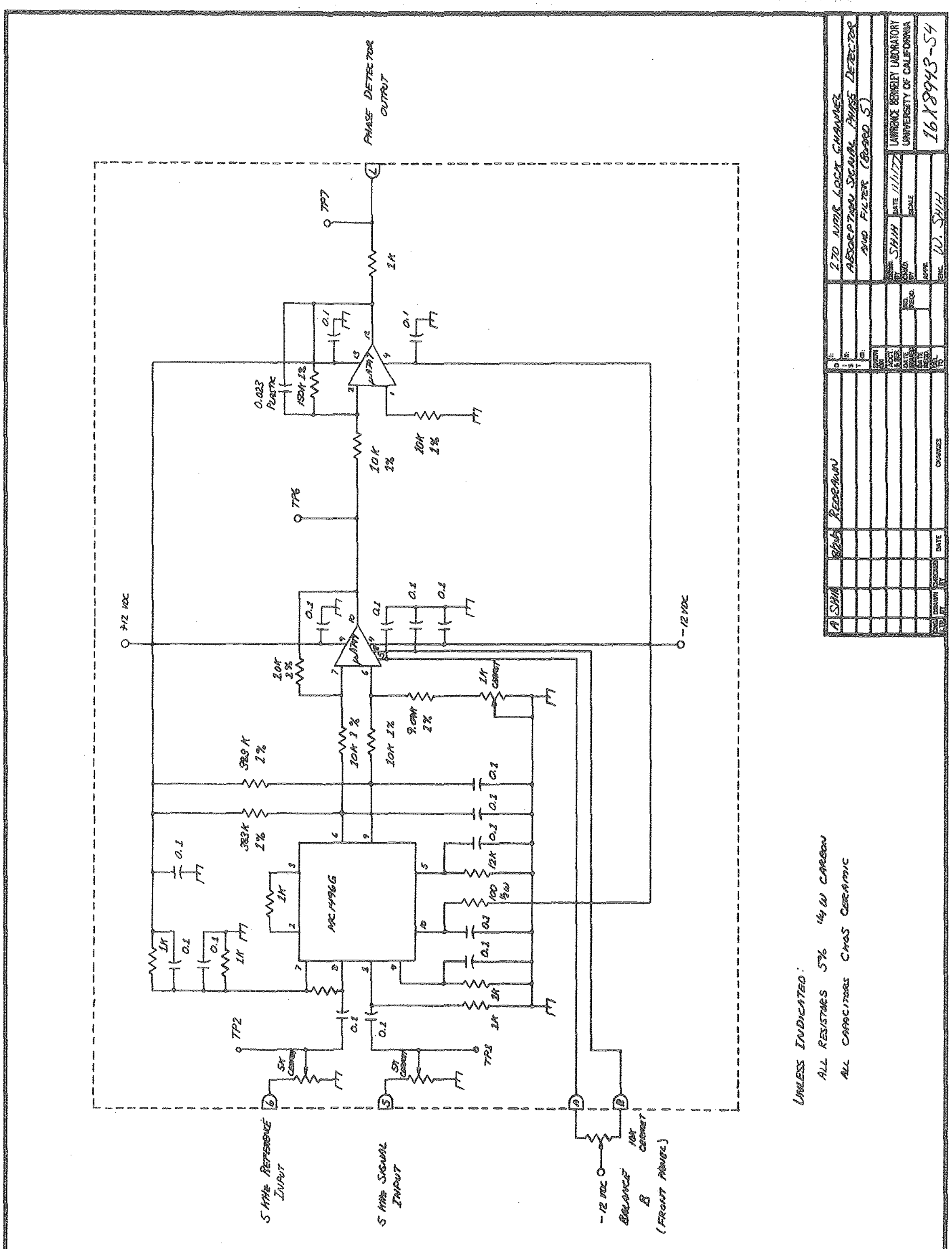

XBL 7910-12492

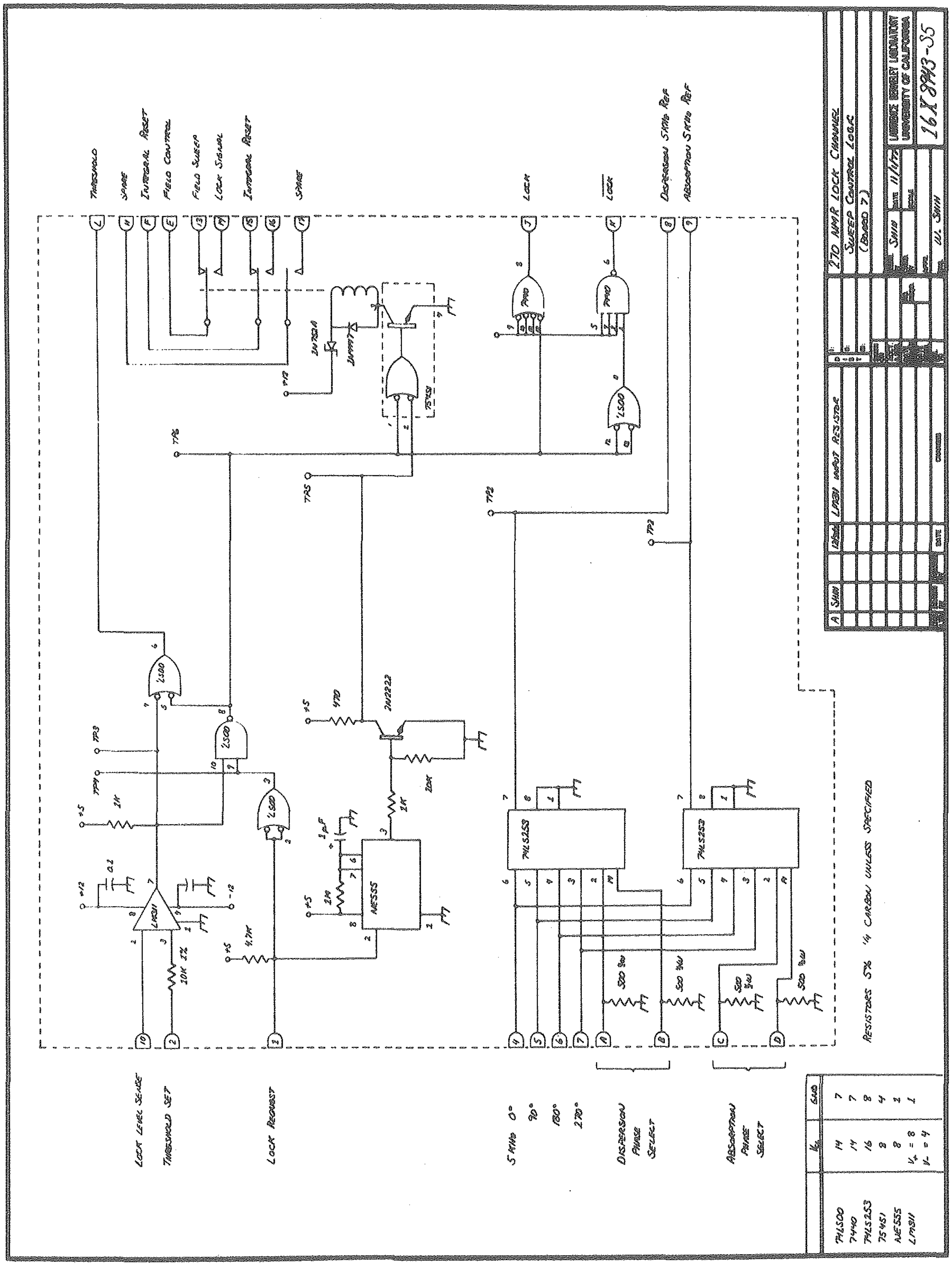
270 NMR LOCK CHANNEL
SWEEP CONTROL LOGIC
(BOARD 7)
LAWRENCE BERKELEY LABORATORY
UNIVERSITY OF CALIFORNIA
RESISTORS 5% 1/4 CARBON UNLESS SPECIFIED
LOCK LEVEL SENSE
THRESHOLD SET
LOCK REQUEST
DISPERSION PHASE SELECT
ABSORPTION PHASE SELECT
THRESHOLD
SPARE
INTEGRAL RESET
FIELD CONTROL
FIELD SWEEP
LOCK SIGNAL
LOCK
DISPERSION 5KHz REF
ABSORPTION 5KHz REF
74LS00
7440
74LS253
75451
NE555
LM311
2N2222

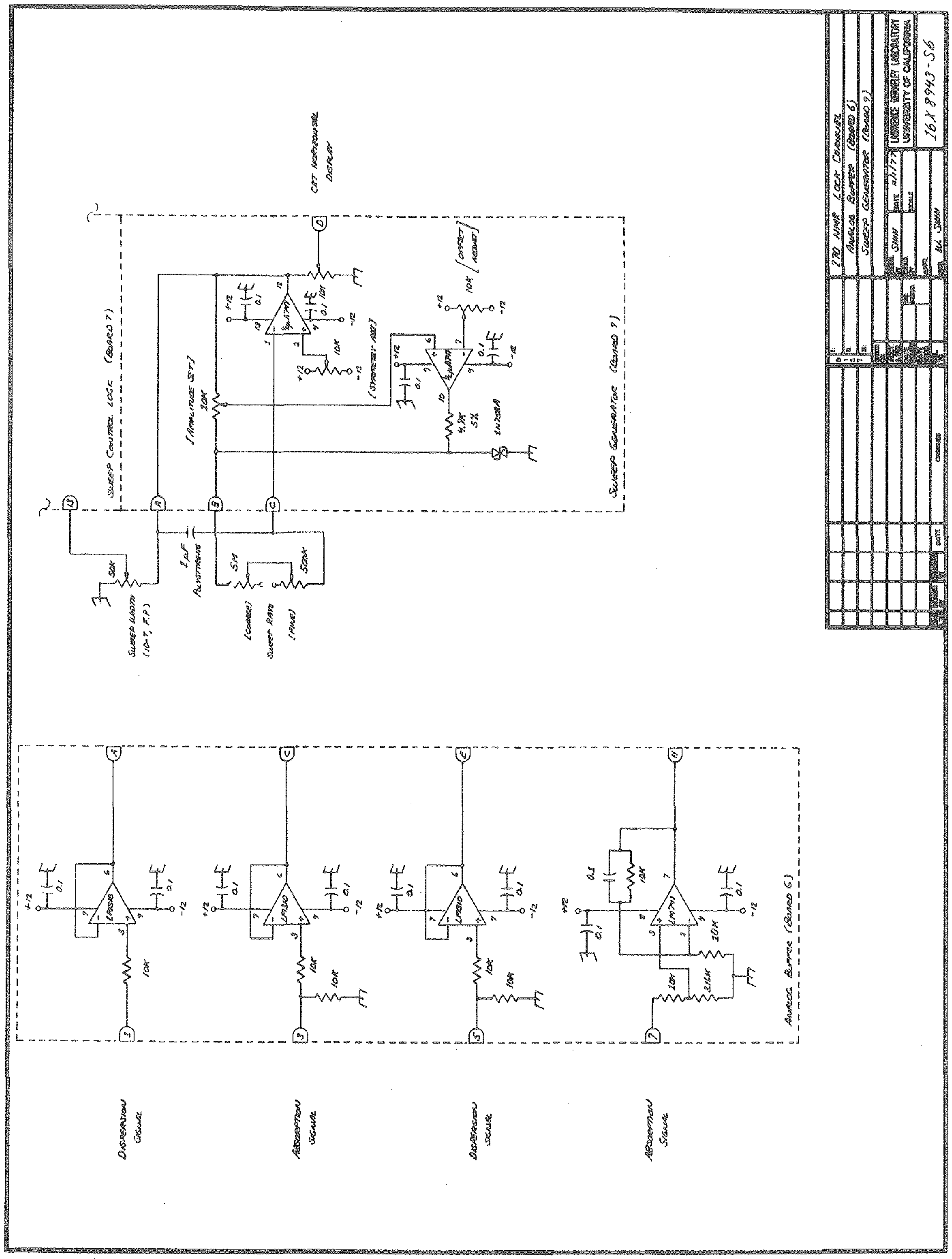

270 NMR LOCK CHANNEL
ANALOG BUFFER (BOARD 6)
SWEEP GENERATOR (BOARD 9)
LAWRENCE BERKELEY LABORATORY
UNIVERSITY OF CALIFORNIA
16X8943-S6
SWEEP CONTROL LOGIC (BOARD 7)
SWEEP GENERATOR (BOARD 9)
CRT HORIZONTAL DISPLAY
SWEEP WIDTH (10-T, F.P.)
SWEEP RATE
ANALOG BUFFER (BOARD 6)
DISPERSION SIGNAL
ABSORPTION SIGNAL
DISPERSION SIGNAL
ABSORPTION SIGNAL

selection of various lock channel modes of operation. Two 74LS253 multiplexers are used to select relative phases of the reference 5 KHz for the absorption and dispersion signal phase detectors. The inputs are the 0°, 90°, 180°, and 270° relative phase TTL pulse trains from board 1, and the outputs are fed to boards 4 (dispersion) and 5 (absorption).

The LM311 comparator is used to compare the absorption channel signal amplitude (when the unit is locked) to a variable (front panel adjustable) threshold. When the unit is unlocked and sweeping through a resonance, if the lock request line is grounded (by turning the front panel lock switch on), when the lock level sense comparator detects signal amplitude in the absorption channel that is above threshold, the field control relay is latched. After a locked state is attained, if the lock level falls below threshold, the field control relay is dropped. The field control relay is debounced with the NE555 timer and the 2N2222 inverter. In addition to driving the relay (using a 75451 peripheral driver), the logic also drives two 7440 high current NAND gates that are used to signal presence or absence of lock by driving front panel LEDs or external lines (to the Nicolet 1180 data system).

F. Analog Buffer and Sweep Generator (Figure 2.38)

Board 6 contains three LM310 voltage followers acting as buffers, and an LM741 operational amplifier connected as a low-pass filter and buffer. The LM310 buffers are connected to the absorption and dispersion signal phase detector outputs, and are present to insure adequate current drive capability. The low-pass filter is connected to the absorption signal; the output is fed to the threshold comparator on board 7.

An LM 747 dual operational amplifier is used on board 9 as an adjustable amplitude sawtooth generator. This sawtooth drives the field sweep amplifier in the 16X935 63 KG Magnet Shim Control. A separate fixed amplitude ramp is also provided to drive the horizontal sweep of a display oscilloscope (thus the display sweep width is invariant with field sweep width).

2.5.3 16X902 Remote Controlled Low-Pass Filter

The 16X902 Remote Controlled Low-Pass Filter is used to provide 0 - 40 dB (switch selectable) audio gain between the 10X211 Double Phase Sensitive Detector and the 1180 data system analog-to-digital converter (ADC) inputs. The two filter channels are exact replicates (direct and quadrature channels), and have four-pole Butterworth characteristics. Turnover frequency may be selected either via remote programming via the 1180 I/O bus and the 16X904 I/O Bus Intercept, or by front panel switches.

In remote operation, the 1180 addresses the filter as device 322. An I/O instruction of generic form ACOUT (620000) with IOP2 set (623224) causes the lowest 10 bits of the accumulator to be loaded into a D register in the filter; this number sets the turnover frequency in 100s of Hertz.

The active filter networks are voltage-controlled voltage source realizations of low-pass networks. Turnover frequency is adjusted by switching the resistances with analog switches. The complete filter unit is described in Figures 2.39 - 2.43.

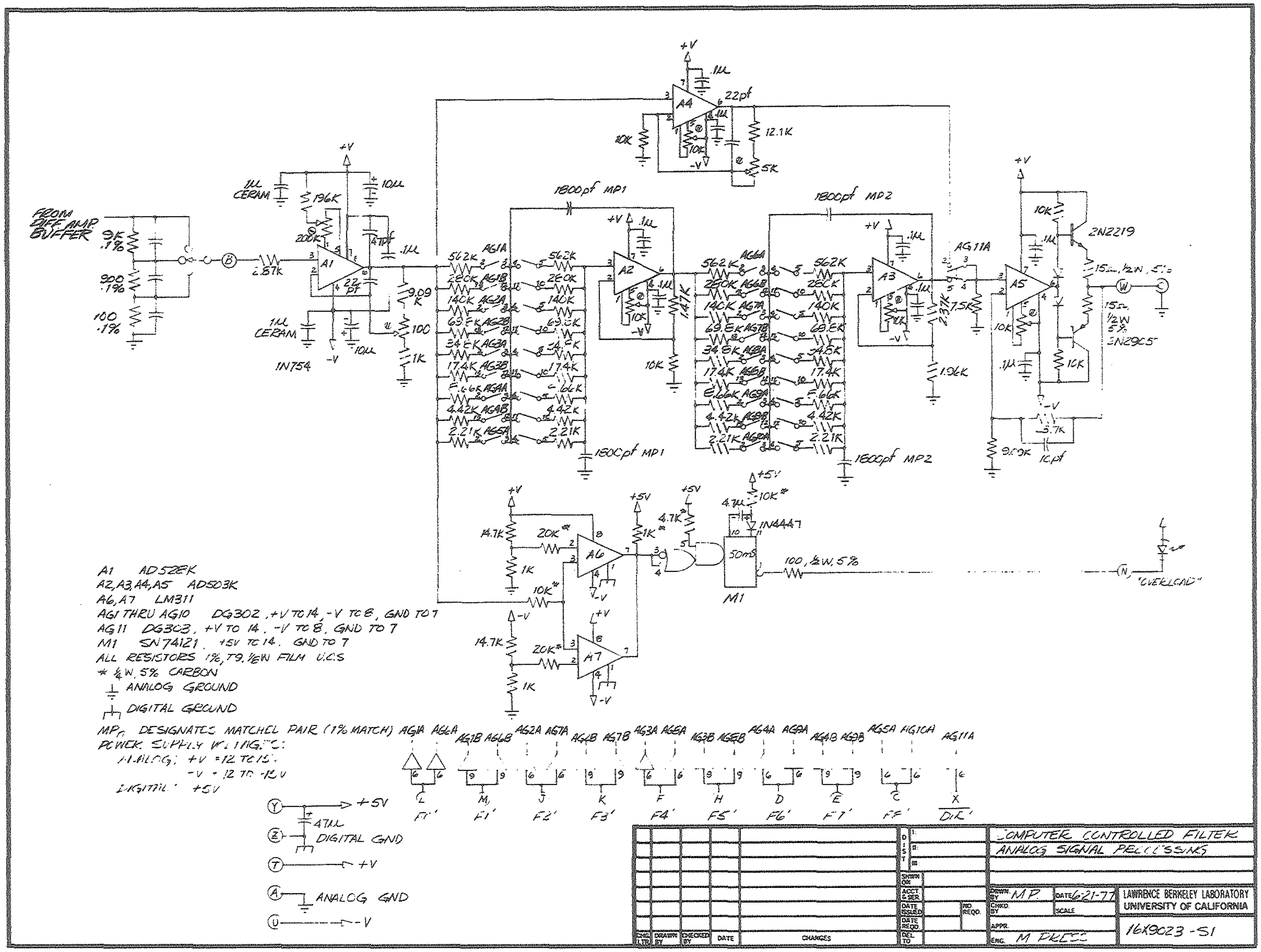
FROM DIFF AMP BUFFER
A1 AD52EK
A2,A3,A4,A5 AD503K
A6,A7 LM311
AG1 THRU AG10 DG302, +V TO 14, -V TO 8, GND TO 7
AG11 DG303, +V TO 14, -V TO 8, GND TO 7
M1 SN74121, +5V TO 14, GND TO 7
ALL RESISTORS 1%, T9, 1/8W FILM U.O.S
* 1/4W, 5% CARBON
ANALOG GROUND
DIGITAL GROUND
1800pf MP1
1800pf MP2
50ms
M1
100, 1/2W, 5%
"OVERLOAD"
2N2219
2N2905
+5V
47μ
DIGITAL GND
+V
ANALOG GND
-V
COMPUTER CONTROLLED FILTER
ANALOG SIGNAL PROCESSING
DRAWN BY M.P.
DATE 6-21-77
LAWRENCE BERKELEY LABORATORY
UNIVERSITY OF CALIFORNIA
ENG. M PRESS
16X9023-S1

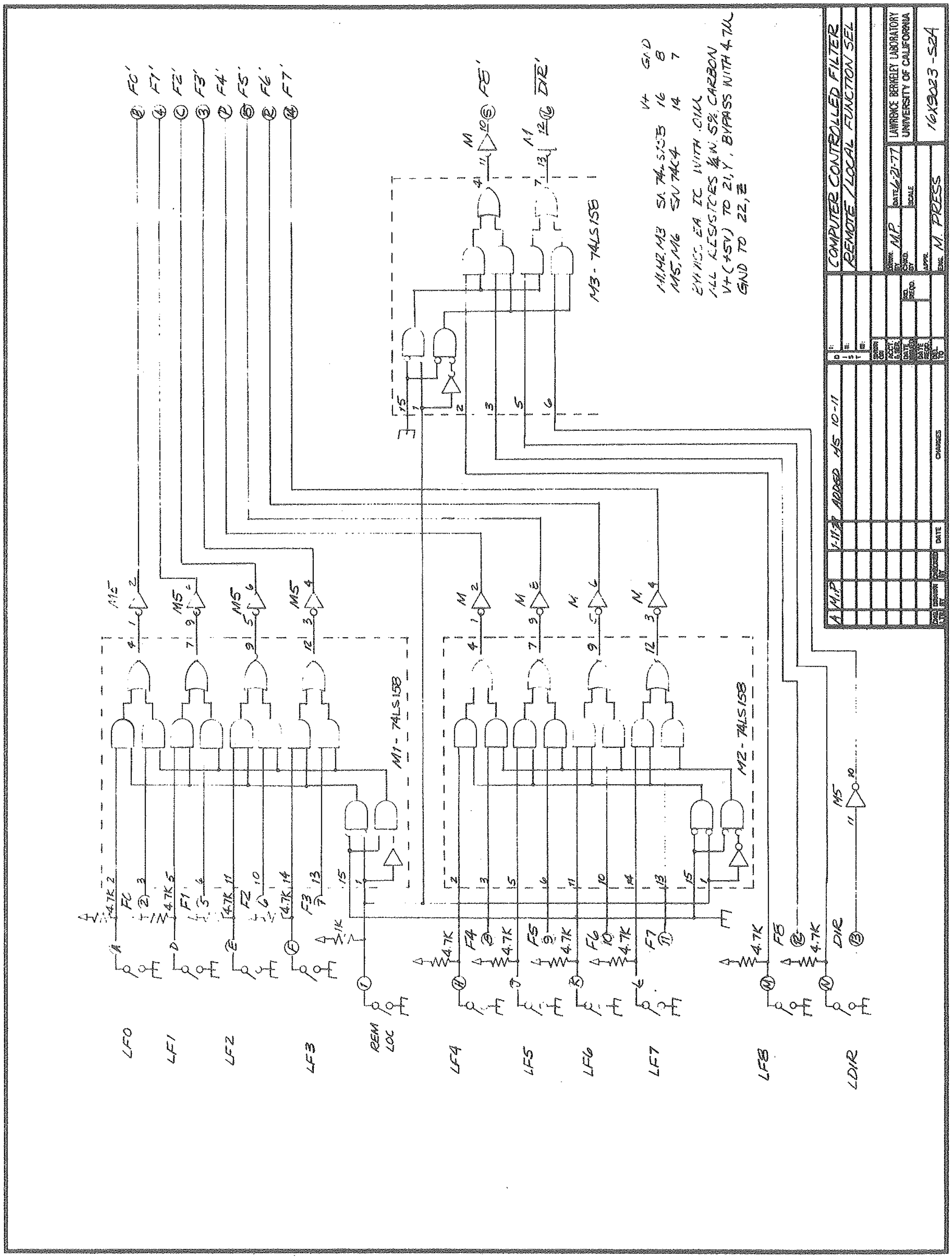
COMPUTER CONTROLLED FILTER
REMOTE / LOCAL FUNCTION SEL
LAWRENCE BERKELEY LABORATORY
UNIVERSITY OF CALIFORNIA
16X3023-S2A
M. PRESS
M1 - 74LS158
M2 - 74LS158
M3 - 74LS158
LF0
LF1
LF2
LF3
REM
LOC
LF4
LF5
LF6
LF7
LF8
LDIR

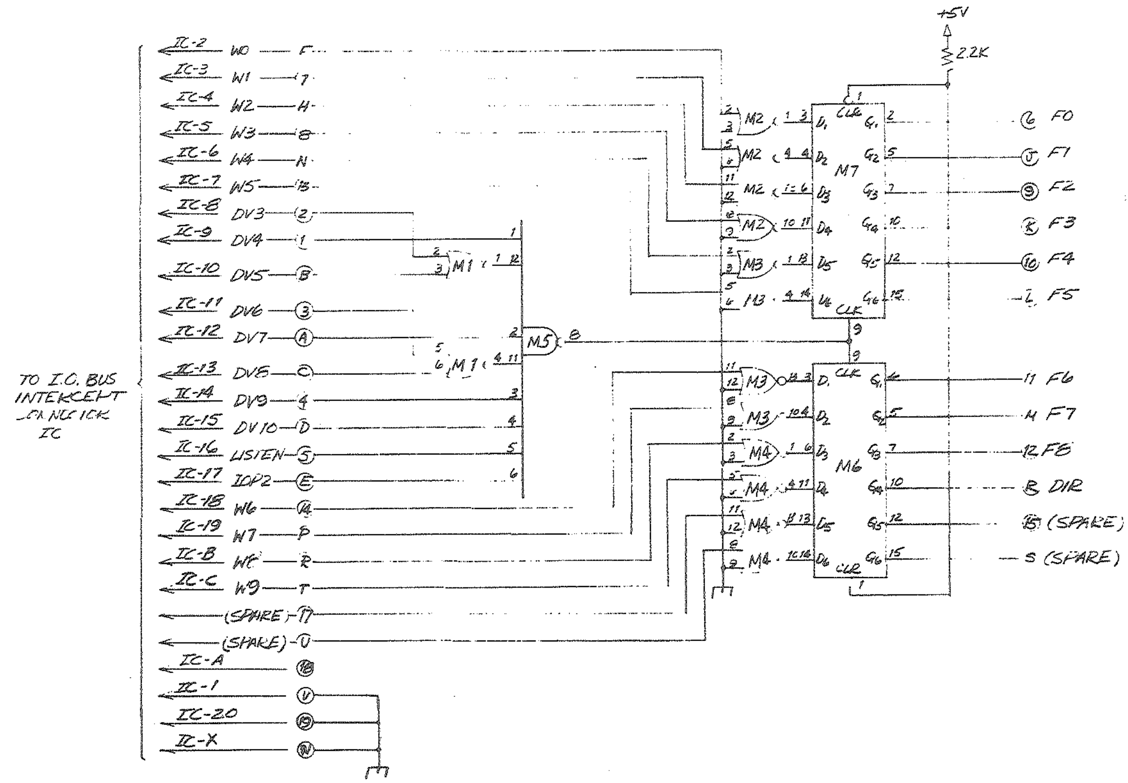

	V+	GND
M1 SN7430	14	7
M2,M3,M4,M5 SN7402	14	7
M6,M8 SN74LS174	16	8

BYPASS EA IC WITH .01µ
ALL RESISTORS ¼W, 5%, CARBON
V+ (+5V) TO 21, Y. BYPASS WITH 4.7µ
GND TO 22, Z

LTR	DRAWN BY	CHECKED BY	DATE	CHANGES
A	M.P		1-11-78	REMOVED GND ON IC-18

COMPUTER CONTROLLED FILTER
DEVICE SELECT & REM. CONTROLLER

DRAWN BY M.P DATE 6-21-77
LAWRENCE BERKELEY LABORATORY
UNIVERSITY OF CALIFORNIA
ENG. M. PRESS
16X9023-534

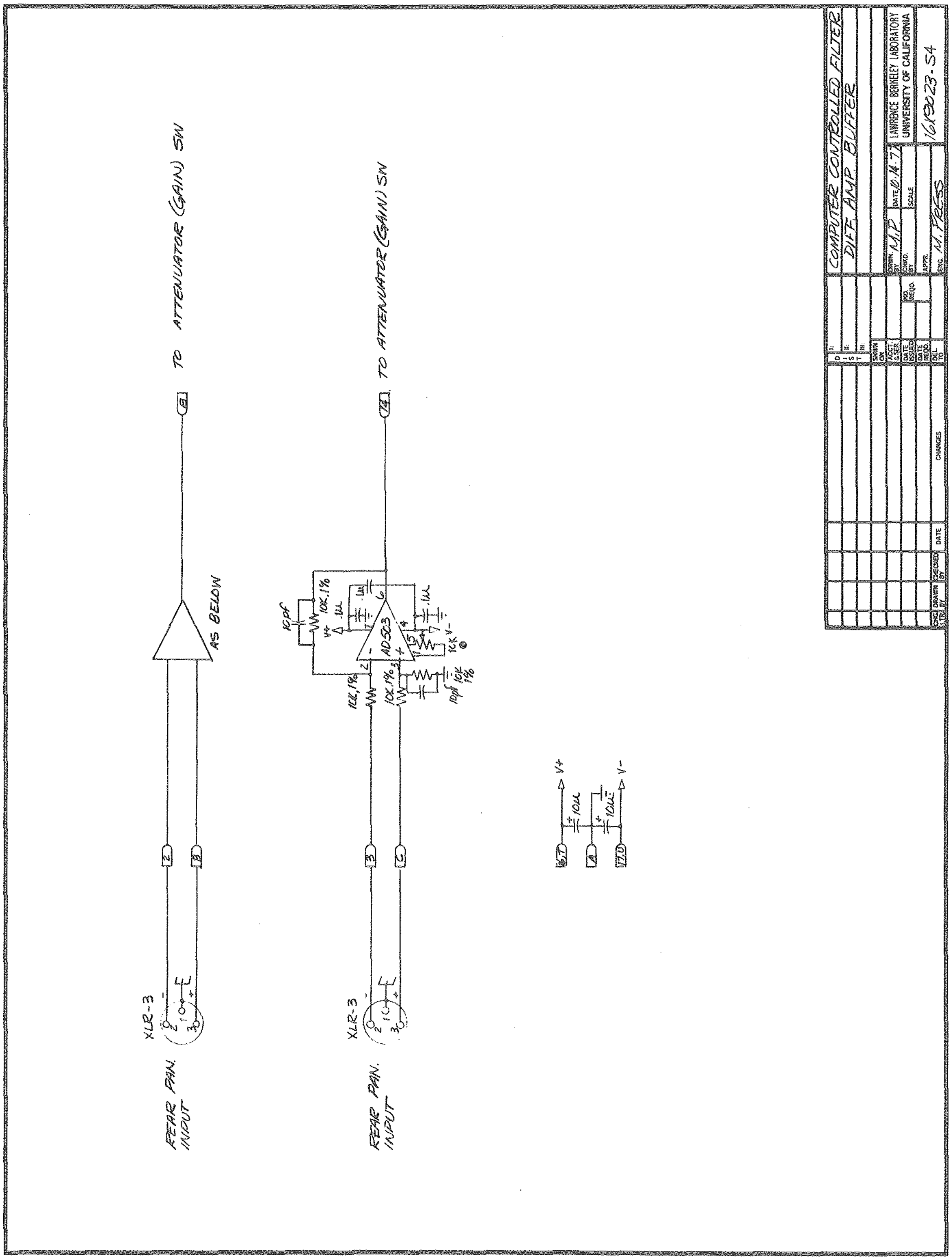
COMPUTER CONTROLLED FILTER
DIFF. AMP. BUFFER
LAWRENCE BERKELEY LABORATORY
UNIVERSITY OF CALIFORNIA
TO ATTENUATOR (GAIN) SW
TO ATTENUATOR (GAIN) SW
AS BELOW
REAR PAN. INPUT
XLR-3
REAR PAN. INPUT
XLR-3
CHANGES

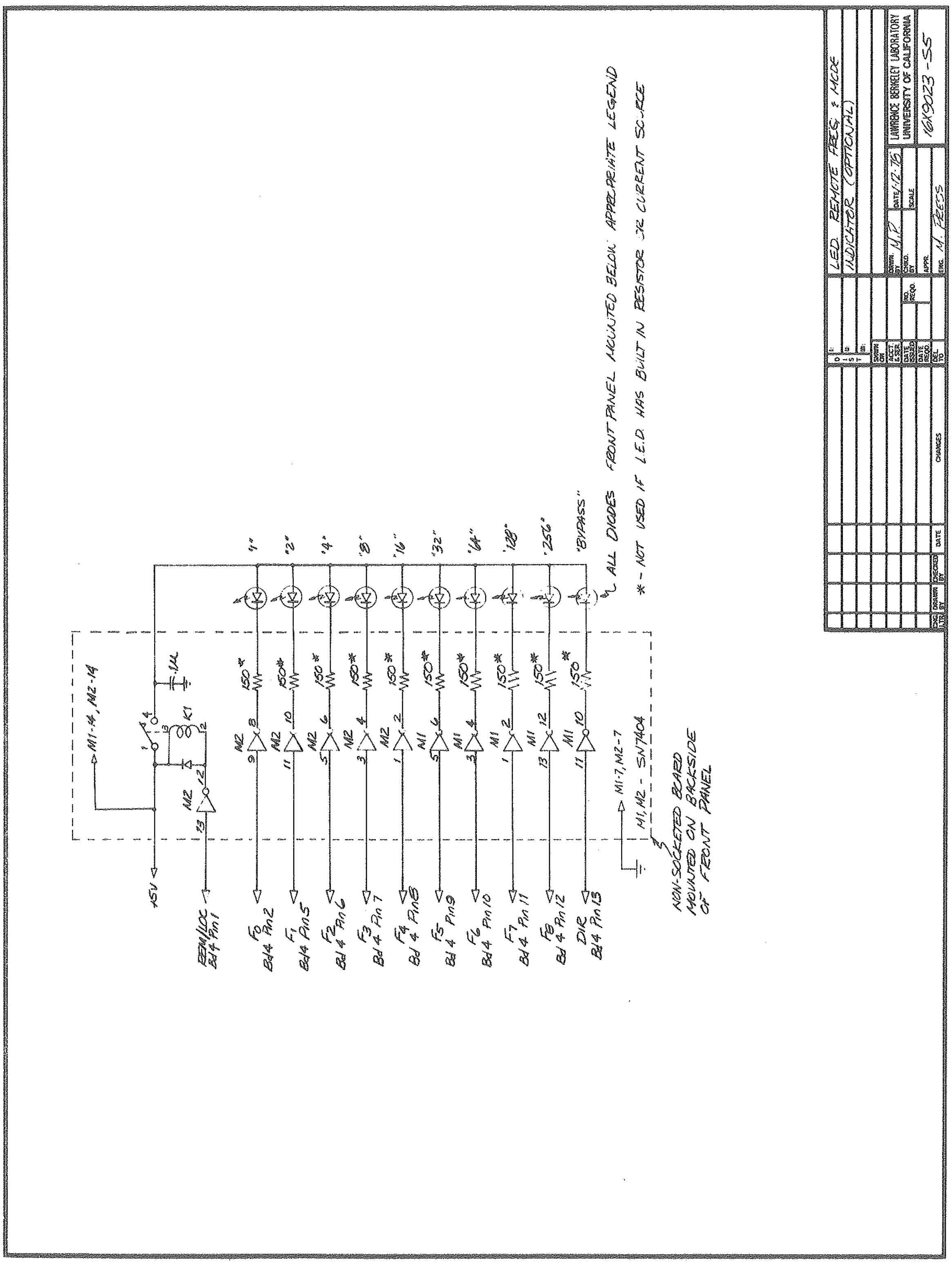
ALL DIODES FRONT PANEL MOUNTED BELOW APPROPRIATE LEGEND
* - NOT USED IF L.E.D. HAS BUILT IN RESISTOR OR CURRENT SOURCE
NON-SOCKETED BOARD MOUNTED ON BACKSIDE OF FRONT PANEL
M1, M2 - SN7404
"BYPASS"
LED REMOTE FREQ. & MODE INDICATOR (OPTIONAL)
LAWRENCE BERKELEY LABORATORY
UNIVERSITY OF CALIFORNIA
16K9023-55

2.5.4 16X903 Low Frequency Rf Preamplifier

The 16X903 Low Frequency Rf Preamplifier is a low noise, moderate gain, FET cascode amplifier that is used at 27.36 MHz and at 41.45 MHz on the 8 - 270 MHz spectrometer system. The circuit is shown in Figure 2.44, with construction details illustrated by the photograph of Figure 2.45. The low level signal input is protected by crossed 1N4447 diodes, and a series resonant 270 MHz trap shunts any stray proton decoupling frequencies to ground.

Gain is provided by a matched pair Siliconix E420 dual J-FET. The identical drain saturation current I_{DSS} for the two FETs insures that neither will have a forward biased gate if direct interstage coupling is used. The input "el" matching network is set to transform the 50 ohm source impedance to the optimum impedance for the lowest noise figure. At 27.36 MHz, the optimum source impedance is about 1850 ohms; at 41.45 MHz the optimum is about 1700 ohms.

Typical measured performance at 27.36 MHz showed a gain of 18 dB, bandwidth of 3.5 MHz, and measured noise figure of 1.5 dB.

Figure 2.44 Low Frequency Rf Preamplifier [16X-9033]

Figure 2.45 Construction Details, Low Frequency Rf Preamplifier

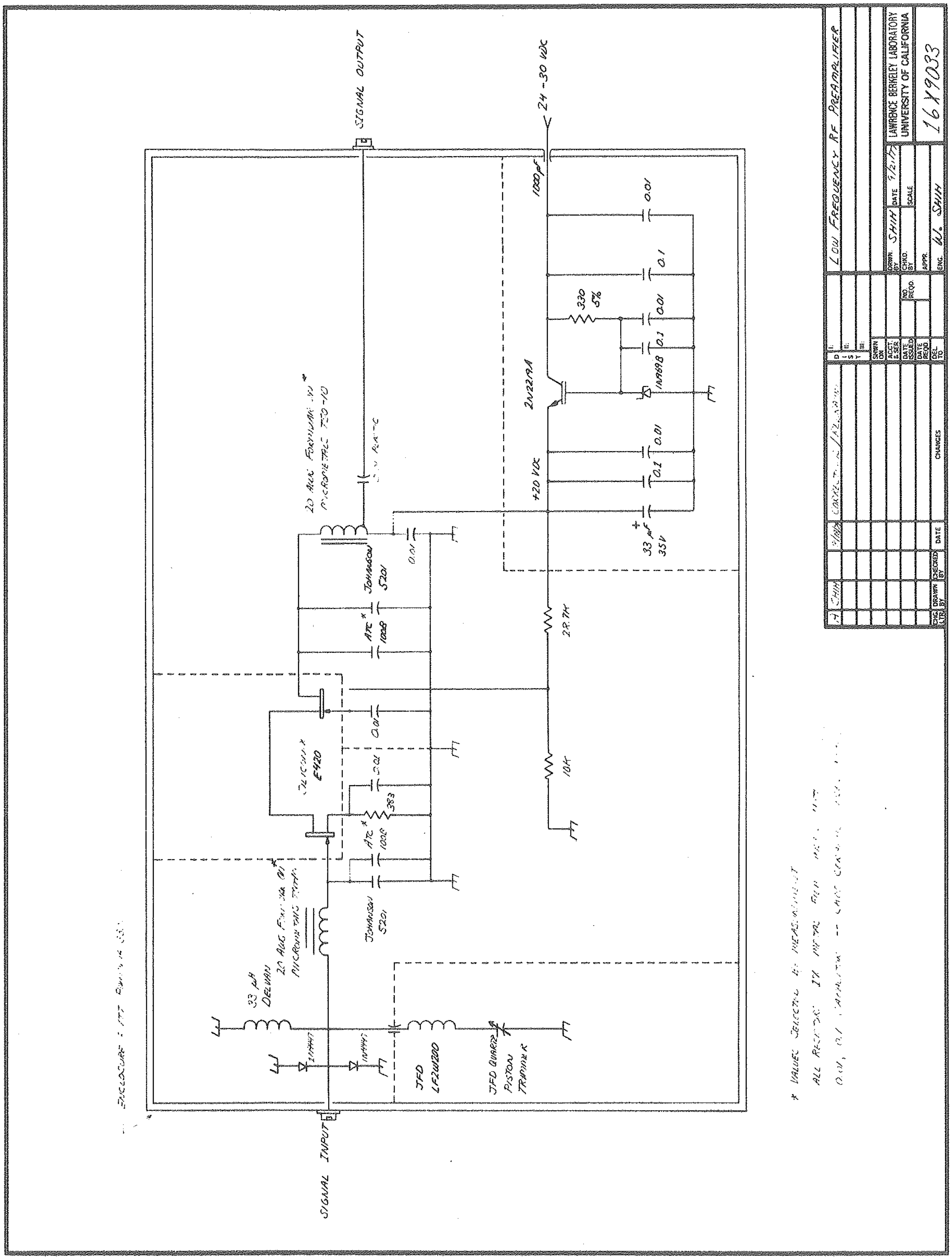
SIGNAL OUTPUT
24-30 VDC
1000pF
0.01
0.1
330
5%
2N2219A
+20 VDC
33 µF
35V
2.7K
10K
E420
JOHANSON
5201
ATC*
100B
383
0.01
33 µH
DELEVAN
JFD
JFD QUARTZ
PISTON
TRIMMER
SIGNAL INPUT
* VALUES SELECTED BY MEASUREMENT
LOW FREQUENCY RF PREAMPLIFIER
LAWRENCE BERKELEY LABORATORY
UNIVERSITY OF CALIFORNIA
16X9033
W. SHIH
CHANGES

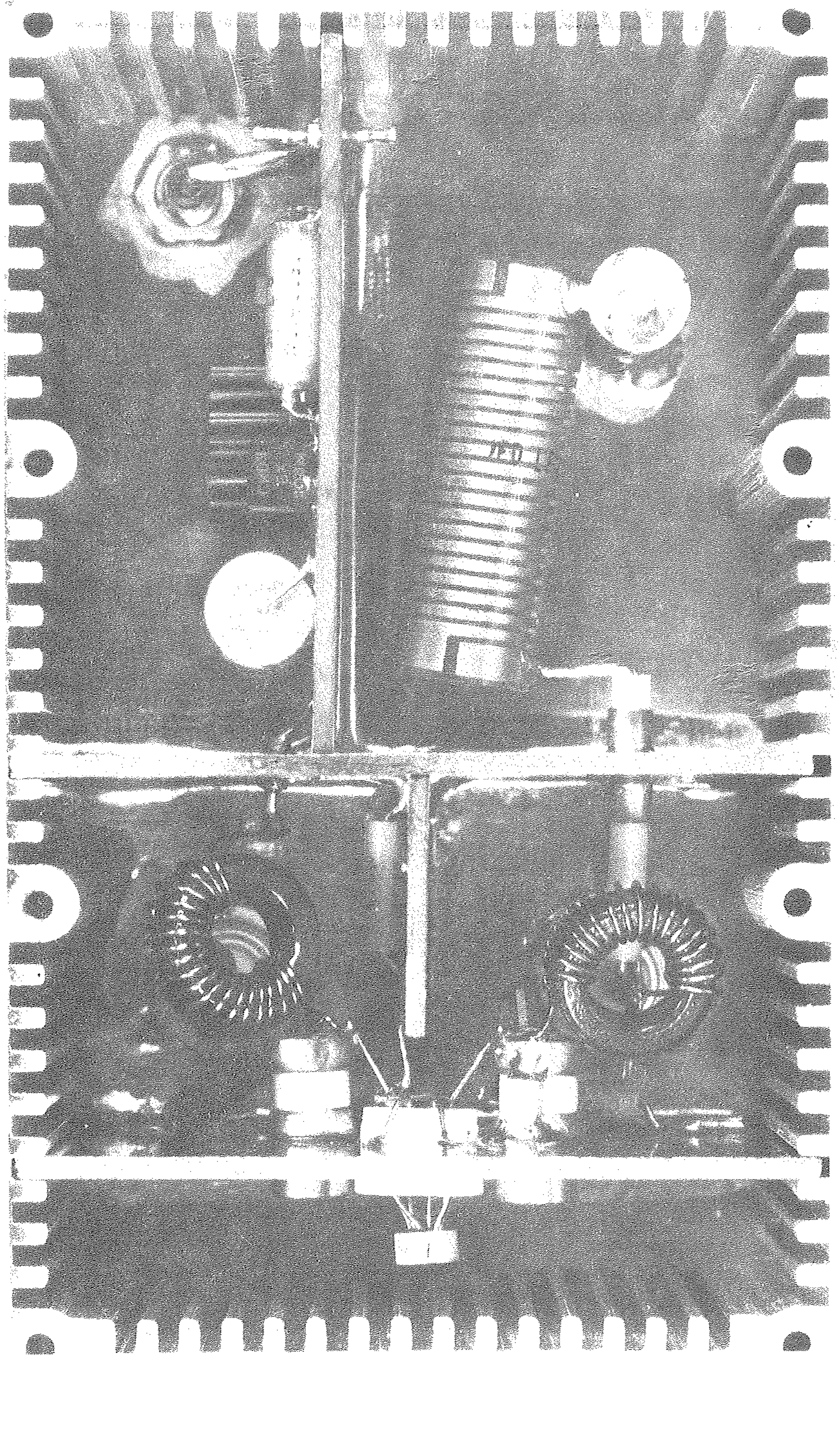

XBB 797-9250

2.5.5 16X904 Nicolet 1180 I/O Bus Intercept

A Nicolet Instruments Corp. Model 1180 Data System is used for data acquisition and control on the LCB 8 - 270 MHz spectrometer system. This processor has three major data busses: memory (M), data (D), and world (W). Only the world lines are available for connections outside of the main processor; and they function as part of a general purpose I/O bus.

The 1180 world lines are bidirectional three-state lines. Data may be transmitted or received by any device attached to the lines. Each I/O device that is attached to the world lines is identified by a unique device address. The processor may address any device; it does this by presenting the device address on address lines DV3 - DV10. The processor may request actions by that device by simultaneously presenting certain control signals: IOP0, IOP1, IOP2, TALK, LISTEN, or ACK.

Peripheral devices attached to the I/O bus may signal a request for service to the processor using the interrupt lines INT0- through INT6-. These lines are wired-or lines, that is all devices that output to the lines have open-collector outputs and the normal line state is held up by pull-up resistors. When a device wishes to signal the processor, it pulls down one of these lines (depending on the interrupt level to which that device is assigned). When the processor senses that an interrupt line is pulled down, it branches to a software interrupt service routine whose address is stored in the interrupt vector, and it deposits the return address at the first location of the service routine for a indirect return jump upon completion.

The three input/output pulses IOP0, IOP1, and IOP2, are usually used to clock the transfer of data to or from the 1180 accumulator to a peripheral device. All three pulses are 400 nsec long, and their occurrence is governed by bits 0 - 2 of the I/O instruction. Bits 3 - 10 of the I/O instruction set DV3 - DV10, the device address selection.

When the I/O bus leaves the 1180 chassis, connections are made with a 175 conductor ribbon cable. 86 signal lines are used; the remaining lines are interleaved grounds. Normally the 1180 is only connected to a 293A Programmable Pulser and a Nicolet I/O Tee. A bus termination is provided within the 293A. Each three-state line is terminated with a 220 ohm pull-up to + 5 VDC and 330 ohms to ground. Wired-or lines are terminated with a 4.7 Kohm pull-up to + 5 VDC.

Locally constructed devices that require connection to the 1180 I/O bus are connected via the 16X904 I/O Bus Intercept. This unit has two 86 conductor edge connectors for the 1180 I/O bus daisy-chain, and four 44 conductor edge connectors for use with Control Logic Corp. (CLC) 40 conductor interleaved ground cables. Only the signal lines that are commonly used are tied to the CLC connectors; this simplifies the construction of peripheral devices and reduces cabling costs. All world lines (W0 - W19), device lines (DV3 - DV10), IOPs, ACK, TALK, LISTEN, and INIT- lines are connected. Of the interrupt lines, only INT6- is connected. In general, locally constructed peripherals will only use interrupt level 6, as higher levels are reserved for the disk memory, the 293A, and internal processor functions such as clocks. Devices attached to the CLC bus are also daisy-chained, so each device must have two 44 conductor connectors on the rear panel. The last device in the chain must have a bus termination board in the extra slot.

Because the terminator board employs powered resistive terminations, the I/O peripheral must be capable of supplying at least 0.5 amps at + 5 VDC to the rear connectors. Since any device may be the last in the chain, all devices should be capable of supplying this current.

Signal definitions and bus conductor assignments are summarized in Table 2.7. Interface details for particular devices are contained in the documentation for the respective device.

Table 2.7 Nicolet 1180 I/O Bus Intercept Wire-Wrap Cross Reference

SIGNAL DEFINITION	*1180 I/O BUS ASSIGNMENT*	*1-43A/B BUS ASSIGNMENT*	*CLC I/O BUS ASSIGNMENT*
GND	1	1B	
GND	2	1A	
+5 VDC	3	2B	
+5 VDC	4	2A	
	5	3B	
DV10	6	3A	15
	7	4B	
DV9	8	4A	14
	9	5B	
DV6	10	5A	11
	11	6B	
DV8	12	6A	13
SKIP-	13	7B	W
W16	14	7A	L
DV3	15	8B	8
W17	16	8A	M
DV4	17	9B	9
W18	18	9A	N
DV5	19	10B	10
W19	20	10A	P
ACK	21	11B	U
W12	22	11A	F
IOP2	23	12B	17
W13	24	12A	H
IOP1	25	13B	S
W14	26	13A	J
IOP0	27	14B	R
W15	28	14A	K
DV7	29	15B	12
	30	15A	
	31	16B	
	32	16A	
	33	17B	
	34	17A	
INIT-	35	18B	A
	36	18A	
TALK	37	19B	T
	38	19A	
LISTEN	39	20B	16
W8	40	20A	B

Table 2.7 (continuation)

SIGNAL DEFINITION	*1180 I/O BUS ASSIGNMENT*	*1-43A/B BUS ASSIGNMENT*	*CLC I/O BUS ASSIGNMENT*
UPPER8-	41	21B	
W9	42	21A	C
SETNEG-	43	22B	
W10	44	22A	D
INT0	45	23B	
W11	46	23A	E
INT1-	47	24B	
	48	24A	
INT2-	49	25B	
	50	25A	
INT3-	51	26B	
	52	26A	
INT4-	53	27B	
W4	54	27A	6
INT5-	55	28B	
W5	56	28A	7
INT6-	57	29B	V
W6	58	29A	18
SPARE1	59	30B	
W7	60	30A	19
SPARE2	61	31B	
W0	62	31A	2
SPARE3	63	32B	
W1	64	32A	3
SPARE4	65	33B	
W2	66	33A	4
SPARE5	67	34B	
W3	68	34A	5
SPARE6	69	35B	
	70	35A	
SPARE7	71	36B	
	72	36A	
SPARE8	73	37B	
	74	37A	
SPARE9	75	38B	
	76	38A	
SPARE10	77	39B	
	78	39A	
SPARE11	79	40B	
	80	40A	

Table 2.7 (continuation)

SIGNAL DEFINITION	*1180 I/O BUS ASSIGNMENT*	*1-43A/B BUS ASSIGNMENT*	*CLC I/O BUS ASSIGNMENT*
SPARE12	81	41B	
	82	41A	
	83	42B	
	84	42A	
GND	85	43B	20,22
GND	86	43A	X,Z

2.5.6 16X919 Lock Channel Single Sideband Generator

The 16X919 Lock Channel Single Sideband Generator performs frequency conversion of a synthesized local oscillator to the desired lock observation frequency. The unit also provides for lock channel transmitter gating and output level controls.

The 8 - 270 MHz spectrometer system uses a 30 MHz intermediate frequency, hence with lower sideband mixing the local oscillator frequency is the desired operating frequency + 30 MHz. Frequency conversion is again via a term-by-term realization of the trigonometric identity (1). Quadrature components of the IF and local oscillator frequencies are generated using quadrature hybrids. The products are then realized using double-balanced mixers, and the sum is formed with an in-phase power combiner.

Design Summary (Figure 2.46)

The IF and local oscillator frequencies are fed in via rear panel TNC connectors. Since a 30 MHz Active Power Divider (10X223) is available on the system, no pass-through 30 MHz output is provided. The local oscillator is fed to a reactive power divider (Anzac TU-50); one output is then returned to the rear panel and the other output is fed to a 3 dB pad followed by a Watkins-Johnson A7 hybrid wideband amplifier. The 3 dB pad adjusts the output level of the amplifier as it feeds the Anzac JH-14 40-400 MHz broadband quadrature hybrid. The attenuation value of this pad was found to give the maximal output level within the constraint of desired spectral purity at the output. The quadrature components of the local oscillator available at the quadrature hybrid outputs are then fed through matched cables to dual phase/amplitude trim networks. It was found that the quadrature hybrid outputs did not have perfectly matched characteristics, therefore to increase the spectral purity of the output when operating at 41.451 MHz (the deuterium observe frequency) it was necessary to add this network. The trim network outputs are fed via another pair of matched cables to the R ports of matched Hewlett-Packard 10514A double balanced mixers.

The input 30 MHz IF is fed to a Merrimac QH-2-30 30 MHz quadrature hybrid. The outputs of this unit were found to have excellent phase and amplitude balance, therefore no trim network was necessary. The outputs are fed via matched cables to the L ports of the two mixers.

The X port outputs were routed via another pair of matched cables to an Anzac TU-50 in-phase power combiner. The power combiner output was fed to a Wavetek 5080 (TNC) 0 - 79 dB step attenuator and another Watkins-Johnson A7 amplifier. The amplifier output was gated by a Watkins-Johnson/Relcom S1 Rf switch, which was controlled from the rear panel switch drive input by a driver circuit (variation of 16X980). The S1 switch was placed last in the signal chain because it has an excellent on/off ratio (approaching 90 dB at low frequencies). Thus when the unit is gated off, there is minimal transmitted noise at the rear panel output. This was significant because the unit generated sufficient output power for internal deuterium locking on the 8 - 270 MHz spectrometer system, and the absence of a higher power transmitter followed by additional non-linear switching devices (*e.g.* series crossed diodes) was found to minimize phase shifts and DC level changes as the lock power level was varied.

Construction Details

Internal construction details of the 16X919 Lock Channel SSB Generator are similar to a number of other devices on the system. Figures 2.47 - 2.49 illustrate the construction methods used.

Figure 2.46 Lock Channel Single Sideband Generator [16X9193]

Figure 2.47 16X919 Lock Channel SSB Generator, Internal Construction Detail (1)

Figure 2.48 16X919 Lock Channel SSB Generator, Internal Construction Detail (2)

Figure 2.49 16X919 Lock Channel SSB Generator, Internal Construction Detail (3)

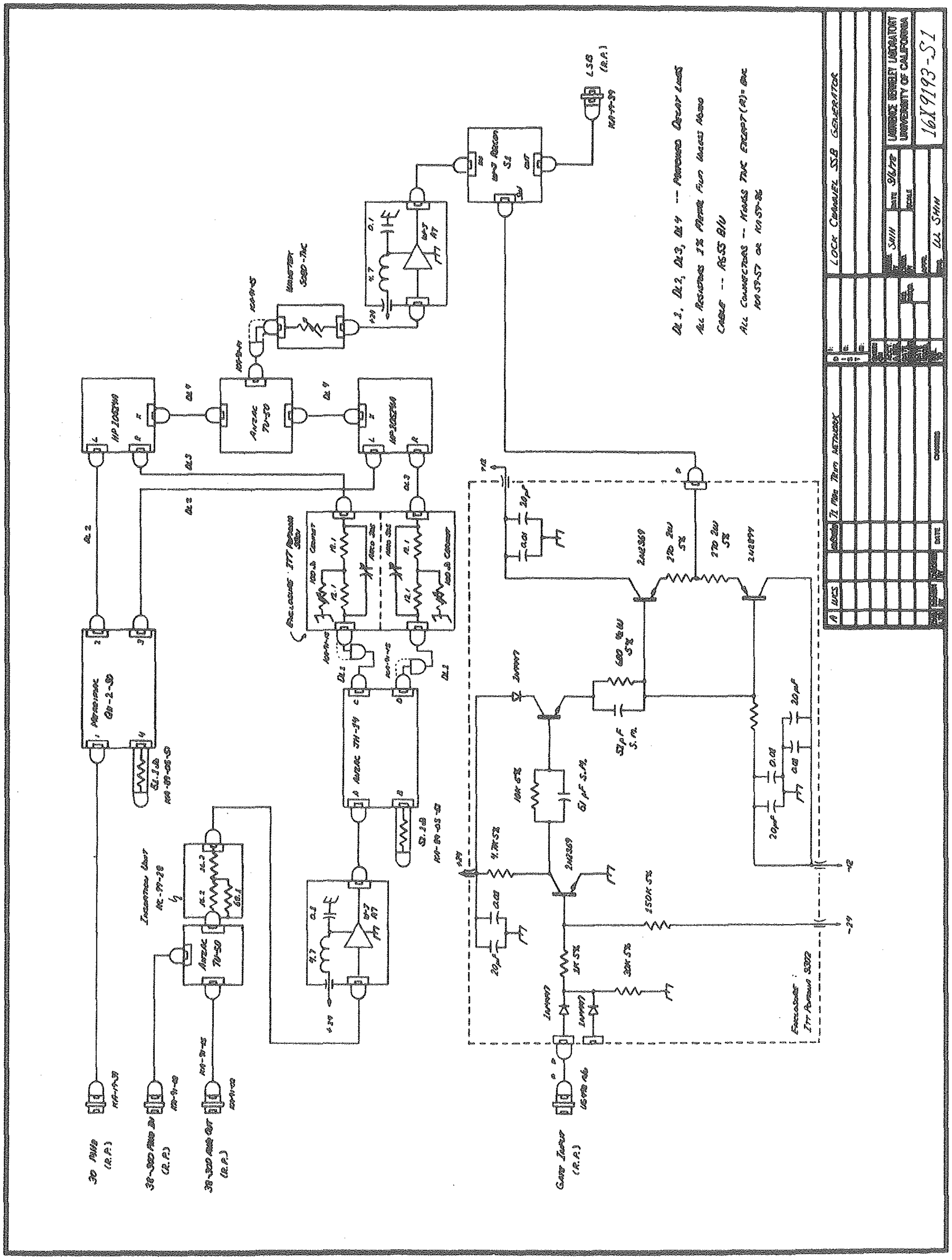
LOCK CHANNEL SSB GENERATOR
LAWRENCE BERKELEY LABORATORY
UNIVERSITY OF CALIFORNIA
16X9193-S1
DL1, DL2, DL3, DL4 -- PREFORMED DELAY LINES
ALL RESISTORS 1% METAL FILM UNLESS NOTED
CABLE -- RG55 B/U
LSB (R.P.)
GATE INPUT (R.P.)
30 PULSE (R.P.)

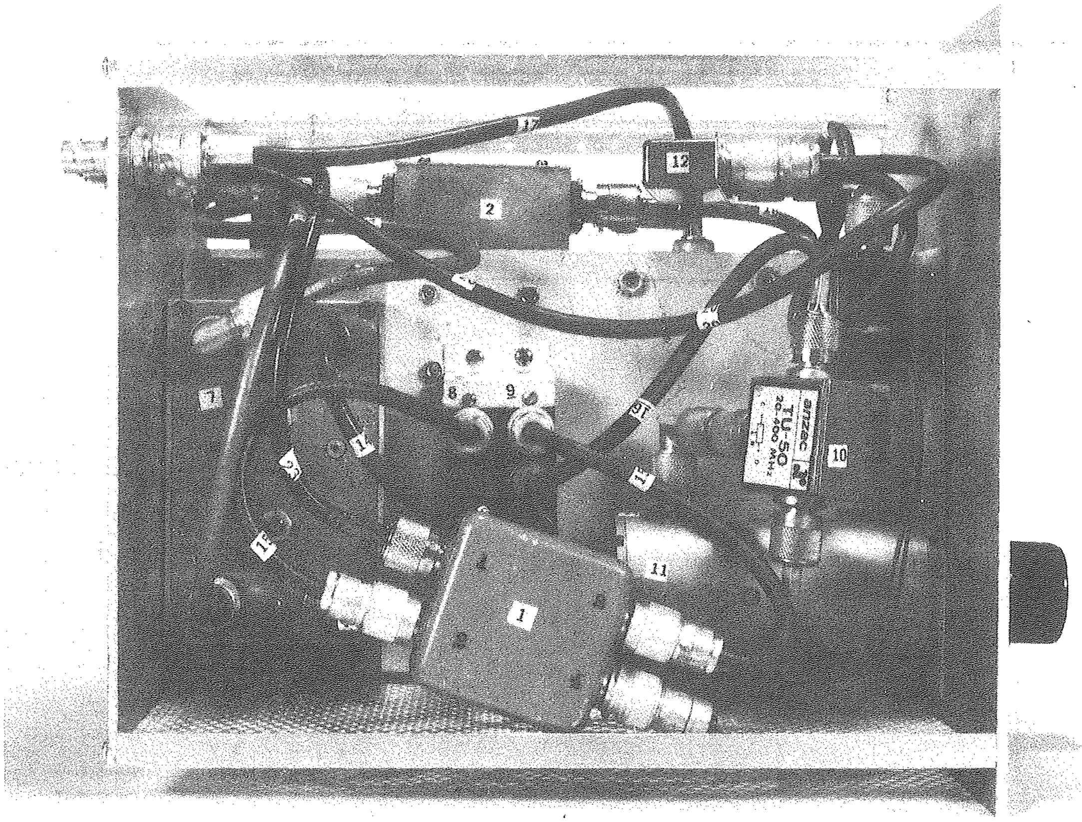

XBB 797-9252

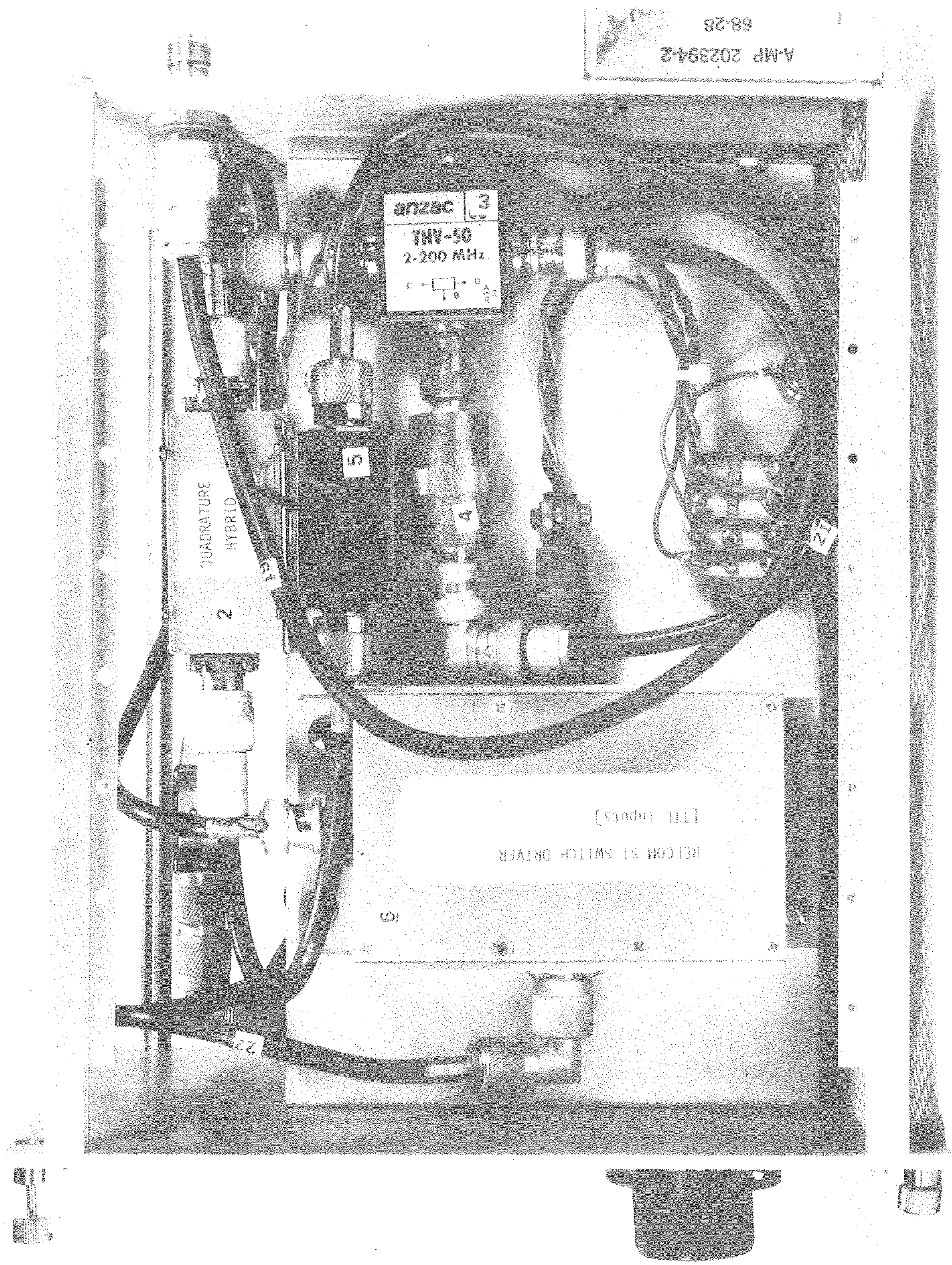
A-MP 202394-2
68-28
anzac
3
TNV-50
2-200 MHz.
QUADRATURE
HYBRID
RELCOM S1 SWITCH DRIVER
[TTL Inputs]

XBB 797-9249

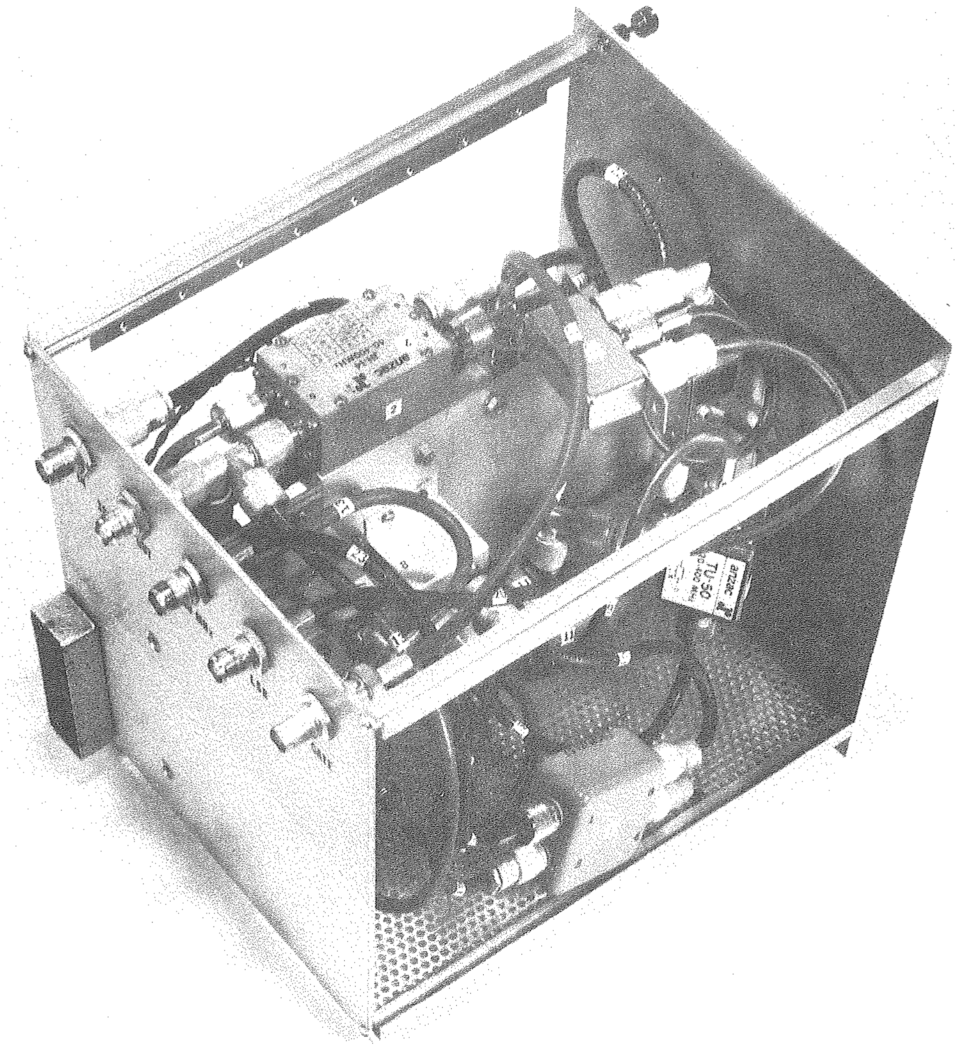

XBB 797-9251

2.5.7 16X935 63.42 KGauss Magnet Room Temperature Shim Control

The 16X935 63.42 KGauss Magnet Room Temperature Shim Control replaces a unit originally supplied with the magnet system. Principal changes are in the four Z shim controls; the original +/- range switch plus potentiometer arrangement was changed to a continuous (500 center) 10 - turn potentiometer adjustment. In the original configuration, it was not possible to reach zero shim current.

Fine controls are provided for all four Z shims, and coarse and fine H_0 field offset controls are brought to the front panel. The Z/H_0 summing amplifier board has incorporated minor changes. A high stability LM108A operational amplifier is used for the field sweep summing amplifier, and an Analog Devices AD741 has been substituted for the original LM741 in the Z summing amplifier.

The unit also incorporates switching and display metering of the lock channel signal amplitude, for convenience in shimming adjustments. An X-Y oscilloscope display, when connected to the 'scope vertical and horizontal outputs, may be switched to display a dispersion, absorption, or undetected 5 KHz signal (along the ordinate) coupled with either a sawtooth or the field correction signal amplitude (along the abscissa). Circuit details are summarized in Figures 2.50 and 2.51.

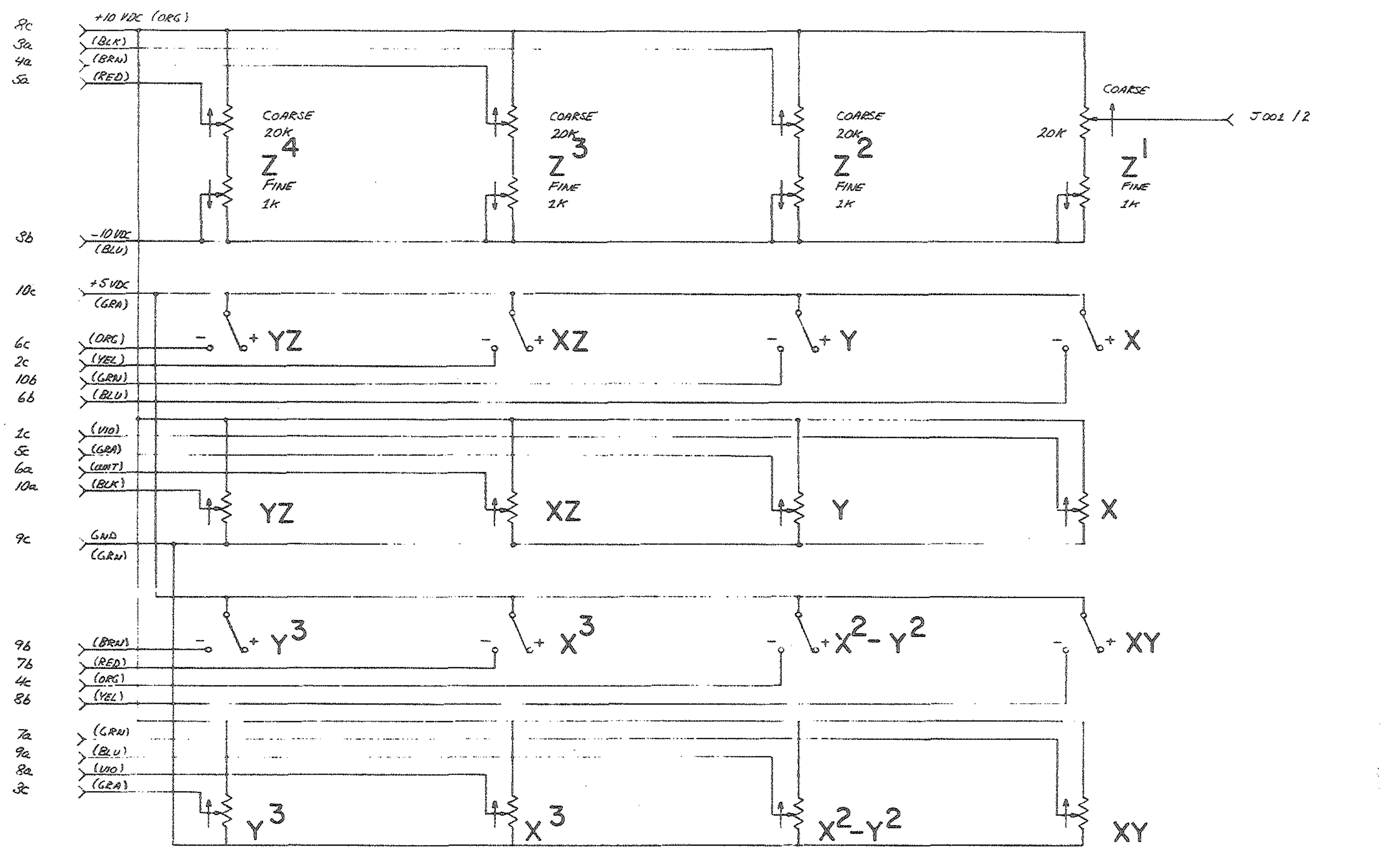

ALL POTENTIOMETERS : 10-TURN LINEAR, 5%
2 WATT

CHG. LTR.	DRAWN BY	CHECKED BY	DATE	CHANGES
A	SHIH		9/16/77	REDRAWN W/ ADDITIONS

63 KG MAGNET SYSTEM -- ROOM TEMPERATURE SHIM CONTROL
FRONT PANEL WIRING

DRAWN BY SHIH | DATE 9/16/77 | CHKD. BY | SCALE | APPR. | ENG. W. SHIH

LAWRENCE BERKELEY LABORATORY
UNIVERSITY OF CALIFORNIA

16X9353-S1A

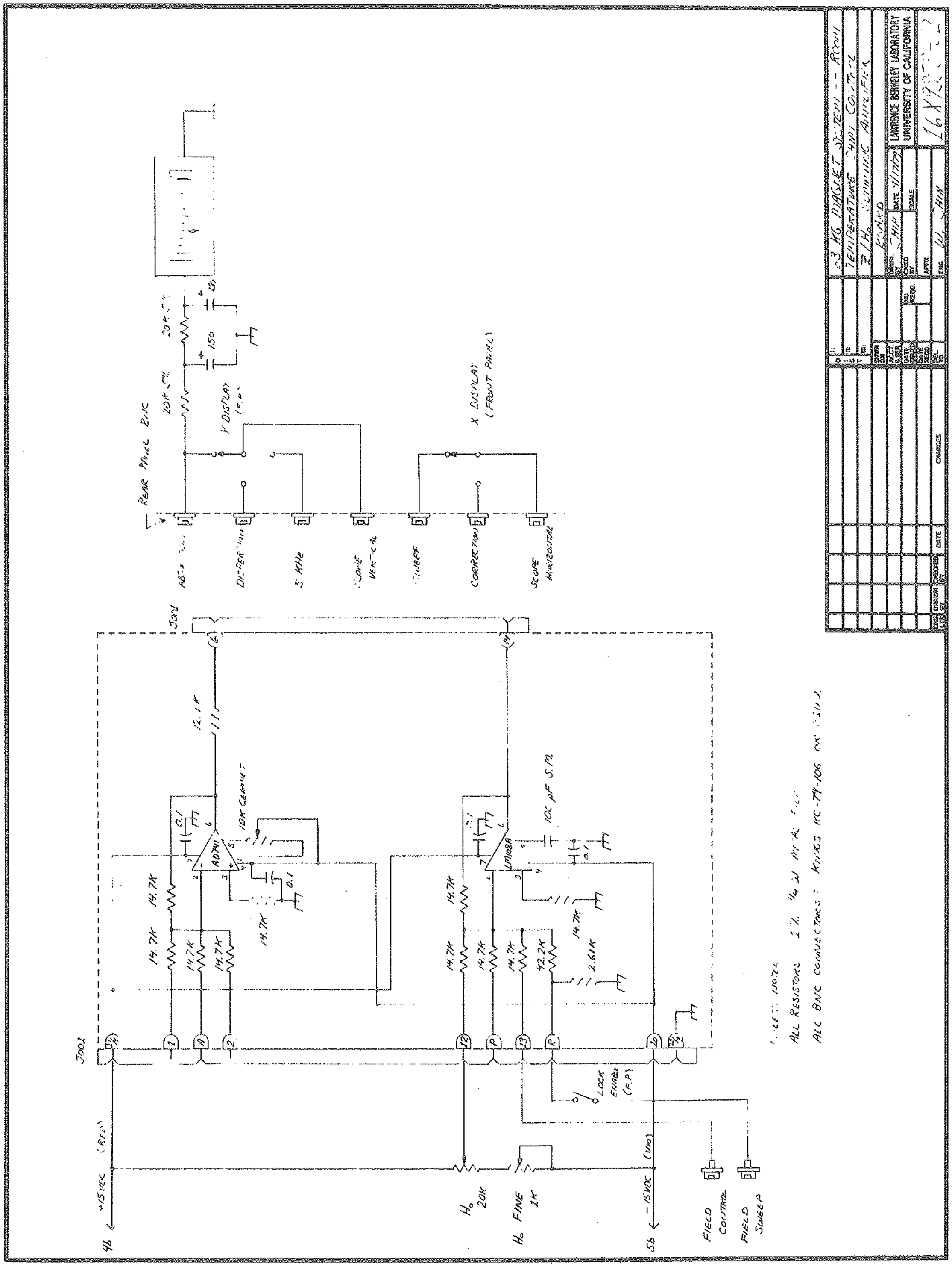
LAWRENCE BERKELEY LABORATORY
UNIVERSITY OF CALIFORNIA
REAR PANEL BNC
Y DISPLAY
X DISPLAY (FRONT PANEL)
5 KHz
SWEEP
CORRECTION
SCOPE HORIZONTAL
ADPH
LM108A
J002
+15VDC
-15VDC
FIELD CONTROL
FIELD SWEEP
ALL RESISTORS 1% 1/4 W
ALL BNC CONNECTORS: KINGS KC-79-106

2.5.8 16X950 Nicolet 1180 Driven Probe Temperature Control

The 16X950 Probe Temperature Control unit is part of a direct digital control system that is designed to maintain software selected temperatures in the probes used in the 63 KG Bruker Instruments solenoid that is the heart of the LCB 8 - 270 MHz Spectrometer System. The complete control system is outlined in Figure 2.52 [16X9503-B1]; it consists of the 16X950 unit attached to the Nicolet Instruments 1180 Data System, a Nicolet 293A Programmable Pulser, a programmable power supply (16X949 or equivalent), and the required heater and gas transfer line assemblies.

Actual probe temperature is measured by a copper/constantan thermocouple that is an integral part of each probe. The temperature control unit generates periodic interrupts on 1180 Interrupt Level 6, and an interrupt service routine that is written as an overlay to the Nicolet Technology Corp. NTCFT-1180 software package reads this temperature, compares it to the desired setpoint, and adjusts the output of the programmable power supply/heater accordingly. Because the thermocouple is physically located in the gas stream just ahead of the sample tube, temperature measurements actually only reflect the probe temperature, which may not be the same as the actual sample temperature. In instances when the decoupling is not in use and the sample has been equilibrated for 15 minutes or more, these temperatures are generally quite close. When proton decoupling is in use with aqueous samples, dielectric heating will increase the sample temperature above the indicated reading by a significant amount, depending on decoupler power level. If the actual sample temperature must be known quite accurately, an external calibration should be run. The measurement error may be minimized to some extent by using a high variable temperature gas flow rate. When proton decoupling is used with non-aqueous samples, the dielectric heating problem is less serious. It is not expected that homonuclear decoupling should cause any measurement errors, because of the much lower Rf power levels involved.

Design Summary

A. Interface Hardware

The 16X950 unit utilizes a Fluke 2170A Digital Thermometer equipped with the Option -02 Digital Output Unit. The thermocouple connections on the 2170A are connected to a rear panel thermocouple plug with a copper/constantan pair that is wound through several ferrite beads. This aids in the suppression of decoupling frequencies that are picked up in the thermocouple. Rectified common-mode input can otherwise lead to significant measurement errors.

The 2170A makes approximately 2.5 readings per second. At the end of each measurement period, the output register in the digital output unit is updated. While updating is in progress, the BUSY line is held high to indicate invalid data.

Interface circuitry is contained on two Control Logic Corp. (CLC) breadboards -- the Device Select and Interrupt Generator Board (Figure 2.53) and the 20-Bit D-Register Board (Figure 2.54). The 2170A is connected via a 34 conductor ribbon cable to the D-register board, and both boards plug into a CLC cardcage that is connected to rear panel

44 conductor edge connectors that are compatible with the 16X904 extended 1180 I/O Bus (refer to 16X904 description, Section 2.5.6).

The falling edge of the BUSY pulse is used to clock a 74LS196 divide-by-ten counter that drives a 74LS221. The 74LS221 monostable issues a 150 nsec pulse approximately every four seconds. This pulse is used to set the interrupt flip-flop (74LS74) using the preset line. When the Q output is high, the device is requesting a Level 6 interrupt. The 74LS38 NAND on the preset line checks to insure that an interrupt service is not currently in progress. The 74LS38 NAND on the Q output has an open collector output, which is compatible with the wired-or nature of the INT6- line of the 1180.

The temperature controller is assigned device address 311. When the INT6- line is pulled down, the processor jumps to the interrupt 6 service routine. Since all slow I/O devices are also on Level 6, the processor must first determine which device caused the interrupt. This is done by polling all devices on Level 6 in a skip-chain. Each possible device code (among those known to be attached to the system as set in the configuration number) is presented on device address lines DV3 - DV10 along with an ACK pulse. If device code 311 is presented, it will be decoded by the 8836s and the 74LS30. The NAND of this signal with ACK (74LS132) are compared to the output state of the interrupt flip-flop with the 74LS38 NAND. If the interrupt flip-flop was set, the SKIP- (wired-or) line is pulled down, signalling the processor that it was the temperature controller that caused the interrupt.

The processor reads out the temperature on to the World lines

W0 - W19 by issuing a device address 311 with a TALK and an IOPØ pulse. This causes the generation of a LOAD BUS signal at the output of the DS8836. This is inverted and routed to the OUTPUT CONTROL inputs of the five 74LS173s that make up the 20 bit D-register. Upon enabling these three-state outputs, the current temperature (in BCD format) and sign and check bits are placed on the I/O bus and loaded into the 1180 accumulator (read temperature control instruction = RTCIN = 603111).

The 20 bit D-register is loaded from the 2170A-02 by the rising edge of the $\overline{\text{BUSY}}$ signal. Thus at the end of each updating cycle in the 2170A, the outputs are dumped into the 20 bit D-register.

The temperature control unit may be switched between ACTIVE and STANDBY states by the processor. A device select 311 coupled with an IOP1 pulse (1180 instruction TCON = 643112) turns on the ACTIVE/STANDBY flip-flop, and a device select 311 with an IOP2 (1180 instruction TCOFF = 643114) turns the unit off. This control line is also brought to the rear panel so that the programmable power supply may also be controlled (using a solid state relay). The ACTIVE/STANDBY flip-flop must indicate that the controller is active for the 74LS38 on the INT6- line to be capable of generating interrupts.

The processor INIT- line is used to clear all registers on power up or in the event of a front panel (1180) clear command. The INIT- line is used in the controller to generate a pulse that clears both the ACTIVE/STANDBY flip-flop and the interrupt flip-flop. This insures that abnormal conditions will force the controller into a STANDBY state.

The processor calculates the desired setpoint for the programmable power supply, and outputs a voltage on DAC2 of the 293A. This signal is available on the DX rear panel connector. The DX lines are routed to a daisy-chain pair of Canon DP-25 rear panel connectors on the 16X950 chassis, and the DAC2 signal is routed to the Analog Output Buffer Board (Figure 2.55, 16X9503-S3). A differential amplifier picks up this signal, and after passing through a front panel 10-turn pot (LOOP GAIN control) and an LM310 voltage follower, it is routed to the programmable power supply via a rear panel BNC connector.

B. Interrupt Service Software

Interrupt service software modifications to NTCFT-1180 Version 90622 are contained in the system ASCII file VT.ASC on the 1180 system. This file is assembled using either FASM, the Fast 1180 Assembler, or DASM, the old 1180 Disk Assembler.

The overlay compensates for the incompatibilities between the 16X950 unit and hardware supplied by Nicolet Technology Corp. Differences are summarized in the internal program documentation. The assembled listing is shown in Figure 2.56, appended to the end of this section.

The direct digital control algorithm used is the velocity form of the proportional-integral-differential (PID) 3-mode control algorithm. Term weightings are determined empirically.

The interrupt service routine also outputs the measured temperature on DAC3 of the 293A. It was found to be useful to monitor the temperature with an analog Y-T recorder when setting control loop gains.

Provisions have been made for adding an alarm board to sense the absence of gas flow or other malfunctions. Error conditions are transmitted to the 1180 by holding bit 19 (W19) high.

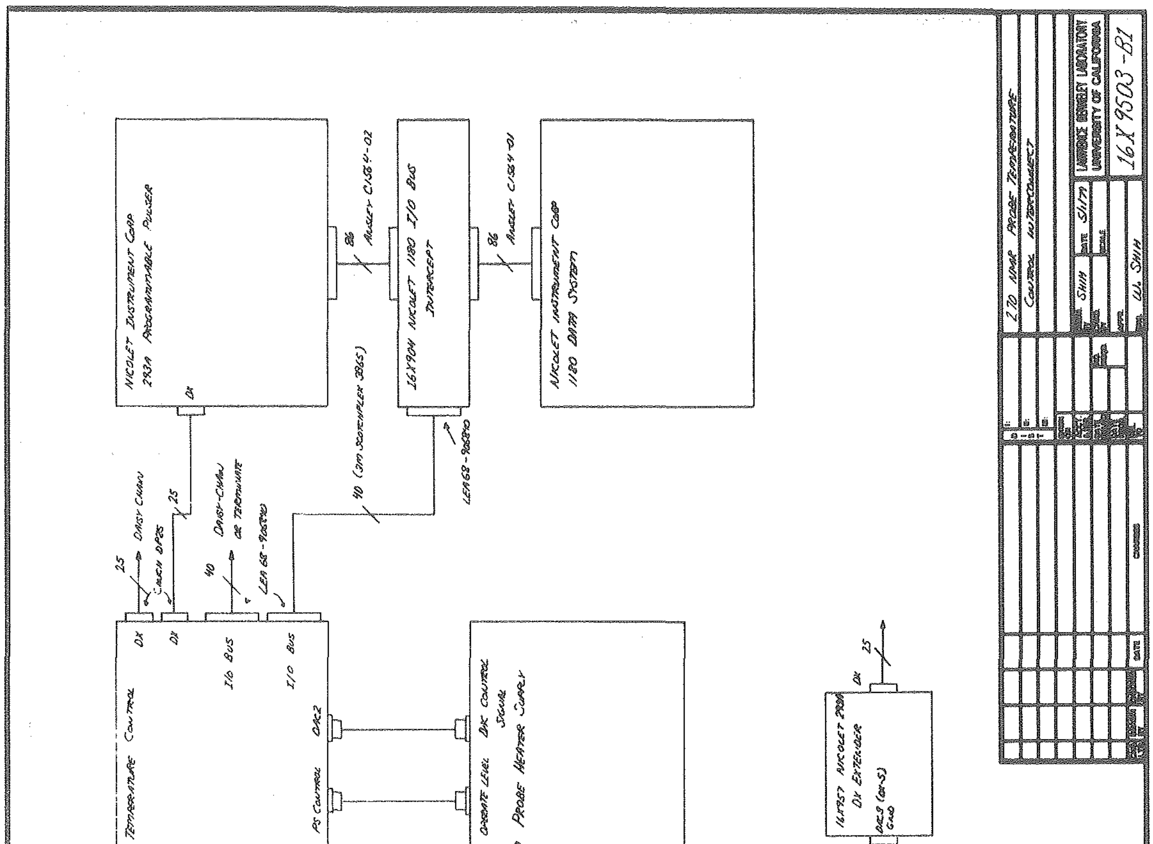
Nicolet Instrument Corp
293A Programmable Pulser
DX
86
Ansley C1564-02
16X904 Nicolet 1180 I/O Bus
Intercept
86
Ansley C1564-01
Nicolet Instrument Corp
1180 Data System
25
Daisy-Chain
25
40
Daisy-Chain
or Terminate
40 (3M Scotchflex 3365)
16X950 Temperature Control
DX
DX
I/O Bus
I/O Bus
DAC2
PS Control
Operate Level DAC Control Signal
16X949 Probe Heater Supply
Output
Thermoelectric
Cu-Constantan
Thermocouple
(Part of Probe)
Nichrome Ribbon
Heater
Assembly
Optional Temperature Monitor :
16X957 Nicolet DX Extender
DX
25
HP 7155B V-T Recorder
or Equivalent
270 MHz Probe Temperature
Control Interconnect
Shih
W. Shih
Lawrence Berkeley Laboratory
University of California
16X9503-B1

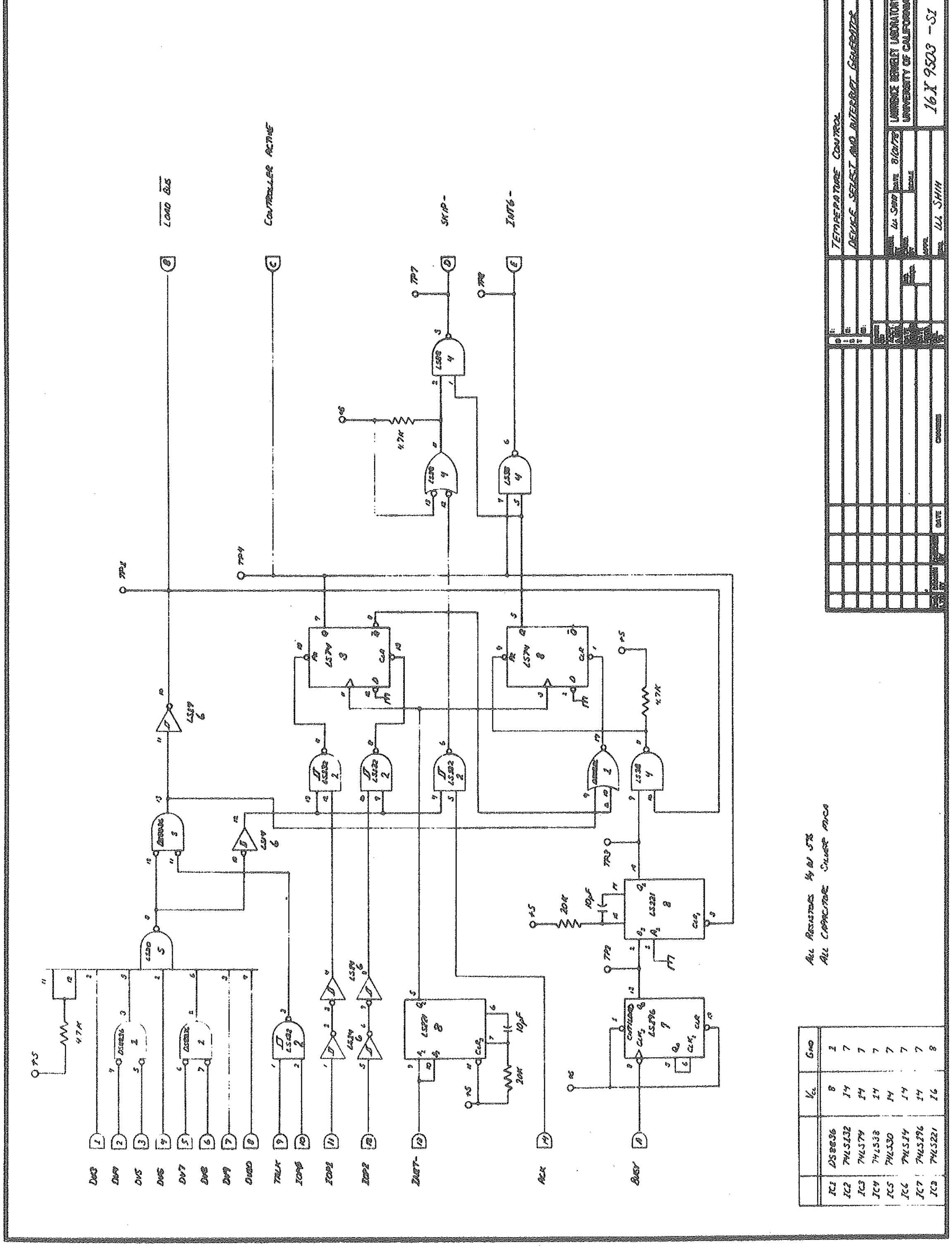
TEMPERATURE CONTROL
DEVICE SELECT AND INTERRUPT GENERATOR
LAWRENCE BERKELEY LABORATORY
UNIVERSITY OF CALIFORNIA
16X 9503 -S1
W. SHIH
LOAD BUS
CONTROLLER ACTIVE
SKIP-
INTG-
ALL RESISTORS 1/4 W 5%
ALL CAPACITORS SILVER MICA

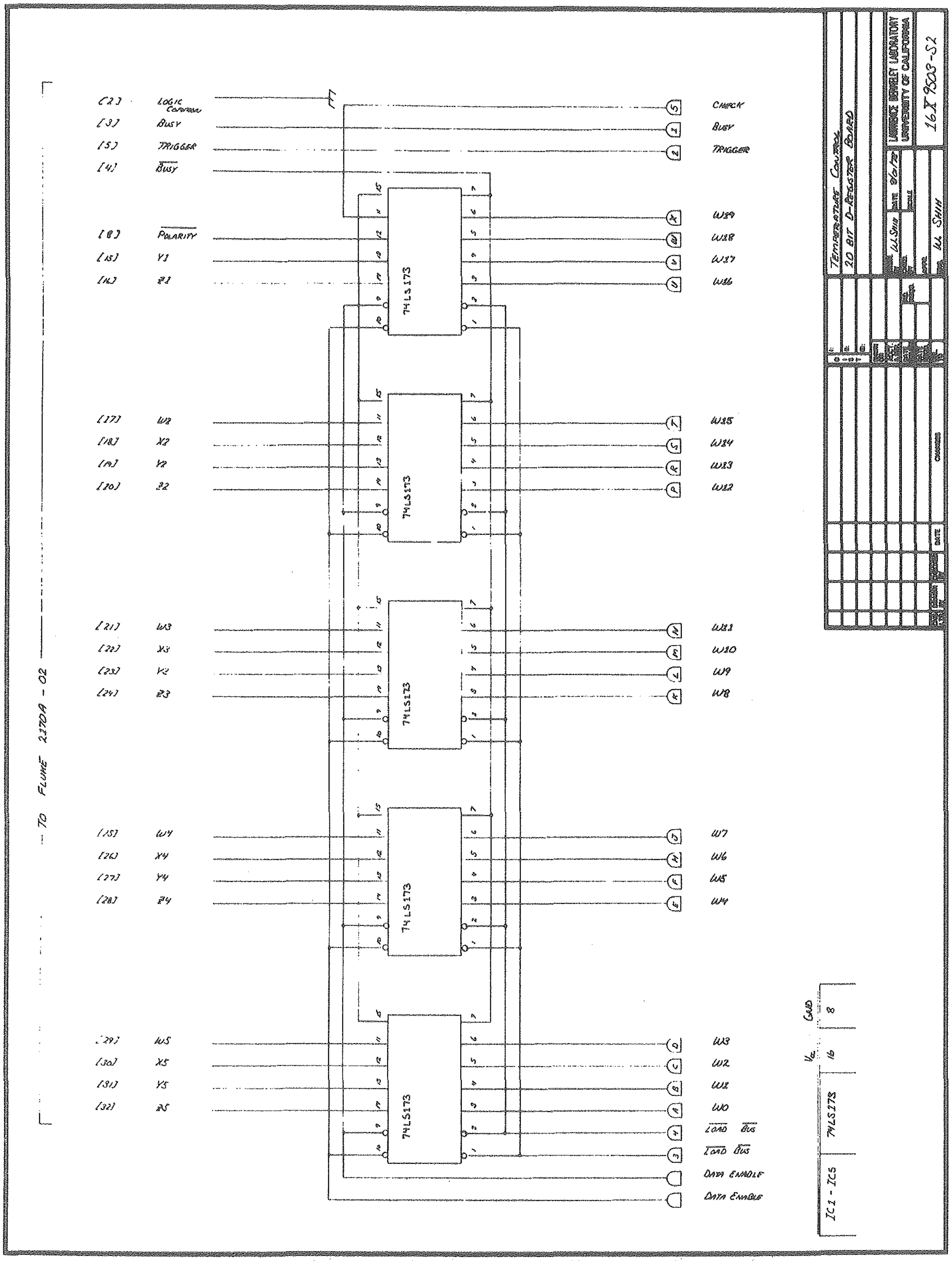
LAWRENCE BERKELEY LABORATORY
UNIVERSITY OF CALIFORNIA
TEMPERATURE CONTROL
20 BIT D-REGISTER BOARD
16X 9503-S2
W. SHIH
TO FLUME 2270A - 02
LOGIC CONTROL
BUSY
TRIGGER
POLARITY
CHECK
74LS173
DATA ENABLE
IC1 - IC5
74LS173
Vcc
GND
16
8

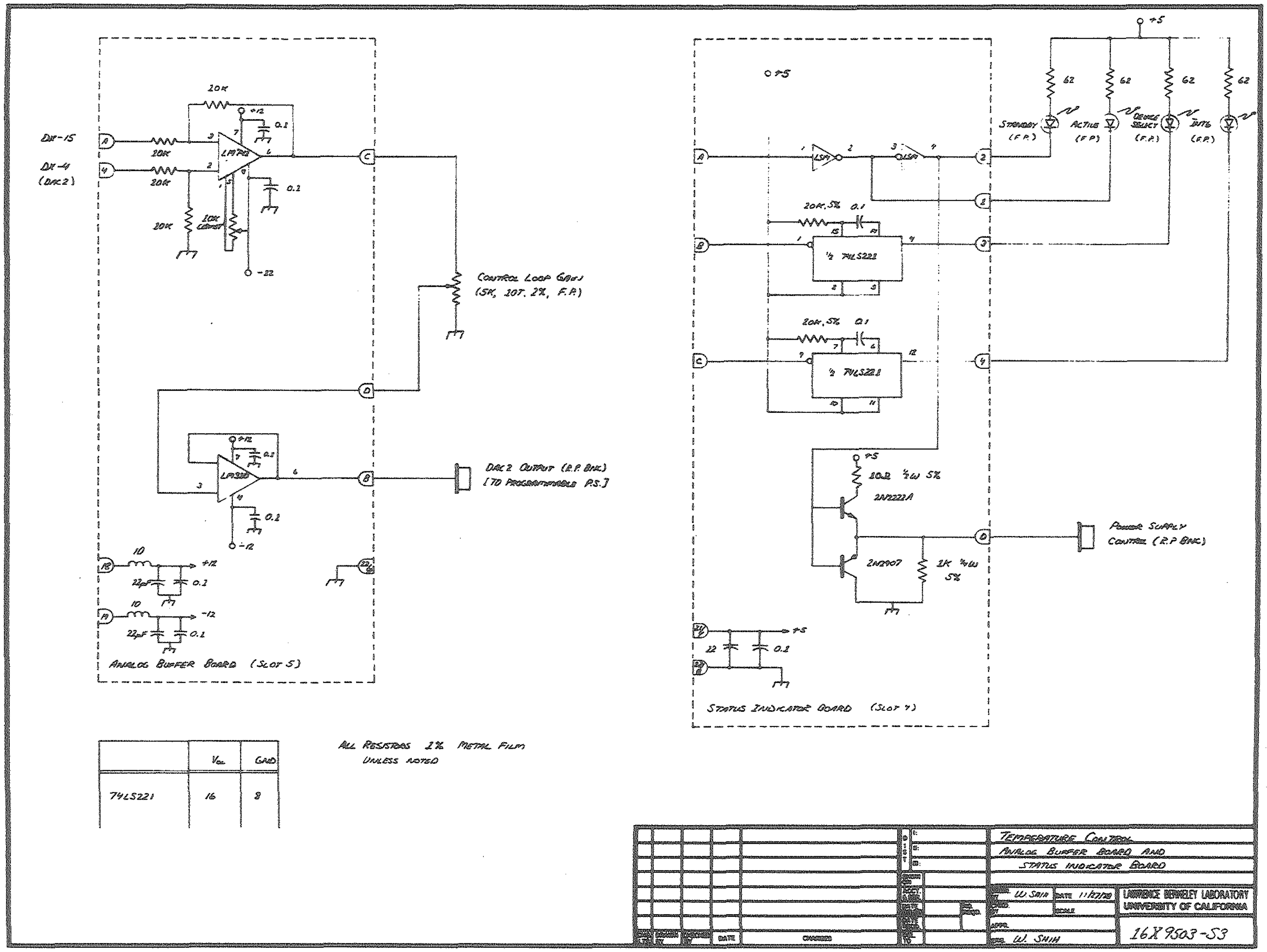

	V_{cc}	GND
74LS221	16	8

Figure 2.56 Assembled Listing of Temperature Control Interrupt Service Overlay to NTCFT-1180

```
 RUN FASM

FASM, E58-90215
@VT.ASC/VT.BIN,-TT:F




        FAST 1180 ASSEMBLER, E58-90215

        08/24/79 16:25   @VT.ASC/VT.BIN,-TT:F

        110 SOURCE STATEMENTS
        27 USER-DEFINED SYMBOLS
        MEMORY NEEDED: 4571 TO 4661
```

```
/OVERLAY TO NTCFT V#90603 FOR 16X950 TE


 /OVERLAY TO NTCFT V#90603 FOR 16X950 TEMPERATURE CONTROL
 .UNDENT
 /
 /
 /
 /       WILLY C. SHIH
 /E90704 *****      4 JULY 1979      *****
 /
 /
 /       This version uses the velocity form of the PID control
 /         algorithm, and reads temperatures to 0.2 deg C.
 /
 /
 /MISCELLANEOUS COMMAND DEFINITIONS
620621          LDAC2=620621             /LOAD DAC2
620631          LDAC3=620631             /LOAD DAC3
603111          RTCIN=603111             /READ TEMPERATURE CONTROL REGISTER ONTO BUS
643112          TCON=643112              /TURN ON TEMPERATURE CONTROL
643114          TCOFF=643114             /TURN OFF TEMPERATURE CONTROL
 /
 /LOCATION EQUIVALENCES
  4047          TSETI=4047
  4050          DTIM1=4050
  4051          EQUILT=4051
  4052          TVOLTS=4052
  4053          TPASS=4053
  4054          TSTORE=4054
  4055          TM0=4055
  4056          TM1=4056
  4057          TM2=4057
  4060          TPT=4060
  4061          TCT=4061
  4060          DTI=TPT
  2666          SLOIOX=2666
   564          GOFLAG=564
   605          QCOUNT=605
   206          TTYOUT=206
 /
  4571          *4571
  4571  603111 TCINT6,RTCIN              /READ TC REGISTER ONTO BUS
  4572  735322         TRLSH 22          /ROTATE ALL BUT SIGN AND CHECK TO MQ
  4573  670400         SKIP AC0          /SIGN BIT=1 => NEG TEMP
  4574 1503060         ZERMZ DTI         /TEMP>0 => STORE 0 @ DTI AND SKIP
  4575 1473060         MONM DTI          /TEMP<0 => STORE -1 @ DTI
  4576  262002         ANDA (2           /CHECK BIT 19 FOR ERROR CONDITION
  4577   44607         JPZ TC1           /JUMP IF NO ERRORS
  4600 1116564         MEMZ GOFLAG       /ACQUISITION IN PROGRESS?
  4601 1436605         MPOM QCOUNT       /YES, STOP IT
  4602  216207         MEMA (207         /RING BELL
  4603 2000206         JMS TTYOUT
  4604    4603         JMP $-1
  4605  722622         TLLSH 22          /RESTORE MQ TO AC VIA ROTATE
  4606    2666         JMP SLOIOX        /IGNORE READING AND QUIT
  4607  216003 TC1,    MEMA (3           /LOAD DIGIT COUNT FOR TEMPERATURE
```

```
/OVERLAY TO NTCFT V#90603 FOR 16X950 TE

                             /THIS VERSION TRUNCATES THE TENTHS OF DEGREES
                             /  FOR THE SAKE OF SIMPLICITY IN GETTING
                             /  OVERLAY WORKING AND GAIN ADJUSTED
 4610 1413061          ACCM TCT          /STORE IN TCT
 4611 1603050          ZERMA DTIM1       /CLEAR TEMP WORD
 4612  722602          TLLSH 2           /GET FIRST 1/2 DIGIT
 4613  701003 TC2,     LASH 3            /BCD TO BINARY CONVERSION OCCURS
 4614 1221050          AFMA DTIM1        /  BY SHIFTING LEFT 3 (*8) AND
 4615 1421050          AFMM DTIM1        /  ADDING DIGIT TO ITSELF TWICE
 4616  722604          TLLSH 4           /GET NEXT DIGIT
 4617  262017          ANDA (17          /MASK FOUR LSB's
 4620 1621050          AFMMA DTIM1       /ADD TO RUNNING SUM
 4621 1535061          MMOMZ TCT         /DECREMENT DIGIT COUNT,SKIP IF DONE
 4622     4613          JMP TC2           /CONTINUE IF NOT DONE
 4623 1117060          MEMZ DTI          /TEMPERATURE < 0?
 4624 1433050          MNGM DTIM1        /YES, COMPLEMENT DTIM1
 4625 1217050          MEMA DTIM1        /OUTPUT TEMPERATURE ON DAC3 +
 4626  220030          AFMA (30          /  30 OFFSET
 4627  620631          LDAC3             /  FOR MONITORING OR LOGGING
 4630 1217054 TC2A,    MEMA TSTORE       /PUSH CURRENT READING ONTO STACK
 4631 1413060          ACCM TPT          /TSTORE POINTS TO TOP OF STACK
 4632  216003          MEMA (3           /STACK IS ONLY LAST 3 READINGS
 4633 1413061          ACCM TCT          /  JUST MOVE 3 LOCATIONS
 4634 1217050          MEMA DTIM1        /GET TEMPERATURE READING
 4635 3657060          SWP ^ TPT         /  AND PUSH ONTO STACK
 4636 1535061          MMOMZ TCT         /DECREMENT DIGIT COUNT,SKIP IF DONE
 4637     4635          JMP *-2
 4640 1735053 TC2B,    MMOMAZ TPASS      /TIME TO EVALUATE?
 4641   62666          JPP SLOIOX        /NO,EXIT INTERRUPT SERVICE

/DIRECT DIGITAL CONTROL ALGORITHM:
/
/      DV = 4*(E + 10*E' - E")
/
/      WHERE:  DV = CHANGE IN DAC OUTPUT
/               E = CURRENT TEMPERATURE ERROR
/               E' = 1ST DERIVATIVE OF ERROR
/               E" = 2ND DERIVATIVE OF ERROR
/
/      E(0) = T(S) - T(0)
/      E'(0) = E(0) - E(-1)
/            = T(-1) - T(0)
/      E"(0) = E'(0) - E'(-1)
/            = 2*T(-1) - T(0) - T(-2)

 4642 1217055          MEMA TM0          /T0
 4643 1223056          AMMA TM1          /T0 - T1
 4644  701002          LASH 2            /4*T0 - 4*T1
 4645 1221055          AFMA TM0          /5*T0 - 4*T1
 4646  701001          LASH 1            /10*T0 - 8*T1
 4647 1223057          AMMA TM2          /10*T0 - 8*T1 - T2
 4650 1225047          MMAA TSETI        /TS - 10*T0 + 8*T1 + T2
 4651     4661          JMP TC3
 4661          *4661
```

```
/OVERLAY TO NTCFT V#90603 FOR 16X950 TE


  4661  701002 TC3,     LASH 2           /*4  (GAIN CONTROL)
```

-3-

```
/OVERLAY TO NTCFT V#90603 FOR 16X950 TE
```

DTI	4060	DTIM1	4050	EQUILT	4051	GOFLAG	564
LDAC2	620621	LDAC3	620631	QCOUNT	605	RTCIN	603111
SLOIOX	2666	TCINT6	4571	TCOFF	643114	TCON	643112
TCT	4061	TC1	4607	TC2	4613	TC2A	4630
TC2B	4640	TC3	4661	TM0	4055	TM1	4056
TM2	4057	TPASS	4053	TPT	4060	TSETI	4047
TSTORE	4054	TTYOUT	206	TVOLTS	4052		

*

2.5.9 16X955 270 MHz Preamplifier

The 16X955 270 MHz Preamplifier is designed for a 270 MHz center frequency with a 1 dB bandwidth of approximately 50 MHz. The unit employs four grounded-gate FET stages, capacitively coupled, yielding about 35 dB of Rf gain. Measured noise figure (cascaded with the 10X210 8-270 MHz to 30 MHz Linear Converter) is 2.2 dB.

Circuit details are summarized in Figure 2.57. The unit employs Siliconix U310 with a common-gate forward transconductance of 20,000 μmho, with a figure of merit (g_m/C) of greater than 2.35×10^9.

Figure 2.57 270 MHz Preamplifier [16X9553]

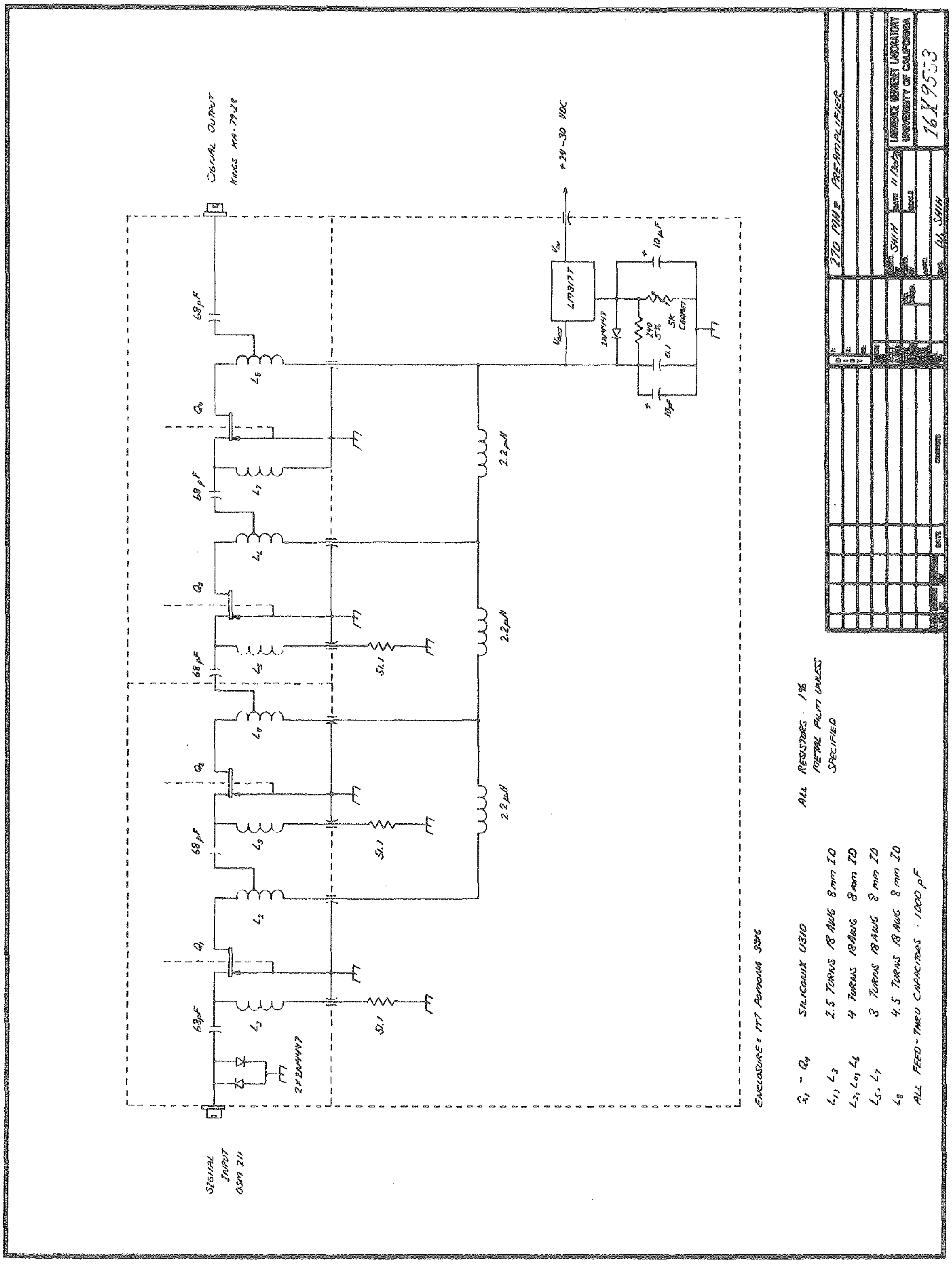
SIGNAL OUTPUT KINGS KA-79-29
+24-30 VDC
LM317T
Vin
Vadj
10 µF
1N4447
240 5%
5K CERMET
0.1
10µF
68pF
68pF
68pF
68pF
68pF
2.2µH
2.2µH
2.2µH
51.1
51.1
51.1
Q1
Q2
Q3
Q4
L1
L2
L3
L4
L5
L6
L7
L8
SIGNAL INPUT OSM 211
2×1N4447
ENCLOSURE: ITT POMONA 3306
Q1 - Q4 SILICONIX U310
L1, L3 2.5 TURNS 18 AWG 8mm ID
L2, L4, L6 4 TURNS 18 AWG 8mm ID
L5, L7 3 TURNS 18 AWG 8mm ID
L8 4.5 TURNS 18 AWG 8mm ID
ALL FEED-THRU CAPACITORS: 1000 pF
ALL RESISTORS: 1% METAL FILM UNLESS SPECIFIED
270 MHz PREAMPLIFIER
LAWRENCE BERKELEY LABORATORY
UNIVERSITY OF CALIFORNIA
SHIH
16X9553

2.5.10 16X956 Nicolet 1180/CalComp 565 Incremental Plotter Interface

The CalComp 565 incremental plotter (California Computer Products) is an industry standard drum-type digital plotter. Control inputs are required at a rear panel Cannon SK-19 connector. These inputs control carriage step left and right, drum step up and down, and pen lift and lower. Inputs are ten volt pulses with a minimum duration of four microseconds.

The Nicolet Instrument Corp. 1180 Data System is normally intended to operate with a Nicolet Zeta Research Model 160 Incremental Plotter system. Connection is made via the supplementary "I/O Tee". This I/O tee is attached to the 1180 I/O bus, which is a three-state bus providing 20 data lines, 8 device address lines, 3 IOP lines, and assorted other control signals. The 16X956 Nicolet 1180/CalComp 565 Interface is connected to the I/O bus via the 16X904 I/O Bus Intercept (refer to Section 2.5.6 16X904 Nicolet 1180 I/O Bus Intercept).

A. Design Summary

The interface unit is connected to the 16X904 I/O Bus Intercept via two 40 conductor ribbon cables (3M Scotchflex 3365). Two rear panel I/O connectors are provided so that the unit may be conveniently daisy-chained. If the unit is the last connection on the bus, a bus terminator board must be inserted in the unused connector.

The rear panel connectors are connected to board 1. The plotter is assigned device address 374. When a plot command is issued, the lowest six bits of the 1180 accumulator contain the desired plot action (Table 2.8).

Table 2.8 16X956 Nicolet 1180/CalComp 565 Plot Command Summary

Accumulator Bit	Desired Action
ACØ = 1	Step carriage right
AC1 = 1	Step carriage left
AC2 = 1	Step drum up
AC3 = 1	Step drum down
AC4 = 1	Lift pen
AC5 = 1	Lower pen

Interface circuit details are summarized in Figures 2.58 and 2.59 [16X9563-S1 and 16X9563-S2]. Upon issuing the plot I/O command (1180 instruction DZETA = 623741), the accumulator is output to the 20 world lines (WØ - W19). The 74LS14 and 74LS30 decode the 374 device select, and with the issuance of the IOPØ pulse, WØ - W5 are clocked on the leading edge into the 74LS174 6 bit D-register. The outputs of this register then reflect which of the 75451 peripheral drivers should issue a pulse.

The device select/IOPØ pulse also triggers two timers (NE556). One timer generates a ten microsecond pulse for the peripheral drivers (in general, only one of the six will have been selected). The other timer generates a delay to allow sufficient time for the plotter to respond. Before issuing a plot command, programs either calculate a software delay or issue a "skip if ready" command. The "skip if ready" command (1180 instruction 647740) generates a device select 374 and an ACK pulse. If the NE556 timer indicates that sufficient time has elapsed since the last plot command, the ANDed device select and ACK will cause the 75452 peripheral driver to pull down the -SKIP line, which is wired-or. When the processor senses that the -SKIP line is pulled down, it assumes that the plotter is ready to receive the next step command.

The board 1 plotter outputs are routed to complementary emiter-followers on board 2. This insures that the plotter step pulses will be driven from a low impedance source with enough current capability for the CalComp. The board outputs are routed to a front panel MS connector, where a shielded cable makes connections to the plotter.

Figure 2.58 Nicolet 1180/CalComp 565 Interface, Plot Control Logic [16X9563-S1]

Figure 2.59 Nicolet 1180/CalComp 565 Interface, Line Driver Detail [16X9563-S2]

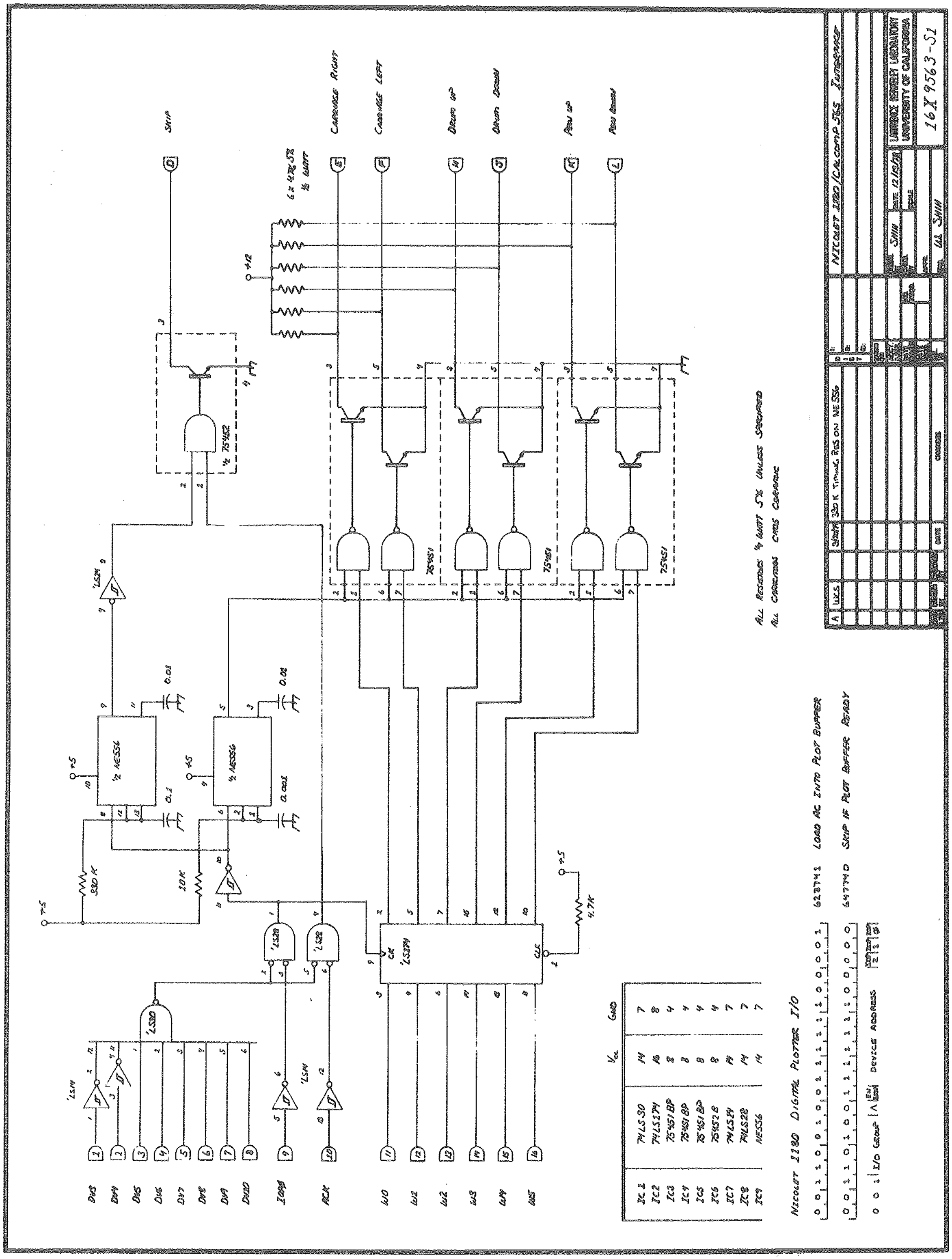
NICOLET 2180/CALCOMP 565 INTERFACE
LAWRENCE BERKELEY LABORATORY
UNIVERSITY OF CALIFORNIA
16X9563-S1
NICOLET 2180 DIGITAL PLOTTER I/O
LOAD AC INTO PLOT BUFFER
SKIP IF PLOT BUFFER READY
DEVICE ADDRESS
ALL RESISTORS 1/4 WATT 5% UNLESS SPECIFIED
ALL CAPACITORS CY15 CERAMIC
SKIP
CARRIAGE RIGHT
CARRIAGE LEFT
DRUM UP
DRUM DOWN
PEN UP
PEN DOWN

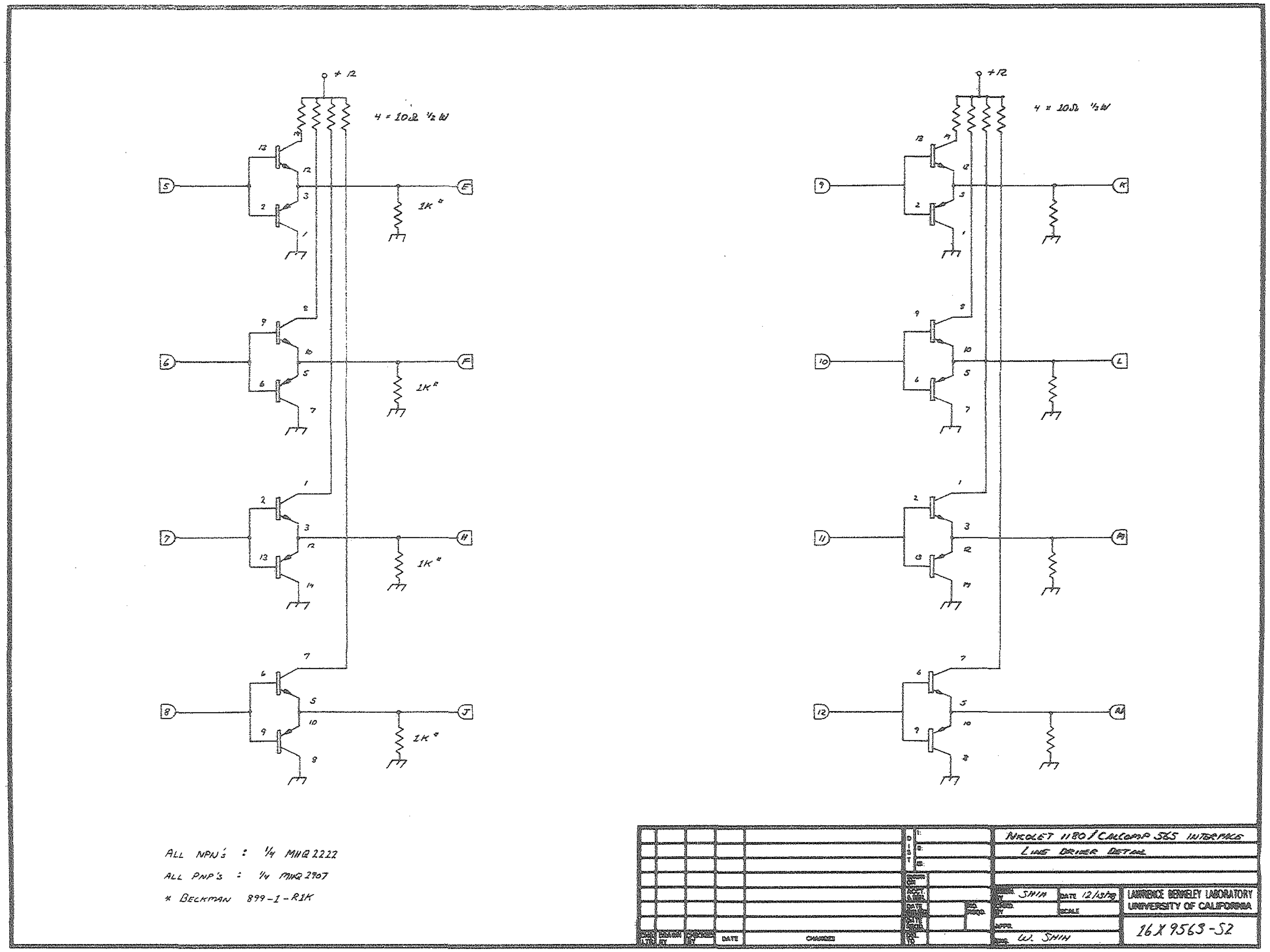
+12
4 = 10Ω ½W
1K*
ALL NPN's : ¼ MHQ 2222
ALL PNP's : ¼ MHQ 2907
* BECKMAN 899-1-R1K
NICOLET 1180 / CALCOMP 565 INTERFACE
LINE DRIVER DETAIL
SHIN
DATE 12/13/78
LAWRENCE BERKELEY LABORATORY
UNIVERSITY OF CALIFORNIA
W. SHIN
16X 9563-S2
DATE
CHANGES

B. Requisite Software Changes

The NTCFT-1180 software package supplied by Nicolet Technology Corp. is designed for use with a Nicolet Zeta Research Model 160 plotter with a step size of 0.005 inch. The CalComp 565 at LCB may use a step size of 0.005 or 0.01 inch, depending on the drive gear selection. Since the LCB CalComp is also used with the general laboratory data acquisition system with a step size of 0.01 inch, a large body of software would have to be modified if the step size were to be changed. It was also deemed to be impractical to change the gears whenever the plotter was moved to a different machine, therefore the only alternative was to modify the NTCFT-1180 software. An assembled listing of these changes is shown in Figure 2.60.

Figure 2.60 Assembled Listing of CalComp 565 Modifications to NTCFT-1180

```
 RUN FASM
FASM, E58-90215
@CALCMP.ASC/CALCMP.BIN,-TT:F



        FAST 1180 ASSEMBLER, E58-90215

        08/23/79 10:01    @CALCMP.ASC/CALCMP.BIN,-TT:F

        70 SOURCE STATEMENTS
        3 USER-DEFINED SYMBOLS
        MEMORY NEEDED: 12640 TO 16107
```

CALCOMP PLOTTER PATCHES - 90615

```
 .TITLE "CALCOMP PLOTTER PATCHES - 90615"
 .UNDENT

 /PATCHES TO NTCFT-1180 - 90622 FOR DRIVING 100 STEP/INCH
 /CALCOMP PLOTTER RATHER THAN ZETA 160 (200 STEPS/INCH)

 /PATCHES TO DIR MODULE

 14227         *14227
 14227  216004          MEMA (4         /TO SLOW DOWN PLOTTER
 14310         *14310
 14310  217730          MEMA (1730      /STEPS/25 CM
 14631         *14631
 14631  114713          114713          /STEPS/1000 CM

 /PATCHES TO OUT MODULE

 12640         *12640
 12640    1522 PAGSIZ, 1522     /STEPS/8.5 IN (=PAGE)
 15507         *15507
 15507  241157          DBMA (1157      /STEPS/PAGE (VERTICAL
 15515         *15515
 15515  216100          MEMA (100       /-> BOTTOM OF PLOT

 /PATCHES TO AXL MODULE

 13010         *13010
 13010       1 CHARSZ,1                 /DEFAULT CHARACTER SIZE
 13063         *13063
 13063  216001          MEMA (1         /CHAR SIZE FOR AXIS
 13073         *13073
 13073  220014          APMA (14        /AXIS Y-OFFSET
 13303         *13303
 13303 3777770          -10             /SMALL TIC SIZE
 13307         *13307
 13307      10          10              / "  "  "
 13324         *13324
 13324 3777757          -21             /LARGE TIC SIZE
 13330         *13330
 13330      21          21              / "  "  "
 13347         *13347
 13347  232050          MNGA (50        /AXIS NUMBER Y-OFFSET
 13402         *13402
 13402  222060          AMMA (60        /= 3 CHAR WIDTHS
 13404         *13404
 13404  222007          AMMA (7         /HALF SPACE
 13432         *13432
 13432  220064          APMA (64        /CHAR Y-OFFSET
 13435         *13435
 13435  220040          APMA (40        /TEST FOR END OF AXIS
 13704         *13704
 13704       7          7               /HALF CHAR SPACE
 15047         *15047
```

CALCOMP PLOTTER PATCHES - 90615

```
 15047  217234           MEMA (1234      /=17 CM
 15051          *15051
 15051  220450           APMA (450       /-> 24.5 CM
 15250          *15250
 15250  220043           APMA (43        /FOR LEFT EDGE OF PLOT
 15260          *15260
 15260 3777634           -144            /PARAMETER POSITIONING
 15261 3777714           -64
 16004          *16004
 16004     1522 PGSIZ,   1522            /=8.5 IN
 16046          *16046
 16046  222006           AMMA (6         /= HALF CHAR  (X)
 16057          *16057
 16057  222007           AMMA (7         /= HALF CHAR  (Y)
 16107          *16107
 16107 3777764           -14             /= 5 MM
```

-2-

CALCOMP PLOTTER PATCHES - 90615

```
CHARSZ   13010        PAGSIZ   12640       PGSIZ    16004
```

*

2.5.11 16X964 41.45 MHz Receiver - T/R Switch

The 16X964 41.45 MHz Receiver T/R Switch operates at a center frequency of 41.451 MHz for ^{2}H observation. The unit serves two principal functions:

- Front-end Rf amplification. The preamplifier in this unit supplies approximately 18 dB of gain. It employs a low noise junction FET amplifier which sets the noise performance of the deuterium receiver channel.

- Transmit/receive switching. When the transmitter produces a pulse, the unit protects the preamplifier from overloading. After the pulse, the unit switches to the receive mode.

Design Summary (Figure 2.61)

The unit employs a 16X903 dual J-FET cascode amplifier (refer to Section 2.5.4). Protective crossed diodes are incorporated in the input, and a series LC shunt tuned to 270 MHz is employed to suppress decoupling frequencies. A semi-rigid UT-141 0.141 quarter-wave line is used as part of the switching arrangement. A Circutel FLT/20-140-13/150-2A/2A 140 MHz low-pass filter is used for additional suppression of decoupling frequencies.

Instead of the conventional diode switch, only a 3 dB pad is used to isolate the lock channel transmitter (16X919) from the receiver. This arrangement was used because the high isolation Rf switch used in the 16X919 final stage has an excellent on/off ratio, and the addition of diode switches only resulted in non-linearities when the Rf power level of the transmitter was varied. The unit employs internal supply voltage regulation, and is normally powered by the 16X974 preamplifier power supply (+24 VDC).

Figure 2.61 41.45 MHz Receiver - T/R Switch [16X9643]

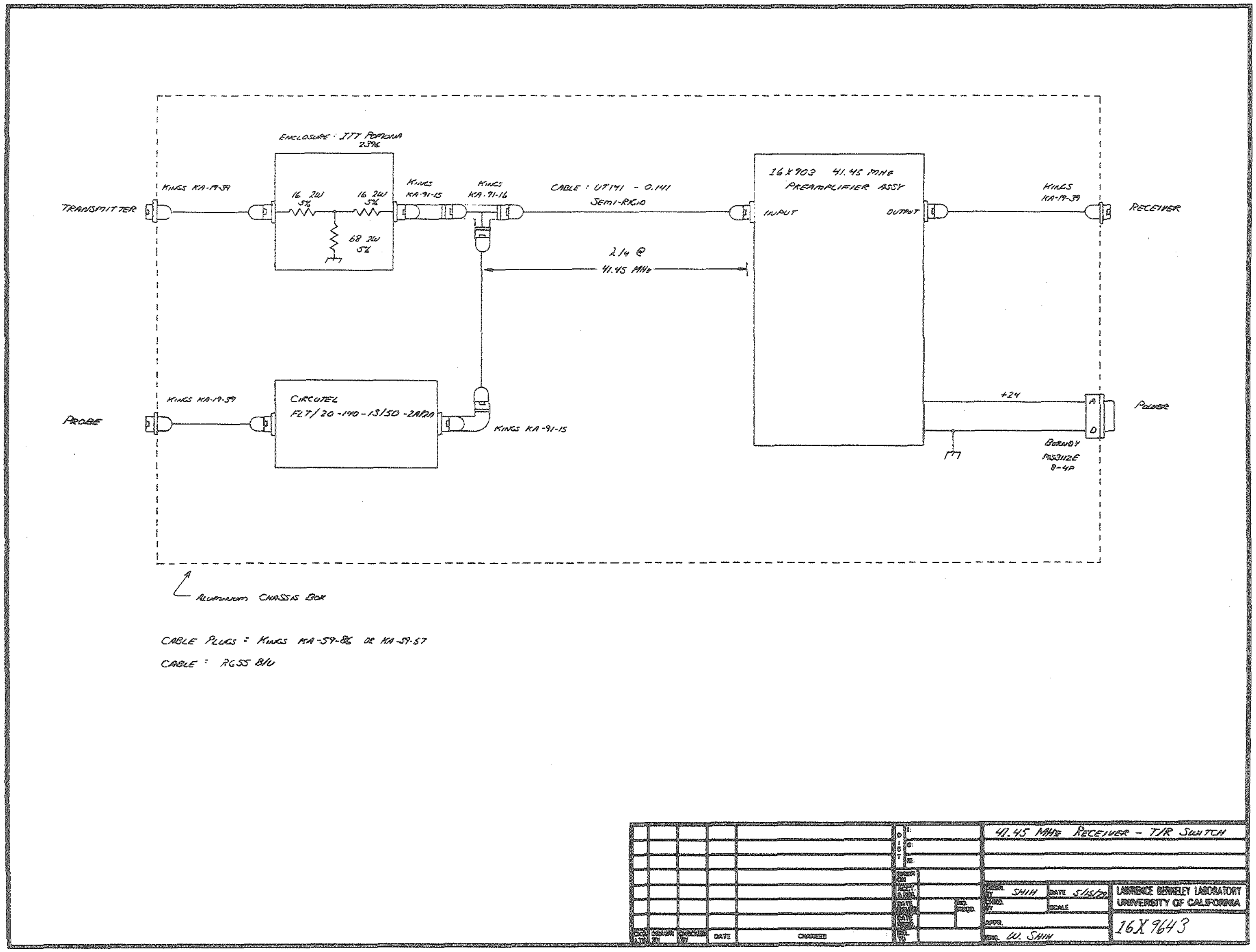
ENCLOSURE : ITT POMONA 2396
KINGS KA-19-39
16 2W 5%
16 2W 5%
68 2W 5%
KINGS KA-91-15
KINGS KA-91-16
CABLE : UT141 - 0.141 SEMI-RIGID
16X903 41.45 MHz PREAMPLIFIER ASSY
INPUT
OUTPUT
KINGS KA-19-39
TRANSMITTER
RECEIVER
λ/4 @ 41.45 MHz
KINGS KA-19-59
PROBE
CIRCUTEL FLT/20-140-13/50-2AP2A
KINGS KA-91-15
+24
POWER
A
D
BURNDY PSS3112E 8-4P
ALUMINUM CHASSIS BOX
CABLE PLUGS : KINGS KA-59-86 OR KA-59-57
CABLE : RG55 B/U
41.45 MHz RECEIVER - T/R SWITCH
SHIH
DATE 5/15/79
LAWRENCE BERKELEY LABORATORY
UNIVERSITY OF CALIFORNIA
SCALE
APPR.
W. SHIH
16X9643
DATE
CHANGES

2.5.12 16X965 27.36 MHz / 270 MHz Dual Frequency Receiver - T/R Switch

The 16X965 dual frequency T/R switch assembly operates at 27.36 MHz for ^{15}N and at 270 MHz for ^{1}H observe. The unit serves three principal functions:

- Front-end Rf amplification -- The two preamplifiers in this unit are the first gain stages encountered by ^{15}N and ^{1}H signals. They provide approximately 36 - 40 dB of gain, and the outputs are fed to the 10X210 8 - 270 MHz to 30 MHz Linear Converter for conversion to the 30 MHz intermediate frequency. Since they are the first gain stages, noise performance is crucial.
- T/R switching -- When the transmitter produces a high power pulse, the unit protects the sensitive front-end receivers. After the pulse, the unit switches to the receive mode.
- Transmitter noise suppression -- Even when the transmitter is gated off, it has a high noise temperature. The 16X965 unit effectively isolates this noise source from the receivers, leading to minimal degradation in system noise performance.

Design Summary

A. 27.36 MHz Section

The 27.36 MHz section uses two cascaded 16X903 low noise dual J-FET cacscode amplifiers (refer to Section 2.5.4). The first amplifier has protective crossed diodes on the input, and it also employs a series LC shunt tuned to 270 MHz to suppress proton decoupling frequencies (see photograph of Figure 2.45). The amplifier cascade, when coupled to the 10X210 Linear Converter, shows a system noise figure of 1.5 dB when measured at the 30 MHz IF output. The T/R switching employs a standard quarter-wave line arrangement. Transmitter isolation was found to be sufficient when four pairs of crossed diodes were placed in series with the transmitter output, and a measured line was used to connect the transmitter.

B. 270 MHz Section

The 270 MHz section employs a 16X955 four stage grounded gate J-FET amplifier to provide 36 - 40 dB of Rf gain (see Section 2.5.9, 16X955 270 MHz Preamplifier). This unit has protective crossed diodes on the input. When coupled to the 10X210 Linear Converter, the system noise figure is approximately 2.2 dB when measured at the 30 MHz IF amplifier output. The T/R switching is done with a standard quarter-wave line arrangement, using UT-141 0.141 semi-rigid coax for the line segment. The junction capacitance of the crossed diodes in the transmitter switch is tuned with a short coil to maximize the impedance at 270 MHz and cancel as much reactive component as possible.

Figure 2.62 27.36 MHz / 270 MHz Dual Frequency Receiver - T/R Switch Assembly [16X9653]

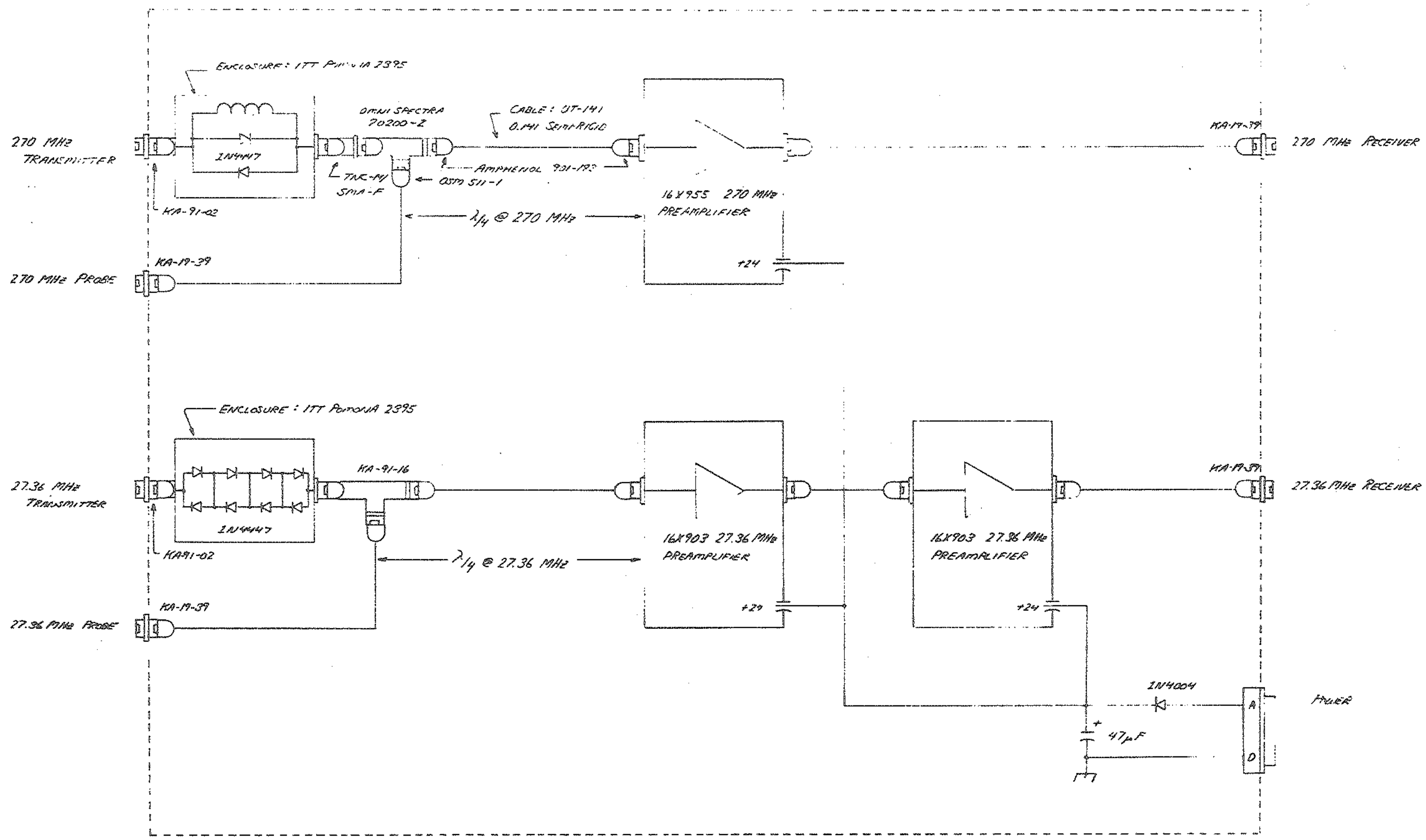

UNLESS SPECIFIED:
ALL CONNECTORS TNC KINGS KA-59-76 OR KA-59-57
ALL CABLE RG55 B/U LBL-SP

Title	27.36 / 270 MHz RECEIVER — T/R SWITCH
DESIGN BY	SHIH
DATE	6/12/79
CHKD. BY	
SCALE	
APPR.	
ENG.	W. SHIH
	LAWRENCE BERKELEY LABORATORY UNIVERSITY OF CALIFORNIA
	16X 9653

CHG. LTR. | DESIGN BY | CHECKED BY | DATE | CHANGES

2.5.13 16X966 67.89 MHz / 109.30 MHz Dual Frequency Receiver T/R Switch

The 16X966 dual frequency T/R switch assembly operates at 67.89 MHz for ^{13}C and at 109.30 MHz for ^{31}P observe. The unit serves three principal functions:

- Front-end Rf amplification -- The two preamplifiers in this unit are the first gain stages encountered by ^{13}C and ^{31}P signals. They provide approximately 30 - 36 dB of gain, and the outputs are fed to the 10X210 8 - 270 MHz to 30 MHz Linear Converter for conversion to the 30 MHz intermediate frequency. Since they are the first gain stages, noise performance is crucial.
- T/R switching -- When the transmitter produces a high power pulse, the unit protects the sensitive front-end receivers. After the pulse, the unit switches to the receive mode.
- Transmitter noise suppression -- Even when the transmitter is gated off, it has a high noise temperature. The 16X966 unit effectively isolates this noise source from the receivers, leading to minimal degradation in system noise performance.

Design Summary

A. 67.89 MHz Section

The 67.89 MHz section uses an RHG ICFT7030 thin-film hybrid preamplifier, protected by passive quarter-wave line switches. For this operating frequency, it was found that additional quarter-wave line sections were necessary for good noise performance (see Figure 2.63).

In the transmit mode, the two quarter wave sections that are terminated with diode pairs will have the diodes turned on, therefore they will look like open circuits $\lambda/4$ away from the diodes. In the receive mode, the diodes will be off; therefore the quarter-wave section closest to the transmitter will look like a short. This sets a boundary condition and forces the transmitter leg of the lower tee to look like an open circuit.

B. 109.30 MHz Section

The 109.30 MHz section uses an RHG ICFT12040 thin-film hybrid preamplifier, with a conventional quarter-wave/diode switching arrangement. It was found that a large number of isolated diode pairs was necessary for the transmitter switch.

Figure 2.63 67.89 MHz / 109.30 MHz Receiver - T/R Switch [16X9663]

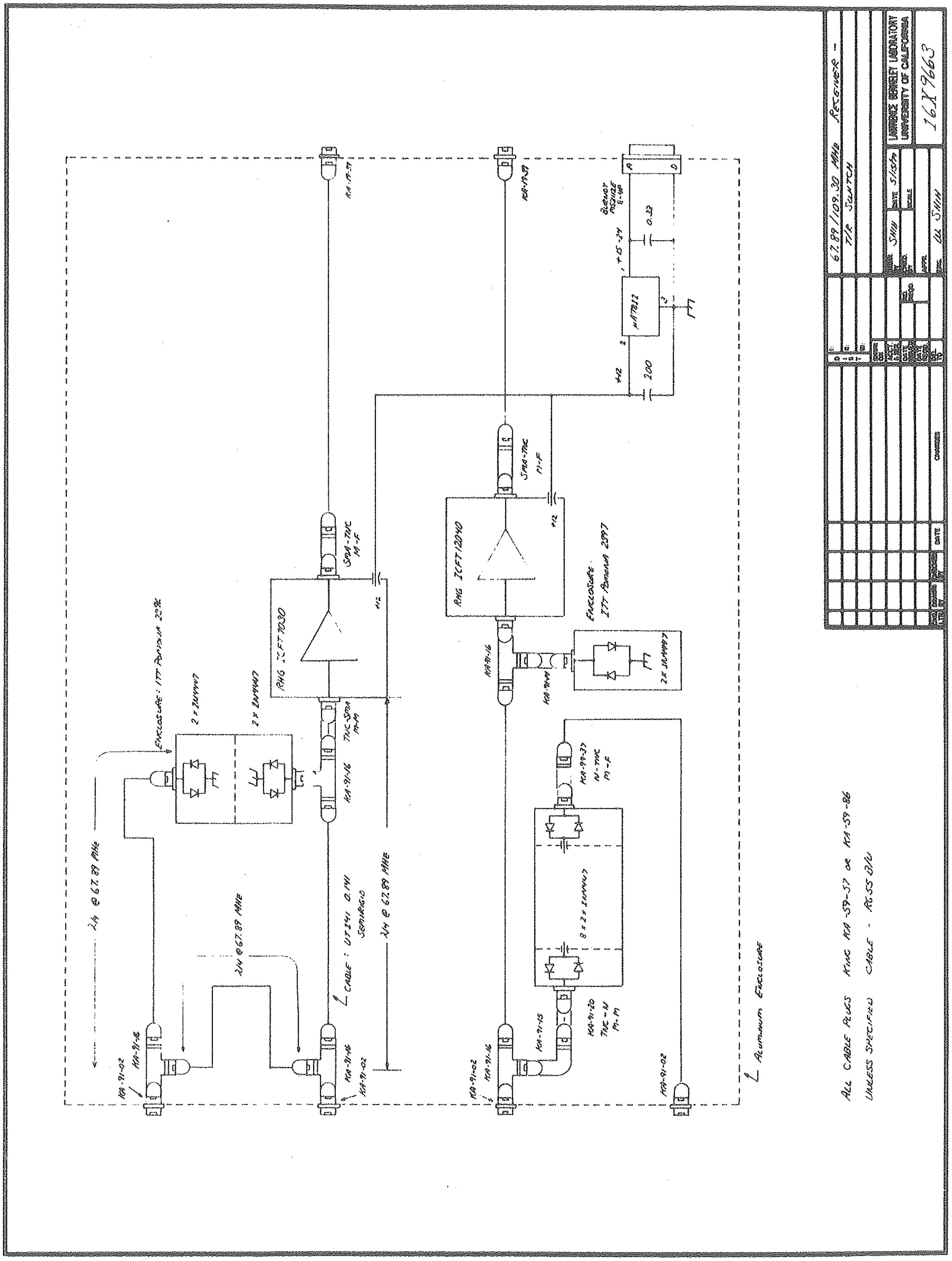
LAWRENCE BERKELEY LABORATORY
UNIVERSITY OF CALIFORNIA
16X9663

2.5.14 Diablo 31 Disk Memory Subsystem -- Power Supply Interconnect

Three Diablo 31 series 2315 type cartridge disk memory subsystems are presently installed on the Nicolet 1180 Data System. Drive unit 0 is powered by a Diablo Model 029 8 amp ± 15 VDC supply; drives 1 and 2 are powered by the supply arrangement shown in Figure 2.64. Because the Dynage 700 KHD series supplies are not as high in current capability as the Diablo 029, capacitor bank buffers are provided. These are attached by very short cables to the drive rear panels.

2.5.15 Rf Power Amplifiers -- Power Supply Interconnect

The 10X224 and 10X229 high power pulse amplifiers are powered by modified Universal Voltronics BRE-3-1000-LRL-1 3 KV 1 A high voltage power supplies. These supplies are buffered by 10X227 Capacitor Banks to minimize pulse droop during long pulses. Upon turn on, the current surge required to charge the capacitor banks would normally trip the current overload shutdown sensor, therefore the supplies were modified to include a time-delayed turn on shunt. Interconnections are shown in Figure 2.65

2.5.16 16X973 Rf Switch

The 16X973 Rf Switch is a relay actuated DPDT Rf switch employing Teledyne 712TN5 miniature Rf relays. The circuit layout is shown in Figure 2.66. The relay is mounted on 0.125 G-10 fiberglass-epoxy circuit board (double-sided), and connections to front panel switch inputs are via 50 ohm microstrip. The double-sided board layout is shown in Figures 2.67 and 2.68

2.5.17 16X974 Preamplifier Power Supply

The 16X974 Preamplifier Power Supply has four switched outputs that may be used to power the 16X964 - 16X965 - 16X966 receiver - T/R switch assemblies. The unit contains two Powermate UNI-88 DC supplies set to provide + 24 VDC and + 15 VDC. Two 15,000 μfd capacitors are used to provide high quality output filtering. Circuit details are shown in Figure 2.69.

2.5.18 16X978 41.45 MHz Amplifier

The 16X978 41.45 MHz Rf Amplifier is used to provide 0 - 80 dB adjustable Rf gain over a 5 MHz bandwidth centered at 41 MHz. The unit is used as part of the ^{2}H internal locking system, providing adjustable Rf gain prior to frequency conversion to the 30 MHz IF.

Circuit details are shown in Figure 2.70. The unit incorporates and RHG EVT40AJ66 amplifier. Gain is regulated by controlling voltage supplied to the AGC input. A trailing Wavetek 5070 0 - 70 dB step attenuator is used to adjust the output level.

2.5.19 16X980 Rf Switch

The 16X980 Rf Switch is a general purpose, fast, high isolation Rf switch unit. The switching element is a Watkins-Johnson/Relcom S1 switch; a drive circuit is provided that accepts TTL level control signals. Circuit details are shown in Figure 2.71.

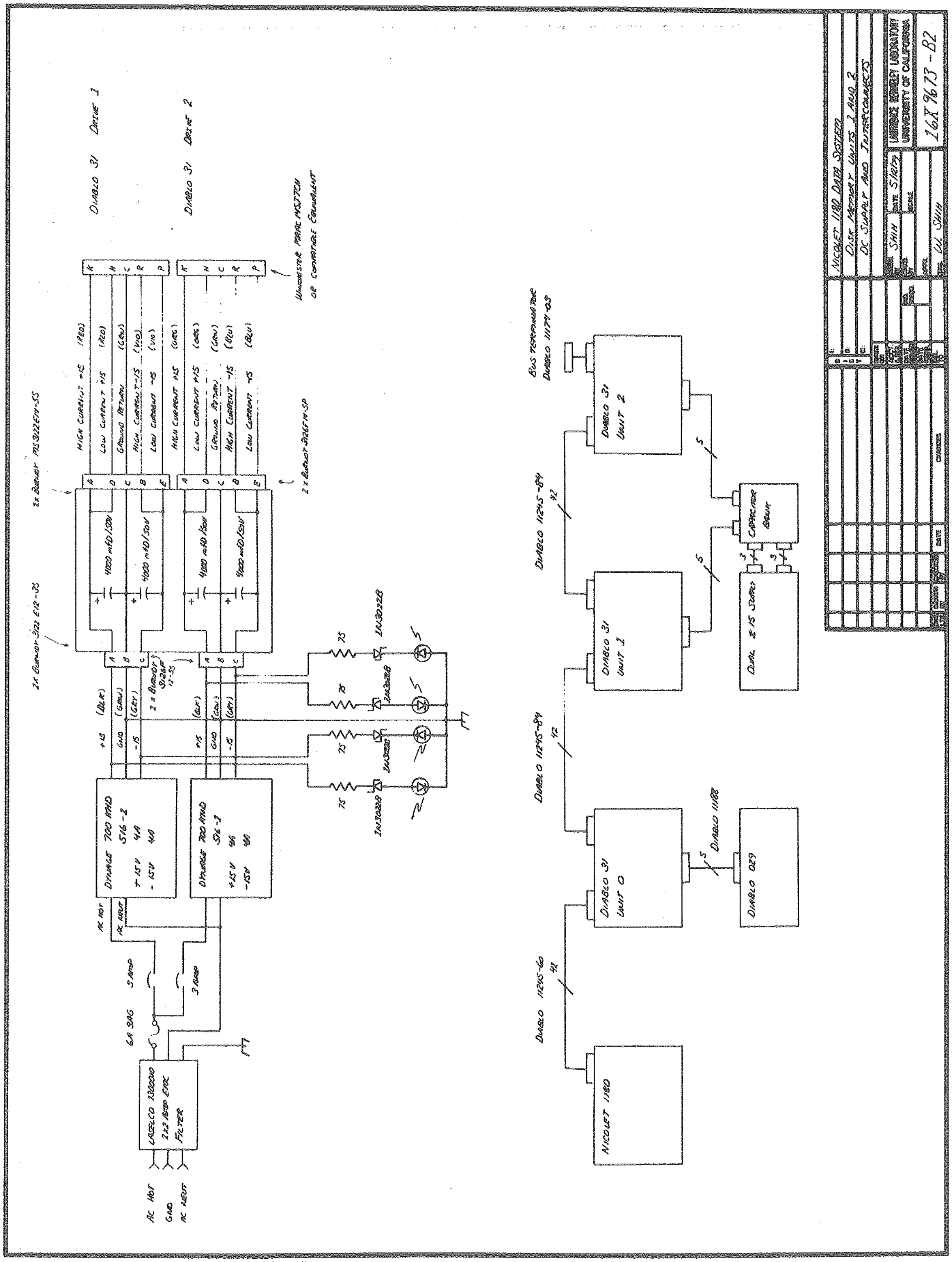

NICOLET 1180 DATA SYSTEM
DISK MEMORY UNITS 1 AND 2
DC SUPPLY AND INTERCONNECTS
SHIH
DATE 5/18/79
W. SHIH
LAWRENCE BERKELEY LABORATORY
UNIVERSITY OF CALIFORNIA
16X9673-B2
DIABLO 31 DRIVE 1
DIABLO 31 DRIVE 2
NICOLET 1180
DIABLO 31 UNIT 0
DIABLO 31 UNIT 1
DIABLO 31 UNIT 2
DIABLO D29
CAPACITOR BANK
DUAL ±15 SUPPLY

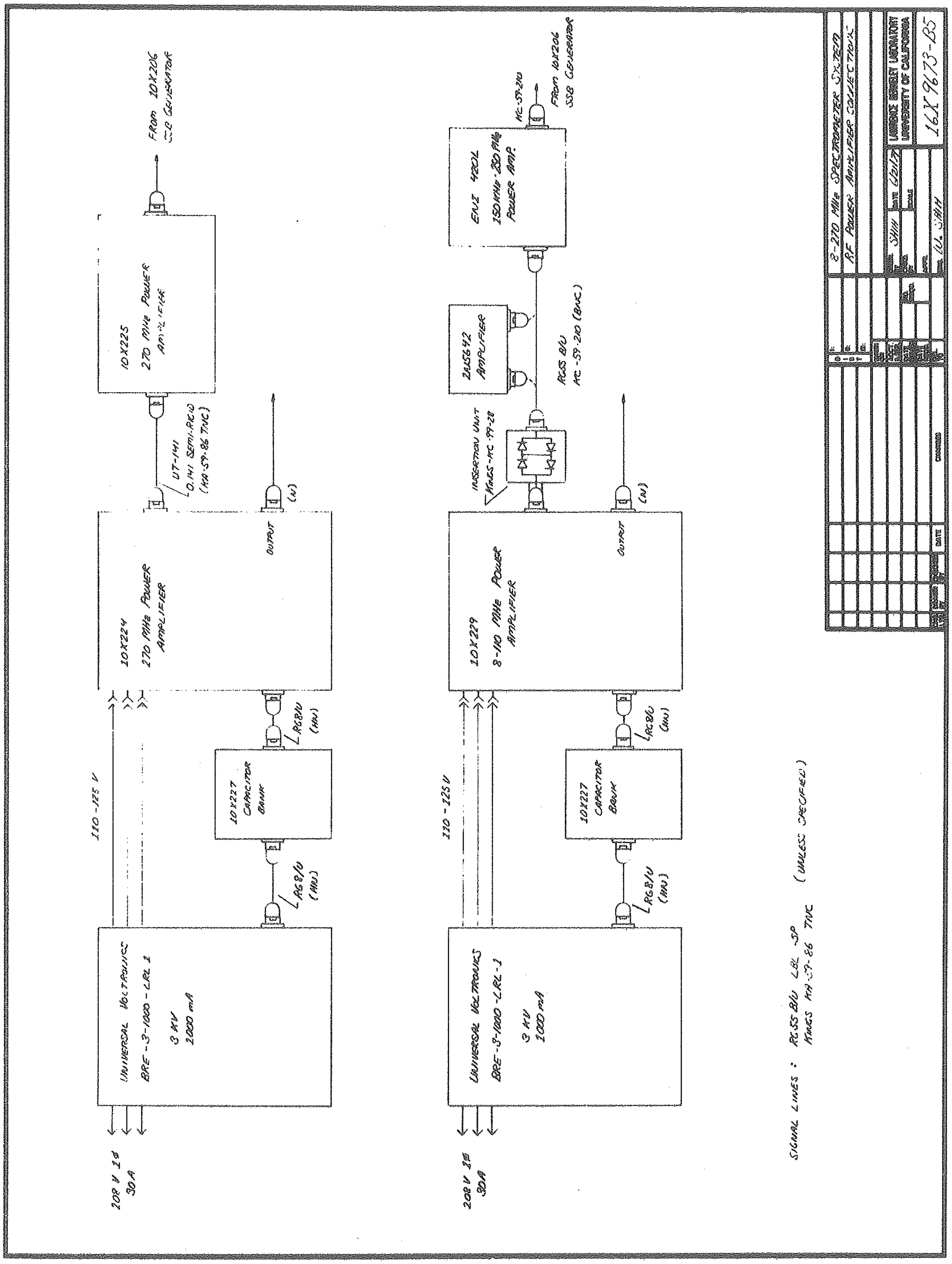
FROM 10X206 SSB GENERATOR
10X225 270 MHz POWER AMPLIFIER
UT-141 0.141 SEMI-RIGID (MA-59-86 TNC)
10X224 270 MHz POWER AMPLIFIER
OUTPUT
(N)
110-125 V
10X227 CAPACITOR BANK
RG8/U (HN)
UNIVERSAL VOLTRONICS BRE-3-1000-LRL-1 3 KV 1000 mA
208 V 1Φ 30A
ENI 420L 150 kHz-250 MHz POWER AMP.
2N5642 AMPLIFIER
RG55 B/U
INSERTION UNIT
10X229 8-110 MHz POWER AMPLIFIER
SIGNAL LINES : RG55 B/U LBL-SP
(UNLESS SPECIFIED)
8-270 MHz SPECTROMETER SYSTEM
RF POWER AMPLIFIER CONNECTION
LAWRENCE BERKELEY LABORATORY
UNIVERSITY OF CALIFORNIA
16X9673-B5
W. SHIH

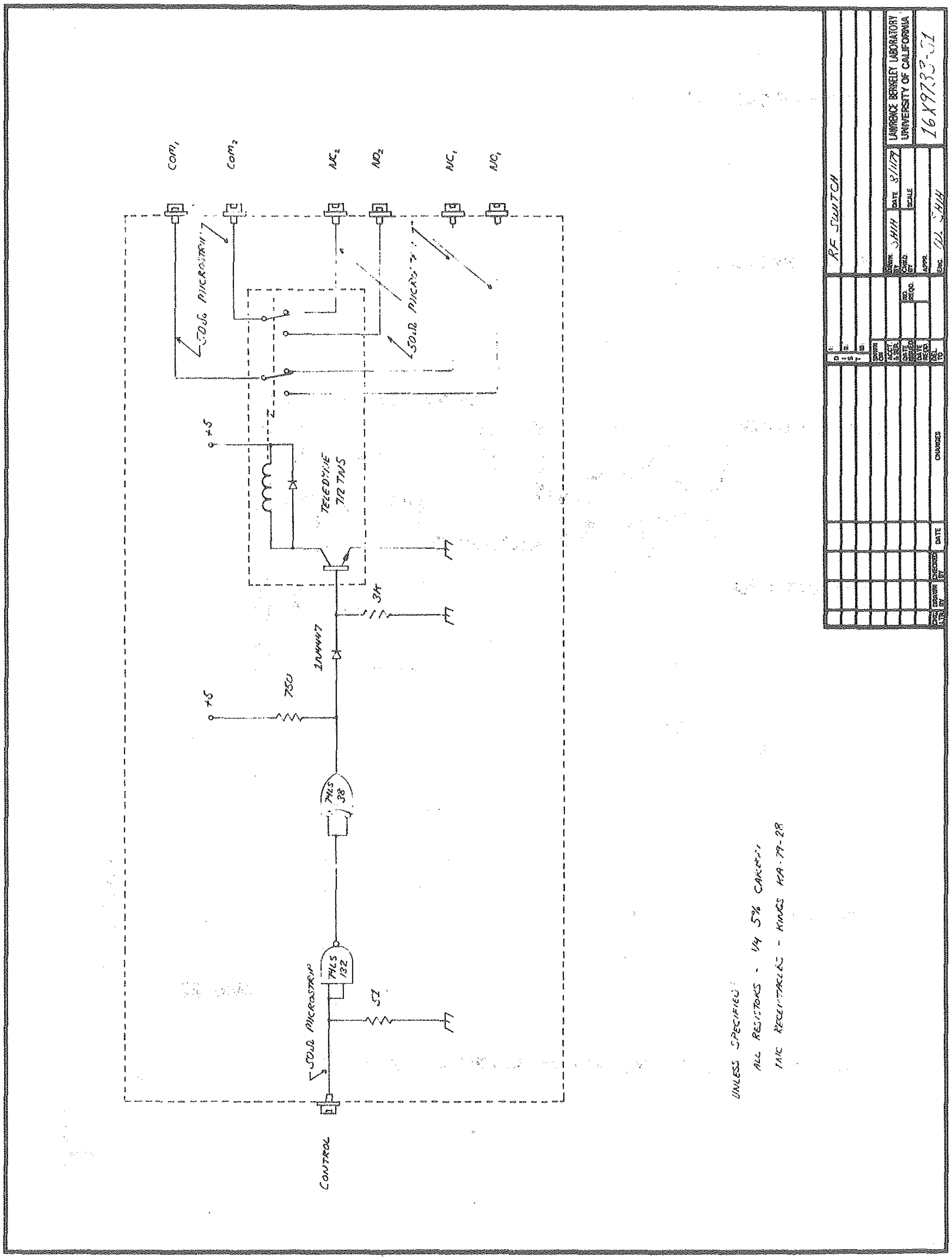
COM1
COM2
NC2
NO2
NC1
NO1
50Ω MICROSTRIP
TELEDYNE 712 TN5
+5
750
1N4447
3K
74LS 38
74LS 132
51
CONTROL
UNLESS SPECIFIED
ALL RESISTORS - 1/4 5% CARBON
RF SWITCH
SHIH
LAWRENCE BERKELEY LABORATORY
UNIVERSITY OF CALIFORNIA

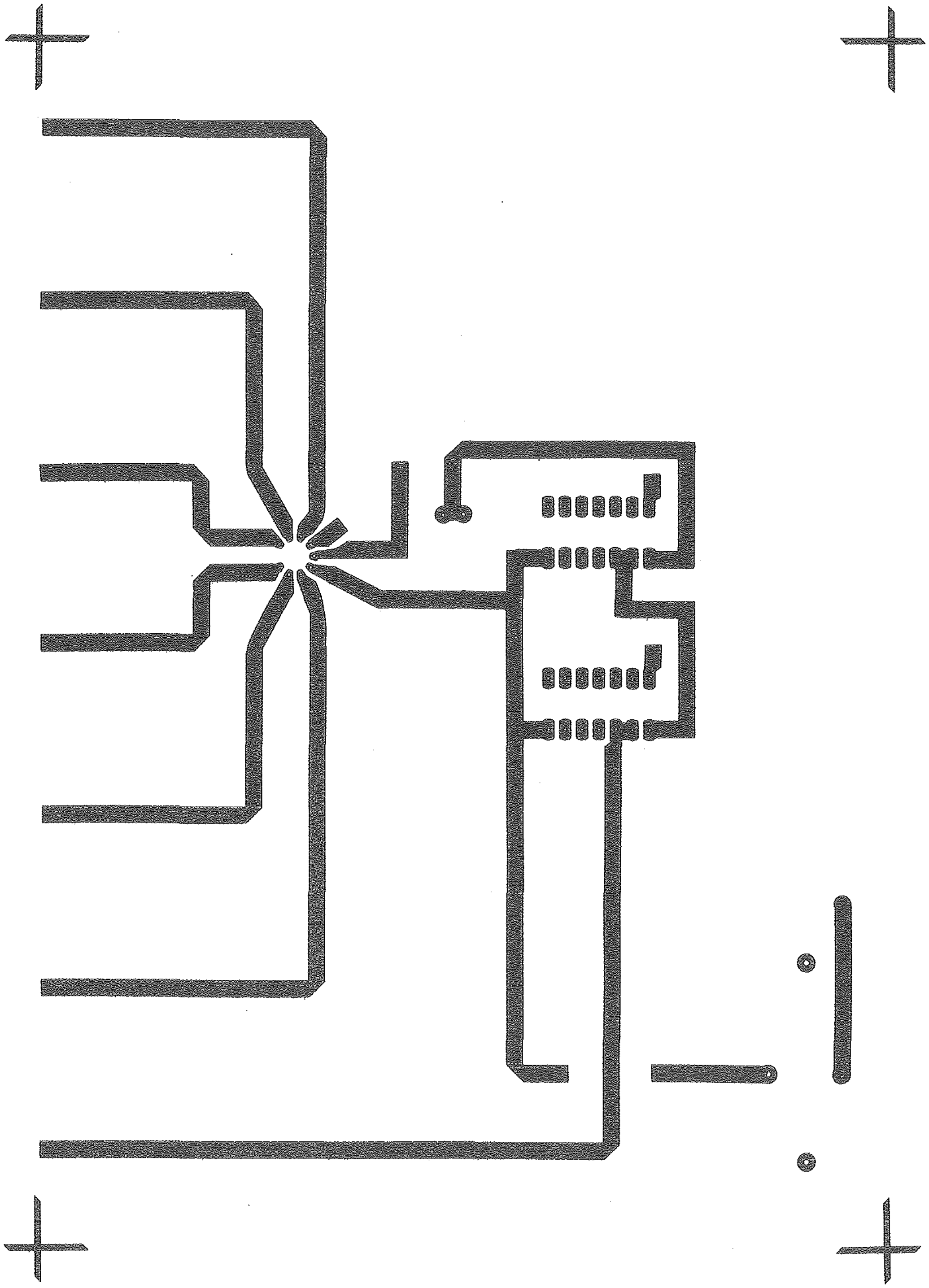

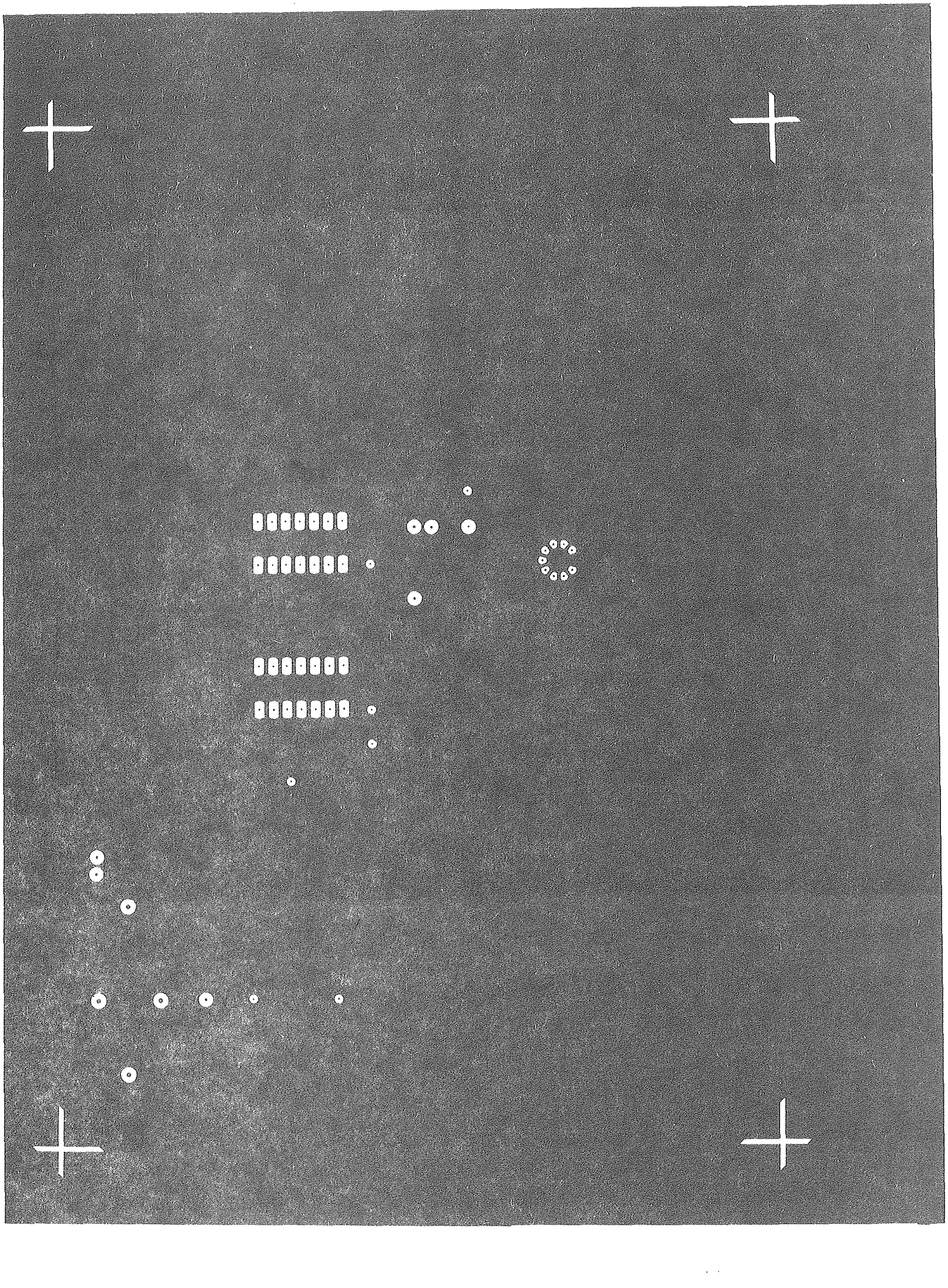

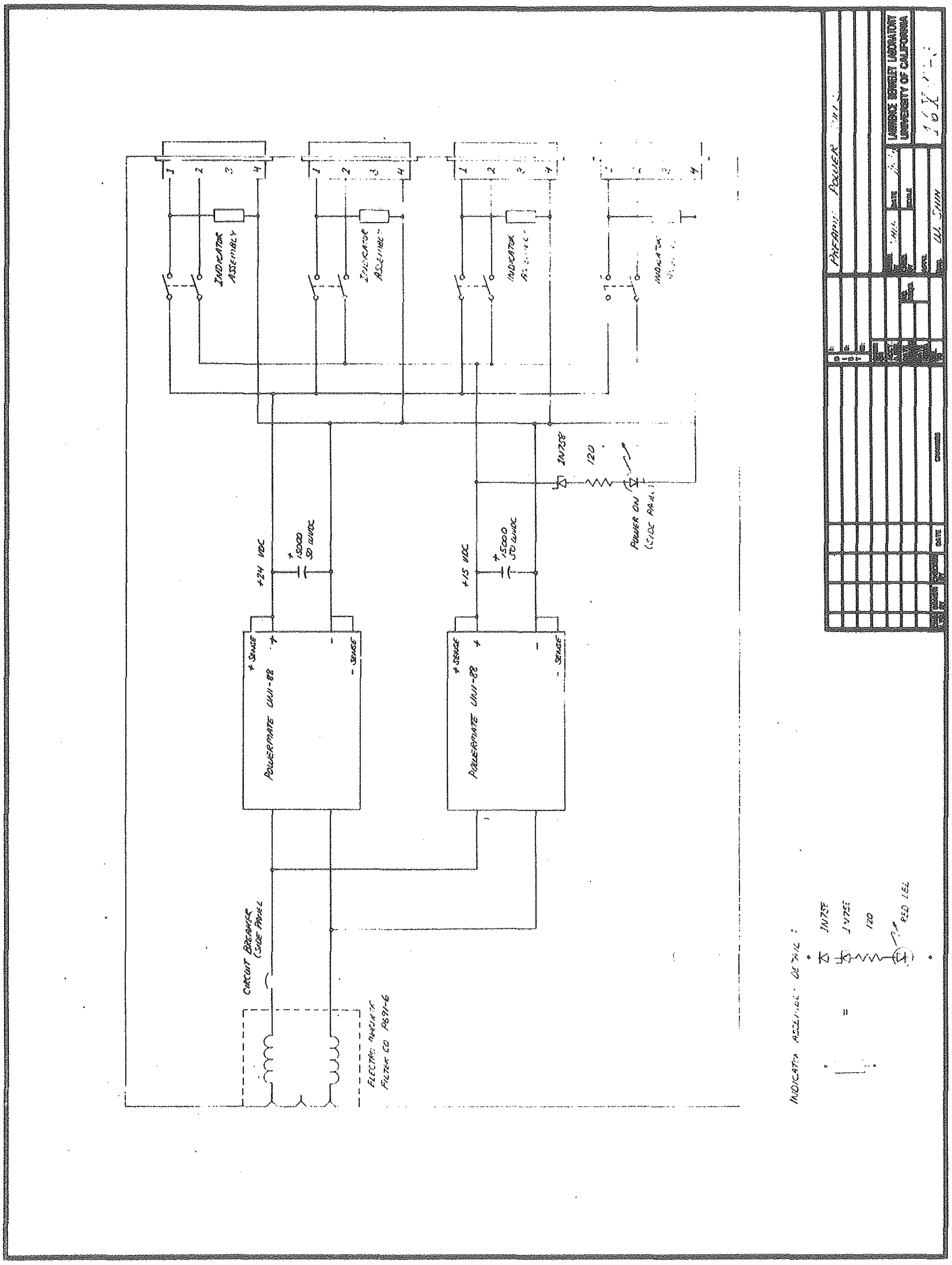
LAWRENCE BERKELEY LABORATORY
UNIVERSITY OF CALIFORNIA
PREAMP POWER
POWERMATE UNI-88
+ SENSE
- SENSE
+24 VDC
+15 VDC
INDICATOR ASSEMBLY
CIRCUIT BREAKER (SIDE PANEL)
POWER ON (SIDE PANEL)
1N758
120
RED LED

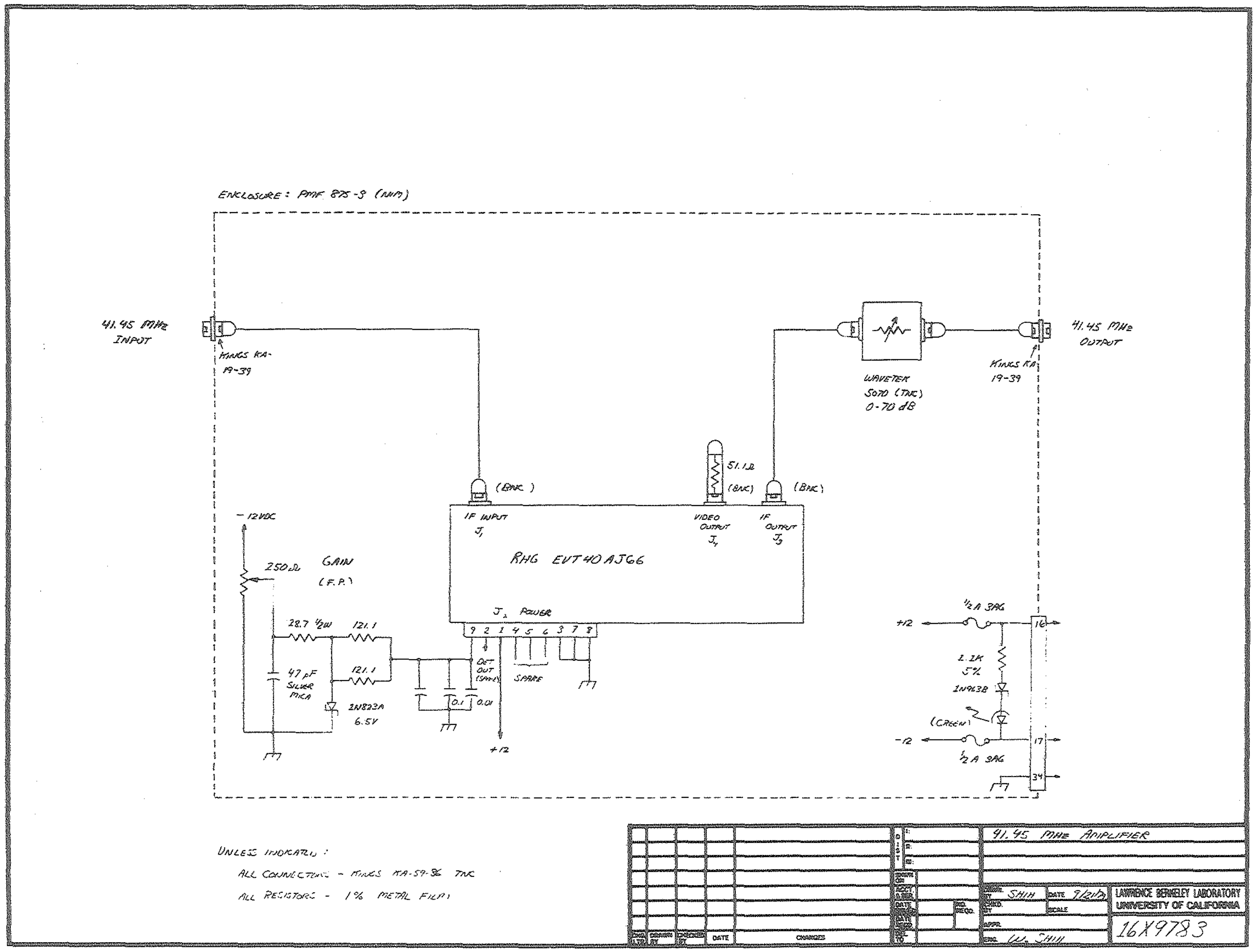

ENCLOSURE: PMF 875-3 (NM)
41.45 MHz INPUT
KINGS KA-19-39
41.45 MHz OUTPUT
KINGS KA 19-39
WAVETEK 5070 (TNC) 0-70 dB
51.1Ω
(BNC)
IF INPUT J1
VIDEO OUTPUT J4
IF OUTPUT J3
RHG EVT40AJ66
J2 POWER
9 2 1 4 5 6 3 7 8
DET OUT
SPARE
-12VDC
250Ω
GAIN (F.P.)
28.7 ½W
121.1
121.1
47 pF SILVER MICA
1N823A 6.5V
0.1
0.01
+12
½A 3AG
+12
2.2K 5%
1N9 63B
(GREEN)
-12
½A 3AG
16
17
34
UNLESS INDICATED:
ALL CONNECTORS - KINGS KA-59-36 TNC
ALL RESISTORS - 1% METAL FILM
41.45 MHz AMPLIFIER
SHIH
LAWRENCE BERKELEY LABORATORY
UNIVERSITY OF CALIFORNIA
16X9783

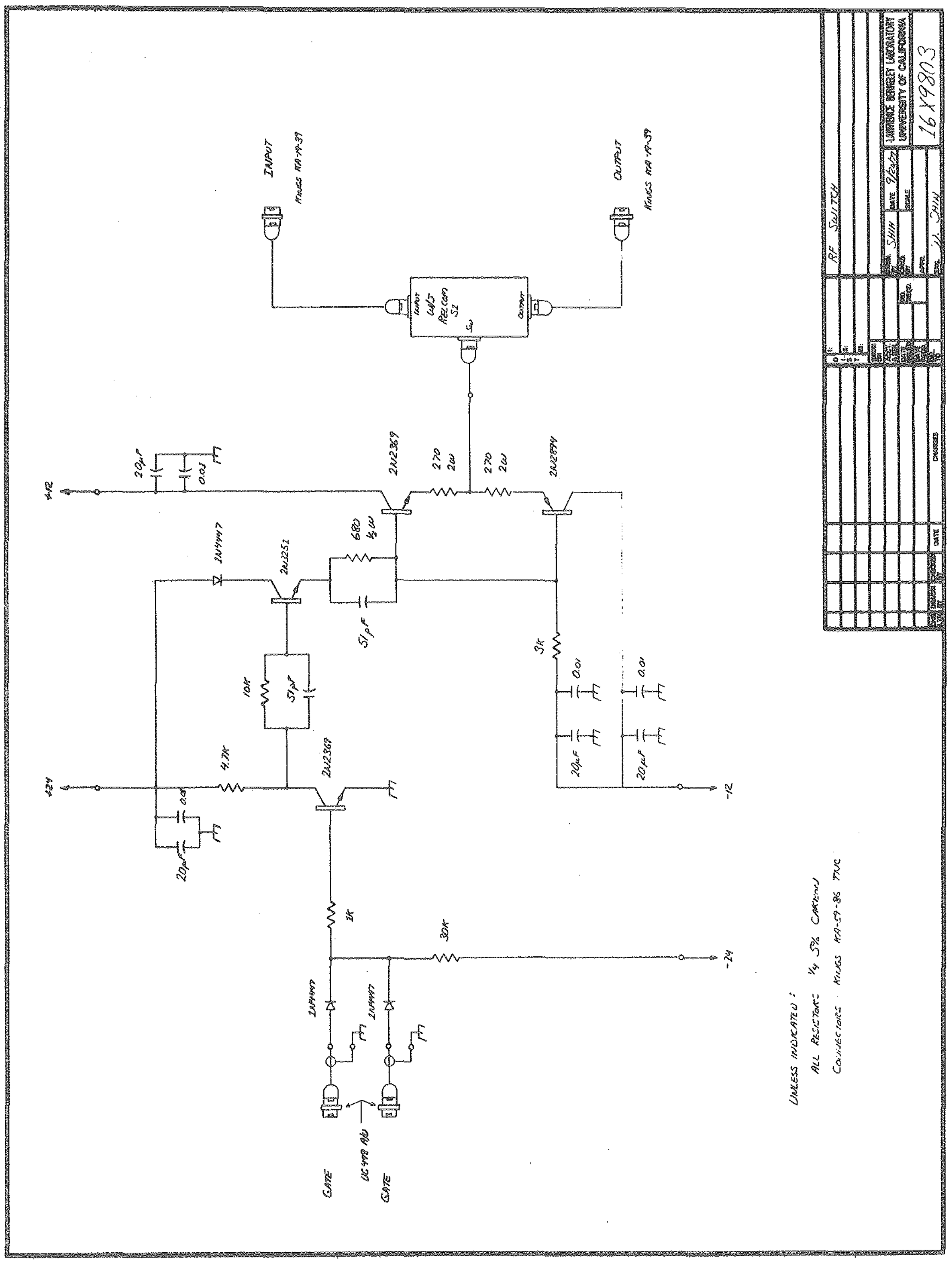

RF SWITCH
LAWRENCE BERKELEY LABORATORY
UNIVERSITY OF CALIFORNIA
16X9803
SHIH
INPUT
OUTPUT
+12
+24
-12
-24
2N2369
2N2894
270
2W
680
1/2W
51pF
10K
4.7K
3K
1K
30K
20μF
0.01
GATE
UNLESS INDICATED:
ALL RESISTORS 1/4 5% CARBON

2.5.20 Data Processor Power Fail Interlock

The 16X981 Data Processor Power Fail Interlock employs a General Electric CR205 high power magnetic contactor to switch system AC power to the 10X225 270 MHz Rf Amplifier, the ENI 420L Rf Power Amplifier, and the programmable power supply used to heat the variable temperature gas. The unit(s) are controlled by attachment to the switched AC line of the 1180 Data System. The units protect the system probes from burn out resulting from sudden CW operation of the transmitters, or from full power heating by the programmable power supply. Such conditions may arise if the 1180 Data System is shut down, leaving system control logic in indefinite states.

Figure 2.72 Data Processor Power Fail Interlock
[16X9813]

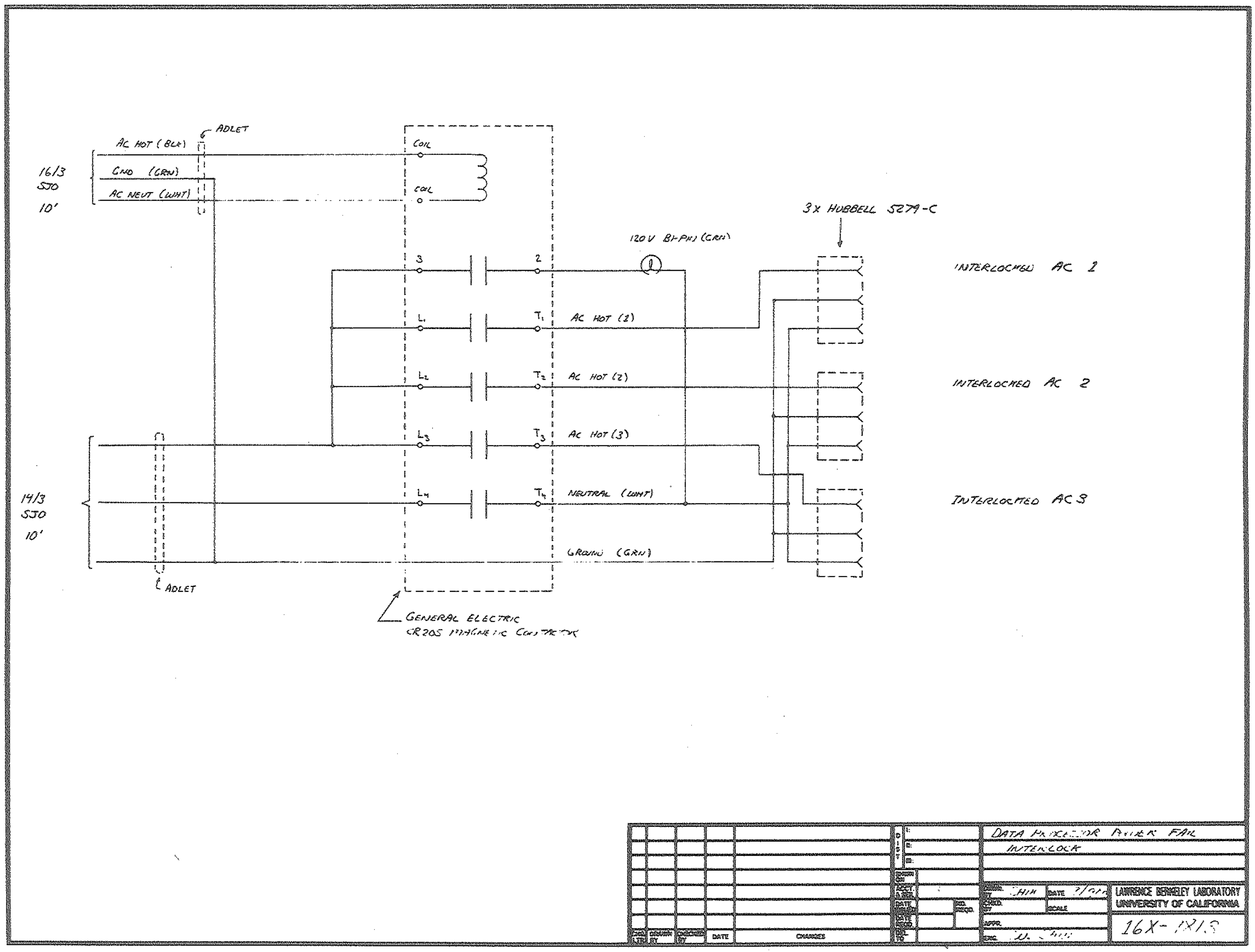

ADLET
AC HOT (BLK)
GND (GRN)
AC NEUT (WHT)
16/3
SJO
10'
COIL
COIL
3
2
L1
T1
L2
T2
L3
T3
L4
T4
120V BYPASS (GRN)
AC HOT (1)
AC HOT (2)
AC HOT (3)
NEUTRAL (WHT)
GROUND (GRN)
14/3
SJO
10'
ADLET
GENERAL ELECTRIC
CR205 MAGNETIC CONTACTOR
3X HUBBELL 5279-C
INTERLOCKED AC 1
INTERLOCKED AC 2
INTERLOCKED AC 3
INTERLOCK
CHG. LTR.
DRAWN BY
CHECKED BY
DATE
CHANGES
DIST
APPR.
ENG.
SCALE
LAWRENCE BERKELEY LABORATORY
UNIVERSITY OF CALIFORNIA
16X-1X13

319

2.6 References

1. J.D. Ellet, Jr., M.G. Gibby, U. Haeberlen, L.M. Huber, M.Mehring, A. Pines, and J.S. Waugh, *Adv. Mag. Res.*, 5, 117 (1971)

2. D.J. Sakrison, "Communication Theory: Transmission of Waveforms and Digital Information," John Wiley & Sons, Inc., New York, NY, 1968

3. R.E. Ziemer and W.H. Tranter, "Principles of Communications," Houghton Mifflin Co., Boston, MA, 1976

4. T.C. Farrar and E.D. Becker, "Pulse and Fourier Transform NMR," Academic Press, New York, NY, 1971

5. M.E. Stoll, A.J. Vega, and R.W. Vaughan, *Rev. Sci. Instrum.*, 48, 800 (1977)

6. I.J. Lowe and C.E. Tarr, *J. Phys. E, Ser. 2*, 1, 320 (1968)

7. I.J. Lowe and M. Eisenberg, *Rev. Sci. Instrum.*, 45, 1159 (1974)

8. K.E. Kisman and R.L. Armstrong, *Rev. Sci. Instrum.*, 45, 1159 (1974)

9. P.D. Murphy and B.C. Gerstein, "Analysis and Computerized Design of NMR Probe Circuits," U.S.D.O.E. Report IS-4436, Ames, Iowa, 1978

10. E. Schwartz, *IEEE Trans. Microwave Theory and Techniques* , MTT-16, 158 (1968)

11. R.M. Fano, *J. Franklin Inst.*, 249, 57 (1950)

12. R.M. Fano, *J. Franklin Inst.*, 249, 139 (1950)

13. D.C. Youla, *IEEE Trans. Circuit Theory*, CT-11, 30 (1964)

14. D.I. Hoult and R.E. Richards, *J. Mag. Resonance*, 24,71 (1976)

15. R.H. Lyddane and A.E. Ruark, *Rev. Sci. Instrum*,10, 253 (1939)

16. W. Franzen, *Rev. Sci. Instrum.*, 33, 933 (1962)

17. W.J.C. Grant and M.W.P. Strandberg, *Rev. Sci. Instrum.*,36, 343 (1965)

18. Service Manual for NIC-1180 Data System, Nicolet Instrument Corp., 1976

19. A. Abragam, "The Principles of Nuclear Magnetism," London, Oxford University Press, 1961, p. 83

20. H.D.W. Hill and R.E. Richards, *J. Phys. E, Ser. 2*, 1, 977 (1968)

APPENDIX 1 Nicolet 1180 / VAX 11/780 Data Transmission Protocol

A1.1 Introduction

The 8 - 270 MHz spectrometer system may be connected via the 1180 data system to two other data processors: the Nicolet NIC-80 attached to the LCB 220 MHz ^1H pulsed Fourier Transform system, or to a Digital Equipment Corporation VAX 11/780. Both connections are implemented with standard RS232 serial links, the former at data rates up to 38.4 Kbaud, and the latter at data rates up to 9600 baud. The purposes of the 1180/VAX connection are:

- Archival storage of data on magnetic tape. The 1180 data system uses IBM 2315 type 2200 bpi 3.0 Mbyte disks for mass storage, which are not ideal for archival storage purposes.
- Data files stored on the VAX are readily manipulated using FORTRAN language routines. Of particular value is the use of FORTRAN display processing routines for 2D NMR data.
- Data files may be readily reformatted on the VAX, making them transportable to other systems for use with foreign analysis and display processing routines (such as the Surface Display Library at the Berkeley CDC 6400 facility).

The current data transmission protocol does not conform to the standards of the CAL Data Acquisition Facility (CALDAF) being implemented on the LCB VAX. The particular approach was chosen because of the speed with which it could be implemented.

A1.2 Data Transmission Protocol

.1 1180 Memory Organization and Interrupt Structure

The 1180 system presently includes 24K × 20 bits of non-ECC memory. Programs are generally written to occupy locations 00000_8 - 17777_8, and data is usually acquired into or processed in the balance (20000_8 - 57777_8). Reserved locations are summarized in Table A1.1.

Memory locations below 400_8 are reserved for DEXTER/2 disk monitor functions. The NTCFT-1180 program package supplied by Nicolet Technology Corp. is the normal resident program. This package consists of a main program (NTCFT) occupying locations 400_8 - 12637_8, an overlay file (NTCFT.OVL) containing 16 blocks of command processing routines that are selected after a command table look-up, and various external routines for spectrum simulation, etc. Overlays are loaded into locations 12640_8 - 16477_8; locations 16500_8 - 17777_8 are used as a scratch area.

VAX data transmission routines are written as part of the USR overlay. They were composed as .ASC (ASCII text) files using the DEDIT disk-based text editor, then assembled using the FASM Fast 1180 Assembler. Stored as a .BIN file (USROVL.BIN), the routines are incorporated into NTCFT via the P↑A command (load overlay). The FASM assembled listing is appended to the end of this section.

.2 1180 Interrupt Structure

The 1180 has a seven-level vectored priority interrupt structure. Interrupt lines are wired-or bus lines (refer to print 16X904) that are asserted by grounding at any point along the bus. The interrupt vector addresses and devices associated with each priority level are summarized in Table A1.2.

When an interrupt occurs, the processor completes the current instruction and then does an indirect subroutine jump through the interrupt vector address corresponding to the priority of the interrupt. The address of a software interrupt service routine must be pointed to by this address; upon performing the JMS, the return address is deposited at the start of the service routine for an indirect jump return upon completion.

Interrupt levels are enabled or disabled using the interrupt level mask register. Devices and levels are enabled only when program dictates require that they be used. When they are no longer needed, they are disabled immediately. The VAX data transmission routines use the Level 5 interrupt for the RS232 B Channel UART (Universal Asynchronous Receiver-Transmitter). Upon entering the routine, Level 5 and the RS232B are enabled in the mask registers. On exiting, a check is done to see if data acquisition is in progress, because the 293A Programmable Pulser is also on Level 5. If data acquisition is in progress, only the RS232B bit is reset in the Slow I/O mask. If data acquisition is not in progress, both the RS232B and the Level 5 bits are reset.

NTCFT-1180 permits simultaneous execution of up to two background processes (plotting and data acquisition) and one foreground process (such as performing a FFT or phasing a spectrum). Data transmission is a foreground process because the serial RS232 format requires partitioning of data words into byte strings; interrupt driven processing would have been very difficult to implement within the framework of NTCFT-1180.

.3 Hardware Connections, VAX Configuration

Hardware connection of the 1180 to the VAX employs the RS232 standard (2 wire + ground). The 1180 connection is to the RS232 B Channel UART (an IM6402 CPD UART was substituted for the slower COM 2502 that was originally supplied, the former has a much higher baud capability); the VAX connection is to one of the ports on the terminal multiplexer. It does not matter which VAX port is connected, but the port number must be known.

Each terminal multiplexer port on the VAX has its own associated buffer space. Communications lines connected to the ports may operate in several modes:

1. HOSTSYNC -- the VAX synchronizes the flow of input into the terminal multiplexer buffer by issuing CTRL-Q to start the data stream or CTRL-S to stop. Default mode is NOHOSTSYNC.
2. TTSYNC -- Device attached to assigned terminal multiplexer port synchronizes output from VAX by issuing CTRL-Q to start data flow and CTRL-S to stop. Default mode is TTSYNC.

A VAX process may accept data from several sources:

1. Interactively, from the terminal that is controlling the process.
2. From a file stored on the system.

3. From an allocated external device attached to an assigned port.

VAX / 1180 data communications programs were written to accept data in the last mode, that is through an allocated port on the terminal multiplexer. This obviates the need to reconnect terminals and computers whenever such a process is to be run. Prior to running any of these programs, it is necessary to ALLOCATE the port, ASSIGN logical files to the port, and to set the port in HOSTSYNC mode. An example sequence that would configure port TTB6 correctly would be:

```
ALLOCATE TTB6 FOR001             /ALLOCATE TTB6, ASSIGN LOGICAL
                                 / NAME FOR001 TO IT
ASSIGN TTB6: FOR002              /ALSO ASSIGN THE LOGICAL NAME
                                 / FOR002 TO IT
SET TERM TTB6/HOSTSYNC           /SET HOSTSYNC CONTROL
```

.4 Data Format

The VAX interprets the input byte stream in terms of ASCII characters and control signals. Because the bit patterns of the 1180 data are random, it is entirely possible that certain data bytes would be misinterpreted as control characters, thereby causing undesired VAX actions. To avoid this possibility, the 1180 segments each 20 bit word into four 5 bit strings, which are then transmitted in an unpacked format with a leading 001. Thus each byte has the format 001XXXXX, where X represents a data bit. The VAX FORTRAN programs FILECOPY and ARRAY then repack each string of four bytes into a 20 bit word, and they then write these to files as 32 bit integers. The ASCII equivalents of 0010 0000 through 0011 0000 do not include any control characters.

Alternatively, the VAX terminal multiplexer port could be set to PASSALL mode, which would permit the input of byte strings without interpretation. This mode is considered dangerous, however, because its use requires I/O priviledges.

.5 Timing

When data transmission is running under HOSTSYNC control, the VAX interrupts the 1180 whenever the terminal multiplexer buffer is full and it is desired to stop transmission. Similarly when the buffer can accept more bytes, the 1180 is interrupted. Data transmission on the 1180 is a foreground process; the flag CTRLCH is inspected prior to any four byte transmission. This flag is set under interrupt control by the VAX control signals. Timing is well illustrated by the flow chart of Figure A1.1.

An 1180 assembly language listing for the data transmission routine, and a VAX FORTRAN IV PLUS listing of the routines FILECOPY and ARRAY are appended to the end of this section.

.6 1180/NIC-80 Data Transmission

The 1180/NIC-80 data link was used to support data storage for the NIC-80, which had no mass storage peripheral. The link was set to operate at 38.4 Kbaud to a NIC-80 modified per drawing 16X943. The 1180 data transmission routine listing is appended to the end of this section.

Table A1.1 1180 Data System -- Resident Monitor Reserved Memory Locations

OCTAL LOCATION	*CONTENTS*
0	JMP to 112, Keyboard Monitor Restart
1-7	Levels 0 - 6 Interrupt Vectors
10	Reserved for DBUG11, NICBUG
11	Software copy of interrupt level enable mask
12	Software copy of slow I/O device enable mask
13	Pointer to overlay exit routine
14	MONR subroutine
17	PUSH subroutine
22	POP subroutine
25	OVRLD overlay loader
30	RDISK disk read service routine
32	WDISK write disk subroutine
34-377	Miscellaneous monitor functions
360007	Paper tape binary loader for high speed reader
360010	Paper tape binary loader for low speed reader
360114	Disk monitor cold start from sector 0, disk drive unit 0
360112	Disk monitor backup bootstrap from sector 6250, disk drive unit 0

Table A1.2 Interrupt Vector Addresses and Device Priority Level Assignment -- Nicolet 1180 Data System

LEVEL	*ADDRESS*	*ASSIGNED DEVICES*
0	1	ADC - in 256 word mode
1	2	ADC - end of sweep
2	3	Clock 1 - general purpose
3	4	Disk
4	5	Clock 2 - Display
5	6	RS232 - B Channel UART, 293A Programmable Pulser
6	7	RS232 - A Channel UART, High speed paper tape reader/punch, 16X950 Variable Temperature Controller

Figure A1.1 Assembled Listing of USR Overlay to NTCFT-1180 for Data Transmission to VAX 11/780

```
 RUN FASM

FASM, E58-90215
@USROVL.ASC/USROVL.BIN,-TT:F




        FAST 1180 ASSEMBLER, E58-90215

        08/24/79 16:16    @USROVL.ASC/USROVL.BIN,-TT:F

        200 SOURCE STATEMENTS
        38 USER-DEFINED SYMBOLS
        MEMORY NEEDED: 4751 TO 16343
```

/USER OVERLAY TO NTCFT V#90615

```
/USER OVERLAY TO NTCFT V#90615
/
.UNDENT
/
/A90823          WILLY C. SHIH
/
/       23 AUGUST 1979
/
/       U1 =>DATA TRANSMISSION TO VAX11/780 VIA TERMINAL
/               MULTIPLEXER.  TERMINAL MULTIPLEXER PORT SHOULD
/               BE SET AS FOLLOWS:
/
/               ALLOCATE TTB6 FOR001
/                       (ASSIGNS PORT TTB6 TO FORTRAN LOGICAL UNIT 001)
/               ALLOCATE TTB6 FOR002
/                       (ASSIGNS PORT TTB6 TO FORTRAN LOGICAL UNIT 002)
/               SET TERM TTB6/HOSTSYNC
/                       (TERMINAL MUX CONTROLS TRANSMISSION)
/               SET TERM TTB6/SPEED=(9600,9600)
/                       (9600 BAUD TRANSMISSION)
/
/
/
/       U1 WILL TRANSMIT THE DISPLAYED AREA, USE THE FS COMMAND
/               TO SET TO A PARTICULAR NUMBER OF POINTS.  U1
/               MAY BE USED IN A LINK FOR SENDING SETS OF FILES
/
/       U2 =>SAME AS U1, EXCEPT WITH ACCOMPANYING PARAMETER TABLE
/               (LOCATIONS 640-1377, 430 OCTAL WORDS)
/
/
  466         DSPSIZ=466              /SIZE OF DISPLAYED REGION
  467         DSPSTA=467              /START OF DISPLAYED REGION
   11         ZILMSK=11               /COPY OF INT LEVEL MASK
   12         SPDMSK=12               /COPY OF SLOW I/O MASK
10061         GADCHK=10061            /CHECK FOR AIP IN DISPLAY REGION
  564         GOFLAG=564              /ACQUISITION IN PROGRESS FLAG
 2301         ZDISPLA=2301            /DISPLAY MEMORY SUBROUTINE
 2533         ZUPKBUF=2533            /MESSAGE OUTPUT ROUTINE
 2627         ZWFCHAR=2627            /CHARACTER INPUT
 2636         ZTTYBUF=2636            /ZWFCHAR+ZACCBUF
  545         DIFLAG=545
10152         BRETRN=10152            /RETURN TO NTCFT INT5 SERVICE
/
/
/ADDITION TO INT5- SERVICE ROUTINE
10121         *10121
10121   44751         JPZ RSBINT      /JMP ON ZERO (i.e. 293A DID NOT
                                      /CAUSE INTERRUPT
 4751         *4751
 4751  644720 RSBINT, RSINF           /RS232B READY TO READ
 4752    4751         JMP *-1         /NO
 4753  600721         RSIN            /READ ONE BYTE
 4754  126021         SNQ (21         /VAX11 START CHAR = CTRL-Q (021)
```

/USER OVERLAY TO NTCFT V#90615

```
 4755 1403761          ZERM CTRLCH      /DEPOSIT 0 FLAG IF START RECEIVED
 4756  126023          SNQ (23          /VAX11 STOP CHAR = CTRL-S (023)
 4757 1471761          ONEM CTRLCH      /DEPOSIT 1 FLAG IF STOP RECEIVED
 4760   10152          JMP BRETRN       /RETURN
 4761       1 CTRLCH, 1
13000        *13000
/ROUTINE FOR UNPACKED DATA TRANSMISSION TO VAX 11 TERMINAL MUX
13000       0 VAXDMP, 0                 /BYTE FORMAT = 001XXXXX
13001 2010061          JMS GADCHK       /CHECK IF ACQ IN PROGRESS IN
                         /CURRENT DISPLAY AREA
13002 2002533          JMS ZUPKBUF      /WRITE MESSAGE
13003   13176            MSG1           /MESSAGE POINTER
13004 2002301          JMS ZDISPLA      /DISPLAY MEMORY ONCE
13005 1403172          ZERM CHKSUM      /ZERO CHECKSUM
13006 1216467          MEMA DSPSTA      /GET START OF DISPLAY REGION
13007 1413174          ACCM START       /  AND PUT IT IN START
13010 1216466          MEMA DSPSIZ      /GET SIZE OF DISPLAY REGION
13011 1413175          ACCM SIZE        /  AND PUT IT IN SIZE
13012 2013114          JMS INTENA       /ENABLE LVL5 INTERRUPTS
13013 2013065          JMS DUMP         /DUMP DISPLAYED REGION(CTRL-E)
13014 1217172          MEMA CHKSUM      /TRANSMIT CHECKSUM
13015 2013127          JMS VAXOUT       /CALL RS232B XMIT WORD ROUTINE
13016 1434545          MMOM DIFLAG      /REENABLE ^O,^X
13017 1217164          MEMA MASK3       /DISABLE RS232B IN SLOW I/O
13020 1462012          ANDM SPDMSK      /  MASK COPY AND MASK
13021  500761          LDMASK           /LOAD SLOW I/O DEVICE MASK
13022      12            SPDMSK
13023 2117171          MEMZ @ GFLAG     /ACQ IN PROGRESS
13024 1013000          JMP @VAXDMP      /RETURN WITHOUT DISABLING LVL5
                         /SINCE 293A IS ALSO ON LVL5
13025 1217165          MEMA MASK4       /OTHERWISE RESET INT5-
13026 1462011          ANDM ZILMSK      /STORE IN MASK COPY AND
13027  503771          LMASK            /LOAD INT LEVEL MASK
13030      11            ZILMSK
13031 1013000          JMP @VAXDMP      /NORMAL RETURN
/
/ROUTINE FOR UNPACKED DATA TRANSMISSION TO VAX11 TERMINAL MUX
/  WITH ACCOMPANYING PARAMETER TABLE
13032       0 LEADER, 0                 /PARM TABLE @ 640-1377 (430 WORDS)
13033 2010061          JMS GADCHK       /CHECK IF ACQ IN PROGRESS
13034 2002533          JMS ZUPKBUF      /WRITE MESSAGE
13035   13213            MSG2           /MESSAGE POINTER
13036 1403172          ZERM CHKSUM      /ZERO CHECKSUM
13037  216640          MEMA (640        /PARAMETER TABLE STARTS AT 640
13040 1413174          ACCM START       /PUT START ADDRESS IN START
13041  216540          MEMA (540        /PARM TABLE IS 540 WORDS (OCTAL)
13042 1413175          ACCM SIZE        /PUT IN SIZE
13043 2013114          JMS INTENA       /ENABLE LVL5 INTERRUPTS
13044 2013065          JMS DUMP         /OUTPUT PARAMETER TABLE
13045 2013075          JMS STATUS       /NOW GET SIZE OF DATA REGION
13046 2013065          JMS DUMP         /DUMP BUTTON REGISTER SELECTED AREA
13047 1217172          MEMA CHKSUM      /LOAD CHECKSUM
13050 2013127          JMS VAXOUT       /AND WRITE IT TO VAX ALSO
13051 1434545          MMOM DIFLAG      /REENABLE ^O,^X
```

/USER OVERLAY TO NTCFT V#90615

```
13052 1217164          MEMA MASK3      /DISABLE RS232B IN SLOW I/O MASK
13053 1462012          ANDM SPDMSK     /AND IT WITH MASK COPY
13054  500761          LDMASK          /LOAD SLOW I/O MASK AND COPY
13055      12            SPDMSK        /  MASK COPY POINTER
13056 2117171          MEMZ @ GFLAG    /ACQ IN PROGRESS?
13057 1013032          JMP @ LEADER    /IF YES, RETURN WITHOUT DISABLING INT5-
13060 1217165          MEMA MASK4      /OTHERWISE RESET INT5-
13061 1462011          ANDM ZILMSK     /AND IT WITH MASK COPY
13062  503771          LMASK           /LOAD INT LEVEL MASK
13063      11            ZILMSK        /  MASK COPY
13064 1013032          JMP @ LEADER    /NORMAL RETURN
13065       0 DUMP,    0               /OUTPUT A MEMORY REGION ROUTINE
13066 2217174 LOOP2,   MEMA @ START    /LOAD FIRST POINTED TO WORD (20 BITS)
13067 1421172          APMM CHKSUM     /ADD IT TO RUNNING CHECKSUM
13070 2013127          JMS VAXOUT      /CALL RS232B XMIT WORD ROUTINE
13071 1437174          MPOM START      /INCREMENT WORD POINTER
13072 1535175          MMOMZ SIZE      /DECREMENT SIZE POINTER
13073   13066          JMP LOOP2       /JMP IF NOT DONE
13074 1013065          JMP @ DUMP      /NORMAL RETURN
13075       0 STATUS,  0               /READ SIZE AND POSITION OF CURRENT
                /DISPLAY REGION FROM BUTTON REGISTER
13076 1217170          MEMA STADDR     /LOAD BASE ADDRESS
13077 1413174          ACCM START      /AND PUT IT IN START
13100  603640          RDBUTN          /READ BUTTONS
13101 1263166          ANDA MASK5      /SELECT START ADDRESS BITS
13102  250000          AMOA            /SEE IF ADDRESS IS ZERO
13103   53106          JPZ SETADR      /START ADDRESS IS ZERO
13104  246000          APOA            /ADD 1 BACK
13105  701007          LASH 7          /CONVERT TO OFFSET
13106 1421174 SETADR,  APMM START      /ADD TO BASE ADDRESS
13107  603640          RDBUTN          /READ BUTTONS AGAIN
13110 1263167          ANDA MASK6      /SELECT SIZE BITS
13111  716001          RISH 1          /CONVERT TO ABSOLUTE SIZE
13112 1413175          ACCM SIZE       /  AND STORE IT IN SIZE
13113 1013075          JMP @ STATUS    /NORMAL RETURN
13114       0 INTENA,  0               /ENABLE INT5- FOR RS232B ROUTINE
13115 1436545          MPOM DIFLAG     /DISABLE ^O,^X
13116  216004          MEMA (4         /LEVEL 5 DEVICE ENABLE
13117 1460012          AOMM SPDMSK     /LOAD COPY OF SLOW I/O MASK
13120  500761          LDMASK          /LOAD SLOW I/O MASK
13121      12            SPDMSK        /  MASK COPY
13122  216040          MEMA (40        /LVL5 ENABLE
13123 1460011          AOMM ZILMSK     /LOAD INT ENABLE MASK COPY
13124  503771          LMASK           /LOAD INT ENABLE MASK
13125      11            ZILMSK        /  MASK COPY
13126 1013114          JMP @ INTENA    /NORMAL RETURN
13127       0 VAXOUT,  0               /RS232B XMIT 20 BIT WORD ROUTINE
13130 1413173          ACCM TEMP       /STORE WORD IN TEMP
13131 2013152          JMS RSXMIT      /OUTPUT LOWEST 5 BITS
13132 1217173          MEMA TEMP       /RESTORE FULL WORD
13133  716005          RISH 5          /SHIFT 5
13134 2013152          JMS RSXMIT      /XMIT NEXT 5 BITS
13135 1217173          MEMA TEMP       /RESTORE FULL WORD
13136  716012          RISH 12         /SHIFT 10
```

/USER OVERLAY TO NTCFT V#90615

```
13137 2013152         JMS RSXMIT      /XMIT NEXT 5 BITS
13140 1217173         MEMA TEMP       /RESTORE FULL WORD
13141  716017         RISH 17         /SHIFT 15
13142 2013152         JMS RSXMIT      /XMIT NEXT 5 BITS
13143  216015         MEMA (15        /LOAD A VAX <CR>
13144 2117163         MEMZ @ XMTFLG   /SKIP IF VAX BUFFER NOT FULL
13145   13144         JMP #-1
13146  644730         RSOUTF          /RS232B OUT READY?
13147   13146         JMP #-1         /NO
13150  620731         RSOUT           /OUTPUT THE <CR>
13151 1013127         JMP @ VAXOUT
13152       0 RSXMIT, 0               /ROUTINE TO OUTPUT 1 BYTE
13153  262037         ANDA (37        /AND AC WITH 00011111
13154  260040         ADMA (40        /SET BITS 001XXXXX
13155 2117163         MEMZ @ XMTFLG   /SKIP IF VAX11 BUFFER NOT FULL
13156   13155         JMP #-1         /NO GO
13157  644730         RSOUTF          /RS232B OUT READY?
13160   13157         JMP #-1         /NO
13161  620731         RSOUT           /OUTPUT 1 BYTE
13162 1013152         JMP @ RSXMIT    /DONE
13163    4761 XMTFLG, CTRLCH
13164 3777773 MASK3,  3777773         /MASK FOR DISABLING SLOW I/O
13165 3777737 MASK4,  3777737         /MASK FOR DISABLING INT5-
13166     777 MASK5,  777             /BUTTON REGISTER MASK
13167  777000 MASK6,  777000          /BUTTON REGISTER MASK
13170   20000 STADDR, 20000           /BASE ADDRESS FOR STATUS ROUTINE
13171     564 GFLAG,  GOFLAG          /ACQ IN PROGRESS FLAG LOC EQUIV
13172       0 CHKSUM, 0               /CHECKSUM
13173       0 TEMP,   0               /TEMP STORAGE
13174       0 START,  0               /LOCATION START POINTER
13175       0 SIZE,   0               /BLOCK SIZE
13176  222362 MSG1,   .TEXT "RS232B DATA XMIT TO VAX (NO LEADER)["
13177  636202
13200  400401
13201  240140
13202  301511
13203  244024
13204  174026
13205   13040
13206  501617
13207  401405
13210   10405
13211  225133
13212  370000
13213  222362 MSG2,   .TEXT "RS232B DATA TRANSMIT TO VAX (LEADER)["
13214  636202
13215  400401
13216  240140
13217  242201
13220  162315
13221  112440
13222  241740
13223  260130
13224  405014
```

/USER OVERLAY TO NTCFT V#90615

```
 13225   50104
 13226   52251
 13227  333700
 16341          *16341
 16341   13000 POINT1, VAXDMP
 16343          *16343
 16343   13032 POINT2, LEADER
```


/USER OVERLAY TO NTCFT V#90615

BRETRN	10152	CHKSUM	13172	CTRLCH	4761	DIFLAG	545
DSPSIZ	466	DSPSTA	467	DUMP	13065	GADCHK	10061
GFLAG	13171	GOFLAG	564	INTENA	13114	LEADER	13032
LOOP2	13066	MASK3	13164	MASK4	13165	MASK5	13166
MASK6	13167	MSG1	13176	MSG2	13213	POINT1	16341
POINT2	16343	RSBINT	4751	RSXMIT	13152	SETADR	13106
SIZE	13175	SPDMSK	12	STADDR	13170	START	13174
STATUS	13075	TEMP	13173	VAXDMP	13000	VAXOUT	13127
XMTFLG	13163	ZDISPL	2301	ZILMSK	11	ZTTYBU	2636
ZUPKBU	2533	ZWFCHA	2627				

*

Figure A1.2 VAX-11 FORTRAN IV-PLUS Listing of the Data Transmission Program FILECOPY.FOR

```
        C  RS232B ENCODED DATA RECEIVE AND PACK ROUTINE
        C
        C  THIS ROUTINE RECEIVES ENCODED DATA FROM THE NICOLET 1180
        C  DATA SYSTEM VIA A TERMINAL MULTIPLEXER INPUT.  1180 DATA
        C  WILL BE IN THE FORM OF VECTORS OR ARRAYS, WITH A MAXIMUM
        C  SIZE OF 16K X 128 20 BIT WORDS.  THE 20 BIT WORDS ARE
        C  TRANSMITTED 5 BITS/BYTE IN THE FORMAT 001XXXXX WHERE XXXXX
        C  ARE THE SIGNIFICANT BITS.  EACH WORD IS TRANSMITTED AS
        C  A STRING OF 4 BYTES FOLLOWED BY A <CR> CHARACTER.  THE 001
        C  HIGH ORDER BITS INSURE THAT NO CONTROL CHARACTERS WILL
        C  APPEAR AS PART OF THE DATA STREAM.
        C
        C  VARIABLE DEFINITIONS:
        C
        C       A(*)              DATA POINT ARRAY, MAX SIZE 16K + 352 WORD
        C                           PARAMETER TABLE
        C       CHECKSUM          RUNNING CHECKSUM CALCULATED DURING DATA RECEIVE
        C       TITLE             A60 HEADER BLOCK WRITTEN ON OUTPUT FILE
        C       MASK1             00011111 MASK USED TO SELECT 5 LSB OF EACH BYTE
        C       MASK2             11111111111111111111 MASK USED TO SELECT
        C                           20 LSBs OF EACH 32 BIT WORD ON VAX
        C       KK                SET TO OCTAL 21 FOR CTRL-Q TO INITIATE
        C                           DATA TRANSMISSION
        C       IP                NUMBER OF DATA POINTS
        C       IJ(*)             VECTOR USED FOR DATA READ-IN, 4 WORDS LONG,
        C                           ONE BYTE PER LOCATION
        C       N                 RECORD COUNT ON DATA READ FROM RS232
        C       ISUM              RUNNING SUM USED IN PACKING DATA
        C
        C----------------------------------------------------------------------
0001            DIMENSION A(16736),IJ(4),TITLE(60)
0002            INTEGER A, CHECKSUM, TITLE, ANS
0003            LOGICAL CONTIN,COUNT,TYPE,LOG
        C  OUTPUT WRITTEN ON FILE 'FOR009.DAT;*' WITH CARRIAGE CONTROL SUPPRESSE
D
0004            OPEN (UNIT=09, NAME='FOR009',TYPE='NEW',
                1CARRIAGECONTROL='LIST')
0005            CONTIN = .TRUE.
0006            COUNT = .FALSE.
0007            TYPE = .FALSE.
0008            LOG = .FALSE.
0009            MAXLIM = 100
        C  SUPPRESS ERROR MESSAGES FROM INTEGER OVERFLOW CAUSED BY CHECKSUM
        C    CALCULATION
0010            CALL ERRSET(70,CONTIN,COUNT,TYPE,LOG,MAXLIM)
0011            MASK1 = "37
0012            MASK2 = "3777777
0013            KK = "21
0014            WRITE (6,1100)
0015    1100    FORMAT ('0ENTER NUMBER OF FILES, POINTS PER FILE')
0016            READ (5,1110) IF,IP
0017    1110    FORMAT (2I6)
        C  OUTPUT FILE MAY BE WRITTEN WITH OR WITHOUT A 352 WORD NTCFT-1180
        C    COMPATIBLE PARAMETER TABLE.  ALL FILES IN A FILEGROUP MUST
        C    HAVE THE SAME OPTION EXERCISED.  ON RELOADING THE 1180 WITH
        C    SUCH A PARAMETER TABLE, LOAD ADDRESS IS 17240.  NTCFT THEN
        C    EXAMINES THE LEADING TWO KEYWORDS TO INSURE THAT THE FILE IS
```

```
        C    AN NTCFT WRITTEN FILE.
0018              WRITE (6,1112)
0019    1112      FORMAT ('OSTORE WITH PARAMETER TABLES (Y OR N)?')
0020    50        READ (5,1114) ANS
0021    1114      FORMAT(1A1)
0022              IF (ANS.EQ.1HY) THEN
0023              IP = IP + 352
0024              GO TO 60
0025              ELSE IF (ANS.EQ.1HN) THEN
0026              GO TO 60
0027              ELSE
0028              WRITE (6,1116)
0029    1116      FORMAT ('OPLEASE ANSWER Y OR N')
0030              GO TO 50
0031              END IF
        C  WRITE A TWO LINE HEADER BLOCK (DEFAULT STANDARD FORMAT)
0032    60        WRITE (6,1120)
0033    1120      FORMAT ('OENTER TWO LETTER ID, 5 DIGIT EXP #, AND 2 DIGIT
                  1 BLOCK # --')
0034              READ (5,1130) IX1,IX2,IX3
0035              WRITE (9,1130) IX1,IX2,IX3
0036    1130      FORMAT (A2,I5,I2)
0037              WRITE (6,1140)
0038    1140      FORMAT (' EXPERIMENT IDENTIFICATION (A60) --')
0039              READ (5,1150) TITLE
0040              WRITE (9,1150) TITLE
0041    1150      FORMAT (60A1)
        C  NOW LOOP THROUGH ONCE FOR EACH FILE.  START BY TRANSMITTING A
        C    CTRL-Q TO INSURE THAT 1180 IS DUMPING DATA.  CTRL-Q SETS INT5-
        C    ON THE 1180 AND CAUSES THE INTERRUPT SERVICE TO SET A DATA
        C    TRANSMIT FLAG.
0042              DO 230, J=1,IF
0043              WRITE (2) KK
0044              CHECKSUM = 0
        C  FOR EACH FILE, LOOP THROUGH IP TIMES TO RECONSTRUCT IP WORDS FROM
        C    IP*4 BYTES.  A 20 BIT WORD IS RECEIVED IN THE FOLLOWING BYTE
        C    SEQUENCE:
        C
        C         AC4-0,AC9-5,AC14-10,AC19-15 <CR>
        C
        C    RECONSTRUCTION (PACKING) OCCURS BY APPROPRIATE LEFT-SHIFTING
        C    AND LOGICAL OR-ING OF THE FOUR BYTES STORED IN IJ(*)
0045              DO 200, K=1,IP
0046    100       READ (1,1000) N,IJ
0047    1000      FORMAT (Q,100A1)
0048              ISUM = 0
0049              DO 120 L=4,1,-1
0050              IJ(L) = IAND(IJ(L),MASK1)
0051              LSHIFT = (L-1)*5
0052    120       ISUM = IOR(ISUM,ISHFT(IJ(L),LSHIFT))
0053              CHECKSUM = CHECKSUM + ISUM
0054    200       A(K) = ISUM
        C  NOW RECEIVE AND RECONSTRUCT THE CHECKSUM CALCULATED BY THE 1180,
        C    AND COMPARE TO THE LOCALLY CALCULATED ONE.
0055              READ(1,1000) (IJ(I),I=1,4)
0056              ISUM = 0
```

```
FILECOPY$MAIN     5-Sep-1979 16:52:07     VAX-11 FORTRAN IV-PLUS V1.2-13       Page
 3
                                          FILECOPY.FOR.12

              DO 220, L=4,1,-1
              IJ(L) = IAND(IJ(L),MASK1)
              LSHIFT = (L-1)*5
      220     ISUM = IOR(ISUM,ISHFT(IJ(L),LSHIFT))
              WRITE (9,2000) (A(KL),KL=1,IP)
              CHECKSUM = IAND(CHECKSUM,MASK2)
              ISUM = IAND(ISUM,MASK2)
      230     WRITE(6,1010) J,CHECKSUM,ISUM
      1010    FORMAT('0FILE =',I3/'0CALCULATED CHECKSUM =',O9/
              1'0RECEIVED CHECKSUM =',O9)
      2000    FORMAT (8I10)
              END
```

```
FILECOPY$MAIN    5-Sep-1979 16:52:07    VAX-11 FORTRAN IV-PLUS V1.2-13      Page
 4
                                        FILECOPY.FOR.12

PROGRAM SECTIONS

    Name                    Bytes   Attributes

  0 $CODE                     635   PIC CON REL LCL   SHR   EXE   RD NOWRT LONG
  1 $PDATA                    313   PIC CON REL LCL   SHR NOEXE   RD NOWRT LONG
  2 $LOCAL                  67396   PIC CON REL LCL NOSHR NOEXE   RD   WRT LONG

ENTRY POINTS

    Address   Type Name

  0-00000000      FILECOPY$MAIN


VARIABLES

    Address   Type Name                Address   Type Name                Address   T
ype Name                  Address   Type Name

  2-00010684  I*4 ANS                2-00010680  I*4 CHECKSUM             2-00010688
L*4 CONTIN            2-0001068C  L*4 COUNT
  2-000106D4  I*4 I                  2-000106A8  I*4 IF                   2-000106AC
I*4 IP                2-000106C8  I*4 ISUM
  2-000106B0  I*4 IX1                2-000106B4  I*4 IX2                  2-000106B8
I*4 IX3               2-000106BC  I*4 J
  2-000106C0  I*4 K                  2-000106A4  I*4 KK                   2-000106D8
I*4 KL                2-000106CC  I*4 L
  2-00010694  L*4 LOG                2-000106D0  I*4 LSHIFT               2-0001069C
I*4 MASK1             2-000106A0  I*4 MASK2
  2-00010698  I*4 MAXLIM             2-000106C4  I*4 N                    2-00010690
L*4 TYPE

ARRAYS

    Address   Type Name                      Bytes  Dimensions

  2-00000000  I*4 A                          66944  (16736)
  2-00010580  I*4 IJ                            16  (4)
  2-00010590  I*4 TITLE                        240  (60)

LABELS

    Address   Label       Address   Label       Address   Label       Address
Label       Address   Label       Address   Label

  0-00000093  50        0-000000EB  60              **      100          **
120            **     200            **     220
      **      230       1-000000EE  1000'     1-000000F4  1010'     1-0000000B
1100'     1-00000035  1110'     1-0000003A  1112'
  1-00000063  1114'     1-00000066  1116'     1-0000007E  1120'     1-000000BC
1130'     1-000000C3  1140'     1-000000E9  1150'
  1-00000134  2000'


FUNCTIONS AND SUBROUTINES REFERENCED

ERRSET              FOR$OPEN            MTH$JISHFT
```

Figure A1.3 VAX-11 FORTRAN-IV PLUS Listing of the Data Transmission Program ARRAY.FOR

```
C  RS232B ENCODED DATA RECEIVE AND PACK ROUTINE
C
C  THIS ROUTINE RECEIVES ENCODED DATA FROM THE NICOLET 1180
C  DATA SYSTEM VIA A TERMINAL MULTIPLEXER INPUT.  1180 DATA
C  WILL BE IN THE FORM OF VECTORS OR ARRAYS, WITH A MAXIMUM
C  SIZE OF 8K X 128 20 BIT WORDS.  THE 20 BIT WORDS ARE
C  TRANSMITTED 5 BITS/BYTE IN THE FORMAT 001XXXXX WHERE XXXXX
C  ARE THE SIGNIFICANT BITS.  EACH WORD IS TRANSMITTED AS
C  A STRING OF 4 BYTES FOLLOWED BY A <CR> CHARACTER.  THE 110
C  HIGH ORDER BITS INSURE THAT NO CONTROL CHARACTERS WILL
C  APPEAR AS PART OF THE DATA STREAM.
C
C  VARIABLE DEFINITIONS:
C
C       A(*,*)          INTEGER ARRAY FOR UP TO 128X128 20 BIT WORDS
C       IJ(*)           4 WORD VECTOR FOR READING 4 UNPACKED BYTES
C       CHECKSUM        RUNNING CHECKSUM CALCULATED ON RECEIVED DATA
C       TITLE(*)        A60 HEADER BLOCK FOR LABLING FILES
C       MASK1           00011111 MASK FOR PICKING OUT SIGNIFICANT BITS
C       MASK2           11111111111111111111 MASK TO PICK OUT 20 BITS
C       KK              SET TO OCTAL 21 (CTRL-Q), USED TO INITIATE
C                         DATA TRANSMISSION
C       IF              NUMBER OF FILES TO BE READ, USUALLY 128
C       IP              NUMBER OF POINTS PER FILE, USUALLY 128
C       N               SET TO CHARACTER COUNT ON EXECUTION OF READ
C                         STATEMENT 100
C       LSHIFT          LEFT SHIFT COUNT
C
C---------------------------------------------------------------------
C
        DIMENSION A(128,128),IJ(4)
        INTEGER A, CHECKSUM, TITLE(60)
        LOGICAL CONTIN,COUNT,TYPE,LOG
        DATA A/16384*0/
C  OUTPUT FILE "FOR010.DAT" WILL CONTAIN THE DATA ARRAY
        OPEN (UNIT=10, NAME='FOR010',TYPE='NEW',
        1CARRIAGECONTROL='LIST')
        CONTIN = .TRUE.
        COUNT = .FALSE.
        TYPE = .FALSE.
        LOG = .FALSE.
        MAXLIM = 100
C  CALL ERRSET TO OVERRIDE INTEGER OVERFLOWS DURING CALCULATION
C       OF CHECKSUMS
        CALL ERRSET(70,CONTIN,COUNT,TYPE,LOG,MAXLIM)
        MASK1 = "37
        MASK2 = "3777777
        KK = "21
        WRITE (6,1100)
1100    FORMAT ('0ENTER NUMBER OF FILES, POINTS PER FILE')
        READ (5,1110) IF,IP
1110    FORMAT (2I4)
C  READ AND WRITE OUT A HEADER BLOCK THAT IS COMPATIBLE WITH THE
C       VAX 11 FORTRAN IV PLUS CONTOUR PLOTTING ROUTINE
C       [KAR120C]NICOLET
20      WRITE (6,1120)
```

```
ARRAY$MAIN       3-Sep-1979 13:55:55    VAX-11 FORTRAN IV-PLUS V1.2-13       Page
 2
                                        ARRAY.FOR.23

       1120     FORMAT ('OENTER TWO LETTER ID, 5 DIGIT EXP #, AND 2 DIGIT
                1 BLOCK # --')
                READ (5,1130) IX1,IX2,IX3
                WRITE (10,1130) IX1,IX2,IX3
       1130     FORMAT (A2,I5,I2)
                WRITE (6,1140)
       1140     FORMAT (' EXPERIMENT IDENTIFICATION (A60) --')
                READ (5,1150) TITLE
                WRITE (10,1150) TITLE
       1150     FORMAT (60A1)
       C  INITIATE 1180 DATA TRANSMISSION BY SENDING A CTRL-Q OUT
       C        TERMINAL MULTIPLEXER PORT THAT IS ALLOCATED TO 1180
       C        RS232B CHANNEL
                WRITE (2) KK
                DO 230, J=1,IF
                CHECKSUM = 0
                DO 200, K=1,IP
       C  A 20 BIT WORD IS RECEIVED IN THE FOLLOWING SEQUENCE:
       C
       C        AC4-0,AC9-5,AC14-10,AC19-14 <CR>
       C
       C  RECONSTRUCTION OCCURS BY APPROPRIATE MASKING, LEFT SHIFTING,
       C        AND LOGICAL OR-ING OF THE FOUR BYTES STORED IN IJ(*)
       100      READ (1,1000) N,IJ
       1000     FORMAT (Q,100A1)
                ISUM = 0
                DO 120 L=4,1,-1
                IJ(L) = IAND(IJ(L),MASK1)
                LSHIFT = (L-1)*5
       120      ISUM = IOR(ISUM,ISHFT(IJ(L),LSHIFT))
                CHECKSUM = CHECKSUM + ISUM
       200      A(J,K) = ISUM
       C  NOW RECEIVE THE 1180 CALCULATED CHECKSUM AND COMPARE IT TO
       C        THE LOCALLY CALCULATED ONE
                READ(1,1000) (IJ(I),I=1,4)
                ISUM = 0
                DO 220, L=4,1,-1
                IJ(L) = IAND(IJ(L),MASK1)
                LSHIFT = (L-1)*5
       220      ISUM = IOR(ISUM,ISHFT(IJ(L),LSHIFT))
                CHECKSUM = IAND(CHECKSUM,MASK2)
       230      WRITE(6,1010) J,CHECKSUM,ISUM
       1010     FORMAT('OFILE =',I3/'OCALCULATED CHECKSUM =',O9/
                1'ORECEIVED CHECKSUM =',O9)
                WRITE (10,2000) ((A(M,N),N=1,128),M=1,128)
       2000     FORMAT (8I10)
       C  [KAR120C]NICOLET LOOKS FOR TAGWORDS AS DELIMITERS OF SERIALLY
       C        STORED DATA BLOCKS.  AS MANY 128 X 128 BLOCKS AS
       C        DESIRED MAY BE STORED SEQUENTIALLY, OR THEY MAY BE
       C        LATER COMBINED USING THE VMS COMMAND <APPEND>.
       C
                WRITE (6,2100)
       2100     FORMAT ('OAPPEND ANOTHER ARRAY (Y OR N)?')
       300      READ (5,2110) IANS
       2110     FORMAT (A1)
                IF (IANS.EQ.1HY) THEN
```

```
ARRAY$MAIN        3-Sep-1979 13:55:55     VAX-11 FORTRAN IV-PLUS V1.2-13       Page
 3
                                          ARRAY.FOR.23

                GO TO 20
                ELSE IF (IANS.EQ.1HN) THEN
                GO TO 400
                ELSE
                WRITE (6,2120)
        2120    FORMAT ('0ANSWER Y OR N')
                GO TO 300
                END IF
        400     END
```

```
ARRAY$MAIN        3-Sep-1979 13:55:55     VAX-11 FORTRAN IV-PLUS V1.2-13       Page
 4
                                          ARRAY.FOR.23

PROGRAM SECTIONS

    Name                   Bytes   Attributes

  0 $CODE                    852   PIC CON REL LCL   SHR   EXE   RD NOWRT LONG
  1 $PDATA                   299   PIC CON REL LCL   SHR NOEXE   RD NOWRT LONG
  2 $LOCAL                 65988   PIC CON REL LCL NOSHR NOEXE   RD   WRT LONG

ENTRY POINTS

    Address   Type Name

  0-00000000       ARRAY$MAIN


VARIABLES

    Address   Type Name                 Address   Type Name                 Address   T
ype Name             Address   Type Name

  2-00010100  I*4 CHECKSUM        2-00010104  L*4 CONTIN            2-00010108
L*4 COUNT           2-00010150  I*4 I
  2-00010158  I*4 IANS            2-00010124  I*4 IF                2-00010128
I*4 IP              2-00010144  I*4 ISUM
  2-0001012C  I*4 IX1             2-00010130  I*4 IX2               2-00010134
I*4 IX3             2-00010138  I*4 J
  2-0001013C  I*4 K               2-00010120  I*4 KK                2-00010148
I*4 L               2-00010110  L*4 LOG
  2-0001014C  I*4 LSHIFT          2-00010154  I*4 M                 2-00010118
I*4 MASK1           2-0001011C  I*4 MASK2
  2-00010114  I*4 MAXLIM          2-00010140  I*4 N                 2-0001010C
L*4 TYPE

ARRAYS

    Address   Type Name                    Bytes  Dimensions

  2-00000000  I*4 A                        65536  (128,128)
  2-00010000  I*4 IJ                          16  (4)
  2-00010010  I*4 TITLE                      240  (60)


LABELS

    Address   Label        Address   Label        Address   Label        Address
Label        Address   Label        Address   Label

  0-0000007D  20              **     100             **     120             **
200           **      220            **      230
  0-000002FF  300      0-00000350   400       1-000000AA  1000'     1-000000B0
1010'      1-0000000B  1100'     1-00000035  1110'
  1-0000003A  1120'    1-00000078   1130'     1-0000007F  1140'     1-000000A5
1150'      1-000000F0  2000'     1-000000F5  2100'
  1-00000117  2110'    1-0000011A   2120'


FUNCTIONS AND SUBROUTINES REFERENCED

ERRSET            FOR$OPEN            MTH$JISHFT
```

Figure A1.4 Assembled Listing of USR Overlay to NTCFT-1180 for Data Transmission to NIC-80

```
 RUN FASM

FASM, E58-90215
@HR220.ASC/HR220.BIN,-TT:F
```

```
FAST 1180 ASSEMBLER, E58-90215

08/23/79 10:03   @HR220.ASC/HR220.BIN,-TT:F

150 SOURCE STATEMENTS
28 USER-DEFINED SYMBOLS
MEMORY NEEDED: 13000 TO 16343
```

/USR OVERLAY TO NTCFT V#90615

```
 /USR OVERLAY TO NTCFT V#90615
 .UNDENT

 /       LAST UPDATE: 27 JUNE 1979
 /
 /       For transmission of data and programs to the NIC-80 system
 /         attached to the HR-220 spectrometer system
 /
 /         U1 =>read programs/data from NIC-80
 /         U2 => send programs/data to NIC-80
 /
 /         293A SSW      UP => Program, occupying 0000-7577
 /                       down => Data, occupying 100000-117777 max
 /                                    (button selected)

600610          TSPW=600610
 13000          *13000
 13000        0 STATUS, 0                 /READ BUTTONS FOR MEMORY START
 13001 1217172          MEMA STADDR       /LOAD BASE ADDRESS
 13002 1413173          ACCM START        /AND STORE IN START
 13003  603640          RDBUTN            /READ BUTTONS
 13004 1263170          ANDA MASK1        /SELECT START ADDRESS BITS
 13005  250000          AMOA              /SEE IF START ADDRESS IS ZERO
 13006   53011          JPZ SETADR        /START ADDRESS IS 0
 13007  246000          APOA              /ADD 1 BACK
 13010  701007          LASH 7            /CONVERT TO OFFSET
 13011 1221173 SETADR,  APMA START        /ADD TO BASE ADDRESS
 13012 1413173          ACCM START        /STORE FINAL START ADDRESS
 13013  603640          RDBUTN            /READ BUTTONS AGAIN
 13014 1263171          ANDA MASK2        /SELECT SIZE BITS
 13015  716001          RISH 1            /CONVERT TO ABSOLUTE SIZE
 13016 1413174          ACCM SIZE         /STORE SIZE IN SIZE
 13017  600610          TSPW              /LOOK AT SENSE SWITCHES
 13020 1363027          ANDAZ MASK0       /PICK OUT SW 3 (BIT 15)
 13021 2013023          JMS SETSIZ        /SET SIZE = 7600
 13022 1013000          JMP @ STATUS
 13023        0 SETSIZ, 0                 /SET SIZE TO 7600
 13024 1217030          MEMA PSIZE
 13025 1413174          ACCM SIZE
 13026 1013023          JMP @ SETSIZ
 13027  100000 MASK0,   100000            /MASK TO PICK OUT SSW 3
 13030    7600 PSIZE,   7600
 13031       0 RSREAD,  0                 /START OF RS232B READ
 13032 1403175          ZERM CHKSUM       /ZERO CHECKSUM
 13033 2013000          JMS STATUS        /FIND ADDRESSES TO USE
 13034 2013114 LOOP1,   JMS XON           /TRANSMIT X-ON
 13035  644720          RSINF             /RS232 READY TO LOOK FOR X-ON?
 13036   13035          JMP #-1           /NOT READY
 13037  600721          RSIN              /READ RS232
 13040  322021          AMMAZ (021        /IS IT X-ON?
 13041   13034          JMP LOOP1         /NO, KEEP LOOKING
 13042 2013101 LOAD,    JMS READ          /READ 8 BITS FROM RS232
 13043 2413173          ACCM @ START      /STORE LOWEST BITS
 13044 2013114          JMS XON           /SEND CONFIRMING X-ON
```

/USR OVERLAY TO NTCFT V#90615

```
13045 2013101          JMS READ         /READ NEXT MSB'S
13046  701010          LASH 10          /SHIFT
13047 2421173          AFMM @ START     /ADD ON AFTER SHIFT
13050 2013114          JMS XON          /SEND CONFIRMING X-ON
13051 2013101          JMS READ         /READ MSB'S
13052  701020          LASH 20          /SHIFT L6
13053 2421173          AFMM @ START     /ADD ON AFTER SHIFT
13054 2013114          JMS XON          /SEND CONFIRMING X-ON
13055 2217173          MEMA @ START     /LOAD WHOLE WORD AND
13056 1421175          AFMM CHKSUM      /  ADD TO CHECKSUM
13057 1437173          MFOM START       /ADVANCE POINTER
13060 1535174          MMOMZ SIZE       /DECREMENT SIZE, SKIP ON 0
13061   13042          JMP LOAD         /NEXT POINT
13062 2013101          JMS READ         /NOW RECEIVE CHECKSUM
13063 1413176          ACCM CSUM        /STORE 8 LSB'S
13064 2013114          JMS XON          /SEND
13065 2013101          JMS READ         /NEXT 8 MSB'S
13066  701010          LASH 10          /SHIFT
13067 1421176          AFMM CSUM        /STORE SHIFTED
13070 2013114          JMS XON          /SEND CONFIRMING X-ON
13071 2013101          JMS READ         /MSB'S
13072  701020          LASH 20          /SHIFT
13073 1421176          AFMM CSUM        /ADD ON
13074 2013114          JMS XON          /SEND CONFIRMING X-ON
13075 1217176          MEMA CSUM        /NOW COMPARE WITH COUNTED
13076 1323175          AMMAZ CHKSUM     /  CHECKSUM
13077 2013106          JMS ERROR
13100 1013031          JMP @ RSREAD     /RETURN TO NTCFT
13101       0 READ,    0                /RS232 READ ROUTINE
13102  644720          RSINF            /RS232B READY?
13103   13102          JMP #-1
13104  600721          RSIN             /READ 8 BITS INTO ACC
13105 1013101          JMP @ READ
13106       0 ERROR,   0                /CHECKSUM ERROR ROUTINE
13107  216207          MEMA (207        /RING BELL
13110  644710          TTYPF
13111   13110          JMP #-1
13112  620711          PRTTY
13113 1013106          JMP @ ERROR
13114       0 XON,     0                /TRANSMIT X-ON ROUTINE
13115  644730          RSOUTF           /RS232B READY TO XMIT?
13116   13115          JMP #-1          /NO
13117  216021          MEMA (021        /X-ON
13120  620731          RSOUT            /TRANSMIT X-ON
13121 1013114          JMP @ XON
13122       0 RSDUMP,  0                /START OF RS232B TRANSMIT
13123 1403175          ZERM CHKSUM      /ZERO CHECKSUM
13124 2013000          JMS STATUS       /FIND ADDRESSES TO USE
13125 2013160          JMS RXON         /WAIT UNTIL X-ON RECEIVED
13126 2013114          JMS XON          /SEND ACKNOWLEDGING X-ON
13127 2217173 LOOP2,   MEMA @ START     /LOAD POINTED TO WORD
13130 1421175          AFMM CHKSUM      /ADD TO CHECKSUM
13131 2013140          JMS WORFUN       /TRANSMIT WORD
13132 1437173          MFOM START       /INCREMENT POINTER
```

/USR OVERLAY TO NTCFT V#90615

```
 13133 1535174         MMOMZ SIZE      /DECREMENT SIZE COUNT
 13134   13127         JMP LOOP2       /NEXT WORD
 13135 1217175         MEMA CHKSUM     /NOW TRANSMIT CHECKSUM
 13136 2013140         JMS WORPUN
 13137 1013122         JMP @ RSDUMP
 13140       0 WORPUN, 0               /20 BIT WORD XMIT ROUTINE
 13141 1413167         ACCM TEMP       /STORE WORD IN TEMP
 13142 2013152         JMS OUT         /DUMP LOWEST 8 BITS
 13143 1217167         MEMA TEMP       /RESTORE WORD AND
 13144  716010         RISH 10         /  SHIFT OVER 8
 13145 2013152         JMS OUT         /DUMP NEXT 8
 13146 1217167         MEMA TEMP       /RESTORE WORD AGAIN AND
 13147  716020         RISH 20         /  SHIFT OVER 16
 13150 2013152         JMS OUT         /DUMP 4 MSB'S + JUNK
 13151 1013140         JMP @ WORPUN
 13152       0 OUT,    0               /RS232B OUTPUT ROUTINE
 13153  644730         RSOUTF
 13154   13153         JMP #-1
 13155  620731         RSOUT
 13156 2013160         JMS RXON        /WAIT FOR REC X-ON
 13157 1013152         JMP @ OUT
 13160       0 RXON,   0               /RECEIVE X-ON ROUTINE
 13161  644720         RSINF           /WAIT FOR RS232B INPUT READY
 13162   13161         JMP #-1
 13163  600721         RSIN
 13164  322021         AMMAZ (021      /IS IT X-ON?
 13165   13161         JMP #-4         /NO
 13166 1013160         JMP @ RXON
 13167       0 TEMP,   0               /TEMP STORAGE
 13170     777 MASK1,  777
 13171  777000 MASK2,  777000
 13172   20000 STADDR, 20000
 13173       0 START,  0
 13174       0 SIZE,   0
 13175       0 CHKSUM, 0
 13176       0 CSUM,   0
 13177       0 COUNT1, 0               /TEMP COUNTER
 16341         *16341
 16341   13031 POINT1, RSREAD
 16343         *16343
 16343   13122 POINT2, RSDUMP
```

-3-

/USR OVERLAY TO NTCFT V#90615

CHKSUM	13175	COUNT1	13177	CSUM	13176	ERROR	13106
LOAD	13042	LOOP1	13034	LOOP2	13127	MASK0	13027
MASK1	13170	MASK2	13171	OUT	13152	POINT1	16341
POINT2	16343	PSIZE	13030	READ	13101	RSDUMP	13122
RSREAD	13031	RXON	13160	SETADR	13011	SETSIZ	13023
SIZE	13174	STADDR	13172	START	13173	STATUS	13000
TEMP	13167	TSPW	600610	WORPUN	13140	XON	13114

APPENDIX 2 Complex Impedance Calculation

Figure A2.1 BASIC Program Listing for Calculating the Complex Impedance from the Magnitude and Phase of the Reflection Coefficient

```
100 REM  CALCULATE COMPLEX IMPEDANCE FROM REFLECTION COEFFICIENT
110 PRINT "Enter A amplitude --";
120 INPUT A
130 PRINT "Enter B amplitude --";
140 INPUT B
150 PRINT "Enter relative phase --";
160 INPUT P
170 LET B=1.0532*B
180 PRINT
190 PRINT "B CORRECTION = 1.0532"
200 PRINT "CORRECTED B =";B
210 LET G=B/A
220 PRINT "GAMMA =";G;"    (Reflection Coefficient)"
230 LET P1=P*3.14159265/180.
240 LET X1=G*COS(P1)
250 LET Y1=G*SIN(P1)
260 LET N1=(X1+1.)*(X1+1.)+(Y1*Y1)
270 LET A1=SQR(N1)
280 LET A2=ATN(Y1/(X1+1.))*180./3.141592654
290 LET N2=(1.-X1)*(1.-X1)+(Y1*Y1)
300 LET A3=SQR(N2)
310 LET A4=ATN(-Y1/(1.-X1))*180./3.141592654
320 LET N3=51.1*A1/A3
330 LET N4=(A2-A4)*3.141592654/180.
340 LET R1=N3*COS(N4)
350 LET R2=N3*SIN(N4)
360 PRINT "REAL PART OF IMPEDANCE --";R1;" OHMS"
370 PRINT "IMAGINARY PART OF IMPEDANCE --";R2;"J OHMS"
380 PRINT
390 PRINT "MAGNITUDE =";N3
400 PRINT "PHASE ANGLE =";(A2-A4);" DEG"
410 PRINT
420 PRINT
430 PRINT "TO QUIT, TYPE 0, OTHERWISE Enter A amplitude --";
440 INPUT A
450 IF A=0. THEN    470
460 GO TO    130
470 END
```

APPENDIX 3 Supplementary Schematic Documentation

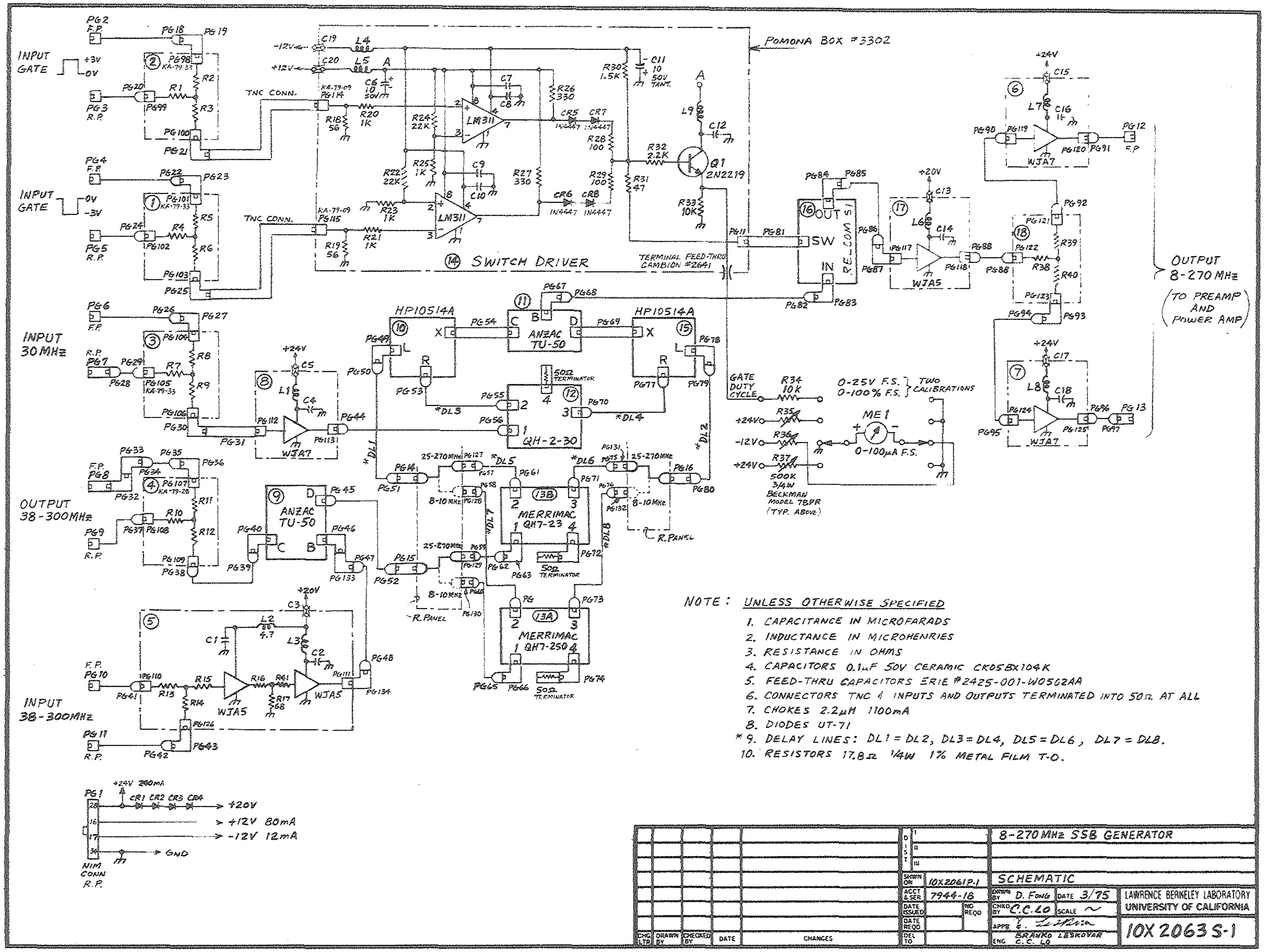

NOTE: UNLESS OTHERWISE SPECIFIED

1. CAPACITANCE IN MICROFARADS
2. INDUCTANCE IN MICROHENRIES
3. RESISTANCE IN OHMS
4. CAPACITORS 0.1μF 50V CERAMIC CK05BX104K
5. FEED-THRU CAPACITORS ERIE #2425-001-W0502AA
6. CONNECTORS TNC & INPUTS AND OUTPUTS TERMINATED INTO 50Ω AT ALL
7. CHOKES 2.2μH 1100mA
8. DIODES UT-71
*9. DELAY LINES: DL1 = DL2, DL3 = DL4, DL5 = DL6, DL7 = DL8.
10. RESISTORS 17.8Ω 1/4W 1% METAL FILM T-O.

8-270 MHz SSB GENERATOR

SCHEMATIC

SHOWN ON	10X2061P-1
ACCT & SER	7944-18
DRAWN BY	D. FONG
DATE	3/75
CHKD BY	C.C. LO
SCALE	~
APPR	[signature]
ENG	BRANKO LESKOVAR, C.C. LO

LAWRENCE BERKELEY LABORATORY
UNIVERSITY OF CALIFORNIA

10X 2063 S-1

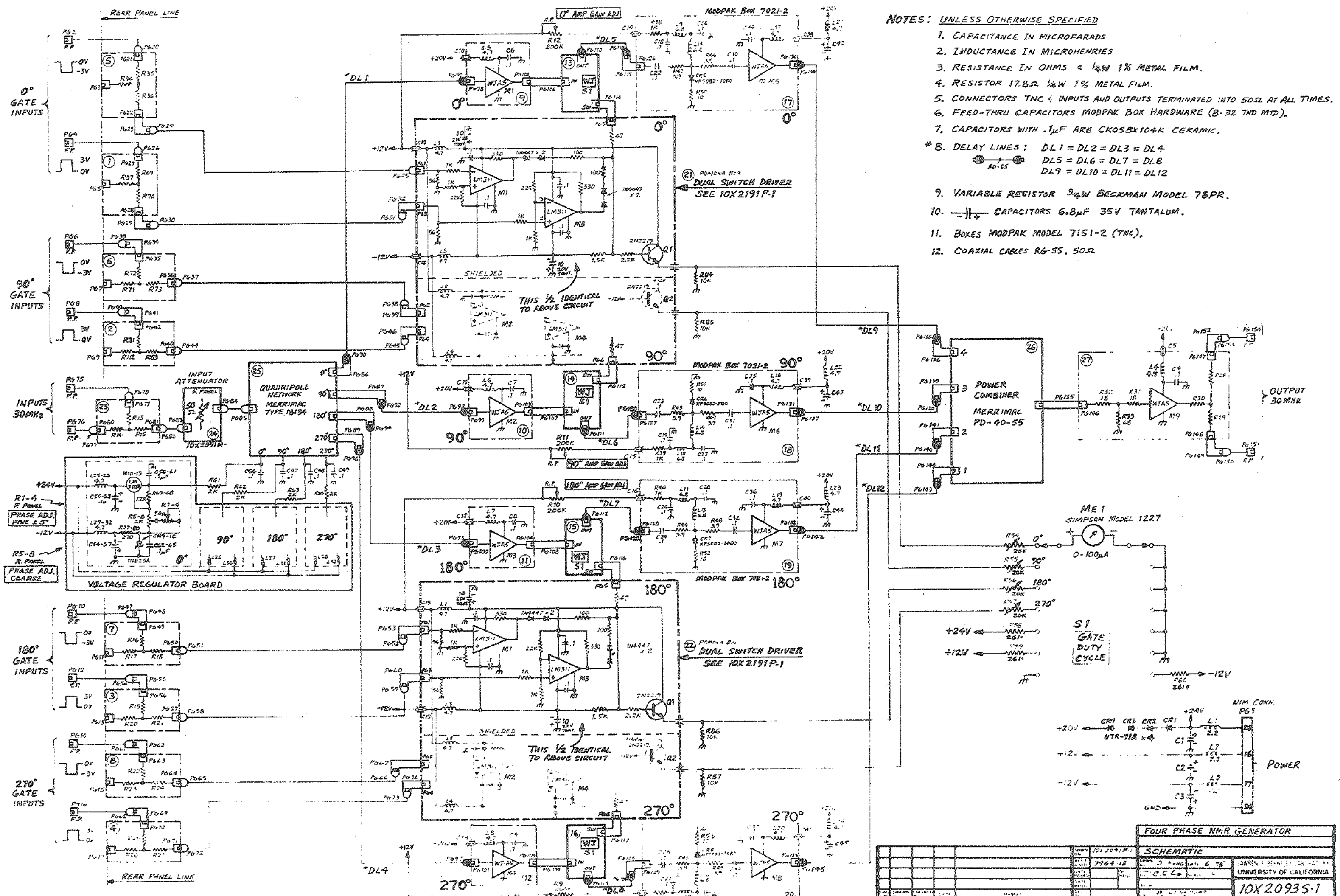
NOTES: UNLESS OTHERWISE SPECIFIED
1. CAPACITANCE IN MICROFARADS
2. INDUCTANCE IN MICROHENRIES
3. RESISTANCE IN OHMS & ¼W 1% METAL FILM.
4. RESISTOR 17.8Ω ¼W 1% METAL FILM.
5. CONNECTORS TNC & INPUTS AND OUTPUTS TERMINATED INTO 50Ω AT ALL TIMES.
6. FEED-THRU CAPACITORS MODPAK BOX HARDWARE (8-32 THD MTD).
7. CAPACITORS WITH .1μF ARE CKO5BX104K CERAMIC.
*8. DELAY LINES: DL1 = DL2 = DL3 = DL4
RG-55
DL5 = DL6 = DL7 = DL8
DL9 = DL10 = DL11 = DL12
9. VARIABLE RESISTOR ¾W BECKMAN MODEL 78PR.
10. CAPACITORS 6.8μF 35V TANTALUM.
11. BOXES MODPAK MODEL 7151-2 (TNC).
12. COAXIAL CABLES RG-55, 50Ω
REAR PANEL LINE
0° GATE INPUTS
90° GATE INPUTS
180° GATE INPUTS
270° GATE INPUTS
INPUTS 30MHz
INPUT ATTENUATOR
QUADRIPOLE NETWORK MERRIMAC TYPE IB134
VOLTAGE REGULATOR BOARD
PHASE ADJ. FINE ±5°
PHASE ADJ. COARSE
0° AMP GAIN ADJ
90° AMP GAIN ADJ
180° AMP GAIN ADJ
270° AMP GAIN ADJ
MODPAK BOX 7021-2
DUAL SWITCH DRIVER SEE 10X2191P-1
SHIELDED
THIS ½ IDENTICAL TO ABOVE CIRCUIT
POWER COMBINER MERRIMAC PD-40-55
OUTPUT 30MHz
ME 1 SIMPSON MODEL 1227
0-100μA
S1 GATE DUTY CYCLE
NIM CONN. P61
POWER
FOUR PHASE NMR GENERATOR
SCHEMATIC
UNIVERSITY OF CALIFORNIA
10X2093S-1

XBL 761-126

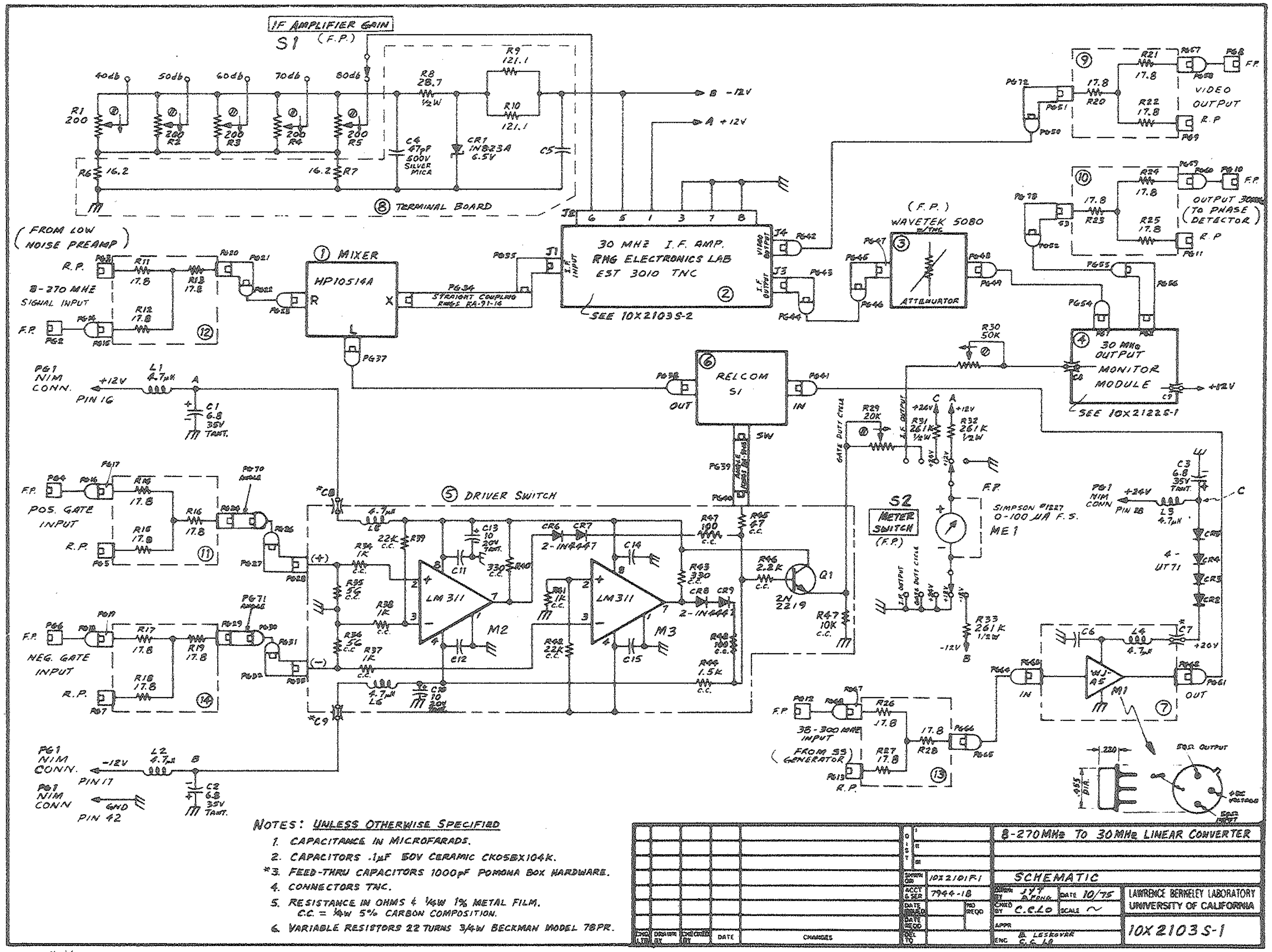
IF AMPLIFIER GAIN
S1 (F.P.)
40db
50db
60db
70db
80db
R8 28.7 ½W
R9 121.1
R10 121.1
CR1 IN823A 6.5V
C4 47pF 500V SILVER MICA
⑧ TERMINAL BOARD
B -12V
A +12V
(FROM LOW NOISE PREAMP)
R.P.
8-270 MHZ SIGNAL INPUT
① MIXER
HP10514A
PG34 STRAIGHT COUPLING RG58 KA-91-16
30 MHZ I.F. AMP.
RHG ELECTRONICS LAB
EST 3010 TNC
SEE 10X2103S-2
(F.P.)
WAVETEK 5080
③ ATTENUATOR
VIDEO OUTPUT
OUTPUT 30MHz (TO PHASE DETECTOR)
⑥ RELCOM S1
④ 30 MHz OUTPUT MONITOR MODULE
SEE 10X2122S-1
PG1 NIM CONN. +12V PIN 16
C1 6.8 35V TANT.
POS. GATE INPUT
NEG. GATE INPUT
⑤ DRIVER SWITCH
LM311
M2
M3
2-IN4447
Q1 2N2219
S2 METER SWITCH (F.P.)
SIMPSON #1227 0-100 μA F.S.
ME1
PG1 NIM CONN +24V PIN 28
4-UT71
WJ-A5
M1
⑦
38-300 MHz INPUT
(FROM SS GENERATOR)
PG1 NIM CONN. -12V PIN 17
C2 6.8 35V TANT.
PG1 NIM CONN GND PIN 42
NOTES: UNLESS OTHERWISE SPECIFIED
1. CAPACITANCE IN MICROFARADS.
2. CAPACITORS .1μF 50V CERAMIC CK05BX104K.
*3. FEED-THRU CAPACITORS 1000pF POMONA BOX HARDWARE.
4. CONNECTORS TNC.
5. RESISTANCE IN OHMS ¼ ¼W 1% METAL FILM. C.C. = ¼W 5% CARBON COMPOSITION.
6. VARIABLE RESISTORS 22 TURNS 3/4W BECKMAN MODEL 78PR.
8-270MHz TO 30MHz LINEAR CONVERTER
SCHEMATIC
10X2101F-1
7944-18
DATE 10/75
C.C.LO
LAWRENCE BERKELEY LABORATORY
UNIVERSITY OF CALIFORNIA
10X2103S-1
CHANGES

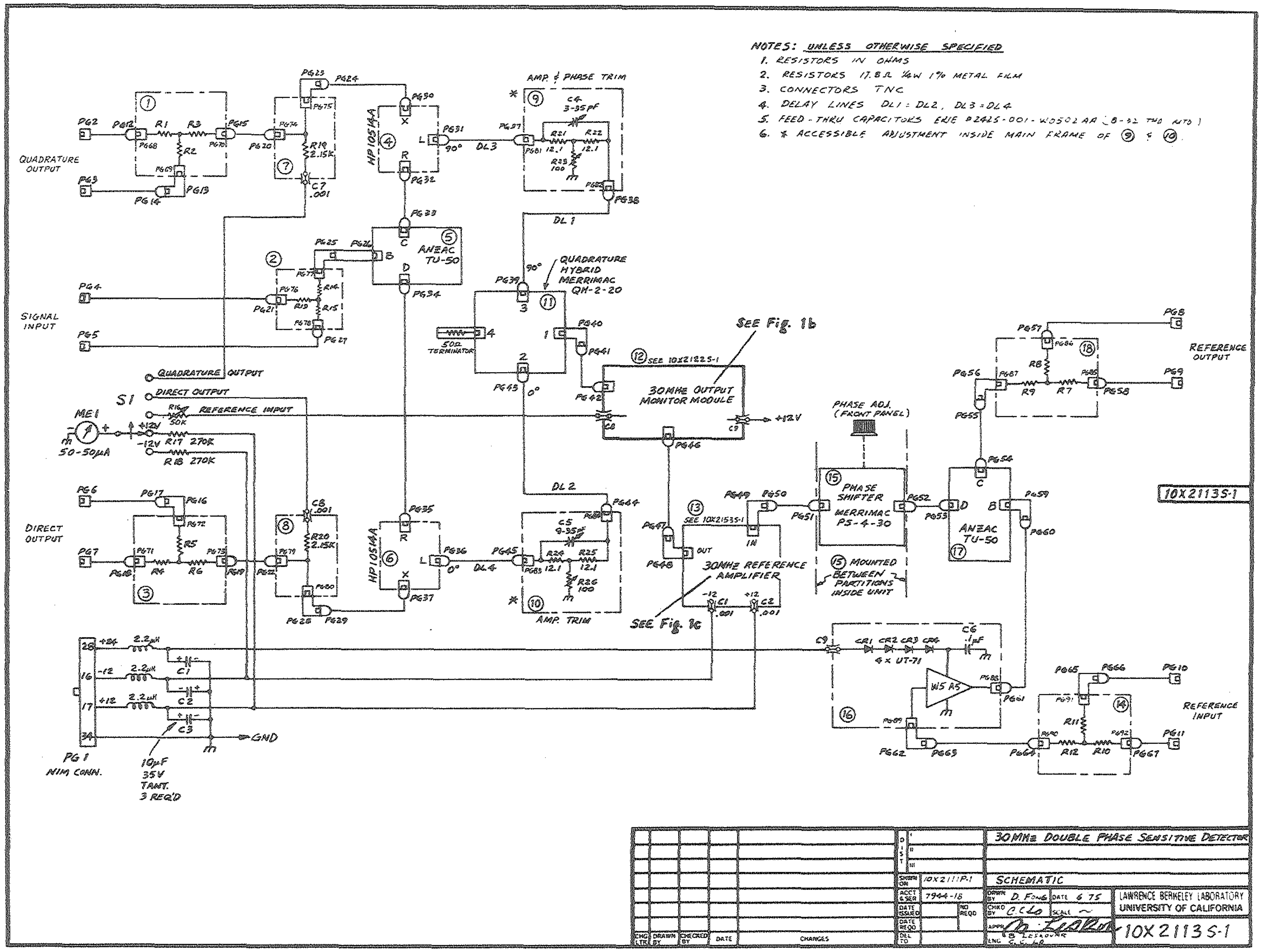
NOTES: UNLESS OTHERWISE SPECIFIED
1. RESISTORS IN OHMS
2. RESISTORS 17.8Ω ¼W 1% METAL FILM
3. CONNECTORS TNC
4. DELAY LINES DL1 = DL2, DL3 = DL4
6. * ACCESSIBLE ADJUSTMENT INSIDE MAIN FRAME OF ⑨ & ⑩
QUADRATURE OUTPUT
SIGNAL INPUT
DIRECT OUTPUT
REFERENCE OUTPUT
REFERENCE INPUT
ANZAC TU-50
QUADRATURE HYBRID MERRIMAC QH-2-20
30MHz OUTPUT MONITOR MODULE
30MHz REFERENCE AMPLIFIER
PHASE SHIFTER MERRIMAC PS-4-30
PHASE ADJ. (FRONT PANEL)
SEE Fig. 1b
SEE Fig. 1c
AMP. & PHASE TRIM
AMP. TRIM
PG 1 NIM CONN.
10μF 35V TANT. 3 REQ'D
10X2113S-1
30MHz DOUBLE PHASE SENSITIVE DETECTOR
SCHEMATIC
D. FONG 6 75
LAWRENCE BERKELEY LABORATORY
UNIVERSITY OF CALIFORNIA
10X2113S-1

XBL 761-432

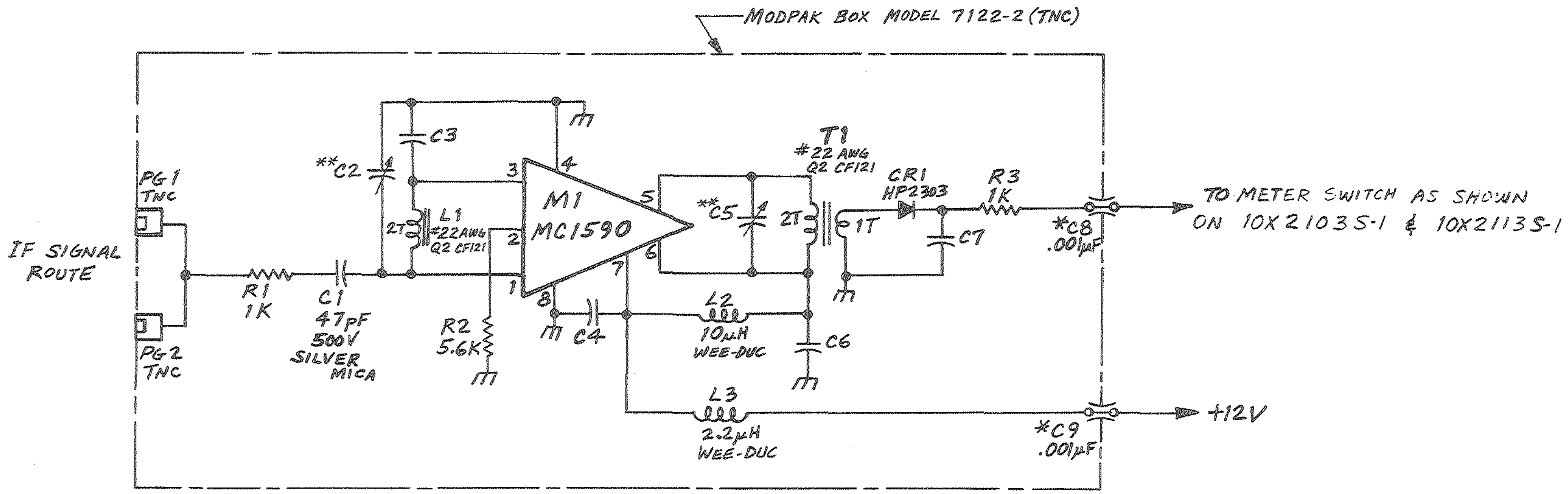

NOTES: UNLESS OTHERWISE SPECIFIED

1. CAPACITORS 0.01μF 100V CERAMIC CK05BX103M.
*2. FEED-THRU CAPACITORS ERIE #2425-001-W0502AA (8-32 THD MTD).
3. RESISTORS ¼W 1% METAL FILM.
**4. VARIABLE CAPACITORS 9-35pF CERAMIC ERIE MODEL #538-000.

CHG. LTR.	DRAWN BY	CHECKED BY	DATE	CHANGES

DIST I.	
II.	
III.	10X2121P-1
SHWN ON	10X2103S-1 & 10X2113S-1
ACCT. & SER.	7944-18
DATE ISSUED	NO REQD.
DATE REQD	
DEL TO	

30MHz OUTPUT MONITOR MODULE

SCHEMATIC

DRWN BY D. FONG	DATE 6/75	LAWRENCE BERKELEY LABORATORY UNIVERSITY OF CALIFORNIA	
CHKD BY C.C.LO	SCALE ~		
APPR. [signature]		10X2122S-1	
ENG. C. C. LO			

RL 2009.2 (REV 12.71)

XBL 761-401

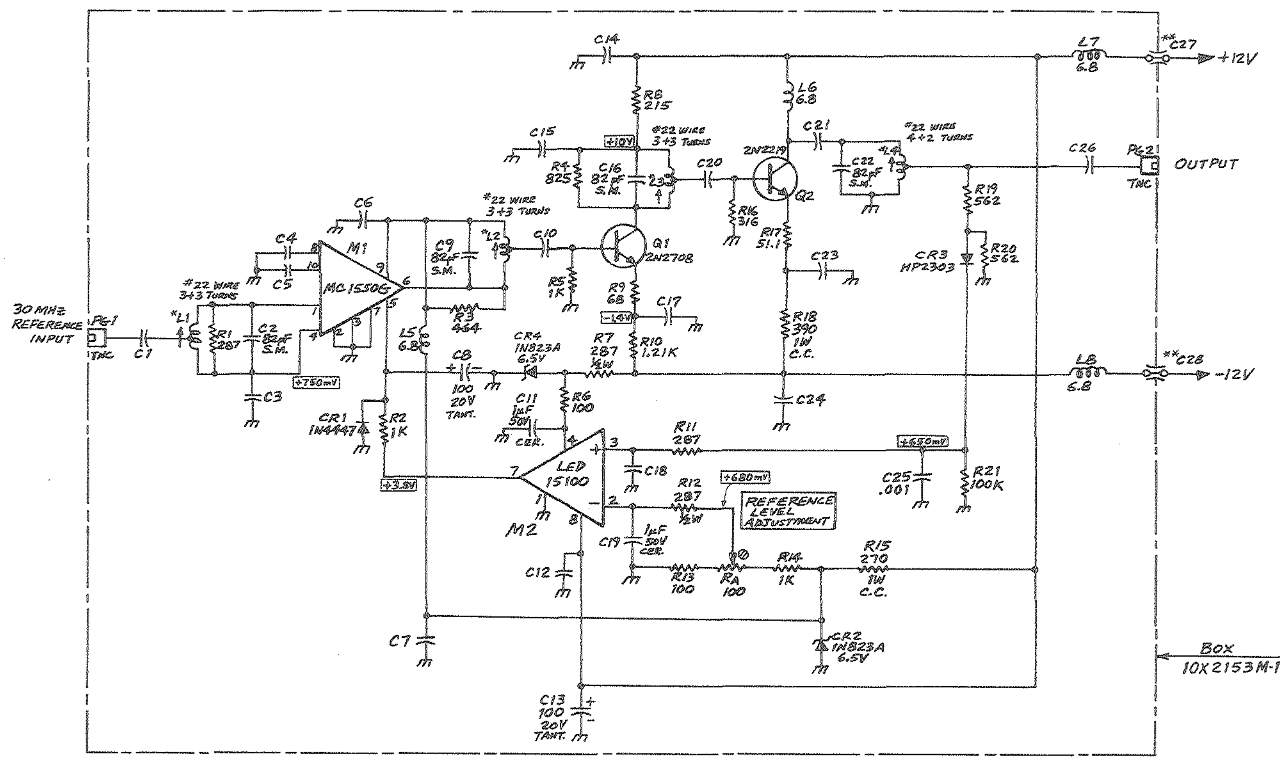

NOTES: UNLESS OTHERWISE INDICATED

1. RESISTANCE IN OHMS
2. CAPACITANCE IN MICROFARADS
3. INDUCTANCE IN MICROHENRIES
4. CAPACITORS .01µF CK05 CERAMIC.
**5. CAPACITOR FEED-THRU ERIE #2425-001-W0502AA (8-32 THD MTD).
*6. ADJUSTABLE COILS WOUND ON MILLER COIL FORM #47A024-4.
7. RESISTORS ⅛W 1% T.O. METAL FILM.

SHOWN ON	10X2151 P-1 / 10X2113 S-1
ACCT 4-SER	7944-18
DATE ISSUED	
DATE REQD	NO. REQD
DEL TO	
CHG LTR / DRAWN BY / CHECKED BY / DATE / CHANGES	
Title	30MHz REFERENCE AMPLIFIER — SCHEMATIC
DRWN BY	D. FONG
DATE	6/75
SCALE	~
APPR	B. Leskovar
ENG	BRANKO LESKOVAR / IRVING KO
	LAWRENCE BERKELEY LABORATORY UNIVERSITY OF CALIFORNIA
	10X 2153 S-1

XBL 761-430

"To do is to be."	- J.P. Sartre
"To be is to do."	- E. Kant
"Do be do be do."	- F. Sinatra

U.S.GPO:1980-698-102 F-102